

**The author(s) shown below used Federal funds provided by the U.S. Department of Justice and prepared the following final report:**

**Document Title:** Application of Fluorescence Line Narrowing Spectroscopy to Forensic Fiber Examination

**Author(s):** Andres D. Campiglia, Ph.D., Michael D. Sigman, Ph.D.

**Document No.:** 240640

**Date Received:** December 2012

**Award Number:** 2006-DN-BX-K036

**This report has not been published by the U.S. Department of Justice. To provide better customer service, NCJRS has made this Federally-funded grant report available electronically.**

**Opinions or points of view expressed are those of the author(s) and do not necessarily reflect the official position or policies of the U.S. Department of Justice.**

## **Final Report**

**Report Title:** Application of Fluorescence Line Narrowing Spectroscopy to Forensic Fiber Examination

**Award Number:** 2006-DN-BX-K036

**Author(s):** *PI:* Dr. Andres D. Campiglia, Department of Chemistry; University of Central Florida, Orlando, FL, 32816-2366; *Co-PI:* Dr. Michael D. Sigman, Department of Chemistry; University of Central Florida, Orlando, FL, 32816-2366 and National Center of Forensic Science

### **Abstract**

We propose to develop nondestructive analytical methodology capable of providing highly discriminating identification of textile fibers encountered as physical evidence in criminal investigations. Trace textile fiber evidence is found at numerous crime scenes and plays an important role in linking a suspect to the respective scene. Several methods currently exist for the analysis of trace fiber evidence. Microscopy based techniques are important tools for discriminating fibers with at least one distinguishable characteristic. The main advantage of these techniques is their non-destructive nature, which preserves the physical integrity of the fibers for further court examination. When fibers cannot be discriminated by non-destructive tests such as those based on microscopic, optical and physical examination, the next reasonable step is to extract the dye from both the known and questioned fiber for further chemical analysis. Many cases exist where the comparison of fibers based on the chemical composition of dyes still leaves the forensic scientist with the difficulty of assigning a probability to the common source determination. The problem stems, in part, from the large amounts of textile produced each year in replicate fiber types and colors. This problem is made more difficult by the fact that it may not be possible to discriminate between two fibers that have been dyed with highly similar dyes. This is not an uncommon situation, as there are many hundred of commercial dyes with indistinguishable colors, and minimal structural variations are encouraged by the patent process and commercial competition. The end purpose of this project is to fulfill this gap with a highly discriminating identification tool that maintains the evidentiary value of the original sample. We focus on the total fluorescence emission of fibers. In addition to the contribution of the textile dye (or dyes) to the fluorescence spectrum of the fiber, we investigate the contribution of intrinsic fluorescence impurities – i.e. impurities imbedded into the fibers during fabrication of garments - as a reproducible source of fiber comparison. The methodology, instrumentation and data analysis we propose obviates the need for destructive dye extractions while significantly increasing the discriminating power of fluorescence microscopy.

**Table of Contents**

Executive Summary	pages 3 - 8
I. Introduction	pages 8 - 10
II. Methods	pages 10 - 24
III. Results	pages 24 - 85
IV. Conclusions	pages 85 - 88
V. References	pages 88 - 90
VI. Dissemination of Research Findings	page 91
VII. Appendix Section	pages 92 - 143

## Executive Summary

Trace textile fiber evidence is found at numerous crime scenes and plays an important role in linking a suspect to the respective scene. Several methods currently exist for the analysis of trace fiber evidence. Microscopy based techniques are important tools for discriminating fibers with at least one distinguishable characteristic. These include polarized light microscopy, infrared microscopy, visible micro-spectrophotometry and scanning electron microscopy coupled to energy dispersive spectrometry. The main advantage of these techniques is their non-destructive nature, which preserves the physical integrity of the fibers for further court examination. Differences in cross-sectional shape, type of fiber material (natural or synthetic), weave and color often make it possible to rule out a common source for the two fiber samples. When fibers cannot be discriminated by non-destructive tests such as those based on microscopic, optical and physical examination, the next reasonable step is to extract the dye from both the known and questioned fiber for further chemical analysis.

Solvent extraction, enzymatic hydrolysis, and alkaline hydrolysis have been used to release dyes from the various types of fibers. Thin-layer chromatography (TLC), high-performance liquid-chromatography (HPLC) and capillary electrophoresis (CE) have been used to separate and identify colored dyes in fiber extracts. TLC is a long-standing tool for the separation of common classes of fiber dyes, with silica gel being the most used stationary phase. Unfortunately, no single solvent system exists that can separate all classes of dyes and some amount of prescreening is usually necessary. This is a major disadvantage for forensic comparisons, mainly if one considers that each loose fiber in a forensic investigation represents and must be handled as a unique item of evidence. HPLC and CE present several advantages over TLC, including better resolution and quantitative capability. When coupled to absorption single channel detectors, the identification of dyes is solely based on their retention times. Additional selectivity is possible with the use of multichannel wavelength detection systems that record real-time absorption spectra for comparison of eluted components to spectral databases.

For the many hundreds of dyes used in the textile industry that appear to be the same color, that have highly similar molecular structures, virtually indistinguishable absorption spectra and identical or highly similar chromatographic retention times or electrophoretic migration times, the best approach is the combination of mass spectrometry (MS) to HPLC (HPLC-MS) or to CE (CE-MS). Unfortunately, MS techniques destroy the fiber just like all the other methods that provide chemical information based on previous dye extraction. Of the nondestructive techniques currently available for comparing dyes in textile fibers diffuse reflectance infrared Fourier transform spectroscopy (DRIFTS) and Raman spectroscopy have shown some promise. When coupled to chemometric methods for spectral interpretation such as principal component analysis (PCA) and soft independent modeling of class analogies (SIMCA), DRIFTS was able to discriminate both dye color and reactive dye state on cotton. Raman microprobe spectroscopy was able to characterize dyes in both natural and synthetic fibers via a combination of Fourier transform-Raman spectra and PCA analysis. Due to the inherently weak nature of the Raman signal, the identification of minor fiber dyes via Raman spectroscopy has not been possible. The inability to detect small concentrations of dyes that could add valuable information to the signature of fibers certainly reduces the discrimination power of the technique. The weak nature of the Raman signal also poses serious limitations in the analysis of lightly dyed fibers.

The common denominator to current methodology is the fact that fiber analysis primarily focus on the dyes used to color the fibers and do not investigate other potential discriminating components present on the fiber. Many cases exist where the comparison of fibers based on the chemical composition of dyes still leaves the forensic scientist with the difficulty of assigning a

probability to the common source determination. The problem stems, in part, from the large amounts of textile produced each year in replicate fiber types and colors. This problem is made more difficult by the fact that it may not be possible to discriminate between two fibers that have been dyed with highly similar dyes. This is not an uncommon situation, as there are many hundred of commercial dyes with indistinguishable colors, and minimal structural variations are encouraged by the patent process and commercial competition. The end purpose of this project is to fulfill this gap with a highly discriminating identification tool that maintains the evidentiary value of the original sample.

We tackle a different aspect of fiber analysis as we focus on the total fluorescence emission of fibers. In addition to the contribution of the textile dye (or dyes) to the fluorescence spectrum of the fiber, we investigate the fluorescence of intrinsic fiber impurities – i.e. impurities imbedded into the fibers during fabrication of garments – and contaminants as a reproducible source of fiber comparison, as well as the methodology for discriminating fibers using fluorescence. To the extent of our literature search, no efforts have been made to investigate the full potential of fluorescence spectroscopy for forensic fiber examination. Previous articles on fluorescence microscopy of fibers report measurements made with excitation and emission band-pass filters which provide no detailed information on the fluorescence features of fibers. The same is true for the fluorescence characteristics of dyes. The lack of information in the open literature regarding fluorescence of fibers prompted us to undertake a systematic study in our lab to better understand the fluorescence of textile fibers. Our experimental approach was then designed to answering several pertinent questions, including the following: (a) should we concentrate on the fluorescence of textile dyes, the fluorescence of intrinsic impurities or the total fluorescence of the fiber?; (b) are intrinsic impurities reproducible sources of fluorescence?; (c) what is the minimum fiber length one can examine via fluorescence spectroscopy?; (d) how do we deal with fluorescence from environmental contaminants?; (e) what is the best fluorescence data format for fiber discrimination?; and (f) what instrumental approach one should use for fiber discrimination on the bases of their fluorescence characteristics?

The investigated fibers were selected to cover a wide range of cloth materials such as acetate, polyester, cotton and nylon. Their respective reagent dyes were the following: Disperse Red 1, Disperse Red 4, Disperse Red 13, Basic Green 4, Basic Red 9, Basic Violet 14, Direct Blue 1, Direct Blue 71, Direct Blue 90, Acid Red 151, Acid Yellow 17, Acid Yellow 23 and Acid Green 27. These reagent dyes are commonly manufactured in the textile industry and fit into one of the following our categories: direct, disperse, basic and acid dyes. Direct dyes are those that have high affinity for cellulose materials such as cotton, rayon, etc. Disperse dyes are slightly soluble in water and typically used for synthetic fibers made of nylon, polyester, etc. Acid dyes are anionic dyes often applied from an acid dye-bath and basic dyes are cationic dyes characterized by their affinity for acrylic fiber and occasionally silk, wool or cotton. Fabric and dyed cloths were purchased from Testfabrics Inc.; West Pittston, PA. All fiber cloths were received in sealed packages. All cloths were kept as received in the dark to avoid environmental exposure. A head-to-head comparison of the fluorescence characteristics of dye reagents with fiber extracts was not possible because Testfabrics did not provide us with the matching reagent dyes for the studied fibers. The unsuccessful outcome of our attempts led us to an investigation of the absorption and fluorescence properties of Sigma-Aldrich dye standards, a popular source of reagent dyes for the textile industry. All Sigma-Aldrich dyes were purchased at reagent grade purity but no information was provided by Sigma-Aldrich on the complete chemical composition of the dye standards. Taking into consideration the possible variations that often exist in the chemical composition of dye reagents from different commercial sources and/or variations that may also exist within dye reagent batches from the same source, the best fluorescence approach for fiber

comparison should only provide a spectral matching for the dye reagent that was used to pre-dye the investigated fiber. If fluorescence impurities were incorporated into the fiber during the fabrication of the cloth, the spectral profile of the Aldrich-Sigma dye should provide a different spectral signature to the one recorded from the “respective” Testfabrics fiber extract.

Our investigations were first conducted with fiber extracts submitted to ultraviolet (UV) and visible (VIS) absorption spectroscopy, room-temperature fluorescence (RTF) spectroscopy and HPLC coupled to UV-VIS absorption and RTF detection. Fibers were extracted via the experimental procedure recommended by the Federal Bureau of Investigations (FBI). Four extracting solvents were investigated for fiber extraction, namely 1:1 methanol – water (v/v), ethanol, 1:1 acetonitrile-water (v/v) and 57% pyridine - 43% water (v/v). The visual comparison of fluorescence spectra from fiber extracts revealed two main types of spectral profiles, i.e. emission spectra with only one and with more than one fluorescent peaks. Spectral comparison within the same type of fiber and the same extracting solvent revealed some cases with strong dependence on the chemical nature of the extracting solvent. The differences observed can be attributed to the chemical affinities of the extracting solvents for fluorescence components in the textile fibers. When fiber extraction was carried out with the best extracting solvent for each type of fiber, all fiber extracts showed excitation and fluorescence profiles different from each other. Considering the disadvantages associated to selecting the best solvent for fiber extraction prior to RTF spectroscopy in forensic comparisons, we propose a 1:1 acetonitrile:water (v/v) mixture as the common extracting solvent for all the studied fibers. Similar to our observations with the best individual extracting solvents, the strong fluorescence intensities of fibers in 1:1 acetonitrile:water (v/v) extracts made possible their analyses with 2mm lengths. The reproducibility of excitation and fluorescence spectral profiles was demonstrated with two types of experiments. Spectral profiles were recorded from individual extracts belonging to adjacent fibers – i.e. single fibers located immediately next to each other –within the same area of cloth - and from single fibers located in four different areas of the cloth. Both types of experiments provided outstanding reproducibility of spectral profiles with minimum variations in fluorescence intensities.

As expected, all Sigma-Aldrich dye standards had strong absorption peaks in the visible range most likely attributed to the presence of the dyes. The fiber extracts showed similar visible peaks, but also showed stronger peaks in the UV region. The majority of dye standards showed relatively weaker fluorescence than their corresponding fiber extracts. Fiber extracts showed the contribution of unknown fluorescence impurities. Since the fluorescence given by the fiber extracts appears to be irrespective of the dyes these fluorescence signals could provide another level of discrimination for forensic fiber analysis beyond examining dyes. The potential exists for differentiating visually indistinguishable fibers, i.e. of the same material, pre-dyed with the same dye but with the presence of different impurities. The separation of fiber extracts via HPLC provides valuable information on the contribution of individual components to the total fluorescence of fibers. The comparison of chromatograms from extracts of fibers collected from different areas of a cloth confirmed the reproducibility of individual fluorescence impurities within the same piece of cloth. The reproducibility of individual impurities agrees well with the fluorescence reproducibility of extracts from fibers of the same cloth. The HPLC analysis of Aldrich-Sigma dyes provided fluorescence chromatograms with different components than those observed from fiber extracts. Further absorption and fluorescence analysis of HPLC fractions confirmed the presence of fluorescence impurities in the fiber extracts that were not present in the Sigma-Aldrich standards.

Two data formats were investigated for comparing fiber extracts to their respective Sigma-Aldrich dye standards, namely two dimensional (2D) - i.e. intensity versus wavelength - excitation and fluorescence spectra and excitation-emission matrices (EEM). Taking into consideration the variations observed in the chemical composition of fiber extracts and their corresponding dye standards, the best fluorescence approach for fiber comparison should only provide a spectral matching for the dye reagent that was used to pre-dye the investigated fiber. If fluorescence impurities were incorporated into the fiber during the fabrication of the cloth, the spectral profile of the Aldrich-Sigma dye should provide a different spectral signature to the one recorded from the "respective" Testfabrics fiber extract. With the exception of Basic Green 4 and Disperse Blue 56, all the remaining fiber extracts presented different 2D spectral profiles to those recorded from their respective dye standards. All RTF-EEM were different from each other. Based on these results, are a more powerful data formats than 2D spectra for fiber discrimination. This advantage results from an intrinsic characteristic of RTF-EEM data formats, which is their ability to convolute the contribution of all fluorescence components within the ultraviolet and visible spectral regions.

The comparison of RTF-EEM recorded from the extracts of visually indistinguishable fibers was best accomplished with the aid of chemometric analysis. Among the algorithms we investigated for this purpose, multivariate curve resolution alternating least squares (MCR-ALS) provided the best results. RTF-EEM data formats were recorded from extracts of nylon fibers pre-dyed with Acid Red 151, Acid Yellow 17 and Acid Yellow 23. Acid Red 151 fibers were collected from two different pieces of cloths, ten fibers per cloth. Ten Acid Yellow 17 fibers were collected from one piece of cloth. The same was true for the Acid Yellow 23 fibers. Each fiber was extracted with ethanol and an RTF-EEM was recorded from each extract. The comparison of Acid Red 151 extracts would allow us to test the ability of to differentiate between two visually indistinguishable fibers pre-dyed with the same dye in the same textile industry but collected from different cloths. The statistical comparison of fiber extracts Acid Yellow 17 and Acid Yellow 23 would allow us to test the ability of RTF-EEM to differentiate between two visually indistinguishable fibers pre-dyed with two different dyes. MCR-ALS analysis of RTF-EEM taken from extracts of nylon fibers pre-dyed with Acid Yellow 17 and 23 predicted five fluorescent components in each type of extract. From differences in the calculated correlation coefficients of two fluorescent components, we were able to discriminate among these two types of visually indistinguishable fibers. MCR-ALS analysis of RTF-EEM taken from extracts of nylon fibers pre-dyed with Acid Red 151 also made possible to discriminate among two visually indistinguishable fibers pre-dyed with the same dye in the same textile industry but from different cloths. Although additional studies should be made with a larger number and types of visually indistinguishable fibers, the results presented in this report provide the foundation to propose the combination of RTF-EEM and MCR-ALS as a promising tool for the forensic analysis of textile fibers.

We examined three possible environmental factors that could alter the fluorescence characteristics of textile fibers, namely cigarette smoke, detergents and fabric softeners. Cigarette smoke is one of the possible contaminants that clothing may be exposed to in a real world environment. Contained within cigarette smoke are a number of strongly fluorescing compounds known as polycyclic aromatic hydrocarbons (PAH). Our investigations exposed fibers to cigarette smoke and examined the resulting extracts to detect the possible presence of PAH. We also investigated the effect of repetitive washing on the intrinsic fluorescence of fibers, the fluorescence characteristics of detergents and fabric softeners and their effects upon repetitive washing of textile fibers. It should be noted that our proposition never intended to provide a definite answer to all the questions related to environmental factors. Our objective was relatively

modest as we merely proposed to initiate an investigation on the potential usefulness of environmental concomitants as an additional source of fiber comparison. Based on the results obtained so far, we are inclined to state that the fluorescence of environmental contaminants could prove useful for fiber comparison, mainly in the specific case of visually indistinguishable fibers with similar inherent chemical composition that provide almost identical RTF-EEM data formats. For instance, the spectral features of PAH adsorbed on the fiber could be used to discriminate between fibers on the basis of their exposure history. The same is true with the spectral changes observed upon washing. In the case of non-polar contaminants such as PAH, one possibility is to remove them from the fiber prior to its extraction. Because of the polar nature of intrinsic fluorescence components, fiber rinsing (or even extraction) with a non-polar solvent should be harmless to the inherent fluorescence of the fiber. Because detergents and softeners are soluble in water, the choice of an appropriate solvent for their selective extraction requires further studies. In addition, we feel that fiber discrimination via RTF spectroscopy should benefit from a comprehensive spectral database of commercial detergents and softeners. Comparison of this database to the spectral characteristics of fiber extracts should aid the analyst to track down the exposure of fibers to laundering contaminants.

Two instrumental approaches were investigated for the non-destructive analysis of fibers. The first approach followed our original proposition based on Fluorescence Line Narrowing (FLN) spectroscopy. The instrumentation for its direct application to fiber analysis had been previously developed in our lab. Its main disadvantage towards fiber analysis was the relatively narrow excitation range of the tunable dye laser. To achieve the full potential of FLN spectroscopy, fluorescence excitation of fibers should occur within both the ultraviolet and the visible spectral range. Our tunable dye laser only provided sufficient output power for fiber excitation in the ultraviolet spectral region. While presenting our results in forensic science meetings and sharing our thoughts with forensic scientists, we noticed skepticism among practitioners on the embracement of FLN spectroscopy as a tool for fiber analysis in forensic science labs. Two arguable reasons apparently contribute to the community's perception, namely the relatively high cost of instrumentation and the pre-conceived idea of sophisticated training for its operation. A more appealing approach for the forensic science community appeared to be RTF- microscopy. With this prospective in mind, our second instrumental approach to non-destructive analysis of fibers was to couple two commercial units, namely a spectrofluorimeter and an epi- fluorescence microscope via commercially available fiber optic bundles. Its installation was successfully accomplished and so it was the alignment of its optical components for best signal-to-background (S/B) ratio. Our studies demonstrate reproducible spectral profiles along the length of single fibers. The same is true for spectral profiles of fibers belonging to the same piece of cloth. The possibility to adjust the diameter of the microscope's pinhole and the excitation and emission band-pass of the spectrofluorimeter made possible to record reproducible spectral profiles from fibers with weak fluorescence emission. This possibility includes un-exposed fibers to pre-dying treatments. The strongest fluorescence signals from all fibers and best spectral profiles were obtained using open pinholes and 40X objectives in both the ultraviolet and visible spectral regions. With the 40X objectives, the open pinhole diameter corresponds to a 150 $\mu$ m (0.15mm) fiber length. This fiber length is considerably shorter than the ~2mm fiber length typically encountered in crime scenes. From this prospective, the combination of an open pinhole and a 40X objective appears to be well suited for the non-destructive RTF analysis of fibers.

The spectral features of the visually indistinguishable fibers studied in this project provided remarkable different RTF-EEMs. Although a larger pool of visually indistinguishable fibers should be examined in the future, we feel we have successfully achieved the goal of this project. We have presented proof of concept that provides a solid foundation for the development of non-

destructive methodology for forensic fiber analysis. Future studies that go beyond the duration of this project should compare the discrimination of visually indistinguishable fibers via RTF-EEM microscopy and micro-spectrophotometry. The new methodology should be tested across multiple types of data frequently encountered in forensic science, in such a way that the practical implications of the results are understandable and the methodology easily explained to juries. If successful, RTF-EEM microscopy should significantly enhance the ‘match’ decision that precedes addressing the question of the weight of the evidence.

## **I. Introduction**

### **I.1. Statement of the problem**

Trace textile fiber evidence is found at numerous crime scenes and plays an important role in linking a suspect to the respective scene. Several methods currently exist for the analysis of trace fiber evidence. When fibers cannot be discriminated by non-destructive tests such as those based on microscopic, optical and physical examination, the next reasonable step is to extract the dye from both the known and questioned fiber for further chemical analysis. Current methods primarily focus on the dyes used to color the fibers and do not investigate other potential discriminating components present on the fiber. Many cases exist where the comparison of fibers based on the chemical composition of dyes still leaves the forensic scientist with the difficulty of assigning a probability to the common source determination. The problem stems, in part, from the large amounts of textile produced each year in replicate fiber types and colors. This problem is made more difficult by the fact that it may not be possible to discriminate between two fibers that have been dyed with highly similar dyes. This is not an uncommon situation, as there are many hundred of commercial dyes with indistinguishable colors, and minimal structural variations are encouraged by the patent process and commercial competition. An additional drawback of the existing methodology is its destructive nature. To extract a dye or contaminant from a fiber essentially destroys the evidence. This leaves the investigator without their original sample in the courtroom. The end purpose of our efforts is to fulfill this gap with a highly discriminating identification tool that maintains the evidentiary value of the original sample.

### **I.2. Literature citations and review**

Analytical techniques that can either discriminate between similar fibers or match a known to a questioned fiber are highly valuable in forensic science [1, 2]. Microscopy based techniques are important tools for discriminating fibers with at least one distinguishable characteristic. These include polarized light microscopy, infrared microscopy [3], visible micro-spectrophotometry [4-10] and scanning electron microscopy coupled to energy dispersive spectrometry [11]. The main advantage of these techniques is their non-destructive nature, which preserves the physical integrity of the fibers for further court examination. Differences in cross-sectional shape, type of fiber material (natural or synthetic), weave and color often make it possible to rule out a common source for the two fiber samples. Beyond microscopy but still under the category of minimally destructive techniques is pyrolysis coupled to gas chromatography. This tool is capable to compare the polymeric nature of synthetic and natural fibers at expenses of small sample consumption [12].

When fibers cannot be discriminated by non-destructive tests, the next step is to extract the questioned and the known fiber for further dye analysis. Solvent extraction, enzymatic hydrolysis, and alkaline hydrolysis have been used to release dyes from the various types of fibers. Thin-layer chromatography (TLC), high-performance liquid-chromatography (HPLC) and capillary electrophoresis (CE) have been used to separate and identify colored dyes in fiber extracts. TLC is a long-standing tool for the separation of common classes of fiber dyes, with

silica gel being the most used stationary phase [13]. Unfortunately, no single solvent system exists that can separate all classes of dyes and some amount of prescreening is usually necessary. Specific methods have been reported for the analysis of dyes in cotton [14, 15], wool [16-19], and various synthetic fabrics [14, 20-22]. This is a major disadvantage for forensic comparisons, mainly if one considers that each loose fiber in a forensic investigation represents and must be handled as a unique item of evidence.

HPLC presents several advantages over TLC, including better chromatographic resolution and quantitative capability. Reversed-phase HPLC has been used to separate and determine anionic, cationic, nonionic, and ionic dyes. When coupled to absorption single channel detectors, the identification of dyes is solely based on their chromatographic retention times. Additional selectivity is possible with the use of multichannel wavelength detection systems that record real-time absorption spectra for comparison of eluted components to spectral databases [23].

Initial attempts to develop CE methods for fiber dyes rendered irreproducible migration times, poor sensitivity, and the inability to separate non-ionizable dyes [24]. The introduction of micelles in the electrophoretic buffer (micellar electrokinetic chromatography or MEKC) has now made possible the separation of water insoluble dyes extracted from wool fiber samples [25]. A considerable improvement in sensitivity was obtained by coupling sample induced isotachopheresis to MEKC. With this approach, it was possible to analyze the dye content of single natural and synthetic fibers [26].

For the many hundreds of dyes used in the textile industry that appear to be the same color, that have highly similar molecular structures, virtually indistinguishable absorption spectra and identical or highly similar chromatographic retention times or electrophoretic migration times, the best approach is the combination of mass spectrometry (MS) to HPLC (HPLC-MS) or to CE (CE-MS). The first report in this area described the use of thermospray HPLC-MS (TSP-HPLC-MS) to identify and quantify dyes in various matrixes [27]. Since then, several authors have discussed the analysis of fiber dyes by HPLC coupled to a mass spectrometer through electrospray ionization (ESI) source [28 – 31]. CE-MS was successfully applied to the discrimination of four types of textile fibers, namely acrylic, nylon, cotton and polyester [32]. The sensitivity of the mass spectrometer allowed fibers as small as 2 mm to be successfully analyzed. Recent advances in MS of textile fibers have focused on matrix-assisted laser desorption ionization (MALDI) time-of-flight (TOF) MS. With this technique, it was possible to discriminate between single fibers pre-dyed with acidic and basic dyes by gathering both positive and negative ion mass spectra [33]. Unfortunately, MS techniques destroy the fiber just like all the other methods that provide chemical information based on previous dye extraction.

Of the nondestructive techniques currently available for comparing dyes in textile fibers diffuse reflectance infrared Fourier transform spectroscopy (DRIFTS) and Raman spectroscopy have shown some promise. When coupled to chemometric methods for spectral interpretation such as principal component analysis (PCA) and soft independent modeling of class analogies (SIMCA), DRIFTS was able to discriminate both dye color and reactive dye state on cotton [34-36]. Raman microprobe spectroscopy was able to characterize dyes in both natural and synthetic fibers via a combination of Fourier transform-Raman spectra and PCA analysis [37-39]. Due to the inherently weak nature of the Raman signal, the identification of minor fiber dyes via Raman spectroscopy has not been possible. The inability to detect small concentrations of dyes that could add valuable information to the signature of fibers certainly reduces the discrimination power of the technique. The weak nature of the Raman signal also poses serious limitations in the analysis of lightly dyed fibers [40-44].

### **I.3. Statement of hypothesis or rationale for the research:**

We tackle a different aspect of fiber analysis as we focus on the total fluorescence emission of fibers. In addition to the contribution of the textile dye (or dyes) to the fluorescence spectrum of the fiber, we investigate the fluorescence of intrinsic fiber impurities – i.e. impurities imbedded into the fibers during fabrication of garments – and contaminants as a reproducible source of fiber comparison, as well as the methodology for discriminating fibers using fluorescence. To the extent of our literature search, no efforts have been made to investigate the full potential of fluorescence spectroscopy for forensic fiber examination. Previous articles on fluorescence microscopy of fibers report measurements made with excitation and emission band-pass filters which provide no detailed information on the fluorescence features of fibers [45-52]. The same is true for the fluorescence characteristics of dyes. The lack of information in the open literature regarding fluorescence of fibers prompted us to undertake a systematic study in our lab to better understand the fluorescence of textile fibers. Our experimental approach was then designed to answering the following questions:

- Should we concentrate on the fluorescence of textile dyes, the fluorescence of intrinsic impurities or the total fluorescence of the fiber?
- Are intrinsic impurities reproducible sources of fluorescence?
- How do we deal with fluorescence from environmental contaminants?
- What is the best fluorescence data format for fiber discrimination?
- What instrumental approach one should use for fiber discrimination on the bases of their fluorescence characteristics?

## **II. Methods**

### **II.1. Absorbance and Fluorescence Investigations Comparing Textile Dyes and Fiber Extracts**

The investigated fibers were selected to cover a wide range of cloth materials (acetate, polyester, cotton and nylon) and reagent dyes commonly manufactured in the textile industry. Table II.1 summaries the fourteen types of fibers investigated in this study, which were purchased in the form of fiber cloths of different shapes and sizes. Appendix A shows the molecular structures of their respective dyes, which fit into one of the following four categories: direct, disperse, basic and acid dyes. Direct dyes are those that have high affinity for cellulose materials such as cotton, rayon, etc. Disperse dyes are slightly soluble in water and typically used for synthetic fibers made of nylon, polyester, etc. Acid dyes are anionic dyes often applied from an acid dye-bath and basic dyes are cationic dyes characterized by their affinity for acrylic fiber and occasionally silk, wool or cotton. The main goals of this section were the following: (a) to select an appropriate extracting solvent for the RTF spectroscopy of each type of fiber; (b) to select a general extracting solvent for room-temperature fluorescence (RTF) spectroscopy of all studied fibers; (c) to find out the minimum fiber length that one needs to perform RTF spectroscopy of fiber extracts; (d) to investigate the reproducibility of spectral profiles recorded from fibers extracts belonging to the same piece of cloth; and (e) to investigate the reproducibility of fluorescence spectral profiles recorded from fluorescence extracts of the same types of fibers belonging to different pieces of the same type of cloth but from the same commercial batch.

Table II.1: Type of Fibers and Respective Dyes

Type of Fiber	Respective Textile Dye	Cloth Size
Acetate 154	Disperse Red 1	1meter x 1meter
Polyester 777	Disperse Red 4	1meter x 1meter
Polyester 777	Disperse Red 13	30cm x 30cm
Polyester 777	Disperse Blue 56	10cm x 10cm
Poly-acrylic 864	Basic Green 4	1meter x 1meter
Polyester 777	Basic Red 9	30cm x 30cm
Polyester 777	Basic Violet 14	30cm x 30cm
Cotton 400	Direct Blue 1	11cm x 15cm (100 pieces)
Cotton 460	Direct Blue 71	10cm x 10cm
Cotton 400	Direct Blue 90	11cm x 15 cm (100 pieces)
Nylon 361	Acid Red 151	11cm x 15cm (100 pieces)
Nylon 361	Acid Yellow 17	30cm x 30cm
Nylon 361	Acid Yellow 23	30cm x 30cm
Nylon 361	Acid Green 27	30cm x 30cm

### II.1.1. Chemicals and Supplies

Fabric and dyed cloths were purchased from Testfabrics Inc.; West Pittston, PA. All fiber cloths were received in sealed packages. All cloths were kept as received in the dark to avoid environmental exposure. All Sigma-Aldrich dyes were purchased at reagent grade purity (see Table II.2). No additional information was provided by Sigma-Aldrich on the complete chemical composition of the dye reagents.

Table II.2: Purity of Dye Standards

Dye	Dye Content (%) <sup>a</sup>
Disperse Red 1	95
Disperse Red 4	NA <sup>b</sup>
Disperse Red 13	95
Disperse Blue 56	NA <sup>b</sup>
Basic Green 4	80
Basic Red 9	85
Basic Violet 14	NA <sup>b</sup>
Direct Blue 1	NA <sup>b</sup>
Direct Blue 71	50
Direct Blue 90	NA <sup>b</sup>
Acid Red 151	40
Acid Yellow 17	60
Acid Yellow 23	90
Acid Green 27	65

<sup>a</sup> (%) = mass/mass x 100; <sup>b</sup> NA = not available.

All solvents used in our studies were HPLC grade and were purchased from Fisher Scientific. Nanopure water was used throughout and obtained from a Barnstead Nanopure Infinity water purifier. Glass culture tubes were purchased from Fisher Scientific.

### II.1.2. Solvent Extraction of Textile Fibers

Fibers were individually pulled from cloths using tweezers. Each fiber was cut into a strand of appropriate length (4cm, 2cm or 5mm) using scissors or razor blades. Tweezers, scissors and razor blades were previously cleaned with methanol and visually examined under ultraviolet light (254nm) to prevent the presence of fluorescence contamination. Each 4cm or 2cm strand was cut into pieces of approximately 5mm in length. 5mm strands were used as such. Fibers were solvent extracted following the procedure depicted in Figure II.1, which is recommended by the Federal Bureau of Investigations (FBI) [53]. All pieces from one fiber were placed in a 6x50mm glass culture tube. 200 $\mu$ L of extracting solvent were added to each tube. The tubes were sealed by melting with a propane torch. Sealed tubes were placed in an oven at 100° C for one hour. Tubes were removed from the oven, scored and broken open. The solvent was removed with a micro-pipette and placed in a plastic vial for storage.

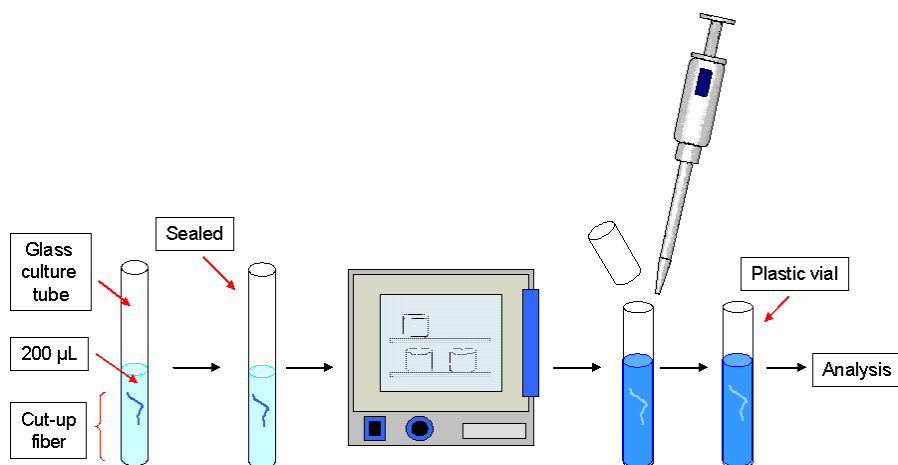


*Figure II.1: Solvent extraction procedure for textile fibers*

### II.1.3. Ultraviolet and Visible Absorption Spectroscopy

Absorbance measurements were made with a single-beam spectrophotometer (model Cary 50, Varian) equipped with a 75 W pulsed xenon lamp, 20 nm fixed band-pass, and 24,000 nm $\cdot$ min<sup>-1</sup> maximum scan rate. Absorption measurements were made with micro-quartz cuvettes (1cm path length x 2mm width) that held a maximum volume of 700 $\mu$ L.

### II.1.4. Room-Temperature Fluorescence (RTF) Spectroscopy

Excitation and fluorescence spectra were recorded using a commercial spectrofluorometer (FluoroMax-P from Horiba Jobin-Yvon) equipped with a continuous 100 W pulsed xenon lamp with broadband illumination from 200 to 2000 nm. Excitation and fluorescence spectra were recorded with two spectrometers holding the same reciprocal linear dispersion (4.2 nm $\cdot$ mm<sup>-1</sup>) and accuracy ( $\pm$ 0.5 nm with 0.3 nm resolution). Both diffraction gratings had the same number of grooves per unit length (1200 grooves $\cdot$ mm<sup>-1</sup>) and were blazed at 330nm (excitation) and 500nm (emission). A photomultiplier tube (Hamamatsu, model R928) with spectral response from 185 to 650 nm was used for fluorescence detection operating at room temperature in the photon-counting mode. Commercial software (DataMax) was used to computer-control the instrument. Measurements were made by pouring un-degassed liquid solutions into micro-quartz cuvettes (1cm path length x 2mm width) that held a maximum volume of 400 $\mu$ L. Fluorescence was collected at 90° from excitation using appropriate cutoff filters to reject straight-light and second order emission.

## **II.2. Comparison of Fiber Extracts with Dye Standards**

A head-to-head comparison of the fluorescence characteristics of dye reagents with fiber extracts should take into consideration the possible variations that often exist in the chemical composition of dye reagents from different commercial sources and/or variations that may also exist within dye reagent batches from the same source. Bearing this possibility in mind, we made several attempts to acquire the dye reagents that were actually used to pre-dye the studied fibers. If fluorescence impurities were incorporated into the fiber during the fabrication of the cloth, subtraction of the spectral profile of the dye from that of the extract would provide a spectral signature of the impurities and – as such - an additional level of fiber discrimination for forensic comparisons. Unfortunately, Testfabrics did not provide us with matching reagent dyes for the studied fibers.

The unsuccessful outcome of our attempts led us to an investigation of the absorption and fluorescence properties of Sigma-Aldrich dye standards, a popular source of reagent dyes for the textile industry. Bearing these limitations in mind, the main goal of our studies then became to estimate the contribution of dyes and impurities to the overall fluorescence of their respective fiber extracts. Keeping in mind that we are dealing with un-exposed fibers to environmental contamination, possible spectral differences among dye and fiber extracts could originate from the following sources: (a) existing impurities in the reagent dye used to pre-dye the fiber and/or (b) from physical contact with other chemical(s) during their fabrication process. The ideal approach should only provide a spectral matching for the dye reagent that was used to pre-dye the investigated fiber. If fluorescence impurities are incorporated into the fiber during the fabrication of the cloth, the spectral profile of the Aldrich-Sigma dye should provide a different spectral signature to the one recorded from the “respective” Testfabrics fiber extract.

### *II.2.1. Absorbance of Dye Standards and Fiber Extracts*

See section II.1.3 for experimental procedure.

### *II.2.2. RTF Characteristics of Sigma-Aldrich Dye Standards*

See section II.1.4 for experimental procedure.

## **II.3. High Performance Liquid Chromatography (HPLC) of Fiber Extracts**

The broad nature of room-temperature excitation and fluorescence spectra and the possible spectral overlapping that might result from the presence of several fluorescence concomitants makes difficult to track down the individual components of fluorescence fiber extracts. The separation of fiber extracts via HPLC should provide valuable information on the contribution of individual components to the total fluorescence of fibers. The HPLC analysis of Aldrich-Sigma dyes should make possible to observe the fluorescence characteristics of pure dyes without the contribution of impurities. Separation of extracts via HPLC should also give information on the number of individual components that contribute to the total fluorescence of each extract and their reproducibility for forensic fiber comparison. Further analysis of HPLC fractions via RTF spectroscopy should possible the comparison of the spectral characteristics of each concomitant. This information should be valuable to assess the potential advantage of lowering the temperature-temperature to minimize spectral overlapping for better fiber discrimination.

Based on the spectral characteristics of fibers extracts we selected three types of fibers as representative cases of the fourteen types of studied fibers. Extracts from fibers pre-dyed with Dispersed Red 4 showed strong fluorescence in both the ultraviolet and visible spectral regions. Basic Green 4 fiber extracts showed fluorescence solely in the ultraviolet region with spectral profiles virtually identical to those observed from their respective Sigma-Aldrich dye. Extracts

from fibers pre-dyed with Acid Red 151 presented no fluorescence in the visible spectral region and multiple fluorescence peaks in the ultraviolet region. Their spectral profiles were different from those observed from their respective Sigma-Aldrich dye.

Solvent extraction of textile fibers was conducted as previously described in section II.1.2. HPLC analyses of dye standards and fiber extracts were carried out using a computer-controlled HPLC system from Hitachi (San Jose, CA, USA) equipped with the following basic components: a gradient pump (L-7100), a UV (L-7400 UV) and a fluorescence (L-7485) detector, an online degasser (L-761) and a control interface (D-7000). All HPLC operation was computer controlled with Hitachi software. Separation was carried out on an Agilent (Santa Clara, CA, USA) Zorbax EclipseXDB-C18 column with the following characteristics: 15 cm length, 2.1 mm diameter, and 5  $\mu\text{m}$  average particle diameters. All extracts and standards were injected at a volume of 20  $\mu\text{L}$  using a fixed-volume injection loop. HPLC fractions were collected in 2 mL sample vials with the aid of a Gilson fraction collector (model FC 20313). The same procedure and instrumentation described in sections II.1.3 and II.1.4 were used to record absorption and RTF spectra from HPLC fractions, respectively.

#### II.4. Room Temperature Fluorescence –Excitation Emission Matrix Spectroscopy

Recording two dimensional (2D) fluorescence spectra, i.e. intensity versus wavelength, from a mixture with numerous fluorescence components only provides partial information on the total fluorescence of the sample. The resulting spectral profile strongly correlates to the measuring excitation wavelength and its relative position to the excitation maxima of the individual fluorescence components of the mixture. The relative contributions to the total fluorescence spectrum of the sample also depend on the fluorescence quantum yields of the individual components and possible quenching due to synergistic effects. Spectral overlap among broad room-temperature excitation and fluorescence bands makes it difficult to identify single components upon selective excitation of their maximum excitation wavelengths. These limitations make an EEM a useful data format to characterize the total fluorescence of a multi-fluorophor mixture. Although EEM have been extensively applied to environmental [54] and drug analysis [55] our literature search revealed no applications to the forensic analysis of textile fibers or their extracts. In this section, we investigate their potential for the forensic examination of fibers.

##### II.4.1. *Theoretical background on EEM*

Figure II.2 illustrates the process of recording room-temperature fluorescence EEM (RTF-EEM). The instrumentation to record steady-state EEM consists of a relatively simple commercial spectrofluorimeter equipped with a continuous wave xenon excitation source, excitation and emission monochromators and a photomultiplier tube for fluorescence detection. The resulting I by J data matrix (EEM) is compiled from an array of two-dimensional fluorescence spectra while the excitation wavelength is increased incrementally between each scan [56, 57]. Each I row in the EEM corresponds to the emission spectrum at the *ith* excitation wavelength. Each J column in the EEM corresponds to the excitation spectrum at the *jth* emission wavelength. For a single emitting species in a sample, the elements of the EEM are given by:

$$\mathbf{M}_{ij} = 2.303\Phi_F \mathbf{I}_0(\lambda_i) \boldsymbol{\varepsilon}(\lambda_i) b c \boldsymbol{\gamma}(\lambda_j) \boldsymbol{\kappa}(\lambda_j) \quad (1)$$

where  $\mathbf{I}_0(\lambda_i)$  is the intensity of the incident light exciting the sample in units of quanta/s;  $2.303\boldsymbol{\varepsilon}(\lambda_i)bc$  represents the optical density of the sample, which results from the product of the analyte's molar absorptivity  $\boldsymbol{\varepsilon}(\lambda_i)$ , the optical path-length  $b$ , and the concentration of the emitting species  $c$ ;  $\Phi_F$  is the quantum yield of fluorescence;  $\boldsymbol{\gamma}(\lambda_j)$  is the fraction of fluorescence photons emitted at wavelength  $\lambda_j$ ; and  $\boldsymbol{\kappa}(\lambda_j)$  is an instrumental factor that represents the wavelength

dependence of the spectrofluorimeter's sensitivity [56]. The condensed version of equation 1 may be expressed as:

$$\mathbf{M}_{ij} = \alpha x_i y_j \quad (2)$$

where  $\alpha = 2.303 \Phi_f \epsilon c$  is a wavelength independent factor containing all of the concentration dependence,  $x_i = I_0(\lambda_i) \epsilon(\lambda_i)$  and  $y_j = \gamma(\lambda_j) \kappa(\lambda_j)$ . The observed relative fluorescence excitation spectrum may be represented by  $\{x_i\}$ , the wavelength sequenced set, and thought of as a column vector,  $x$  in  $\lambda_i$  space. The wavelength sequenced set,  $\{y_j\}$ , may be thought of as a row vector  $y$  in  $\lambda_j$  space, representing the observed fluorescence emission spectrum. Therefore, for a single component,  $\mathbf{M}$  is simply represented as:

$$\mathbf{M} = \alpha xy \quad (3)$$

Where  $\mathbf{M}$  is the product of the vectors  $x$  and  $y$  multiplied by the compound specific parameter  $\alpha$ . When data is taken from a sample containing multiple,  $r$ , different species,  $\mathbf{M}$  is given by the following expression:

$$\mathbf{M} = \sum_{k=1}^r \alpha_k x^k y^k \quad (4)$$

where  $k$  is used to detail the species. For a recorded  $\mathbf{M}$ , the spectral characterization of single components then relies on finding  $r$ ,  $\alpha_k$ ,  $x^k$ , and  $y^k$ .

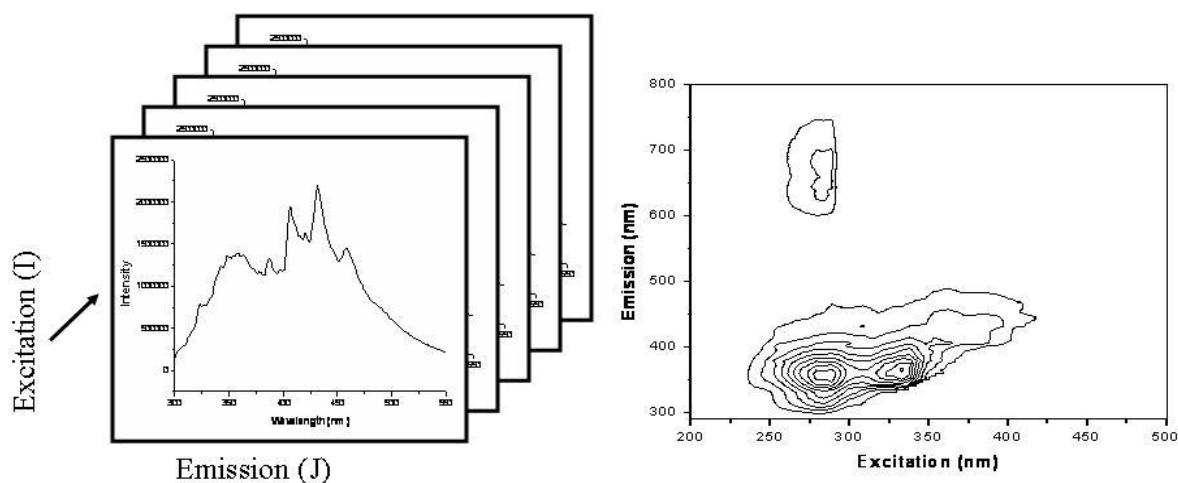


Figure II.2: Layering of fluorescence spectra recorded at different excitation wavelength to compile and EEM data format.

#### II.4.2. Procedure for recording RTF-EEM

Two-dimensional (2D) excitation and 2D-fluorescence spectra were recorded via the classic method of setting one monochromator to the maximum wavelength while scanning the other. RTF-EEM from fiber extracts were collected at 5nm excitation steps from longer to shorter wavelengths to reduce the risk of potential photo-degradation due to extensive sample excitation. The same procedures were used for blank samples to account for fluorescence background subtraction.

## **II.5. Comparison of RTF-EEM Recorded from Fiber Extracts of Visually Indistinguishable Fibers**

The comparison of RTF-EEM recorded from the extracts of visually indistinguishable fibers would be best accomplished with the aid of Chemometric analysis. Among the algorithms we investigated for this purpose, multivariate curve resolution alternating least squares (MCR-ALS) provided the best results. This algorithm has been extensively discussed in the literature [58-61]. In general terms, MCR-ALS predicts the number of fluorescence components that contribute to the data set of excitation and emission spectra and the emission and excitation profiles corresponding to each component. Its application was then extended to fibers from Testfabrics, i.e. our “control” set of fibers, with the aid of commercial and public domain software. RTF-EEM data formats were recorded via procedure described in section II.4.2.

RTF-EEM data formats were recorded from extracts of nylon fibers pre-dyed with Acid Red 151, Acid Yellow 17 and Acid Yellow 23. Acid Red 151 fibers were collected from two different pieces of cloths, ten fibers per cloth. Ten Acid Yellow 17 fibers were collected from one piece of cloth. The same was true for the Acid Yellow 23 fibers. Each fiber was extracted with ethanol and an EEM was recorded from each extract. The comparison of Acid Red 151 extracts allowed us to test the ability of MCR-ALS to differentiate between two visually indistinguishable fibers pre-dyed with the same dye in the same textile industry but collected from different cloths. The statistical comparison of fiber extracts Acid Yellow 17 and Acid Yellow 23 allowed us to test the ability of MCR-ALS to differentiate between two visually indistinguishable fibers pre-dyed with two different dyes.

## **II.6. Effects of Environmental Contaminants on the Fluorescence of Textile Fibers**

From the time of manufacture to the time they are found at the crime scene, textile fibers will most likely be exposed to a wide variety of environmental factors and contaminants. These include, but are not limited to cigarette smoke, food stains, weathering and laundering. Their exposure to these uncontrollable variables might play a role on fiber discrimination via RTF spectroscopy. We examined three possible environmental factors that could alter the fluorescence characteristics of textile fibers, namely cigarette smoke, detergents and fabric softeners. Cigarette smoke is one of the possible contaminants that clothing may be exposed to in a real world environment. Contained within cigarette smoke are a number of strongly fluorescing compounds known as polycyclic aromatic hydrocarbons (PAH). Our investigations exposed fibers to cigarette smoke and examined the resulting extracts to detect the possible presence of PAH. Clothing in a real world environment will be exposed to laundering at some point. It is not unlikely that fibers discovered at a crime scene may have been exposed to multiple launderings previous to becoming evidence. Fibers from suspect clothing may have been laundered after a crime was committed. It becomes then essential to understand the effect that multiple washings might have on the fluorescence characteristics of fibers over time. Repetitive laundering of fibers might be able to remove fluorescence concomitants originally present in the fibers. The repetitive exposure to detergents and fabric softeners might add additional fluorescence spectral components to the total fluorescence of the fiber. We investigated the effect of repetitive washing on the intrinsic fluorescence of fibers, the fluorescence characteristics of detergents and fabric softeners and their effects upon repetitive washing of textile fibers.

### ***II.6.1. Exposure of Textile Fibers to Cigarette Smoke***

Textile fibers were exposed to cigarette smoke as detailed in figure II.3. Two holes were cut into a 591mL plastic bottle. The first hole was made on the top of the cap lid and the second at the bottom of the bottle. The bottom hole was made to partially introduce a lit cigarette into the

bottle. A metal screw with a textile fiber wound around it was introduced into the bottle via the top hole of the screw cap lid. Prior to introducing the cigarette into the bottle, the cigarette was lit with the aid of a rubber pipet bulb. Once the lit cigarette was partially placed into the bottle, the bulb was slowly depressed to simulate “smoking” of the cigarette. Following suggestions from several smokers, the simulation of cigarette smoking was carried out over an average time of seven minutes to expose textile fibers to cigarette smoke. The cigarette was removed from the bottle after it burned down to the filter. The textile fiber was then removed from the bottle with the aid of the metal screw. Clean tweezers were used to place the exposed fiber inside a plastic micro-centrifuge tube. All steps involving cigarette smoking simulations were performed under an exhaust hood. Solvent extraction of PAH from exposed fibers was carried out with n-octane. Blanks of un-exposed fibers were submitted to the same solvent extraction procedure to investigate the possible octane co-extraction of inherent fluorescence components.

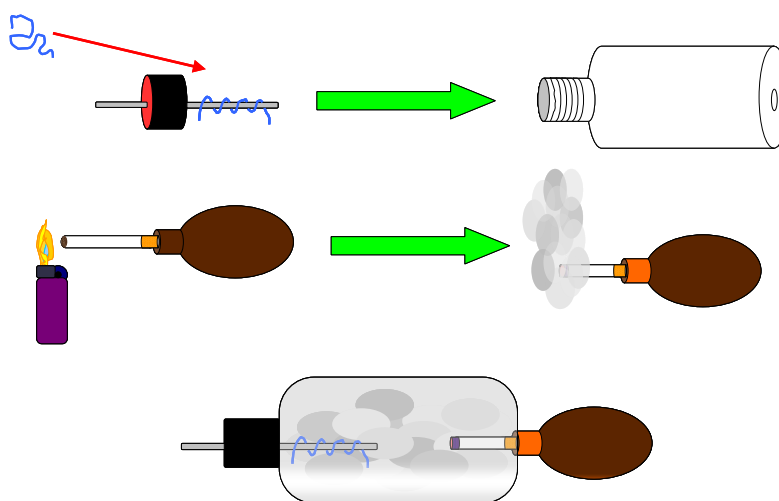


*Figure II.3: Diagram illustrating the procedure of exposing fibers to cigarette smoke.*

### II.6.2. Washing of Textile Fibers

Five square samples (5 cm x 5 cm) of cloth were cut from a 1 m x 1 m piece of cloth pre-dyed with Disperse Red 4. Each sample cloth was placed into a separate plastic bag and set aside in the dark for storage. Four of the five sample cloths were individually washed in the presence of full load of cloths. The remaining cloth sample was kept unwashed for reference purposes. Each washing was carried out using the normal wash cycle setting of the same washing machine located at the Laundromat of a local apartment complex. Each piece of cloth was subsequently washed five times. The only difference among washings of the same sample was the load of cloths in the washing machine, which had previous exposure to unknown potential contaminants. All washing were done in cold water with ALL detergent. After each washing, the sample was dried in the same commercial drier with the entire load of cloths. After each drying, one fiber of 1 cm length was removed from the sample cloth and set aside for further experiments in a plastic micro-centrifuge tube. All collected fibers were storage in the dark at room temperature. Fiber extractions were carried out as described in section III.1.2.

### II.6.3. Instrumental Analysis

Absorption and RTF spectroscopy measurements were made via experimental procedures described previously. PAH separation was carried out on an Agilent (Santa Clara, CA, USA) Zorbax EclipseXDB-C18 column with the following characteristics: 15 cm length, 2.1 mm diameter, and 5  $\mu\text{m}$  average particle diameters. All extracts and standards were injected at a

volume of 20  $\mu\text{L}$  using a fixed-volume injection loop. HPLC fractions were collected in 2 mL sample vials with the aid of a Gilson fraction collector (model FC 20313). The separation of PAH was accomplished using a mixture of methanol/water as the mobile phase. Column conditions include a 1.5 mL/min flow rate, isocratic elution with 40/60 water/methanol for 5 min, and then linear gradient to 99% methanol over 20 min. The total separation time of the 16 EPA-PAH was approximately 40 min.

## II.7. Instrumentation for Non-destructive Analysis of Textile Fibers

The selectivity of room-temperature fluorescence techniques for the determination of targeted compounds in complex matrixes is the broad nature of excitation and emission spectra. In amorphous matrixes, characterized by their lack of long-range order, the local conditions (microenvironments) that influence the transition energies of the solute molecules (predominantly through electron-electron interactions) differ from one solute molecule to another. The observed band broadening then is the result of the superposition of many transition lines having slightly different energies. Aware of this fact, we originally proposed to investigate Fluorescence Line Narrowing (FLN) spectroscopy as a non-destructive tool for the forensic analysis of fibers. FLN spectroscopy reduces spectral broadening by freezing the sample to 4.2K and exciting - with the aid of a narrow band tunable laser - a sub-population of solute molecules within the same microenvironment. Our proposition built upon significant improvements we had made to instrumentation for high-resolution spectroscopy at 77K and 4.2K. Its development and application to the environmental analysis of carcinogenic compounds had been funded by the National Science Foundation (CHE-0138093; period: August 2002 – July 2005).

Figure II.4 shows a schematic diagram of the fiber optic probe (FOP) we had developed to eliminate the complications of traditional low-temperature methodology [62, 63]. The FOP incorporates one delivery and six silica-clad silica collection fibers. At the sample end the fibers are arranged in a conventional six-around-one configuration with the delivery fiber in the center. At the collection end the excitation and collection fibers are separated and vertically aligned with the spectrograph entrance slit.

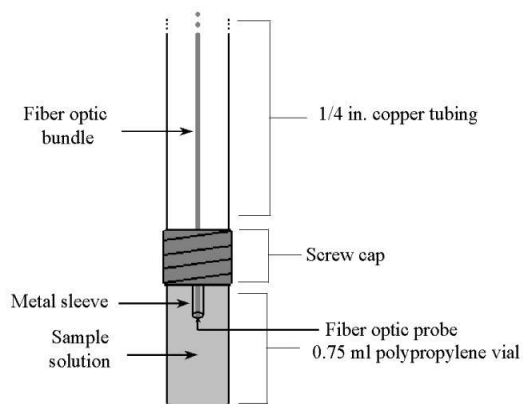
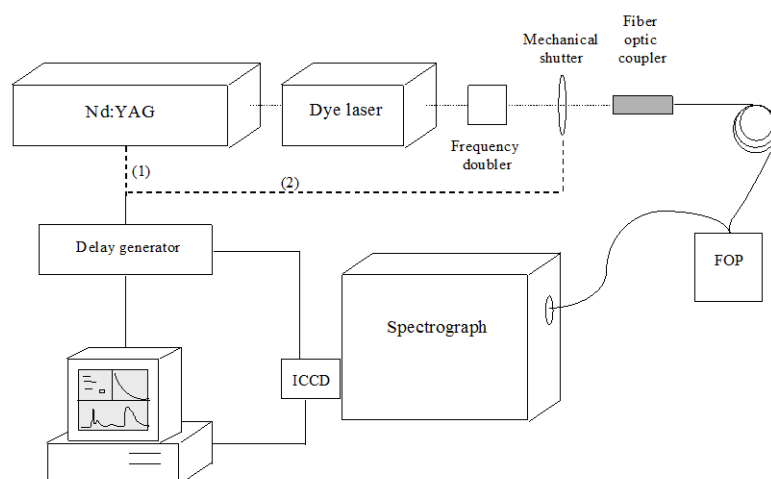


Figure II.4: Fiber optic probe for low-temperature measurements.

Figure II.5 shows a schematic diagram of the instrumental system we had developed for high-resolution spectroscopy [62-64]. As the excitation source, we use a compact frequency doubled pulsed tunable dye laser whose bandwidth ( $< 0.03\text{nm}$ ) is well matched for selective excitation of narrow excitation spectra. The intensified charge-coupled device (ICCD) is coupled to a spectrograph to rapidly

collect a series of emission spectra at different delay times between the laser firing and the opening of the gate on the ICCD. The series of spectra can be assembled into a wavelength-time matrix (WTM), analogous to an excitation-emission matrix (EEM). Because of the spectrograph and the ICCD, EEM are collected in relatively short analysis time. Tuning the excitation wavelength also allows the rapid collection of time-resolved excitation-emission matrices (TREEM). The tuning of the dye laser is computer-controlled, which facilitates the collection of EEM and TREEM. For fluorescence data collection, the electronic shutter is kept open. For phosphorescence data collection, the electronic shutter sets the zero time. Once triggered by the shutter, the pulse delay generator communicates with the ICCD to start collecting multidimensional data. If desired, phosphorescence acquisition can be started after a given delay time to eliminate any detection of fluorescence. For excitation in the ultraviolet region, the tunable dye laser is operated through a KDP frequency-doubling crystal; for fluorescence measurements the delay generator is externally triggered by the laser source (connection 1); for phosphorescence measurements, the delay generator is triggered by the electronic shutter (connection 2).



*Figure II.5: Instrumental system for low-temperature multidimensional fluorescence and phosphorescence analysis.*

The experimental procedure for forensic analysis of textile fibers is rather simple. After introducing the fiber into the sample tube, the tip of the FOP is positioned on top of the fiber and the sample tube is lowered into a container filled with liquid cryogen. The cell is allowed to cool for 90 s prior to fluorescence measurement to ensure complete fiber freezing. With this approach, we were able to record highly-resolved spectra and well-behaved single exponential lifetimes directly from textile fibers in table II.1. Because the data is directly collected from the fiber, solvent extraction is avoided and the physical integrity of the fiber is preserved. We examined several fibers before and after numerous freezing cycles and we noticed no visible change under the microscope. Similarly, their fluorescence properties remained the same. Additional supporting evidence was obtained via attenuated total reflectance (ATR) spectroscopy. The main disadvantage of the instrumental system in Figure III.5 is its relatively narrow excitation range. To achieve the full potential of FLN spectroscopy, fluorescence excitation of fibers should occur

within both the ultraviolet and the visible spectral range. Our tunable dye laser only provides sufficient output power for fiber excitation in the ultraviolet spectral region. Unfortunately, the cost of purchasing a laser excitation source with the appropriate characteristics for fiber analysis did not fit within the approved budget of this project.

While presenting our results in forensic science meetings and sharing our thoughts with forensic scientists, we noticed skepticism among practitioners on the embracement of FLN spectroscopy as a tool for fiber analysis in forensic science labs. Two arguable reasons contributed to the community's perception, namely the high cost of instrumentation and the pre-conceived idea of sophisticated training for its operation. A more appealing approach for the forensic science community appears to be RTF- microscopy. With this prospective in mind, we adapted an instrumental set-up from two commercial units, namely a spectrofluorimeter (FluoroMax-P from Horiba Jobin-Yvon) and an epi- fluorescence microscope (Olympus BX-51). The two units are connected via commercially available fiber optic bundles. The spectrofluorimeter was described in section II.1.4. Its sample compartment was equipped with a fiber optic platform (Horiba Jobin-Yvon) that optimizes collection efficiency via two concave mirrors. Figure III.6 shows the configuration of the microscope. Wavelength ranges can be selected with dichromatic mirrors, filters or beam splitters. The best approach to collect RTF data in the ultraviolet and visible spectral regions is to use two 50/50 beam splitters, one for the ultraviolet and the other for the visible wavelength range. A turret placed immediately above the microscope objective and aligned with both the excitation and the emission optical paths facilitates the use of either one of the two beam splitters. The turret can accommodate up to six optical components. A pinhole plate is located between the 50/50 beam splitter and the mirror that directs fluorescence emission into to the CCD camera of the microscope or the emission fiber bundle of the spectrofluorimeter. The role of the pinhole is to isolate the illuminated area of fiber while rejecting light scattered from the fiber sample.

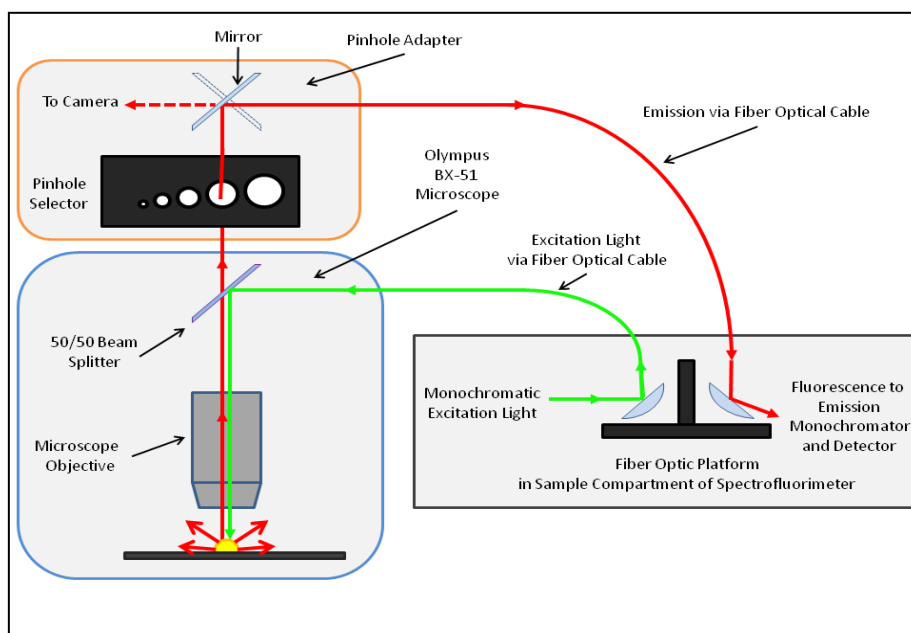


Figure II.6: Schematic diagram of epi-fluorescence microscope for RTF data collection from textile fibers.

Instrument alignment and optimization was carried out using “standard samples” which consisted of sealed capillary tubes (250 micro-meters internal diameter; 3 cm long) filled with micro-litter volumes of methanol solutions of laser dyes with maximum excitation and

fluorescence wavelengths ( $\lambda_{ex}/\lambda_{em}$ ) in the ultraviolet (BPBD-365;  $\lambda_{ex}/\lambda_{em} = 327/373\text{nm}$ ) and visible (Rodhamine 6G;  $\lambda_{ex}/\lambda_{em} = 527/561\text{nm}$ ) spectral regions. Once the relative positions of all optical components were optimized for best signal-to-background ratio, proper functioning of the instrumental set up was verified recording spectra at different spectrofluorimeter's slit-widths and microscope's pinhole diameters.

### II.8. Spectral Reproducibility within the Length of a Single Fiber

Fiber extracts do not provide information on the distribution of fluorescence impurities and/or dyes within the length of a fiber. If the distribution of fluorescence impurities and/or dyes within a fiber happens to be heterogeneous, the spectral profiles recorded directly from the fiber might show some dependence with the fiber area probed under the microscope. Because possible spectral variations within a single fiber might have detrimental implications in the forensic comparison of known and suspect fibers, we initiated an investigation of the reproducibility of spectral profiles within the lengths of single fibers. Three fibers, 4cm in length, were removed from four different regions of a piece of cloth (see figure II.7). Excitation and emission spectra were collected at three different areas of the fiber with the aid of the plate stage and fiber holder shown in figure II.8. These two metal pieces were made in house with the purpose of providing reproducible positioning of fibers under the microscope. Both were painted matte black to minimize the measurement of possible reflection and scatter of light. The 3-mm inner diameter holes located at the fiber holder facilitate the reproducible positioning of the microscope objective with respect to the fiber. As shown in figure II.9, the reproducible positioning of single fibers with respect to the microscope objective was made possible with the aid of two visible grooves on the back of the fiber holder. Grooves were 4cm apart from each other. Spectra were collected by placing the microscope objective at three different locations ( $\alpha$ ,  $\beta$  and  $\gamma$ ) within each 3-mm hole.

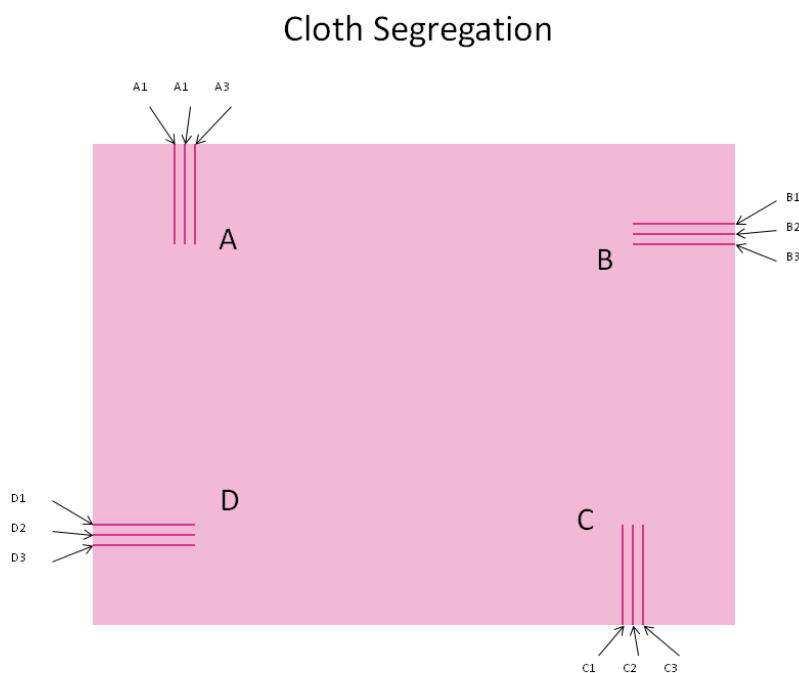


*Figure II.7: Cloth segregation for the analysis of single fibers. "Cloth regions" are denoted by capital letters A, B, C and D. Subscripts under capital letters refer to single fibers collected within the same cloth area.*

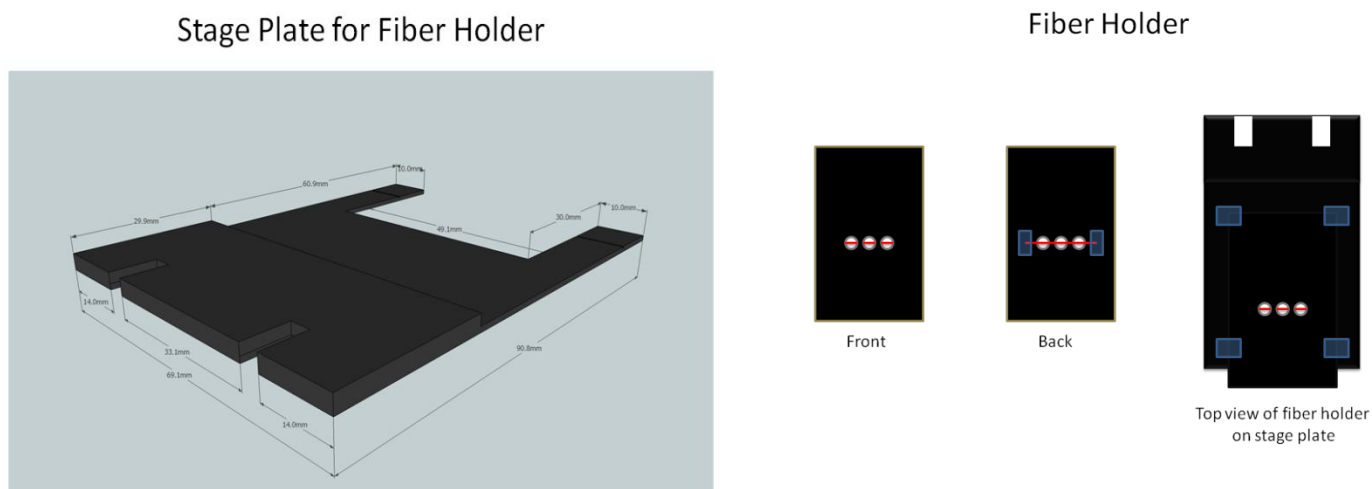


Figure II.8: Stage plate and fiber holder for reproducible positioning of single fibers under the microscope.

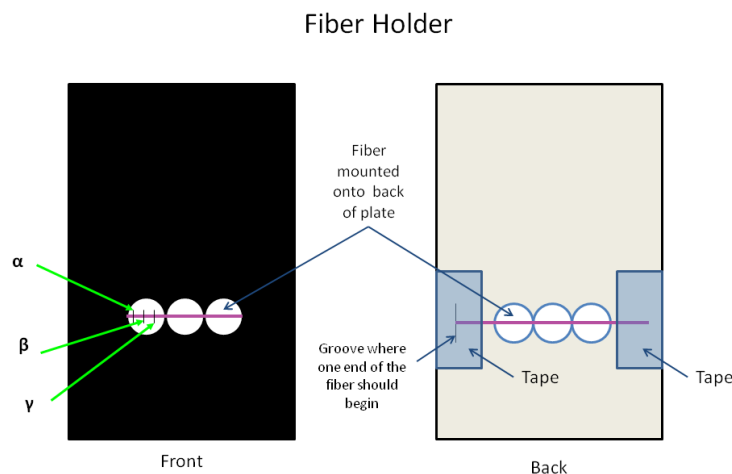


Figure II.9: Procedure for reproducible fiber positioning under the microscope objective.

## II.9. Optimization of Microscope Objectives

The relatively weak fluorescence we observed from some types of fibers in Table II.1 called our attention to the need for the search of a better set of microscope objectives. The collection efficiency (C.E.) of a microscope objective correlates its numerical aperture (N.A.) via the formula  $C.E. = \sin^2[\arcsin(N.A./n)/2]$ ; where  $n$  represents the refractive index of the surrounding medium, which is approximately 1 in our case. Table II.3 correlates typical N.A. of microscope objectives to their respective C. E. values. The N.A. of the 10xUV and 10xVIS objectives we used for measurements in sections II.7 and II.8 were 0.25 and 0.30, respectively. In comparison to other microscope objectives in Table III.3, the C. E. of these two objectives is relatively low. For measurements made under optimum pinhole diameter size and excitation/emission band-

pass, the N. A. of the microscope objective could possibly become the limiting factor for signal-to-background ratio optimization. Under this prospective, we then decided to investigate the effect of the N.A. of microscope objectives on the quality of spectra directly recorded from fibers.

*Table II.3: Correlation between numerical aperture (N.A.) and collection efficiency (C.E.) of microscope objectives<sup>1</sup>*

N. A.	1.0	0.9	0.8	0.7	0.6	0.5	0.4	0.3	0.2	0.1
C.E. (%)	50	28	20	14	10	6.7	4.2	2.3	1.0	0.3

<sup>1</sup>Shaole W. U., Dovichi N. J., *J. Chromatogr.* **1989**, 480, 141.

Table II.4 summarizes the commercial sources and pertinent characteristics of various microscope objectives evaluated in our lab. All Olympus objectives operated in the visible spectral range. The performance of each objective was evaluated recording spectra and measuring the signal-to-background ratio of fibers in Table II.1. Signal measurements were made at the maximum excitation and emission wavelengths of fibers placed on quartz (ultraviolet measurements) or glass (visible measurements) slides. The maximum wavelengths were obtained from two dimensional spectra recorded either in the ultraviolet or visible regions. Background signals were collected at the maximum wavelengths of fibers placing a quartz (ultraviolet measurements) or glass (visible measurements) slide under the microscope objective.

*Table II.4: Microscope Objectives Evaluated in Our Lab for the Non-Destructive Analysis of Fibers via Microscopy-RTF*

<i>Commercial Source</i>	<i>Model</i>	<i>Type</i>	<i>C. E.</i>
OFR	LMU-40x-UVB	Dry	6.7
Olympus	UPlanSApo 20X/0.75; $\infty$ /0.17/FN26.5	Dry	16.9
Olympus	UPlanSApo 20X/0.85 Oil; $\infty$ / - /FN26.5	FF Immersion Oil	9.1
Olympus	UPlanSApo 40X/0.90	Dry	28.2
Olympus	UPlanFln 40X/1.30	FF Immersion Oil	26.2

## **II.10. Fluorescence Microscopy of Visually Indistinguishable Fibers**

Table II.5 list the pairs of fibers we used to evaluate the discrimination power of room-temperature fluorescence microscopy. These test samples were pre-dyed by Testfabrics, Inc. using commercial dyes purchased by us and provided to them. This mechanism avoided proprietary issues and provided us with the possibility to evaluate fibers pre-dyed with dyes of known spectral characteristics. Measurements were carried out with the microscope and spectrofluorimeter described in section II.7 of this report. All measurements were done using 40X objectives. Prior to EEM collection, pinhole aperture diameters and excitation and emission band-passes were optimized for appropriate signal-to-background ratio.

*Table II.5: Pairs of Visually Indistinguishable Fibers*

	<i>Generic Dye Name</i>	<i>Fiber Type</i>
1	Acid Blue 25	Nylon
2	Acid Blue 41	Nylon
3	Basic Green 1	Acrylic
4	Basic Green 4	Acrylic
5	Direct Blue 1	Cotton
6	Direct Blue 53	Cotton
7	Acid Orange 10	Nylon
8	Acid Orange 7	Nylon
9	Disperse Blue 3	Acetate
10	Disperse Blue 14	Acetate
11	Disperse Red 1	Polyester
12	Disperse Red 19	Polyester

*Note: Pairs of visually indistinguishable fibers: 1 and 2, 3 and 4, 5 and 6, 7 and 8, 9 and 10, 11 and 12.*

### III. Results

#### III.1. Absorbance and Fluorescence Characteristics of Fiber Extracts

##### *III.1.1. Selecting the Best Solvent for Fiber Extraction*

Previous reports on fiber analysis via ultraviolet-visible absorption spectrometry, thin-layer chromatography and high-performance liquid chromatography (HPLC) often recommend one of the following solvents for extracting dyes from fibers: 1:1 methanol – water (v/v), ethanol, 1:1 acetonitrile-water (v/v) and 57% pyridine - 43% water (v/v) [53, 65-67]. Each type of fiber in Table II.1 was then extracted with the four types of solvents to select an appropriate solvent for RTF spectroscopy. All measurements were performed with fibers collected from the top left corner of sample cloths, i.e. a cloth area arbitrarily selected with the sole purpose of consistency.

Appendix B compiles the excitation and fluorescence spectra of the extracts from fibers in Table II.1 with the four types of solvent systems. All spectra represent an average of nine spectral runs recorded from three aliquots of three independent fiber extractions. The slit widths of the excitation and emission monochromators were adjusted to obtain a satisfactory compromise between signal intensity and spectral resolution. For comparison purposes, all spectra in Appendix B were recorded with the same excitation (4nm) and emission (2nm) band-pass. Under these conditions, most of the studied fibers showed strong fluorescence in the four types of extracting solvents. For the few cases where relatively weak fluorescence was observed, further adjustment of excitation and emission band-pass was unsuccessfully attempted as weak fluorescence signals – i.e. barely distinguishable from the blanks - were still observed under

10nm excitation and emission band-passes. Under these conditions, the signal intensities of the strongly fluorescent fibers fall beyond the upper linear limit ( $2 \times 10^6$  counts) of our instrument detection unit.

The visual comparison of fluorescence spectra in Appendix B reveals two main types of spectral profiles, i.e. emission spectra with only one and with more than one fluorescent peaks. Assuming the absence of spectral overlapping and synergistic effects among fluorescence components in the fiber extract, fluorescence spectra with a single fluorescence peak suggest the emission of one fluorescence component at the recorded excitation wavelength. Still under the same assumptions but disregarding the possibility of vibronic structural resolution at room temperature, the presence of multiple emission peaks can then be attributed to the emission of multiple fluorescence components at the recorded excitation wavelength. Under this prospective, spectral comparison within the same type of fiber reveals some cases with strong dependence on the chemical nature of the extracting solvent. The differences observed in Figures III.1 – III.5, which compare intensity-normalized spectra recorded from the same types of fibers but extracted with different solvents, could then be attributed to the chemical affinities of the extracting solvents for fluorescence components in the textile fibers.

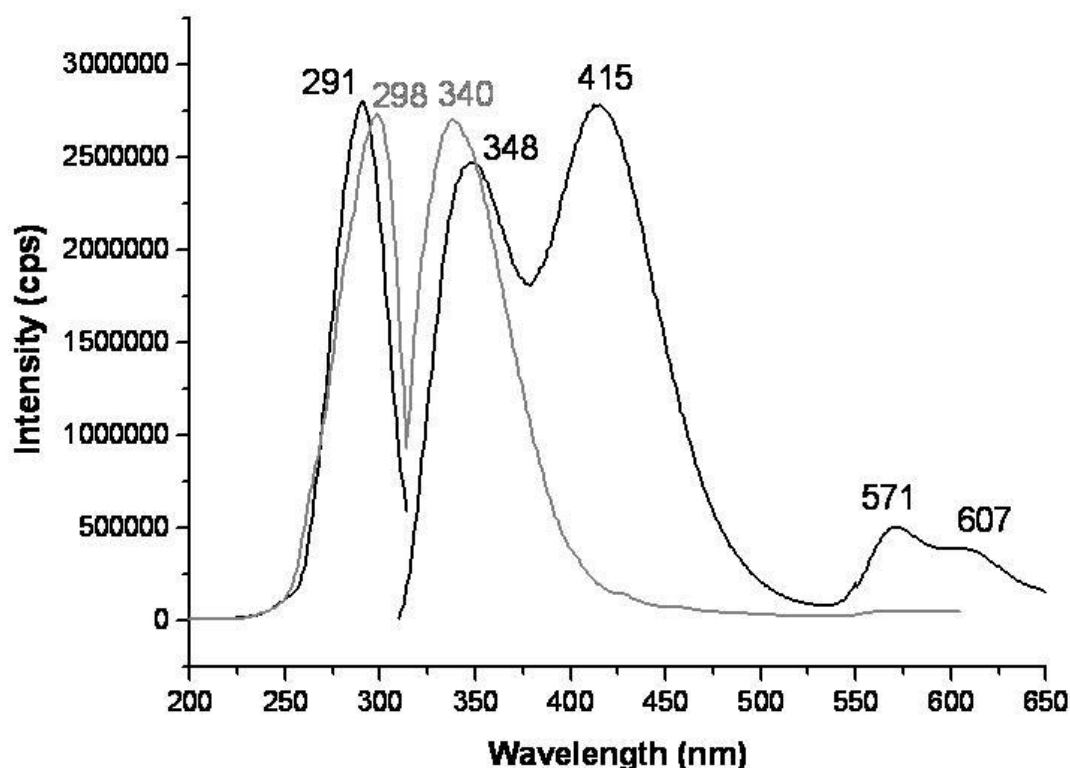


Figure III.1: Fluorescence spectra of extracts in two different solvents from fibers pre-dyed with Disperse Red 4. (—) Extract in 1:1 acetonitrile water (v:v) and (---) extract in ethanol. Maximum excitation wavelength used for each extract, 291nm and 298nm respectively. Excitation and emission slits set for 4nm and 2nm band-pass, respectively.

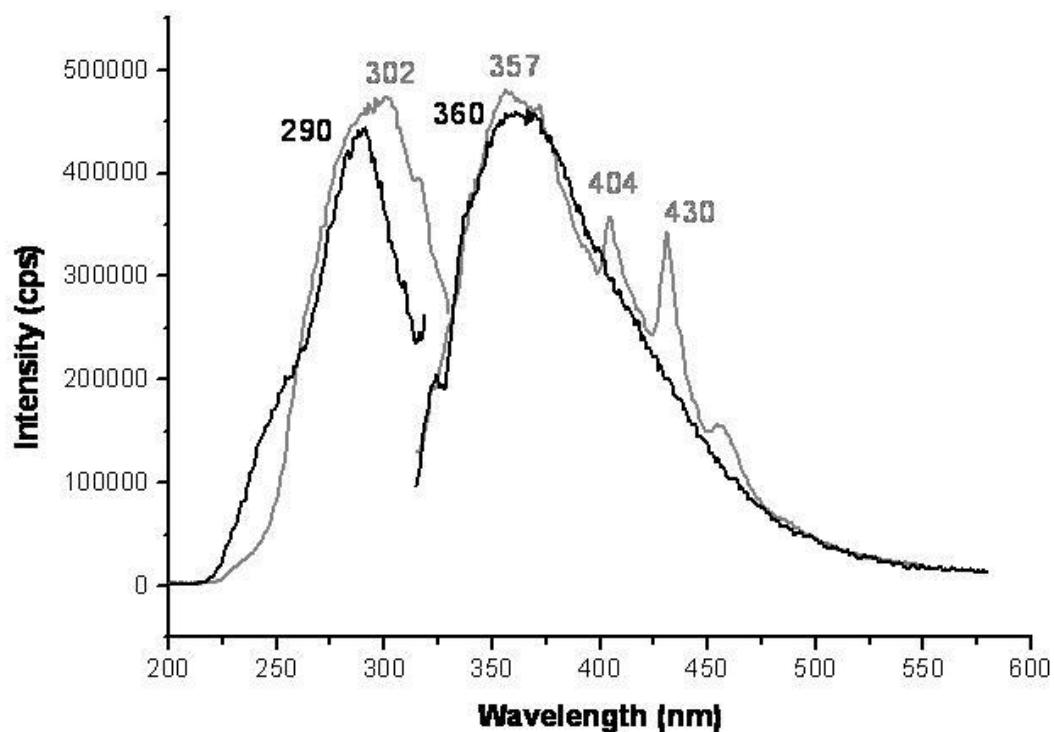


Figure III.2: Fluorescence spectra of extracts in two different solvents from fibers pre-dyed with Disperse Red 13. (—) Extract in 1:1 methanol/water (v:v) and (---) extract in ethanol. Maximum excitation wavelength used for each extract, 290nm and 302nm respectively. Excitation and emission slits set for 4nm and 2nm band-pass, respectively.

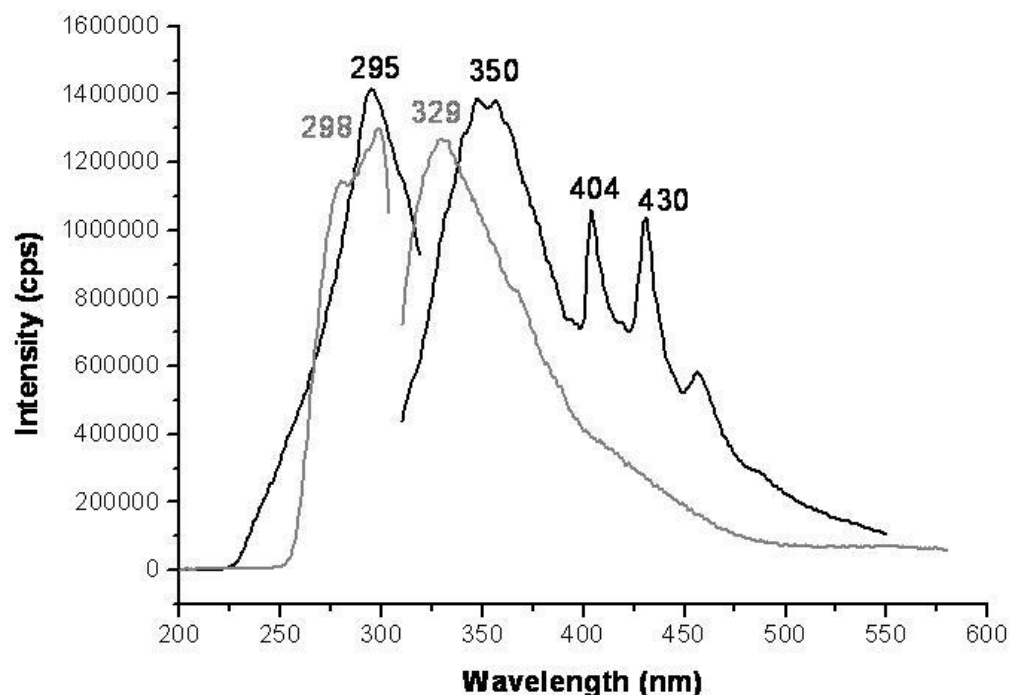


Figure III.3: Fluorescence spectra of extracts in two different solvents from fibers pre-dyed with Basic Red 9. (—) Extract in ethanol and (---) extract in 1:1 acetonitrile/water (v:v). Maximum excitation wavelength used for each extract, 295nm and 298nm respectively. Excitation and emission slits set for 4nm and 2nm band-pass, respectively.

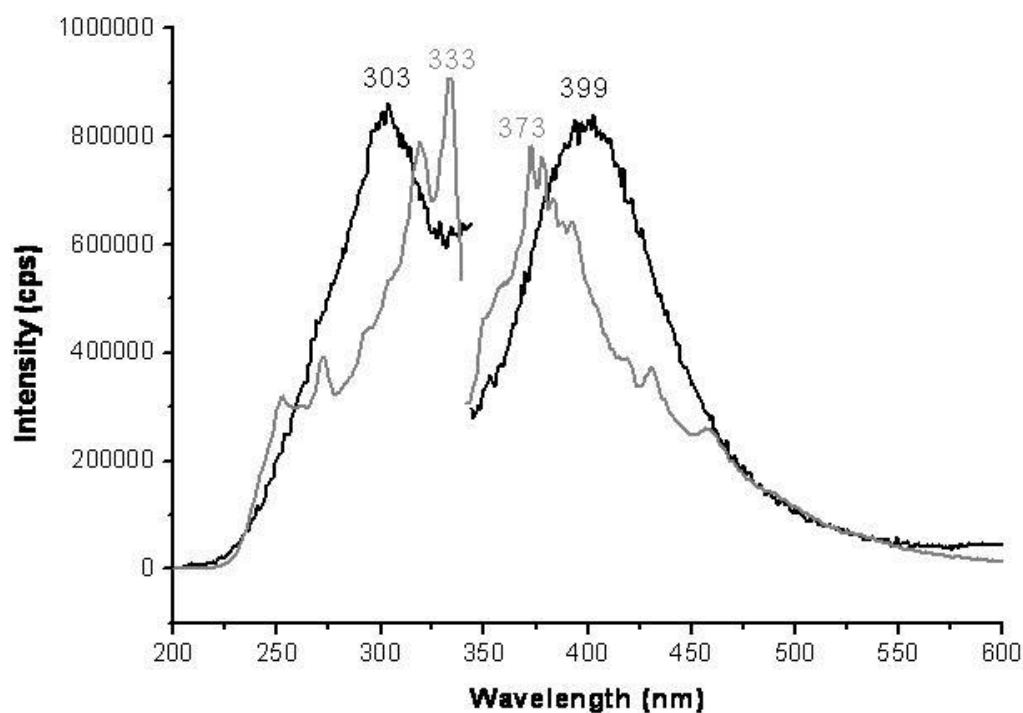


Figure III.4: Fluorescence spectra of extracts in two different solvents from fibers pre-dyed with Direct Blue 1. (—) Extract in 1:1 methanol/water (v:v) and (---) extract in ethanol. Maximum excitation wavelength used for each extract, 303nm and 333nm respectively. Excitation and emission slits set for 4nm and 2nm band-pass, respectively.

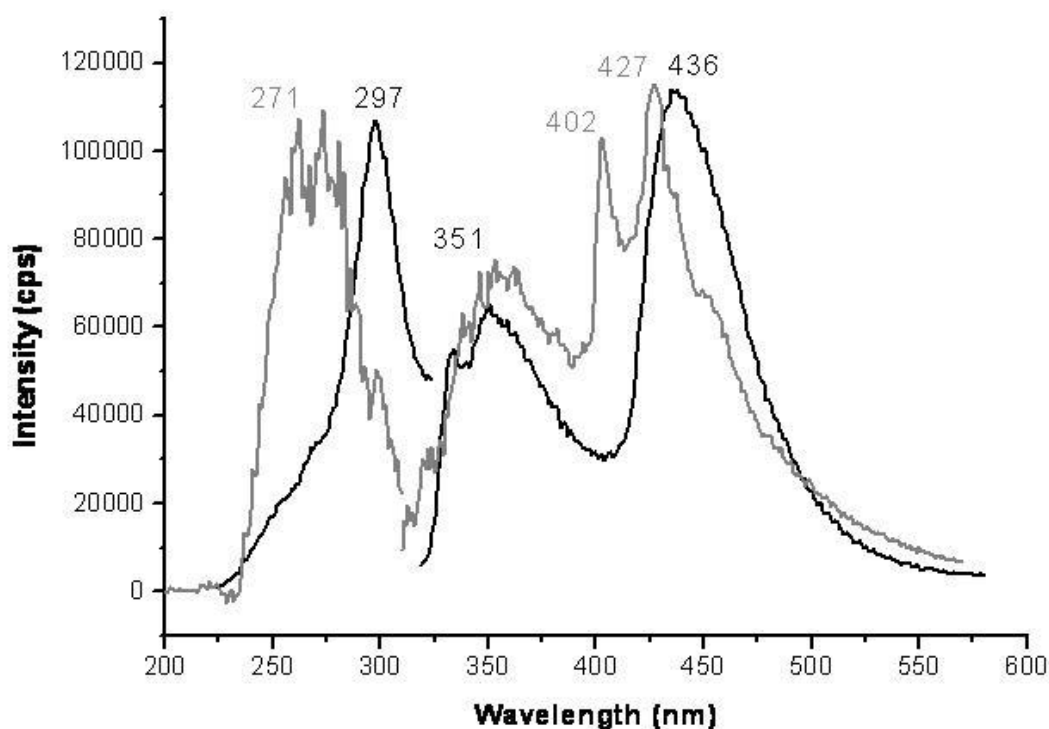


Figure III.5: Fluorescence spectra of extracts in two different solvents from fibers pre-dyed with Direct Blue 71. (—) Extract in 1:1 methanol/water (v:v) and (---) extract in ethanol. Maximum excitation wavelength used for each extract, 297nm and 271nm respectively. Excitation and emission slits set for 4nm and 2nm band-pass, respectively.

Table III.1 summarizes the extracting solvent with the highest fluorescence intensity for each type of studied fiber. The comparison of the maximum excitation and fluorescence wavelengths in Table III.2 shows the possibility to discriminate the studied fibers on the basis of their maximum wavelengths.

Table III.1: Type of Fiber with Dye Used to Pre-dye Fabric and the Best Extracting Solvent for Fluorescence

Type of Fiber	Respective Textile Dye	Solvent
Acetate 154	Disperse Red 1	1:1 acetonitrile/water (v:v)
Polyester 777	Disperse Red 4	1:1 acetonitrile/water (v:v)
Polyester 777	Disperse Red 13	ethanol
Polyester 777	Disperse Blue 56	4:3 pyridine/water (v:v)
Poly-acrylic 864	Basic Green 4	1:1 acetonitrile/water (v:v)
Polyester 777	Basic Red 9	ethanol
Polyester 777	Basic Violet 14	1:1 acetonitrile/water (v:v)
Cotton 400	Direct Blue 1	ethanol
Cotton 400	Direct Blue 71	1:1 acetonitrile/water (v:v)
Cotton 400	Direct Blue 90	4:3 pyridine/water (v:v)
Nylon 361	Acid Red 151	ethanol
Nylon 361	Acid Yellow 17	ethanol
Nylon 361	Acid Yellow 23	ethanol
Nylon 361	Acid Green 27	1:1 methanol/water (v:v)

*Table III.2: Maximum Excitation and Fluorescence Wavelengths of Fiber Extracts with the Highest Fluorescence Intensity*

<i>Fiber Dye</i>	<i>Excitation Peaks (nm)<sup>a</sup></i>	<i>Emission Peaks (nm)<sup>a</sup></i>
Disperse Red 1	256, <u>347</u>	386
Disperse Red 4	291	348, <u>415</u> , 571, 607
Disperse Red 13	303	<u>357</u> , 404, 430
Disperse Blue 56	319	385
Basic Green 4	<u>271</u> , 303	366
Basic Red 9	295	<u>350</u> , 404, 430
Basic Violet 14	284	330
Direct Blue 1	317, <u>333</u>	<u>373</u> , 430
Direct Blue 71	300, <u>355</u>	417
Direct Blue 90	335	406
Acid Red 151	305	358, 387, 406, <u>431</u> , 459
Acid Yellow 17	287	<u>338</u> , 403, 430
Acid Yellow 23	289	<u>345</u> , 430
Acid Green 27	245, <u>303</u>	412

<sup>a</sup> In the case of multiple peaks, most intense is underlined.

### *III.1.2. Selecting a General Solvent for Fiber Extraction*

Numerous methods have been reported for isolating dyestuffs from fibers and for comparing dyes and dye mixtures with thin-layer chromatography (TLC) techniques. These include TLC systems for disperse, acid and basic dyes extracted from polyester, polyamide and acrylic fibers [68], for direct and reactive dyes extracted from cellulose fibers [69], for acid and metallised acid dyes from wool [70] and for disperse, acid and metallised dyes from polypropylene [71]. Some of these methods were compiled and presented as an analytical protocol in 1983 by the Trace Evidence Study Group of the California Association of Criminalists [72]. This work was later extended to cotton and rayon fibers by Laing et al. [73] Typically, the protocol involves three major steps: (a) Identification of the fiber type (usually involving microscopy); (b) selection and application of increasingly powerful extracting solvents to identify dye types; and (c) selection of appropriate TLC systems to discriminate extracted dyes. Although these procedures and their limitations pose few if any problems when large samples of fiber or fabric are available for comparison, they represent substantial difficulties in typical forensic fiber comparisons. These difficulties center on the fact that each loose fiber in a forensic investigation represents, and must be handled as, a unique item of evidence in the case.

Under this prospective, we thought it would be valuable to propose a common extracting solvent for all the studied fibers. Based on the strong fluorescence signals we consistently observed from all its fibers extracts, a 1:1 acetonitrile:water (v/v) mixture appears to be the best solvent choice. Figures III.6 – III.8 compare the excitation and fluorescence profiles of the fourteen types of fibers extracted with this solvent. As shown in figure III.6, fibers pre-dyed with Disperse Red 1, Direct Blue 1, Disperse Red 13 and Acid Green 27 showed extracts with similar excitation and fluorescence profiles. The same is true for fibers pre-dyed with Basic Red 9, Basic Violet 14, Disperse Blue 56 and Acid Yellow 17 (see figure III.7). On the other end, fibers pre-dyed with Basic Green 4, Disperse Red 4, Direct Blue 71, Direct Blue 90, Acid Yellow 23 and Acid Red 151 showed distinct excitation and fluorescence spectra. Although the spectral comparison of fibers would certainly benefit from additional parameters of selectivity, the different excitation

and fluorescence maxima still makes possible their visual discrimination on the basis of spectral profiles.

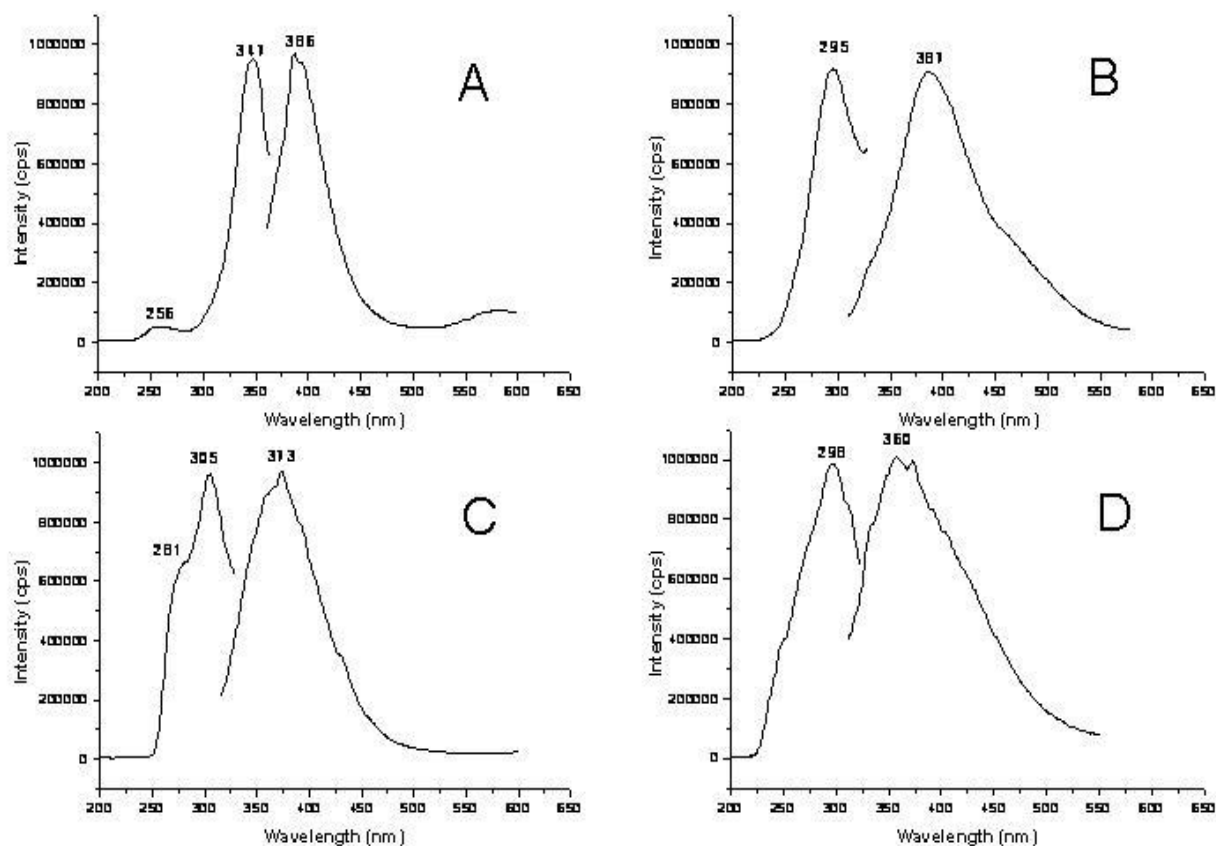


Figure III.6: Comparison of four different fiber extracts in the same solvent, 1:1 acetonitrile/water (v:v). A- Disperse Red 1; B-Direct Blue 1; C-Disperse Red 13; D-Acid Green 27. Excitation set at maximum wavelength for each extract and excitation and emission slits set at 4 and 2 nm band-pass, respectively.

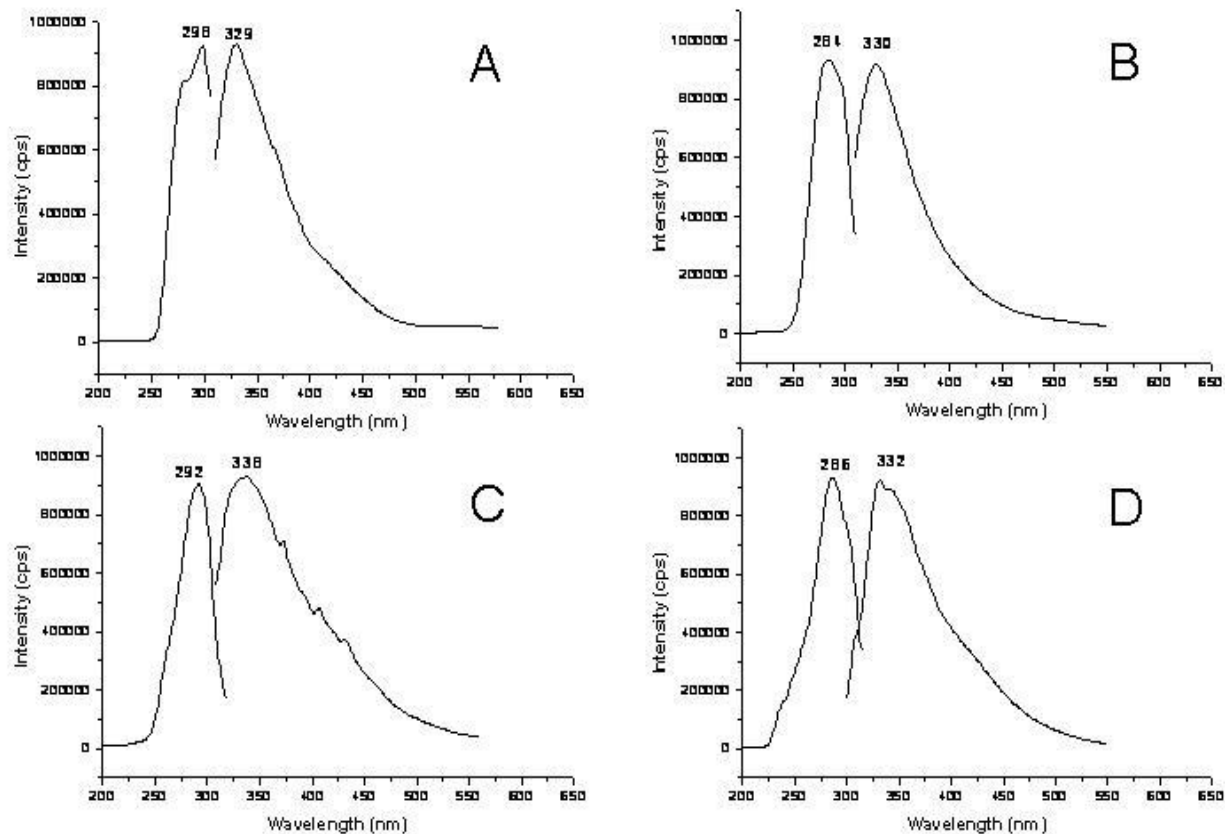


Figure III.7: Comparison of four different fiber extracts in the same solvent, 1:1 acetonitrile/water (v:v). A- Basic Red 9; B-Basic Violet 14; C-Disperse Blue 56; D-Acid Yellow 17. Excitation set at maximum wavelength for each extract and excitation and emission slits set at 4 and 2 nm band-pass, respectively.

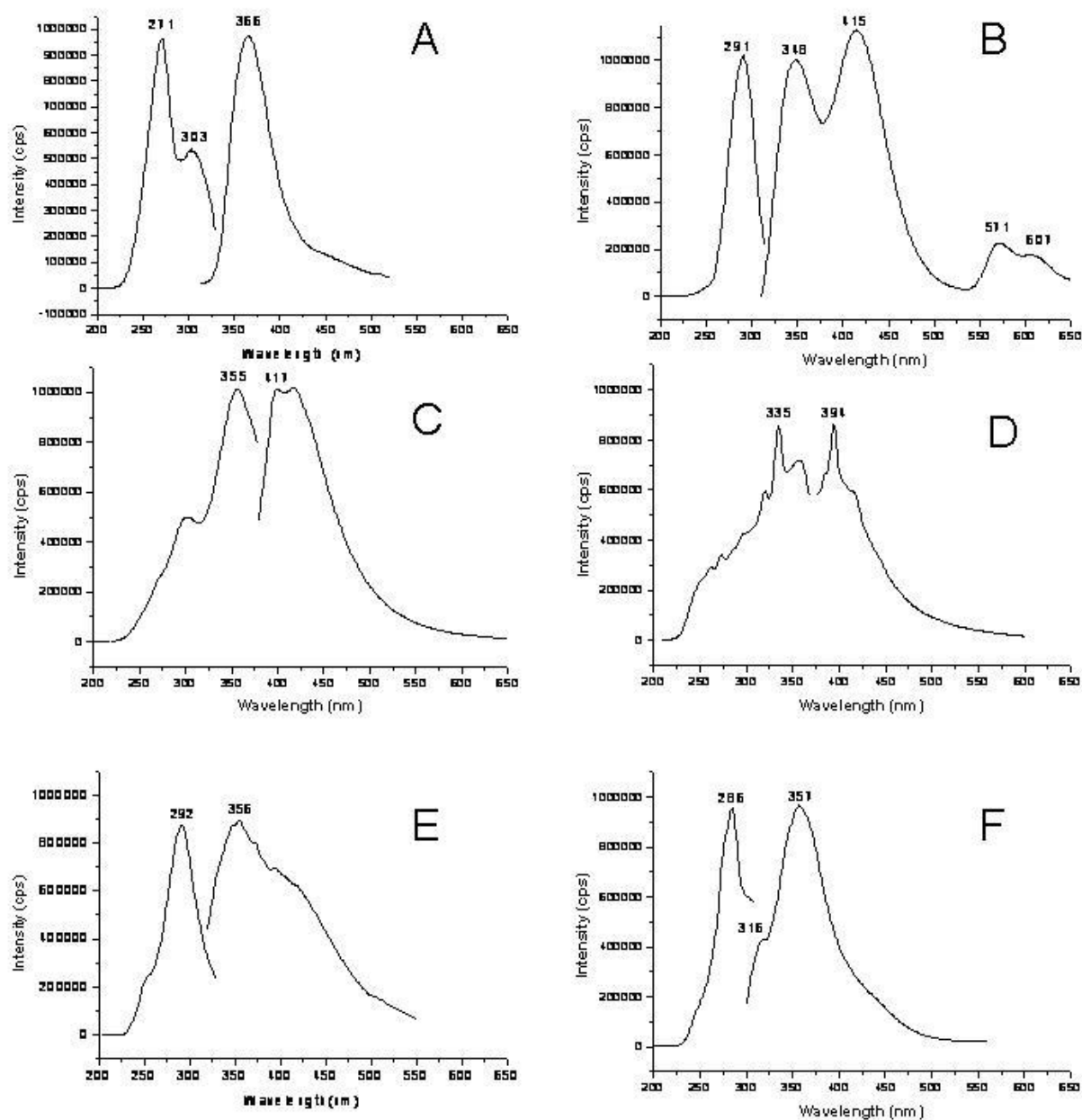


Figure III.8: Comparison of six different fiber extracts in the same solvent, 1:1 acetonitrile/water (v:v). A- Basic Green 4; B-Disperse Red 4; C-Direct Blue 71; D-Direct Blue 9; E-Acid Yellow 23; F-Acid Red 151. Excitation set at maximum wavelength for each extract and excitation and emission slits set at 4 and 2 nm band-pass, respectively.

### III.1.3. Minimum Fiber Length for RTF Spectroscopy of Fiber Extracts

Extensive work in 1974 [74] had shown that the average length fiber transferred between clothing materials was about 5mm. Subsequent work in 1991 reemphasized the limited length and size distribution of retained transferred fibers in typical casework, with the result that the average recovered transferred fiber had a length of less than 2mm, when removed eight hours after the transfer took place [75]. This fiber length poses a significant challenge to current forensic protocols, which require a minimum fiber length between 5 and 20mm. The solvent mixture 1:1 acetonitrile:water (v/v) was then used to investigate the possibility to analyze fibers with 2mm lengths. Figures III.9 and III.10 compare fluorescence spectra of extracts obtained from fibers with different lengths. Although the overall intensities of fluorescence spectra decreased with the lengths of the extracted fibers, 2mm fiber lengths still provided sufficient fluorescence to characterize the fibers on the basis of their spectral profiles. The same type of result was obtained for all investigated fibers.

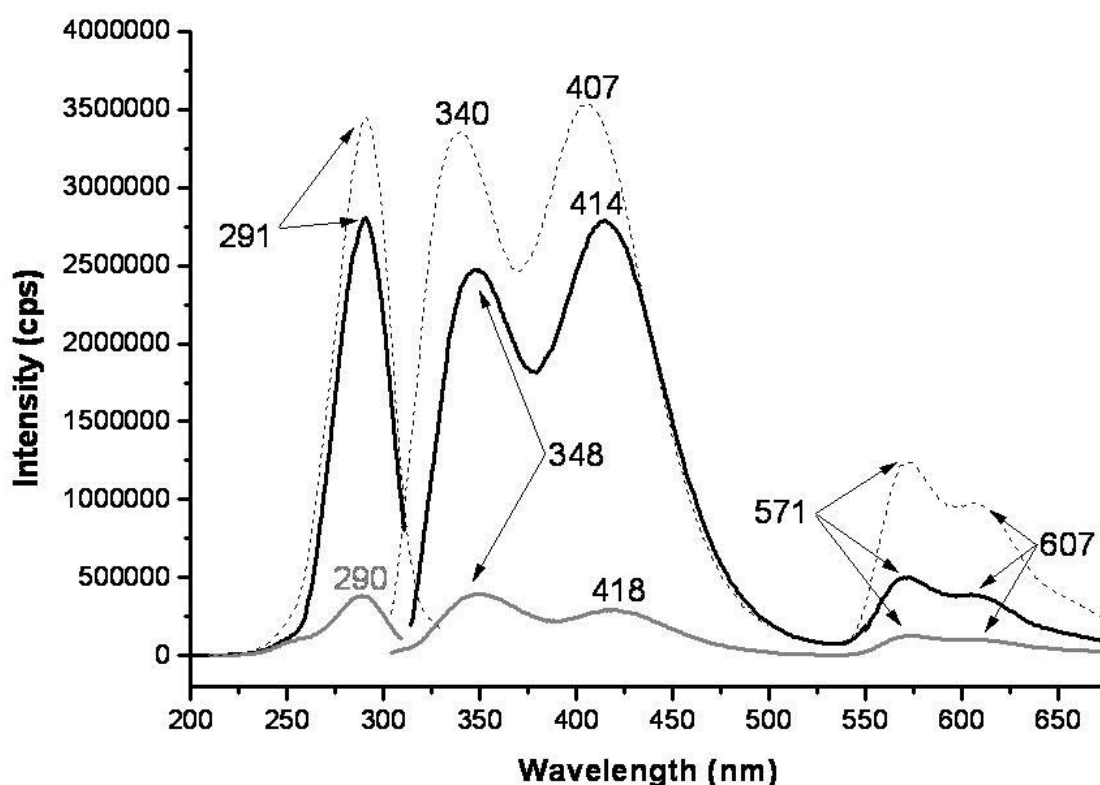


Figure III.9: Excitation and emission spectra of Disperse Red 4 extracts from different lengths of fibers. Extracts in 1:1 acetonitrile/water (v:v) taken from fibers pre-dyed with Disperse Red 4 of lengths (---) 2cm (—) 1cm and (—) 2mm. Extracts excited at 291nm and emission set at 415nm to collect excitation spectra. Slits set at 4 and 2 nm band-pass for excitation and emission, respectively.

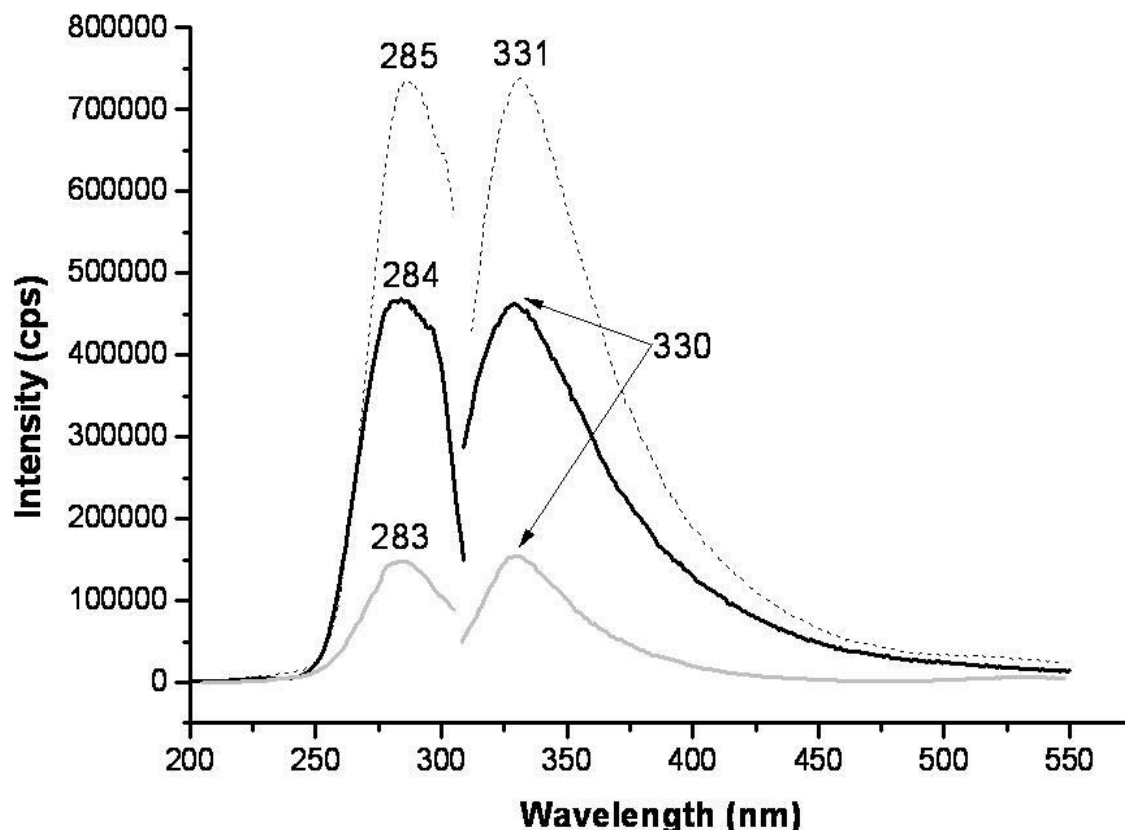


Figure III.10: Excitation and emission spectra of Basic Violet 14 extracts from different lengths of fibers. Extracts in 1:1 acetonitrile/water (v:v) taken from fibers pre-dyed with Basic violet 14 of lengths (---) 2cm (—) 1cm and (—) 2mm. Extracts excited at 284nm and emission set at 330nm to collect excitation spectra. Slits set at 4 and 2 nm band-pass for excitation and emission, respectively.

#### III.1. 4. Reproducibility of Spectral Profiles

Considering reproducible spectra an essential characteristic for forensic fiber comparison, our next goal was to investigate the fluorescence spectral profiles of extracts obtained from single fibers belonging to the same piece of cloth. Two types of experiments were conducted to achieve the following goals: (a) spectral profiles were recorded from individual extracts belonging to adjacent fibers – i.e. single fibers located immediately next to each other – to investigate the reproducibility within the same area of cloth; and (b) single fibers located in four different areas of the cloth were extracted and the spectral profiles recorded to investigate their reproducibility within the entire cloth. Figure III.11 illustrates the four areas of cloth we arbitrarily chose and designated as top middle (TM), top corner (TC), bottom middle (BM) and bottom corner (BC).

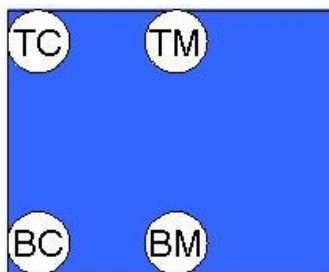
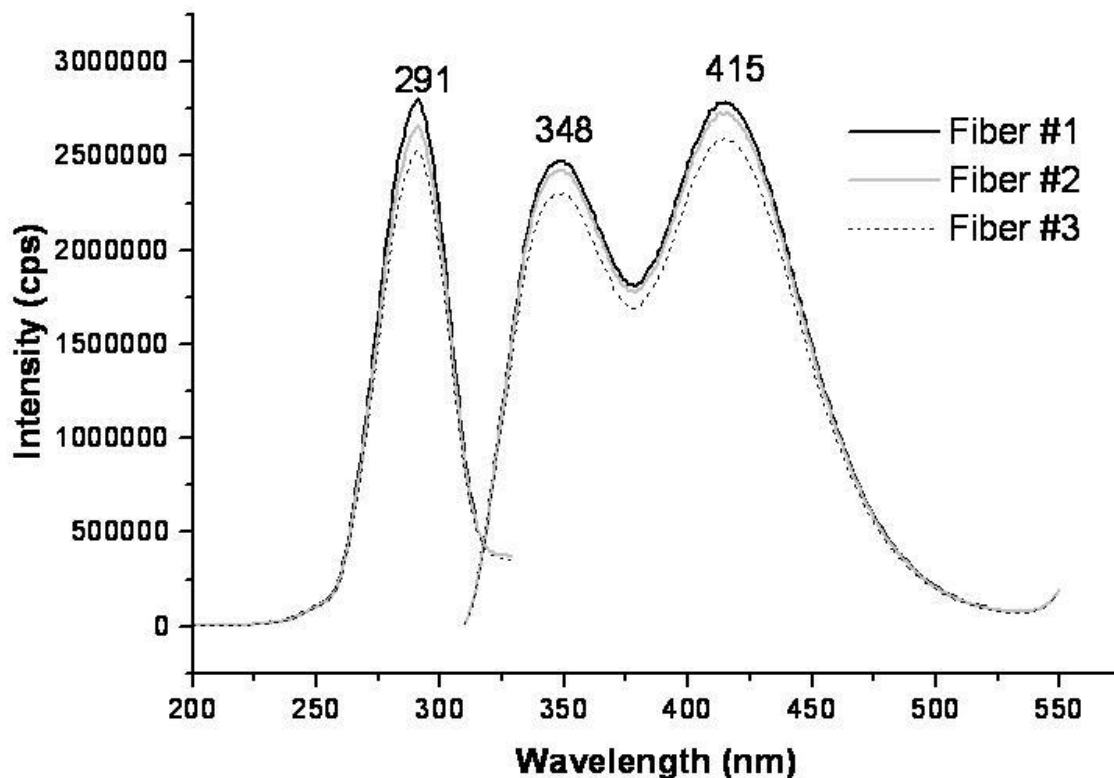


Figure III.11: Abbreviations represent four areas of cloth as follows: TC = top corner, TM = top middle, BC = bottom corner, BM = bottom middle.

Figure III.12 compares the excitation and fluorescence spectra of fiber extracts collected from three single fibers located within the same area of cloth. The extracted fibers were right next to each other so that the first fiber was lying alongside (touching) the second fiber which was alongside the third fiber. Their spectral profiles are clearly reproducible with only a slight variation in intensity.



*Figure III.12: Excitation and fluorescence spectra of 1:1 acetonitrile-water extracts taken from fibers of a polyester cloth garment pre-dyed with Disperse Red 4. Each spectrum corresponds to an extract from a single fiber. All fibers were adjacent to each other and located within the same area of cloth.*

The same behavior was observed for all types of cloths in Table II.1. Figures III.13 and III.14 show additional examples of the excellent reproducibility among the spectral profiles of extracts from adjacent fibers.

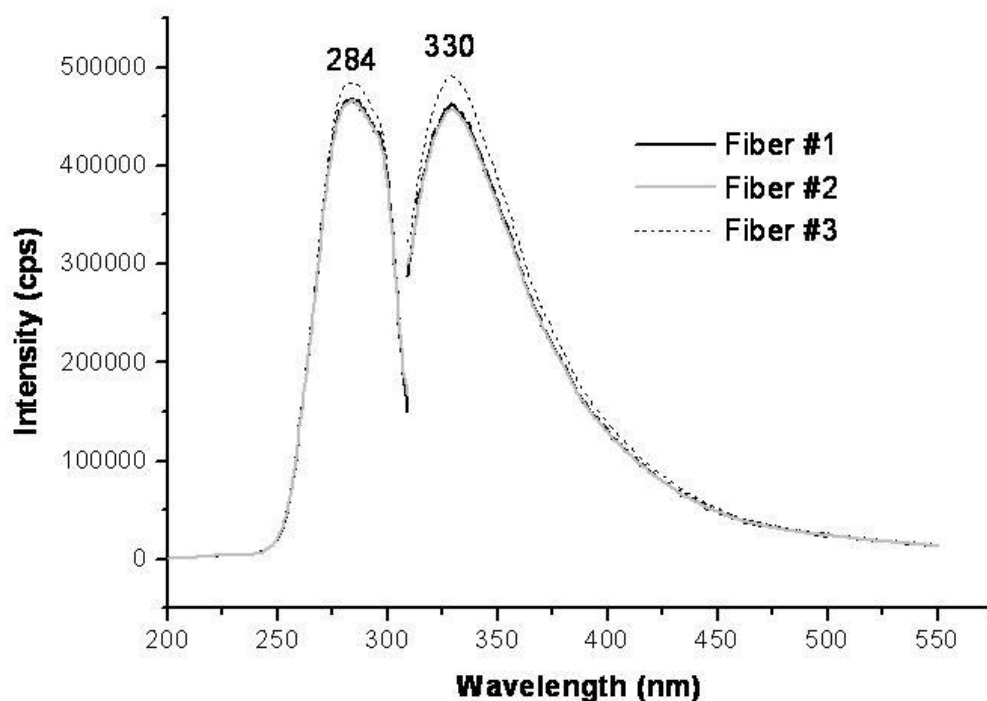


Figure III.13: Excitation and fluorescence spectra of 1:1 acetonitrile-water extracts taken from fibers of a polyester cloth garment pre-dyed Basic Violet 14. Each spectrum corresponds to an extract from a single fiber. All fibers were adjacent to each other and located within the same area of cloth.

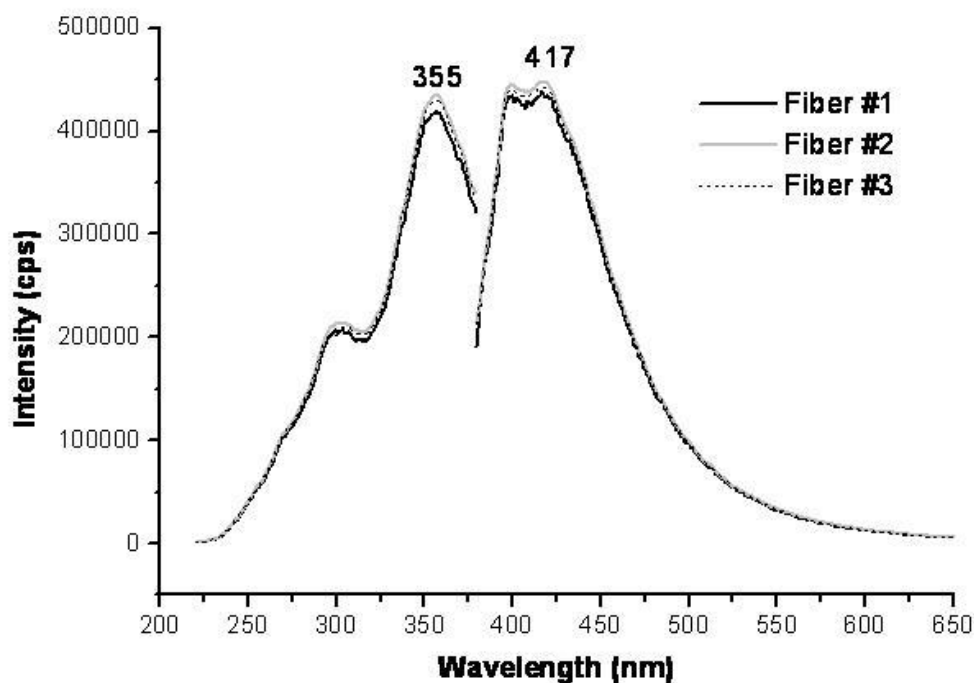
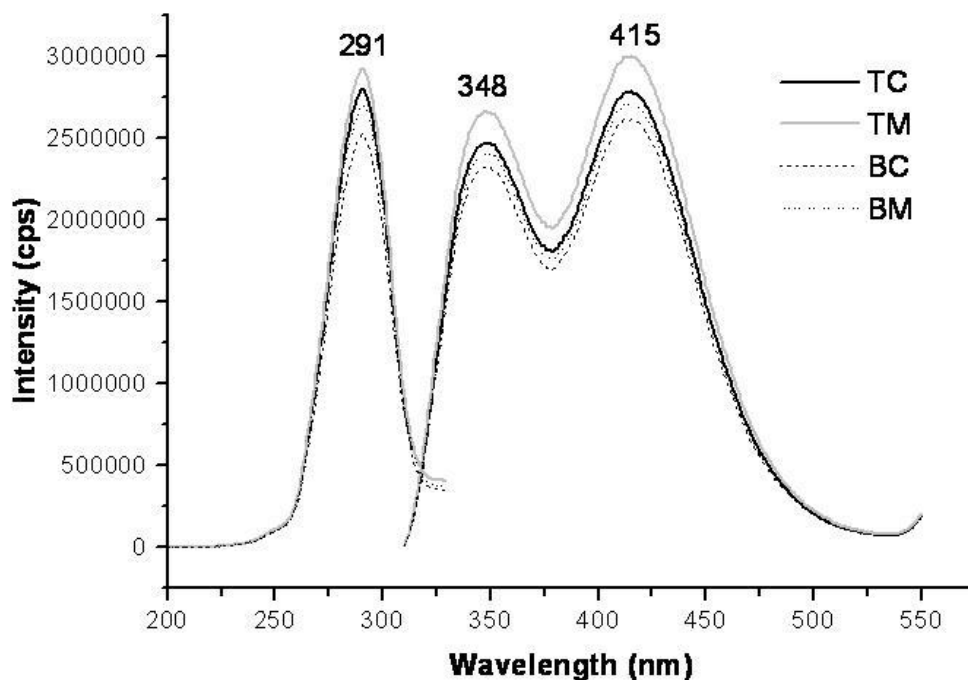


Figure III.14: Excitation and fluorescence spectra of 1:1 acetonitrile-water extracts taken from fibers of a cotton cloth garment pre-dyed with Direct Blue 71. Each spectrum corresponds to an extract from a single fiber. All fibers were adjacent to each other and located within the same area of cloth.

Figure III.15 shows the outstanding spectral reproducibility of single fiber extracts taken from any area across the cloth. Other than a slight difference in intensity, which was within the reproducibility of measurements of the instrumental response, the spectral profiles are virtually the same.



*Figure III.15: Excitation and fluorescence spectra of 1:1 acetonitrile-water extracts taken from fibers of a polyester cloth garment pre-dyed with Disperse Red 4. Each spectrum corresponds to an extract from a single fiber. All fibers were located at different areas within the same cloth.*

For all types of investigated fibers, the spectral profiles recorded from fibers collected from different areas of cloth were extremely reproducible. This is also true for the four types of studied solvents. Additional examples of the observed reproducibility are shown in figures III.16 and III.17.

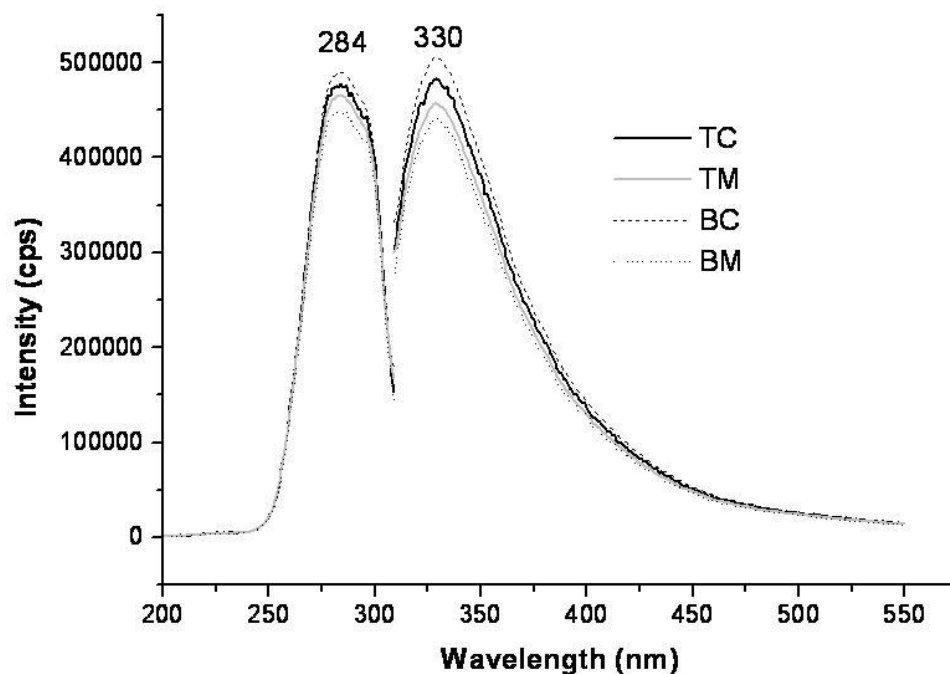


Figure III.16: Excitation and fluorescence spectra of 1:1 acetonitrile/water extracts taken from fibers of a polyester cloth garment pre-dyed with Basic Violet 14. Each spectrum corresponds to an extract from a single fiber. All fibers were located at different areas within the same cloth.

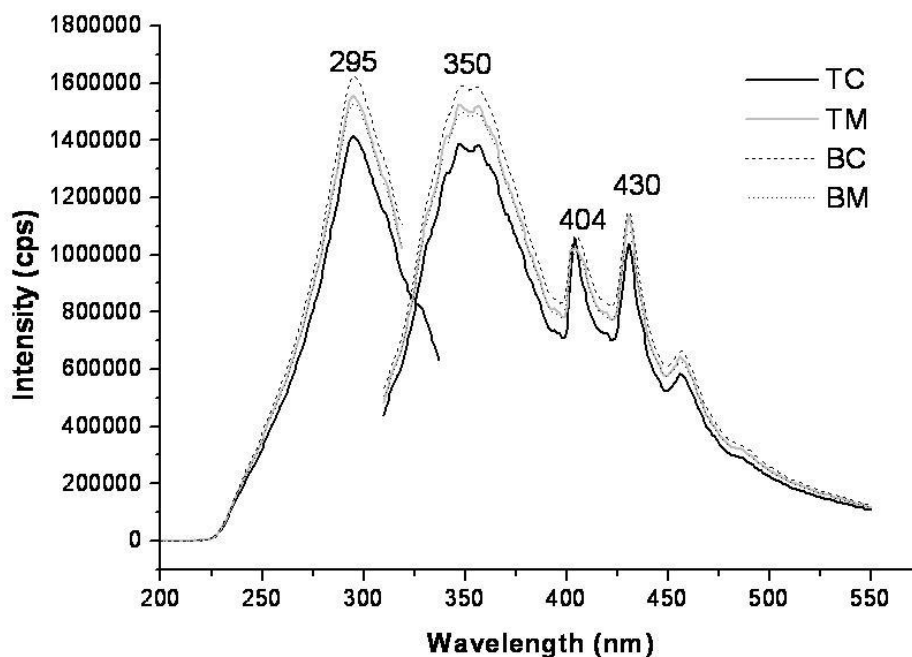
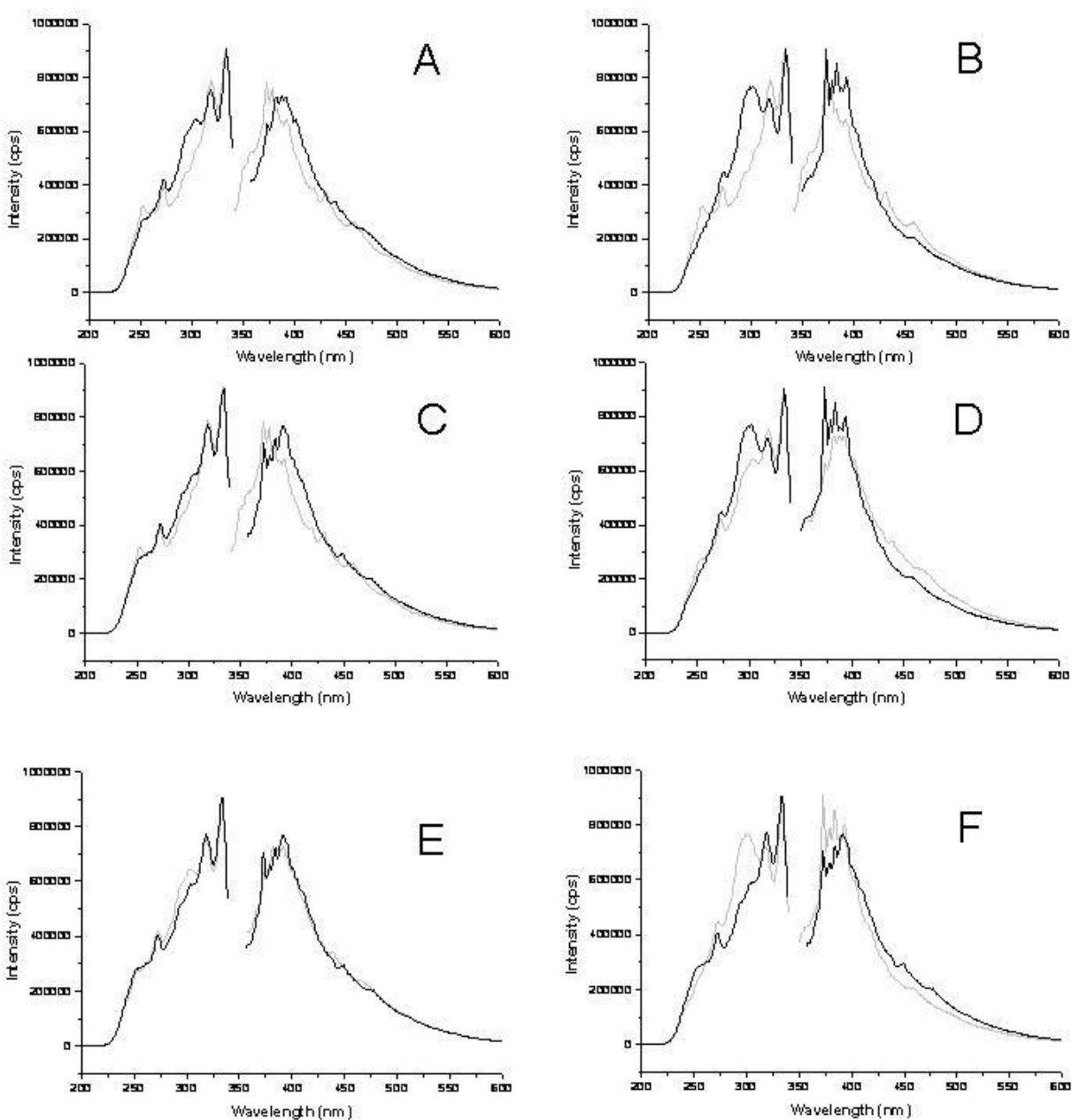


Figure III.17: Excitation and fluorescence spectra of ethanol extracts taken from fibers of a polyester cloth garment pre-dyed with Basic Red 9. Each spectrum corresponds to an extract from a single fiber. All fibers were located at different areas within the same cloth.

### III.1.5. Comparison among the Same Type of Fibers Belonging to Different Pieces of the Same Type of Cloth

This type of comparison was made with fiber cloths pre-dyed with Direct Blue 90, Direct Blue 1 and Acid Red 151. All the remaining fibers were acquired as one piece of cloth. Direct Blue 90, Direct Blue 1 and Acid Red 151 were purchased as a set of 100 pieces of cloths. To the extent of our knowledge (verbal communication from Testfabrics, Inc.), each set of 100 pieces of cloths belongs to the same commercial batch. Our studies, therefore, do not provide information on batch-to-batch reproducibility. Four pieces of each type of cloth were randomly selected to collect one fiber from the top left corner of each garment (see TC area in figure III.11). Each fiber was cut to a 1cm length and extracted with its best extracting solvent for RTF spectroscopy.

Among the three types of fibers, the largest spectral differences were observed with Direct Blue 1 fibers. Figure III.18 compares the excitation and fluorescence profiles of the four Direct Blue 1 fiber extracts in ethanol. With the exception of fiber extracts from cloths 2 and 4, which showed almost identical spectra, the remaining spectral profiles allow one to visually differentiate among the four fiber extracts. Although the differentiation of the same type of fiber from different pieces of cloth appears possible on the basis of two-dimensional excitation and fluorescence spectra, we feel that the forensic examination of textile fibers would certainly benefit from additional selectivity. One should notice that all fluorescence spectra were recorded at the same excitation wavelength (maximum excitation wavelength = 333nm). As such, the possibility to enhance fluorescence spectral differences upon selective excitation was not explored. The same is true for all excitation spectra, which were recorded at the same fluorescence wavelength (maximum fluorescence wavelength = 373nm).



*Figure III.18: Excitation and fluorescence profiles comparing four Direct Blue 1 fiber extracts in ethanol from different cloths. A-Cloth 1 vs. Cloth 2; B-Cloth 1 vs. Cloth 3; C-Cloth 1 vs. Cloth 4; D-Cloth 2 vs. Cloth 3; E-Cloth 2 vs. Cloth 4; F-Cloth 3 vs. Cloth 4.*

## III.2. Comparison of Fiber Extracts with Dye Standards

### *III.2.1. Absorbance of Dye Standards and Fiber Extracts*

The absorption spectra of several dyes in Table II.1 are well documented in the Sigma-Aldrich Handbook of Stains, Dyes and Indicators [67]. Among the four solvent systems we investigate here for fiber extraction, the most common solvent used to record absorption spectra in the Aldrich-Sigma Handbook was methanol/water. "A" spectra in appendix C compiles the absorption profiles of the fourteen dye standards recorded in 1:1 methanol/water (v/v) solutions. All spectra showed strong absorption peaks in the ultraviolet and visible wavelength regions. Based on the visible color of dye standards solutions, the absorption peaks in the visible most likely reflect the presence of the dye in the commercial standard. Because the concentration of the dyes in the commercial standards is always lower than 100% (see Table II.2), the absorption peaks in the ultraviolet range of the spectra could be attributed to the presence of impurities in the commercial mixtures of unknown composition.

The comparison of "A" spectra in appendix C to the absorption spectra of dyes in the best fiber extracting solvent for fluorescence (see "B" spectra in Appendix C) shows the effect of solvent composition and dye solubility in the spectral features of the studied dyes. With the exception of Direct Blue 1, all the other dyes showed very similar spectra in both types of solvents. The absence of the visible peak in the absorption spectrum of Direct Blue 1 is due to the poor solubility of the dye in ethanol, i.e. the best fiber extracting solvent for fluorescence. The presence of ultraviolet peaks in both spectra probably reflects the presence of soluble impurities in both types of solvents.

Comparison of "B" spectra to the absorption spectra of fiber extracts in the best fluorescence extracting solvent (see "C" spectra in Appendix C) should take into consideration possible variations in the composition of the Aldrich-Sigma standards and the dye reagents used to pre-dye Testfabrics fibers. If the visible portion of the spectra results from the presence of the dyes in the fibers, the comparison among "B" and "C" spectra should then provide qualitative information on the ability of the best fluorescence solvents to extract the dyes from the fibers.

Figures C-6 to C-8 and C-12 show the absence of the absorption peak in the visible spectrum of the extract. The lack of visible peak in the absorption spectrum of Direct Blue 1 (figure C-8) can be attributed to the poor solubility of the dye in the best extracting solvent for fluorescence. The lack of visible absorption peaks in Basic Red 9 (figure C-6), Basic Violet 14 (C-7) and Acid Yellow 17 (figure C-12) could be attributed to two possible reasons, namely the inability of the best fluorescence fiber solvent to extract the dye from the fiber and/or the low concentration of the dye to be measured via absorption spectrometry. All the remaining "C" spectra show visible peaks in the fiber extracts. When comparing the relative intensities of the visible peaks to those in "B" spectra, one should consider the unknown amount of dye in the fiber and that their relative intensities do not provide quantitative information on the dye extraction efficiency of the best fluorescence fiber solvent. The comparison only demonstrates the ability of the best fluorescence fiber solvent to extract the dye from the fiber. Table III.3 compares the maximum absorption wavelengths of the Sigma-Aldrich dye standards to those from the respective fiber extracts.

Table III.3: Absorbance Peaks <sup>a</sup> of Dye Standards and Extracts in Best Extracting Solvent

Dye	Standard	Extract
Disperse Red 1	<u>263</u> , 318, 483	274, <u>484</u>
Disperse Red 4	<u>257</u> , 512, 547	<u>287</u> , 513, 548
Disperse Red 13	211, 284, <u>503</u>	253, <u>500</u>
Disperse Blue 56	302, 592, <u>632</u>	<u>299</u> , 637
Basic Green 4	<u>256</u> , 359, 621	<u>268</u> , 316, 619
Basic Red 9	211, 289, 546	<u>290</u> , 317
Basic Violet 14	240, 291, 546	<u>245</u> , 315
Direct Blue 1	<u>214</u> , 274	320
Direct Blue 71	299, <u>591</u>	283, <u>586</u>
Direct Blue 90	631	<u>261</u> , 587
Acid Red 151	230, 351, 511	<u>325</u> , 504
Acid Yellow 17	<u>224</u> , 403	<u>232</u> , 281
Acid Yellow 23	<u>260</u> , 430	<u>225</u> , 282, 409
Acid Green 27	<u>254</u> , 286, 410, 603, 645	<u>288</u> , 412, 605, 647

<sup>a</sup>If more than one peak was observed, the peak of maximum intensity is underlined.

### III.2.2. Room-Temperature Fluorescence Characteristics of Sigma-Aldrich Dye Standards

Not much is published of the RTF characteristics of textile dyes. A comprehensive literature search on fluorescence of reagent dyes from Sigma-Aldrich revealed only two reports [76, 77]. The fluorescence characteristics of Direct Blue 1 and Direct Blue 71 were recorded in water, methanol and aqueous triton-X [76]. The fluorescence features of Disperse Red 1 were investigated in methanol, ethylene glycol, glycerol, and phenol [77]. Both reports use the reagent dyes as received with no attempts of further purification. In the case of Disperse Red 1 [77], the highest fluorescence signal was observed upon sample excitation at 532nm, i.e. an excitation wavelength nominally selected to attempt the exclusive excitation of the dye in the presence of unknown reagent impurities.

With the exception of Disperse Red 13 and Acid Red 151, all the dye standards in Table II.2 showed RTF when dissolved in the best extracting solvent of their corresponding fibers (see Table III.1). One should notice that the lack of fluorescence from Disperse Red 13 and Acid Red 151 does not reflect the solubility of the dyes in the extracting solvent as both dyes were soluble in ethanol, i.e. the best fluorescence solvent for their corresponding fibers. Appendix D compiles the excitation and fluorescence spectra of the remaining dyes recorded with the same excitation and emission band-passes used to record spectra from fibers extracts in Appendix B. Initial wavelength selection for fluorescence excitation was based on absorption spectra. For those dyes that showed absorption peaks in the ultraviolet and visible region, fluorescence excitation was attempted in both spectral regions. Dispersed Red 4 (see spectra D-2) was the only dye to show different fluorescence peaks upon excitation in the ultraviolet (272nm) and the visible (512nm) regions of the spectrum. Upon excitation at 253nm, Basic Red 9 showed two fluorescence peaks with maximum wavelengths at 350nm and 689nm (see spectra D-6). The remaining dyes showed one fluorescence peak either in the ultraviolet or the in visible spectral regions. In some cases, their excitation spectra recorded at the maximum fluorescence wavelength showed more than one prominent peak. The maximum excitation and fluorescence wavelengths of Sigma-Aldrich dyes standards are summarized in Table III.4. Although the unknown and heterogeneous composition of Sigma-Aldrich dyes standards makes difficult the assignment of peaks to impurities and/or dyes, the comparison of spectra in Appendix D clearly shows the possibility to discriminate among commercial dyes on the basis of excitation and fluorescence profiles.

*Table III.4: Maximum Excitation and Fluorescence Wavelengths<sup>a</sup> of Sigma-Aldrich Dye Standards at Room Temperature*

<i>Dye Standard</i>	<i>Excitation (nm)</i>	<i>Emission (nm)</i>
Disperse Red 1	258	307
Disperse Red 4	272, <u>512</u>	300, <u>570</u>
Disperse Red 13	N/A	N/A
Disperse Blue 56	326, <u>586</u>	380, <u>661</u>
Basic Green 4	272	368
Basic Red 9	<u>252</u> , 290	<u>350</u> , 689
Basic Violet 14	257, <u>299</u>	363
Direct Blue 1	267, <u>340</u>	397
Direct Blue 71	250, <u>296</u> , 350	431
Direct Blue 90	250	306
Acid Red 151	N/A	N/A
Acid Yellow 17	278	302
Acid Yellow 23	<u>275</u> , 423	<u>299</u> , 547
Acid Green 27	600	689

<sup>a</sup> In the case of multiple peaks, most intense is underlined.

Figures III.19 to III.22 provide a head-to-head comparison of the spectral profiles of the commercial dyes and their corresponding fiber extracts in the best solvent for fluorescence intensity. With the exception of Basic Green 4 and its corresponding fiber extract, all the remaining pairs showed different spectral profiles. The observed differences provide compelling evidence of the important contribution that fluorescence impurities make on the total fluorescence spectra of fiber extracts. The presence of impurities on the extracts of fibers pre-dyed with Disperse Red 13 and Acid Red 151 make possible their discrimination on the basis of fluorescence spectroscopy.

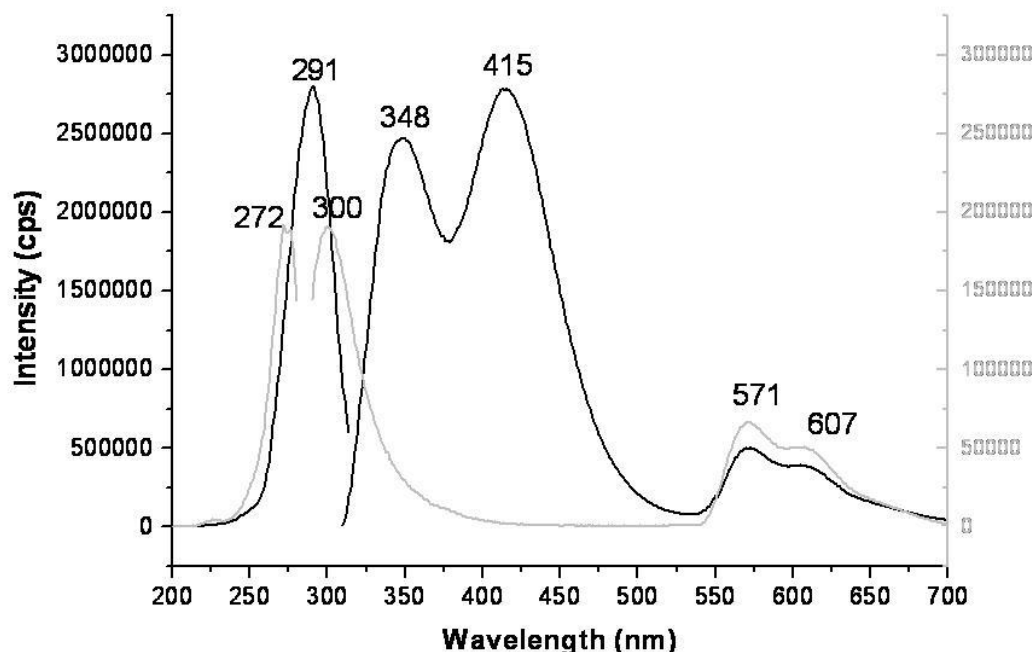


Figure III.19: Excitation and fluorescence comparison of Disperse Red 4 standards and extracts in 1:1 acetonitrile/water (v:v). (—) Fiber extract and (---) Standard. Maximum excitation wavelength for each sample was used to record fluorescence spectra; excitation and emission slits were set at 4 and 2nm band-pass, respectively.

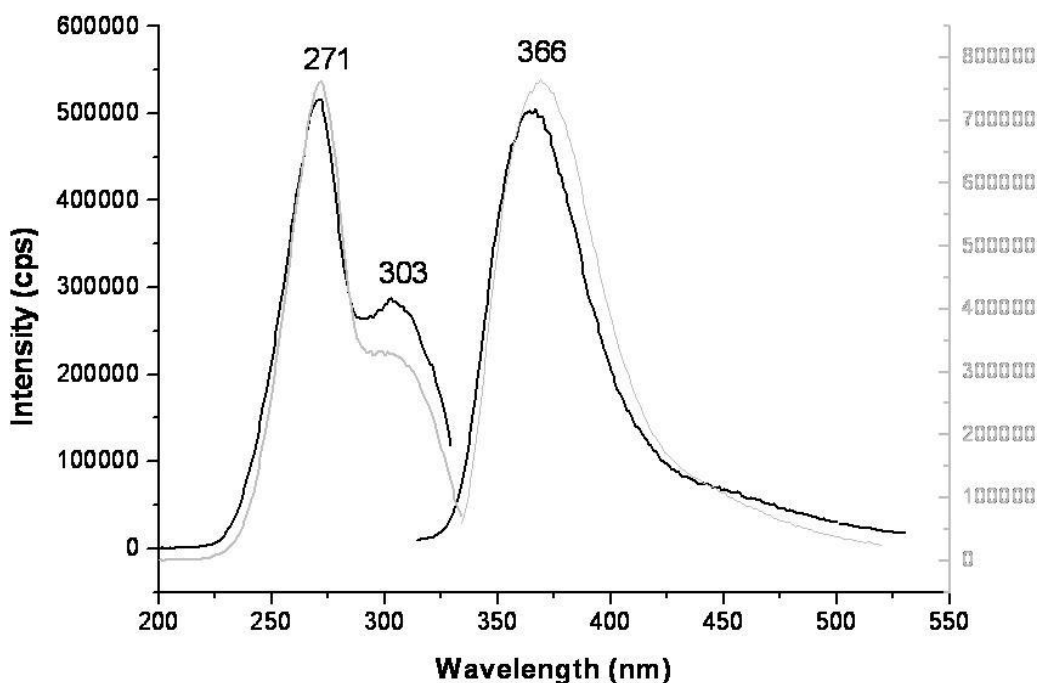


Figure III.20: Excitation and fluorescence comparison of Basic Green 4 standards and extracts in 1:1 acetonitrile/water (v:v). (—) Fiber extract and (---) Standard. Maximum excitation wavelength for each sample was used to record fluorescence spectra; excitation and emission slits were set at 4 and 2nm band-pass, respectively.

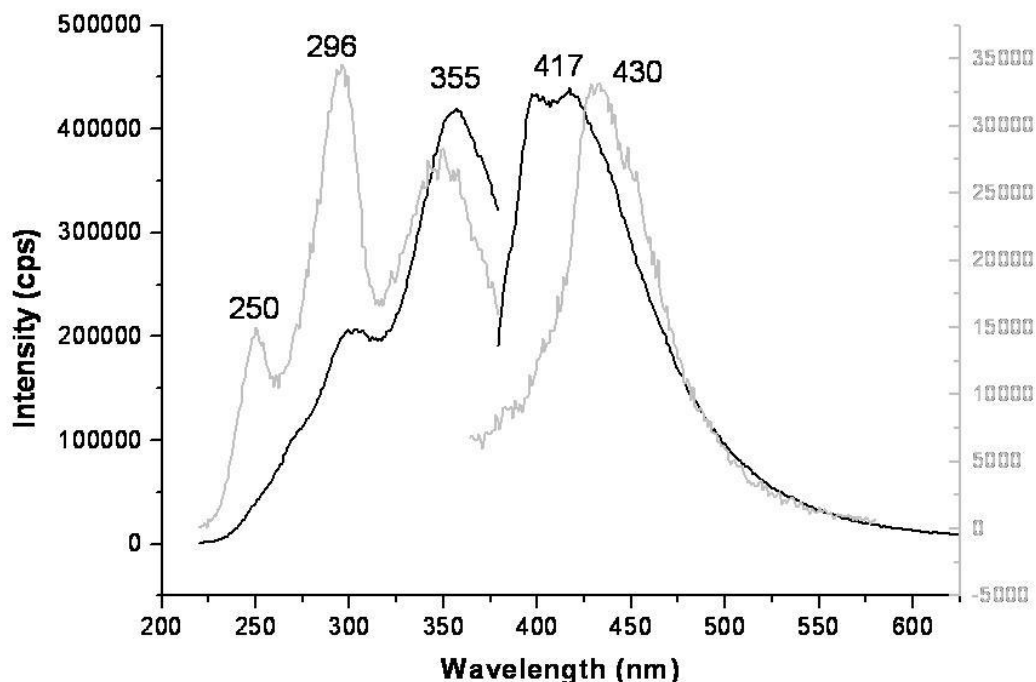


Figure III.21: Excitation and fluorescence comparison of Direct Blue 71 standards and extracts in 1:1 acetonitrile/water (v:v). (—) Fiber extract and (---) Standard. Maximum excitation wavelength for each sample was used to record fluorescence spectra; excitation and emission slits were set at 4 and 2nm band-pass, respectively.

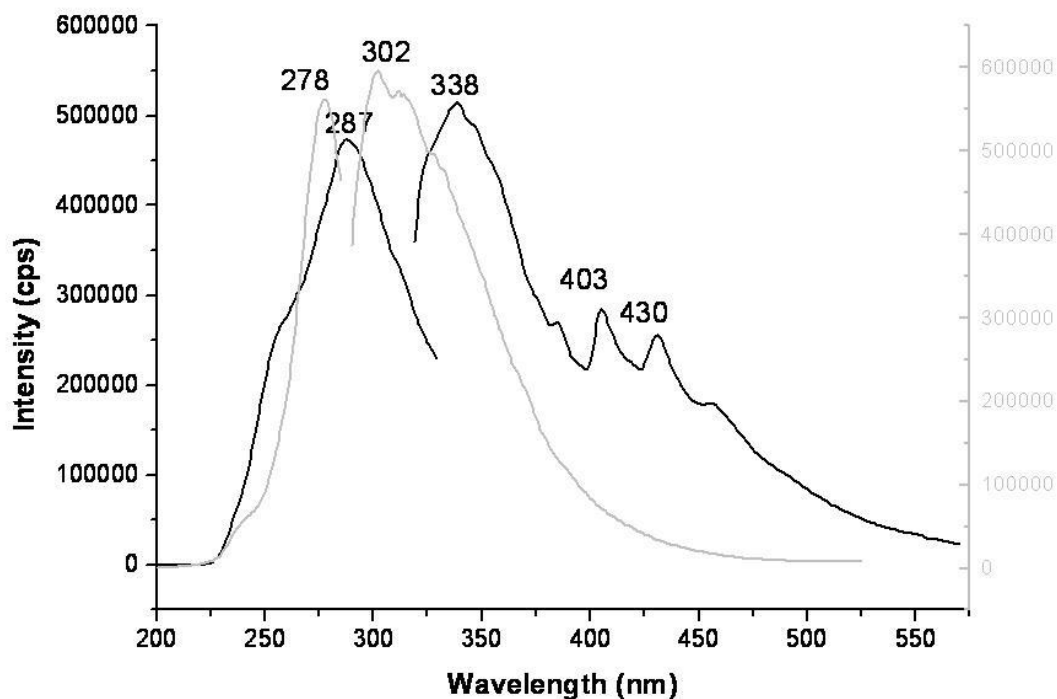


Figure III.22: Excitation and Fluorescence Comparison of Acid Yellow 17 Standards and Extracts in Ethanol. (—) Fiber extract and (---) Standard. Maximum excitation wavelength for each sample was used to record fluorescence spectra; excitation and emission slits were set at 4 and 2nm band-pass, respectively.

### III.3. HPLC of Fiber Extracts

The investigation of the reproducibility of individual components in fiber extracts across the same piece of garment followed the same strategy as the one described in section III.1. 4. Adjacent fibers were collected from four different areas of the same piece of cloth, namely top corner (TC), bottom corner (BC), top middle (TM) and bottom middle (BM). A minimum of three chromatographic runs were carried out per fiber extract and per dye standard solution. Figure III.23 compares the fluorescence chromatograms of four fibers pre-dyed with Disperse Red 4, Basic Green 4 and Acid Red 151. The excitation and emission wavelengths selected for detection were the maximum wavelengths of the fiber extracts (see appendix B). The retention times of each chromatographic peak represents the average of three chromatographic runs of the same extract. The typical relative standard deviations of retention times were no larger than 5%. The agreement observed among the retention times and the fluorescence intensities of the four chromatograms for each type of fiber extract demonstrates the reproducible distribution of the dyes within fibers of the same piece of cloth.

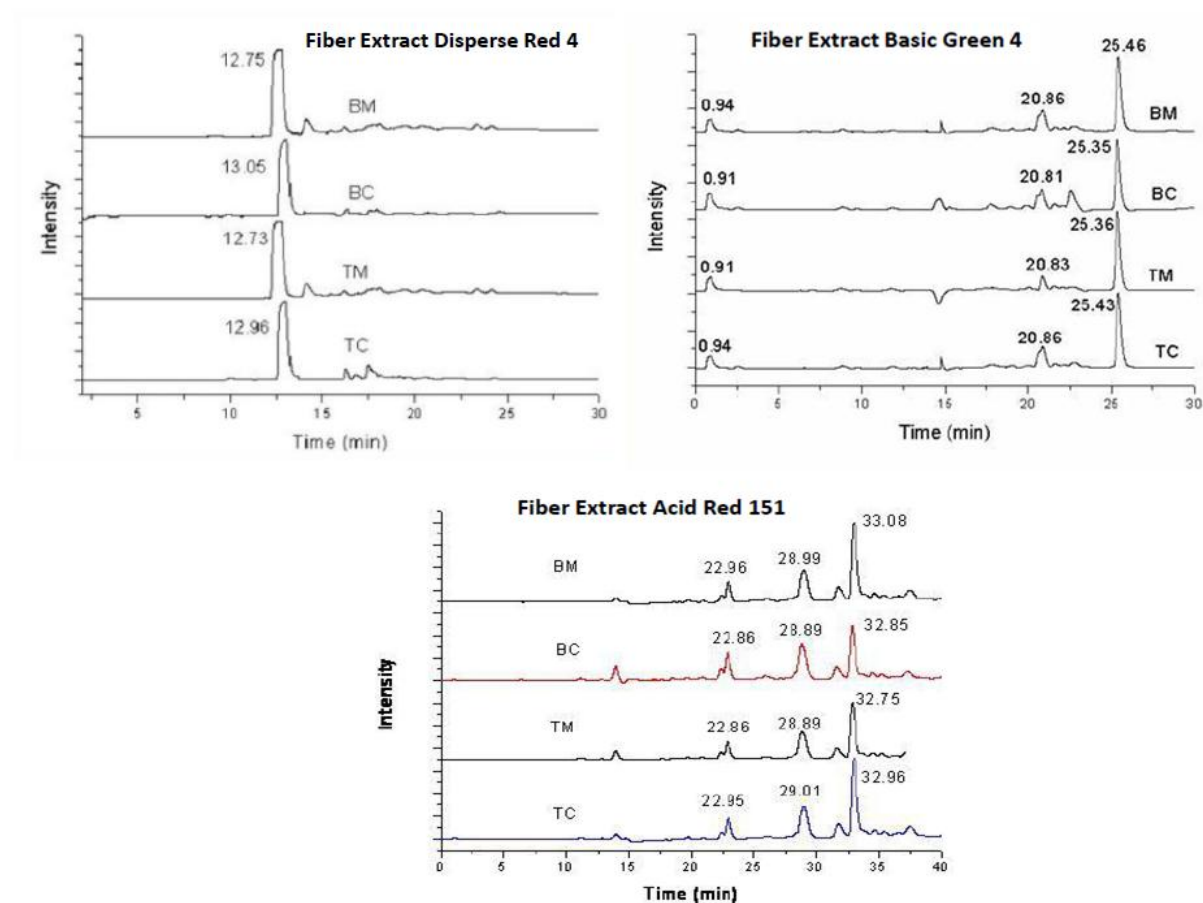


Figure III.23: HPLC absorption chromatograms of Disperse Red 4 standards and fiber extracts. Excitation and fluorescence detection wavelengths set as follows: 291/345nm (Disperse Red 4), 272/366nm (Basic Green 4) and 305/431nm (Acid Red 151).

Figure III.24 – III.26 compare the absorption and fluorescence chromatograms of the Sigma-Aldrich standards to those recorded from the fiber extracts. The excitation and emission wavelengths selected for fluorescence detection correspond to the maximum excitation and emission wavelengths of the fiber extracts (see appendix B). The statistical comparison of retention times of absorption peaks confirms the presence of the dye in both the standard and the fiber extract. The comparison of the fluorescence chromatograms clearly shows the presence of fluorescence impurities in the fiber extracts not present in the Sigma-Aldrich standards. Interesting to note is the less intense absorption peaks of all the extracts when compared to their respective standards. The lower intensities reveal dye concentrations in the extracts below 10ppm, i.e. the concentrations of dyes in the standard solutions. A direct correlation between the concentration of the dye in the extract and its mass on the extracted fiber requires the knowledge of the extraction efficiency of the solvent, which was not investigated in these studies.

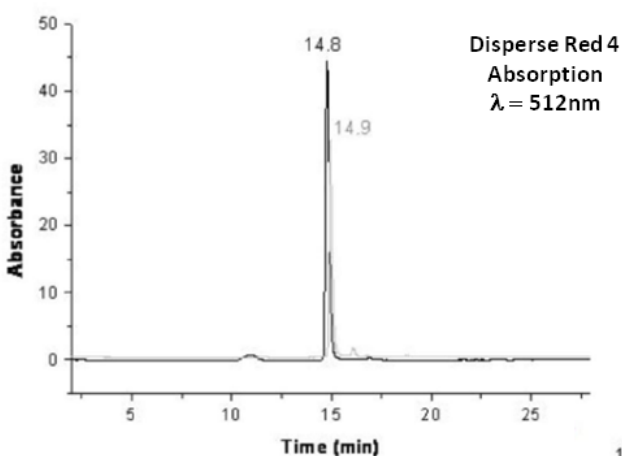
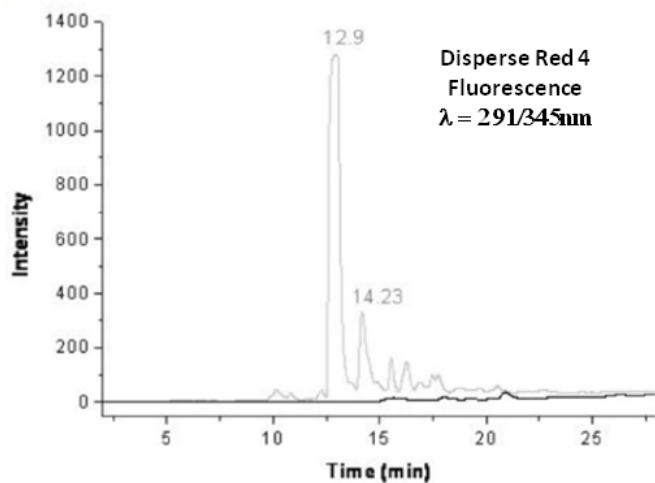


Figure III.24: HPLC chromatograms of Disperse Red 4 standard (dark trace) and fiber extract (clear trace).



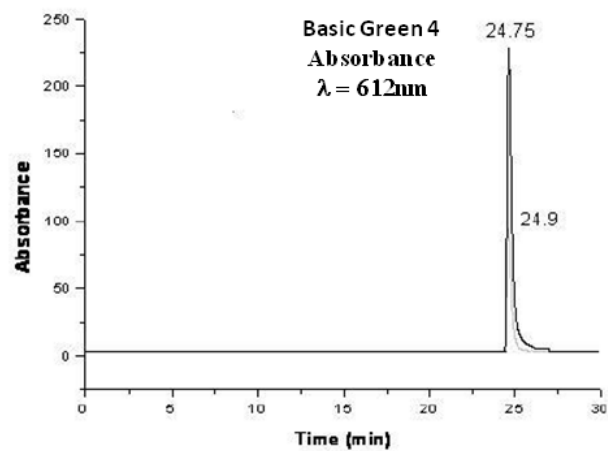
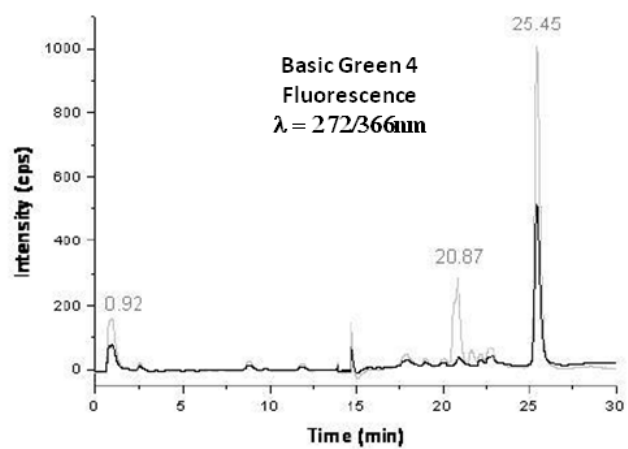


Figure III.25: HPLC chromatograms of Basic Green 4 standard (dark trace) and fiber extract (clear trace).



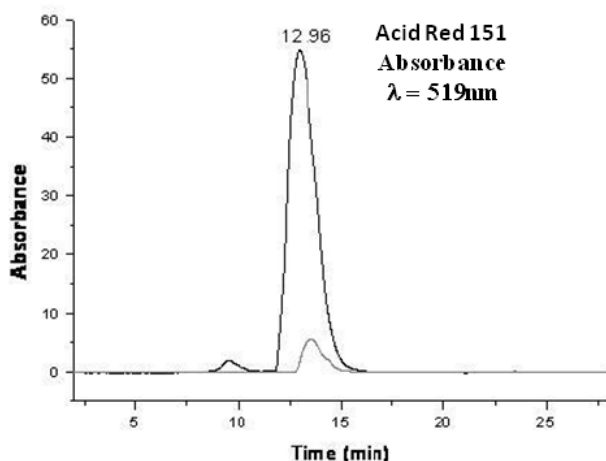
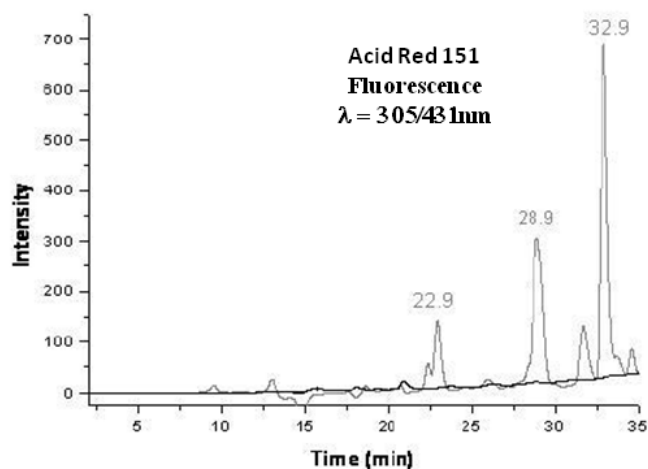


Figure III.26: HPLC chromatograms of Acid Red 151 standard (dark trace) and fiber extract (clear trace).



In the case of Basic Red 4, the retention times of the main peaks in the absorption and fluorescence chromatograms are statistically different. This is an indication that the dye and the main fluorescence impurity have different chemical structures. Figure III.27-A compares the absorption spectrum of a 10ppm Disperse Red 4 dye standard solution in 50% methanol-water (v/v) to the absorption spectrum of the HPLC fraction collected from the extract at 14.9 min (refer to figure III.24 for chromatographic time). The agreement between the two spectra in III.27-A can be attributed either to the similarity of the spectral features of the commercial dye reagent and the purified dye via HPLC analysis or to the unsuccessful separation of impurities from the dye via HPLC analysis of the extract. Considering the strong probability of the chemical composition of the commercial dye reagent to be different from the chemical composition of the extract, the latter appears to be unlikely. Figure III.27-B shows the absorption spectrum of the HPLC fluorescence fraction collected from the extract at 12.9 min (refer to figure III.24 for chromatographic time). The lack of extract absorbance with similar characteristics to those from the dye confirms the assignment of fluorescence peaks in figure III.24 to the presence of impurities and not to the presence of the dye. Similar results are shown for fibers pre-dyed with Acid Red 151 in figure III.28. Similar to Basic Red 4, the main peaks in the absorption and fluorescence chromatograms of Acid Red 151 are different.

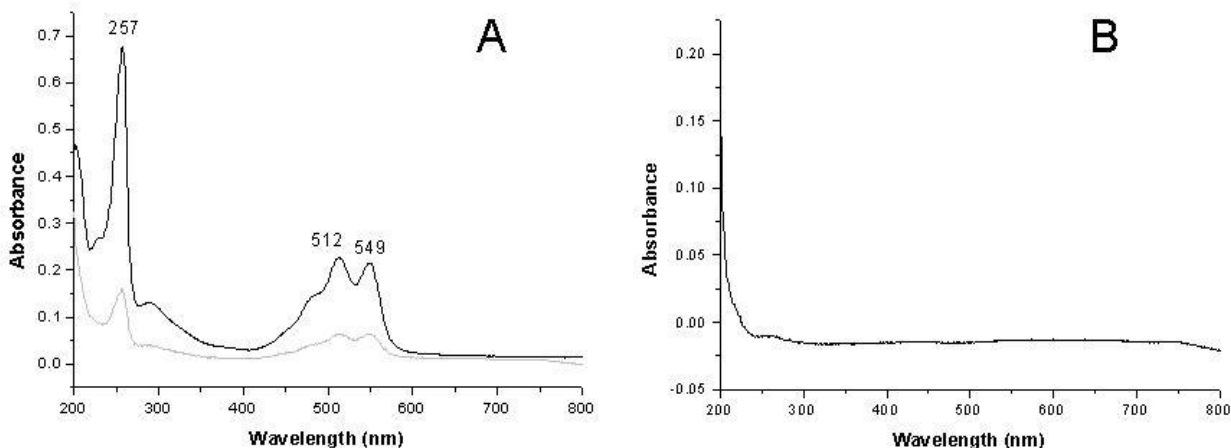


Figure III.27: Absorbance spectra of HPLC fractions from extracts of fibers pre-dyed with Disperse Red 4. A-Absorbance spectra of 10ppm Disperse Red 4 standard in 1:1 methanol/water (v:v) (dark trace) and fraction collected at 14.9 minutes from HPLC chromatogram of Disperse Red 4 extract (clear trace). B-Absorbance spectra of fraction collected at 12.9 minutes from HPLC chromatogram of Disperse Red 4 extract.

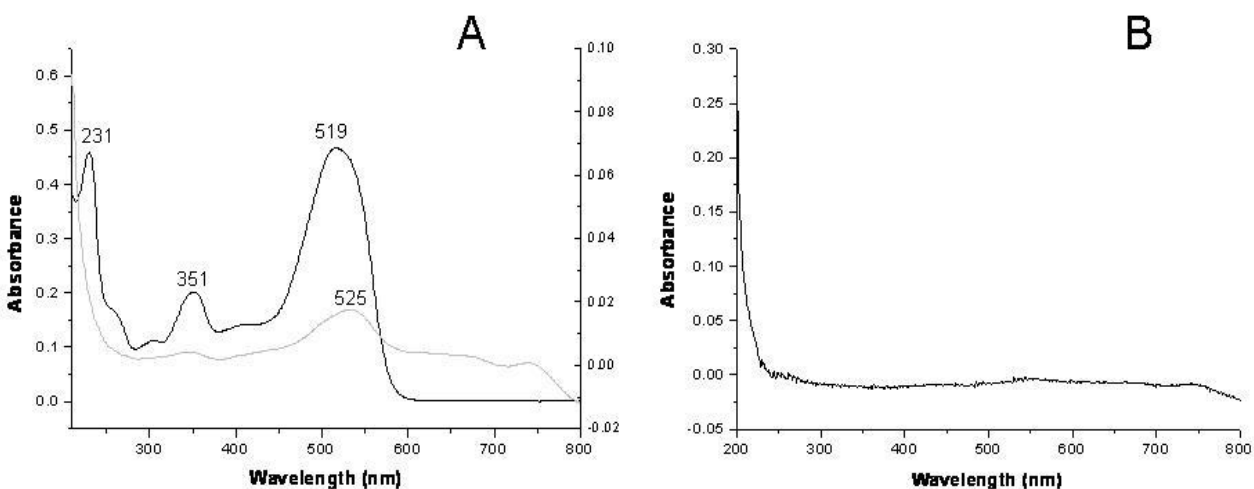


Figure III.28: Absorbance spectra of HPLC fractions from extracts of fibers pre-dyed with Acid Red 151. A-Absorbance spectra of 10ppm Acid Red 151 standard in 1:1 methanol/water (v:v) (dark trace) and fraction collected at 12.96 minutes from HPLC chromatogram of Acid Red 151 extract (clear trace). B-Absorbance spectra of fraction collected at 32.9 minutes from HPLC chromatogram of Acid Red 151 extract.

Additional evidence for Basic Red 4 is provided in figure III.29-A, which compares the excitation and fluorescence spectra of a 10ppm Disperse Red 4 dye standard solution in 50% methanol-water (volume/volume) to the fluorescence spectrum of the HPLC fraction collected from the extract at 14.9 min (refer to figure III.24 for chromatographic time). Figure III.29-B shows the excitation and emission spectra of the HPLC fraction collected from the extract at 12.9 min (refer to figure III.24 for chromatographic time). These spectra were recorded at the same excitation (512nm) and emission (570nm) wavelengths as the spectra in figure III.29-A. The similarity of the spectral features in figure III.29-A, and the lack of fluorescence in figure III.29-

B, confirm the assignment of the main fluorescence peak at 12.9 min to an impurity and not to the presence of the dye.

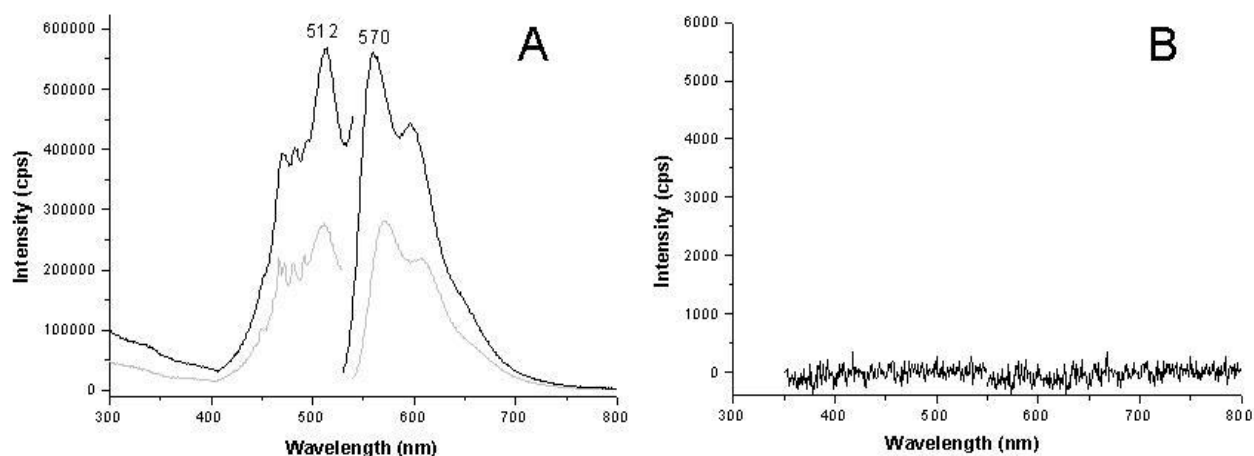


Figure III.29: Visible excitation and emission spectra of HPLC fractions from extracts of fibers pre-dyed with Disperse Red 4. A-Fluorescence spectra of 10ppm Disperse Red 4 standard in 1:1 methanol/water (v:v) (dark trace) and fraction collected at 14.9 minutes from HPLC chromatogram of Disperse Red 4 extract (clear trace). B-Fluorescence spectra of fraction collected at 12.9 minutes from HPLC chromatogram of Disperse Red 4 extract. Exciting at maximum excitation (512nm) and collecting excitation with emission set at (570nm). Excitation slits set at 4 and emission slits set at 2 nm band-pass respectively.

Figure III.30-A compares the excitation and fluorescence spectra of the extract from fibers pre-dyed with Disperse Red 4 to those recorded from the HPLC fluorescence fraction of the same extract collected at 12.9min. Figure III.30-B shows the excitation and emission spectra recorded from the HPLC absorption fraction of the same extract collected at 14.9min. The similarity of the spectral features in figure III.30-A, and the lack of fluorescence in figure III.30-B, confirm that the fluorescence of the extract in the ultraviolet spectral region is due to the presence of fluorescence impurities and not to the presence of the dye. One should notice that similar differences in the relative intensities of the two fluorescence peaks with maximum wavelengths at 348 and 415nm were also observed in the spectra of extracts from fibers with different lengths. Spectra from extracts of fibers with 2cm and 1cm lengths showed the highest peak at 415nm. Extracts from 2 mm fibers showed the highest fluorescence peak at 348nm. These facts indicate a correlation between the spectral features of the extract and the concentration of its fluorescence impurities. Further studies are needed to understand the role of the concentration of fluorescence impurities on synergistic and inner filter effects.

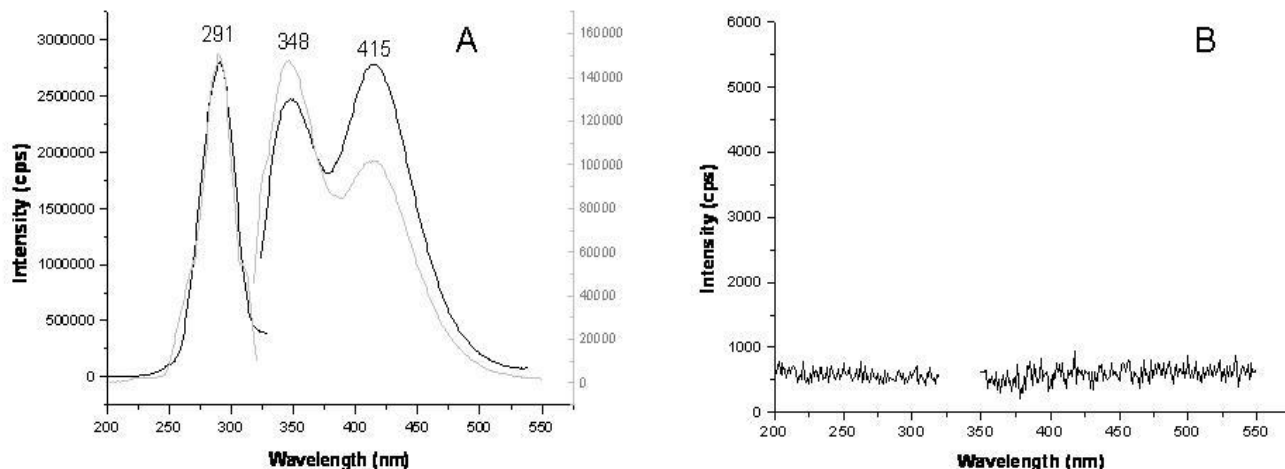


Figure III.30: UV excitation and emission spectra of HPLC fractions from extracts of fibers pre-dyed with Disperse Red 4. A-Fluorescence spectra of extract from fibers pre-dyed with Disperse Red 4 in 1:1 methanol/water (v:v) (dark trace) and fraction collected at 12.9 minutes from HPLC chromatogram of Disperse Red 4 extract (clear trace). B-Fluorescence spectra of fraction collected at 14.9 minutes from HPLC chromatogram of Disperse Red 4 extract. Exciting at maximum excitation (291nm) and collecting excitation with emission set at (348nm). Excitation slits set at 4 and emission slits set at 2 nm band-pass respectively.

Figure III.31 overlays the excitation and fluorescence spectra of the extract from fibers pre-dyed with Acid Red 151 to those recorded from the HPLC fluorescence fraction of the same extract collected at 22.9min (III.31-A) and 28.9 min (III.31-B). The reader should refer to fluorescence chromatogram in III.26 for retention time guidance. Their comparison clearly demonstrates the main contribution of two different fluorescence impurities to the total fluorescence spectrum of the extract.

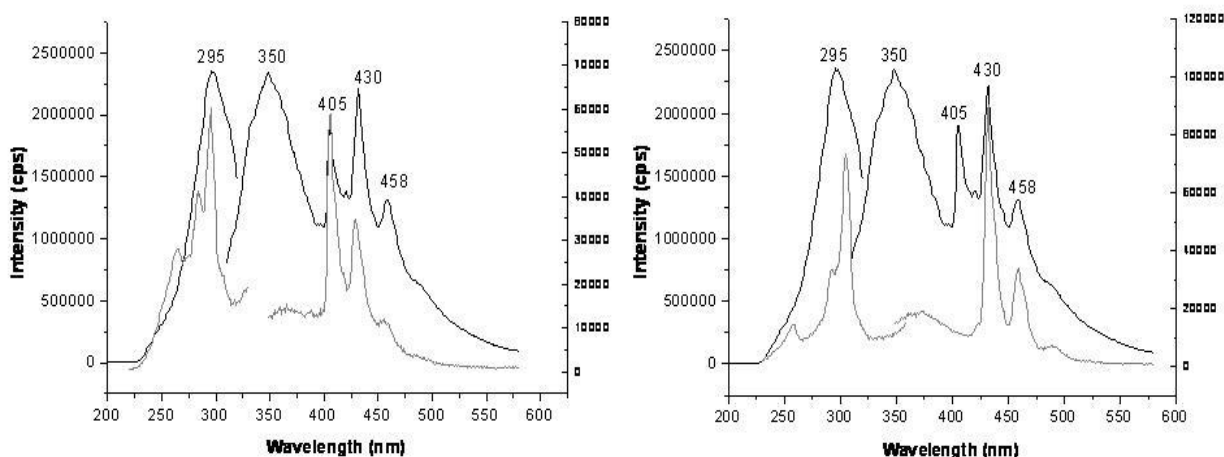


Figure III.31: UV excitation and emission spectra of HPLC fractions from extracts of fibers pre-dyed with Acid Red 151. A-Fluorescence spectra of extract from fibers pre-dyed with Acid Red 151 in ethanol (dark trace) and fraction collected at 22.9 minutes from HPLC chromatogram of Acid Red 151 extract (clear trace). Exciting at maximum excitation (295nm) and collecting excitation with emission set at (405nm). B-Absorbance spectra of fraction collected at 28.9 minutes from HPLC chromatogram of Acid Red 151 extract. Exciting at maximum excitation

(303nm) and collecting excitation with emission set at (430nm)Excitation slits set at 4 and emission slits set at 2 nm band-pass respectively.

### III.4. Room Temperature Fluorescence –Excitation Emission Matrix Spectroscopy

Eight types of textiles fibers were investigated via RTF – EEM spectroscopy. For the purpose of comparison, EEM were also recorded from their respective Sigma-Aldrich standards. Appendix E compares the EEM of the fiber extracts to those recorded from the Sigma-Aldrich dye standards. Clearly, all the EEM of the fiber extracts are different to their respective counterparts. Table III.5 provides a visual comparison of the spectral profiles obtained via 2D and EEM fluorescence spectroscopy. When examining this table, the reader should keep in mind that the HPLC fluorescence chromatograms of the nine fiber extracts were different than those recorded from the respective Sigma-Aldrich standards. The fact that two of the fiber extracts provide very similar 2D spectral profiles to those recorded from the Sigma-Aldrich standards indicates insufficient selectivity of the 2D data format for forensic fiber discrimination.

*Table III.5 Profile comparison of 2D RT-excitation and fluorescence spectra and RTF-EEM recorded from dye reagents and fiber extracts*

<i>Type of Fiber</i>	<i>2D-Excitation</i>	<i>2D-Fluorescence</i>	<i>EEM</i>
Disperse Red 4	different	different	different
Disperse Blue 56	<i>very similar</i>	<i>very similar</i>	different
Basic Green 4	<i>very similar</i>	<i>very similar</i>	different
Basic Red 9	different	different	different
Acid Red 151	different	different	different
Acid Yellow 17	different	different	different
Acid Yellow 23	different	different	different
Acid Green 27	different	different	different

Figure III.20 – which is shown in section III.2 - compares the 2D-excitation and 2D-fluorescence spectra of the fiber extracts pre-dyed with Basic Green 4 to those recorded from their respective Sigma-Aldrich dye standard. The spectral profiles of the extracts and the standard are virtually the same, which makes visual discrimination within these two not possible. As shown in figure E.3 (see appendix E), recording RTF-EEM makes their visual discrimination possible.

Figure III.32 compares the EEM of Disperse Blue 56 and the fluorescence chromatograms of the standard and the fiber extract recorded with two sets of excitation and emission wavelengths. Considering the chromatographic retention times of 20.5 min (583/660nm) and 20.88 (320/385nm) statistically similar ( $P = 95\%$ ,  $N_1 = N_2 = 3$ ) [78], the several peaks with different retention times indicate the presence of several fluorescence concomitants in the extract not present in the standard. The main reason RTF-EEM data formats were able to differentiate between the extract and the standard is their ability to convolute the contribution of all fluorescence components within the ultraviolet and visible spectral regions.

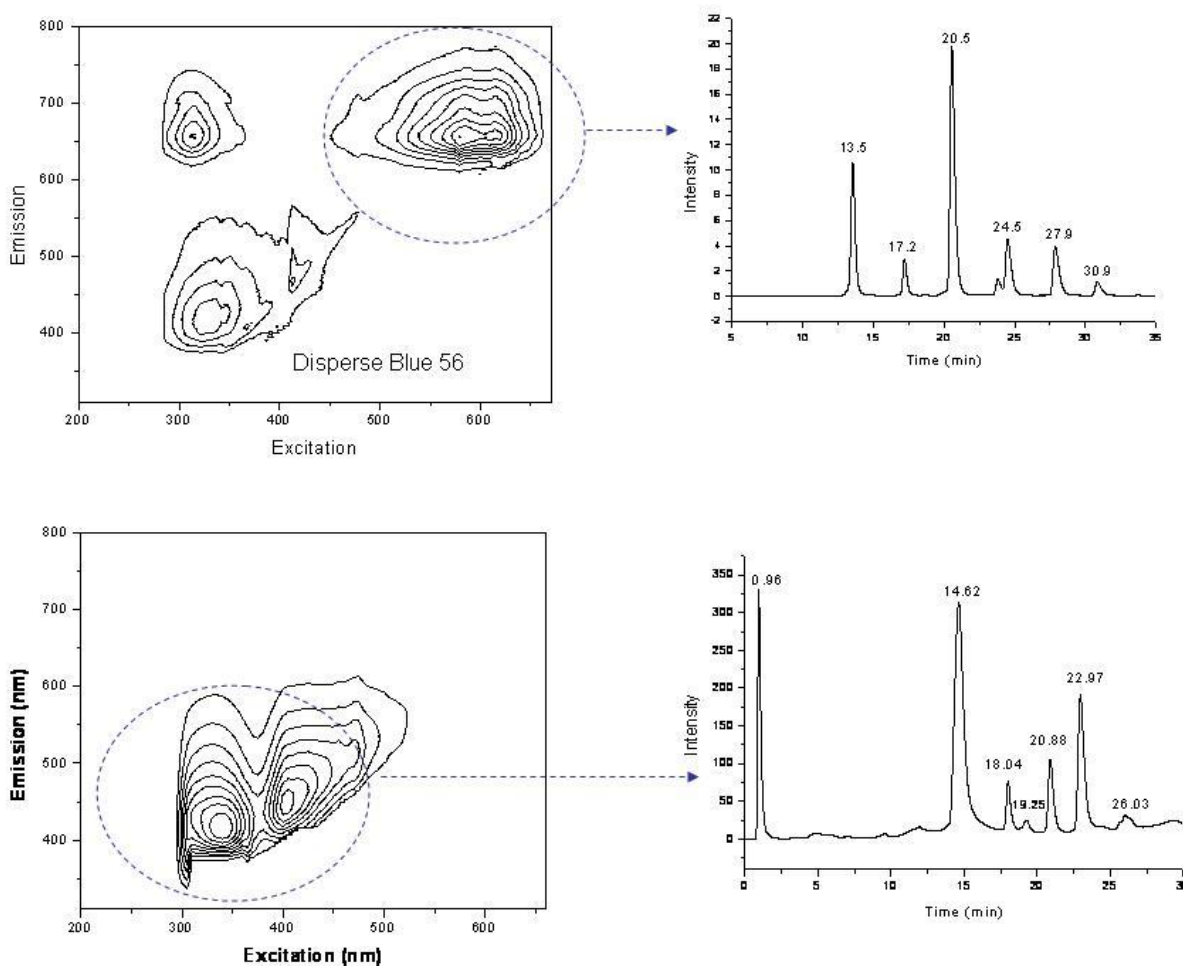


Figure III.32: RTF-EEM and HPLC chromatograms of Disperse Blue 56 Sigma-Aldrich standard and extract from fibers pre-dyed with Disperse Blue 56. Top-EEM and fluorescence chromatograms of Disperse Blue 56 standard with excitation set at 583nm and the emission detector set at 660nm. Bottom- EEM and fluorescence chromatograms of Disperse Blue 56 fiber extract with excitation set at 320nm and the emission detector set at 385nm.

### III.5. Comparison of RTF-EEM Recorded from Fiber Extracts of Visually Indistinguishable Fibers

Figure III.33 shows examples of EEM recorded from fiber extracts Acid Yellow 17 and Acid Yellow 23. Examples of EEM recorded from the two sets of fiber extracts Acid Red 151 are shown in figure III.34 and III.35.

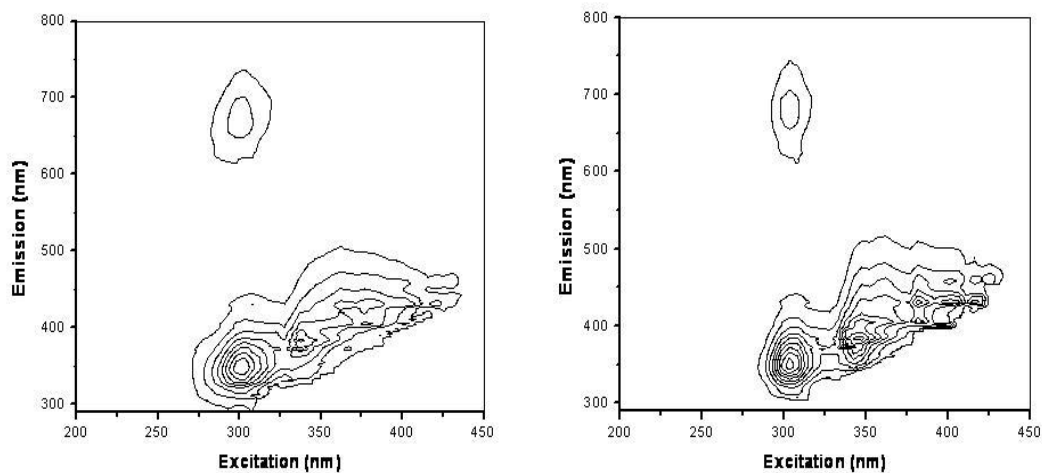


Figure III.33: RTF-EEM recorded from extracts of fibers pre-dyed with Acid Yellow 17 (left) and Acid Yellow 23 (right)

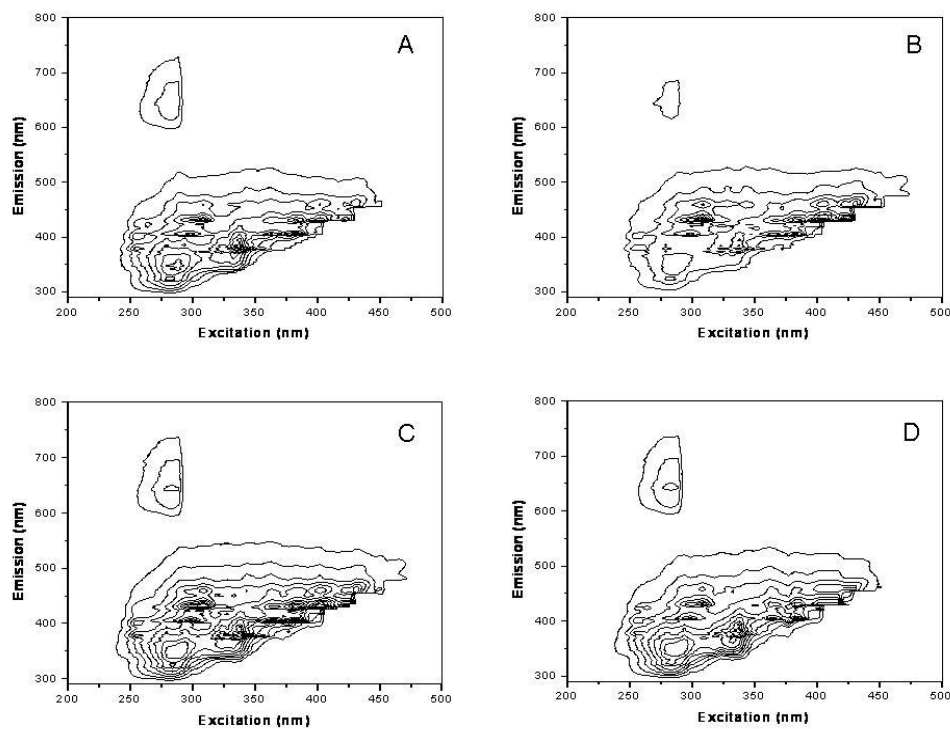
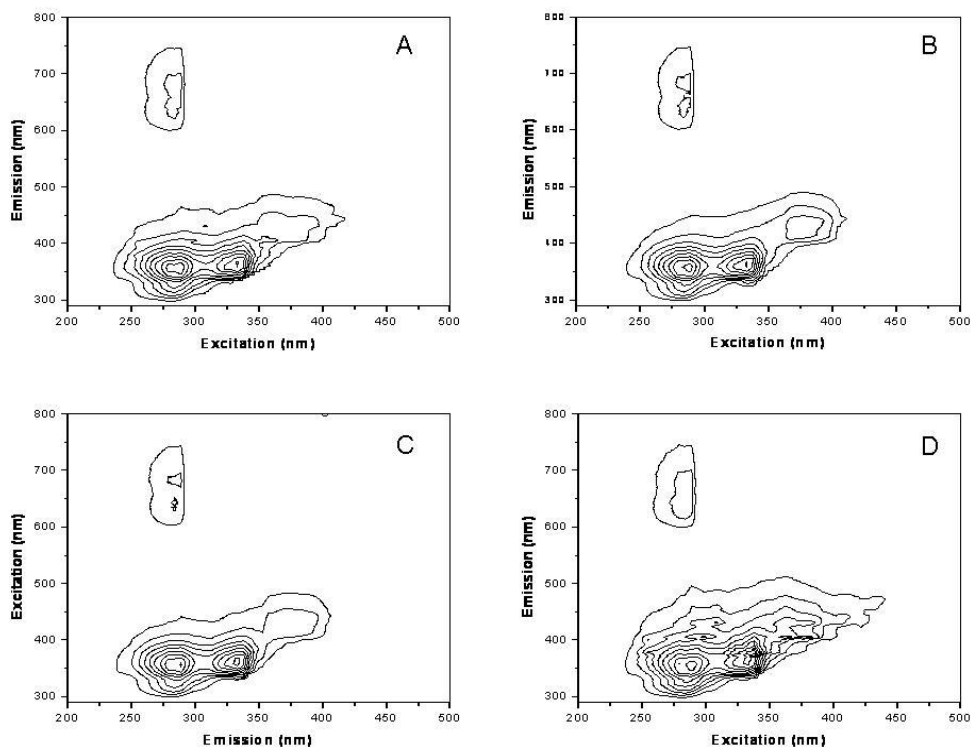


Figure III.34: RTF-EEM from fiber samples of set #1, nylon cloth pre-dyed with Acid Red 151.



*Figure III.35: Four EEM from fiber samples of set #2, second nylon cloth pre-dyed with Acid Red 151*

MCR-ALS analysis of EEM recorded from fiber extracts Acid Yellow 17 and Acid Yellow 23 provided five fluorescence components per extract. Their predicted excitation and fluorescence spectra are shown in figure III.36 (Acid Yellow 17) and figure III.37 (Acid Yellow 23). Although the number of fluorescence components in both types of extracts is the same, the spectral profiles of the individual components of Acid Yellow 17 are considerably different to those observed from the individual components in Acid Yellow 23. Their excitation and emission spectra are overlaid in figures III.38 and III.39, respectively. Interesting to note is the good agreement between the number of fluorescence components in the EEM of Acid Yellow 23 and the number of fluorescence peaks in the chromatogram of the same type of extract (see figure III.40).

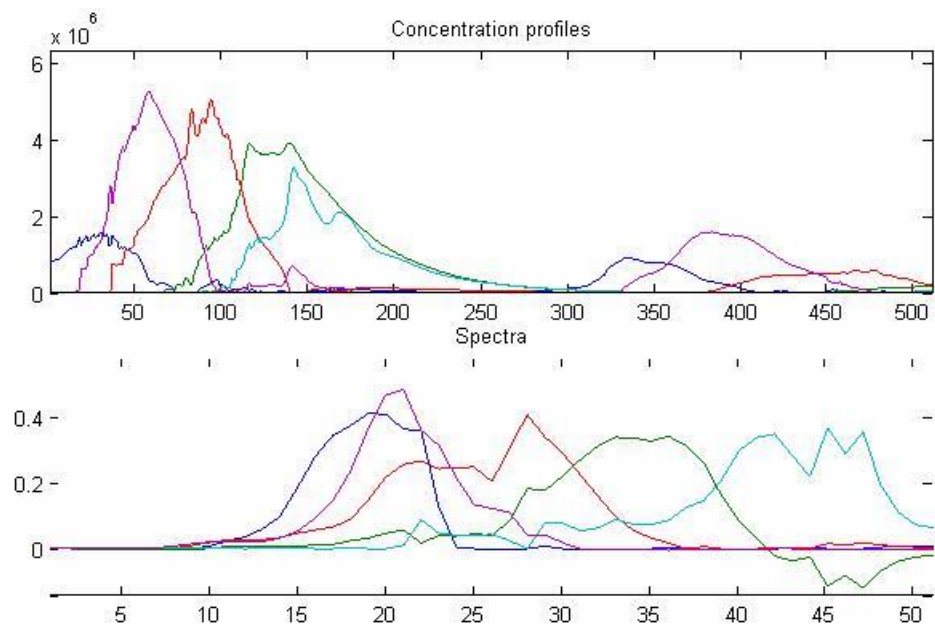


Figure III.36: Emission (top) and excitation (bottom) profiles predicted from EEM of extracts from nylon fibers dyed with Acid Yellow 17.

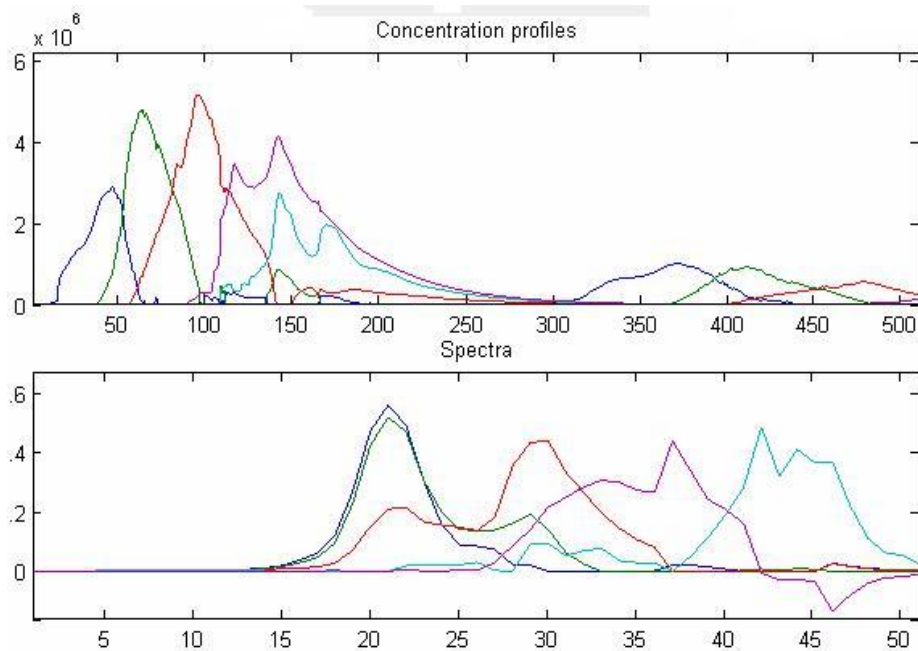
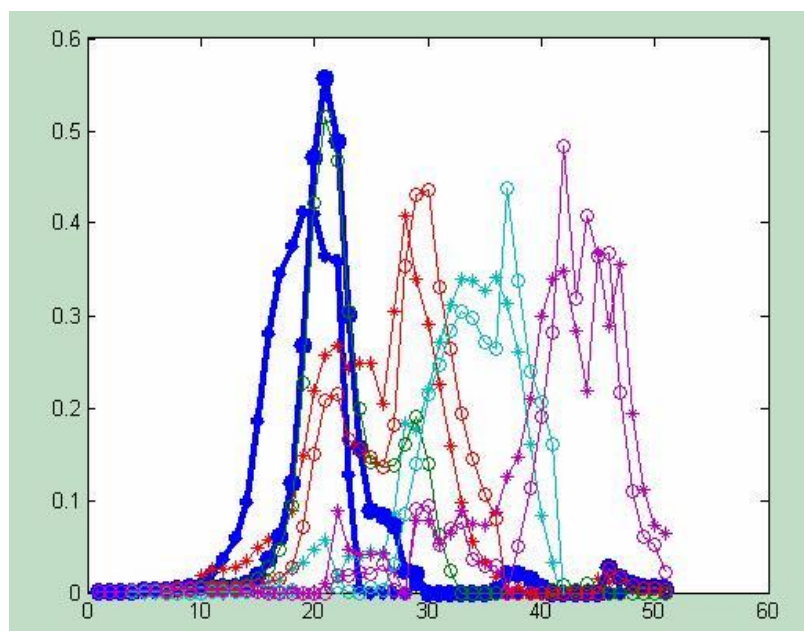
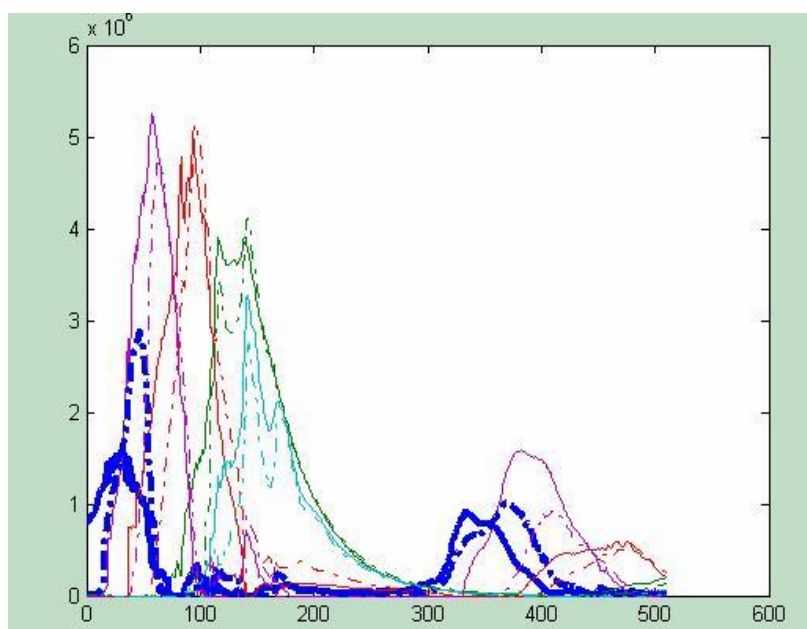


Figure III.37: Emission (top) and excitation (bottom) profiles predicted from EEM of extracts from nylon fibers dyed with Acid Yellow 23.



*Figure III.38: Overlay comparison of the five extracted excitation profiles taken from EEM of nylon fibers dyed with Acid Yellow 17 and 23. Stars represent profiles of Acid Yellow 17 and Spectra represented by circles are profiles from Acid Yellow 23. Components two (red spectra), four (cyan spectra) and five (green spectra) show the strongest correlation.*



*Figure III.39: Overlay comparison of the five emission profiles extracted from EEM of Extracts from Nylon Fibers Pre-Dyed with Acid Yellow 17 and 23. Solid lines represent profiles of Acid Yellow 17 and spectra represented by dotted lines are profiles from Acid Yellow 23. Components two (purple spectra), three (red spectra) and four (green spectra) show the strongest correlation.*

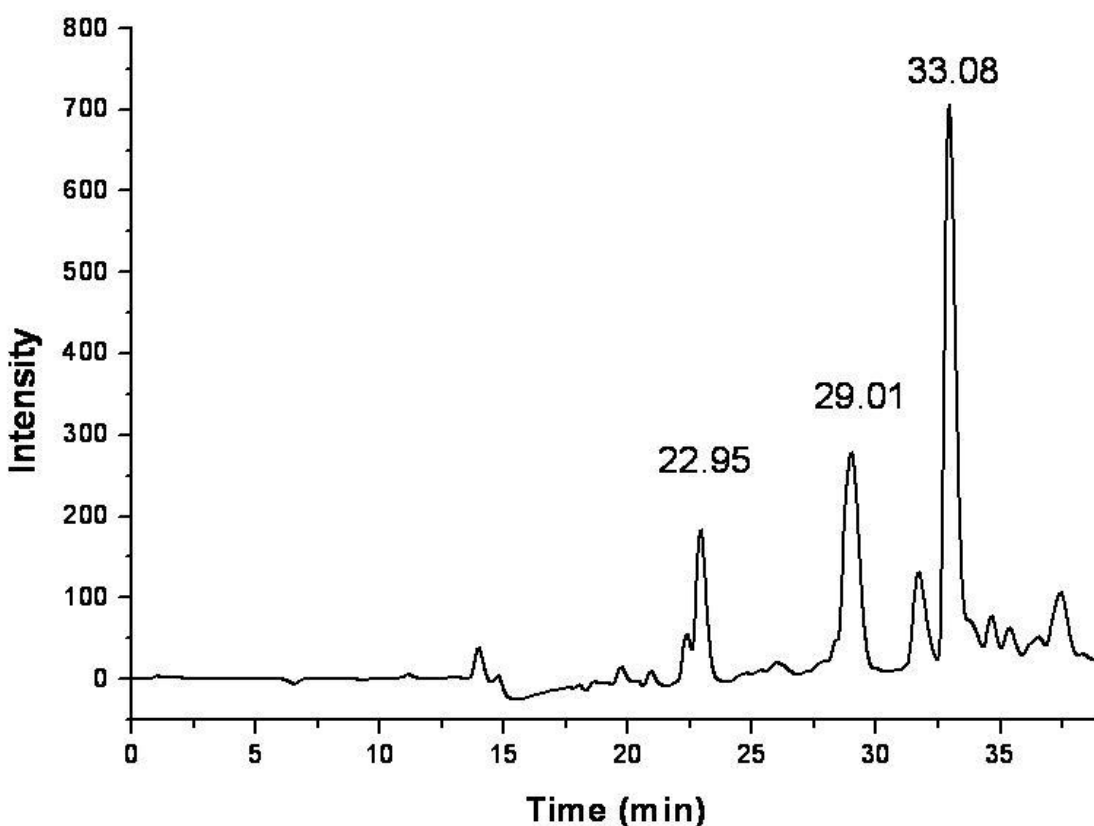


*Figure III.40: Fluorescence chromatogram of extracts from fibers pre-dyed with Acid Yellow 23. Excitation set at 290nm and emission detector set at 345nm.*

Figures III.41 and III.42 correlate the excitation and fluorescence spectra of the five fluorescence components in each type of fiber extract. The five correlations were made comparing the spectral intensities of the corresponding components in each type of extract at each excitation and fluorescence wavelength. From the calculated values of the correlation coefficients, it becomes readily apparent that only three of the five components exhibit similar spectral profiles. Close comparison of the five pairs of excitation and fluorescence spectra support correlation coefficients close to unity for three predicted components. Based on the prediction that two components only exist in one type of fiber extract, MCR-ALS is able to discriminate among these two types of visually indistinguishable fibers.

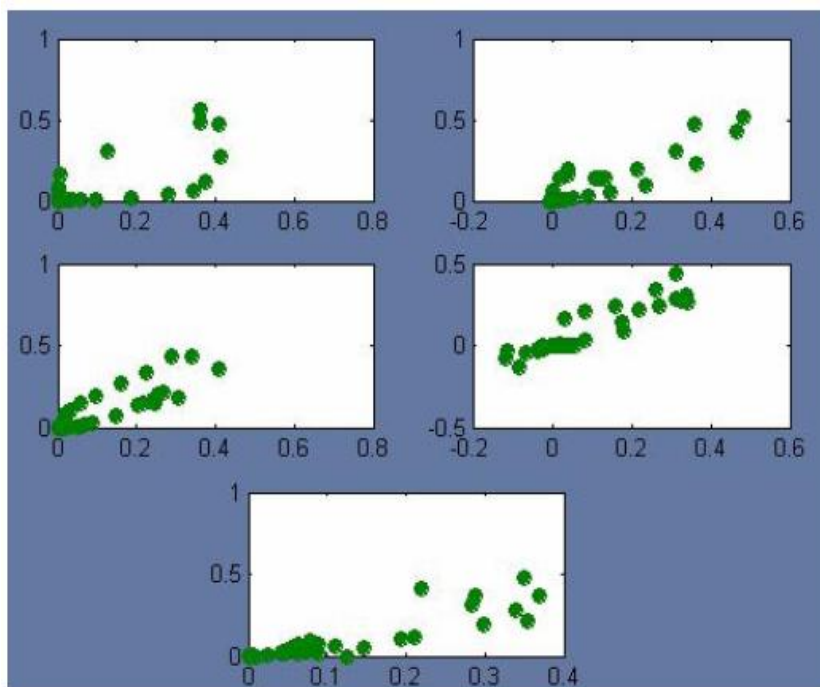


Figure III.41: correlation of the five excitation profiles predicted from EEM of extracts of nylon fibers pre-dyed with Acid Yellow 17 and 23. Correlation is done by comparing intensities of the excitation profiles from each component versus wavelength. Five correlation coefficients are as follows top left-0.7562; top right-0.9186; middle left-0.8875; middle right-0.9301, bottom-0.8956.

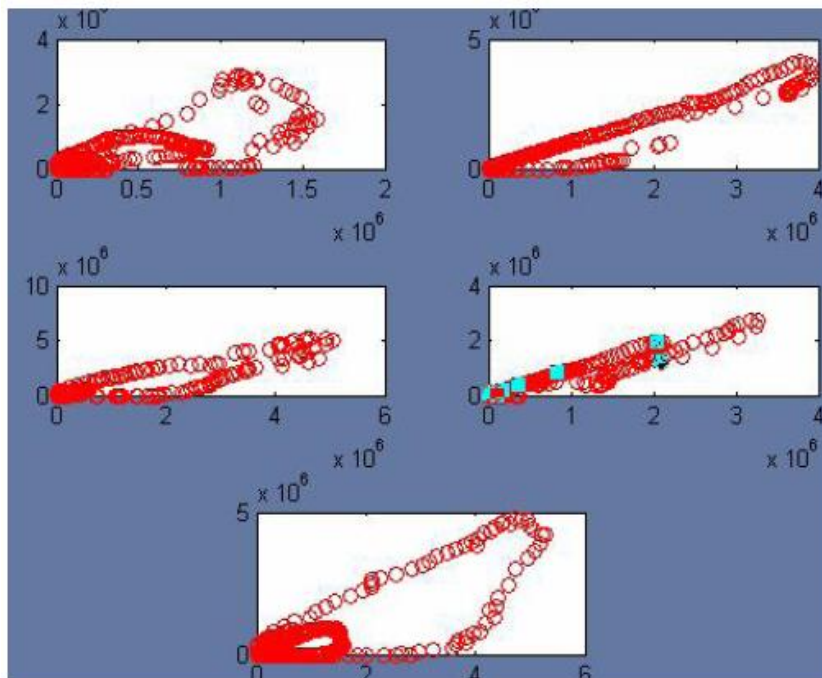
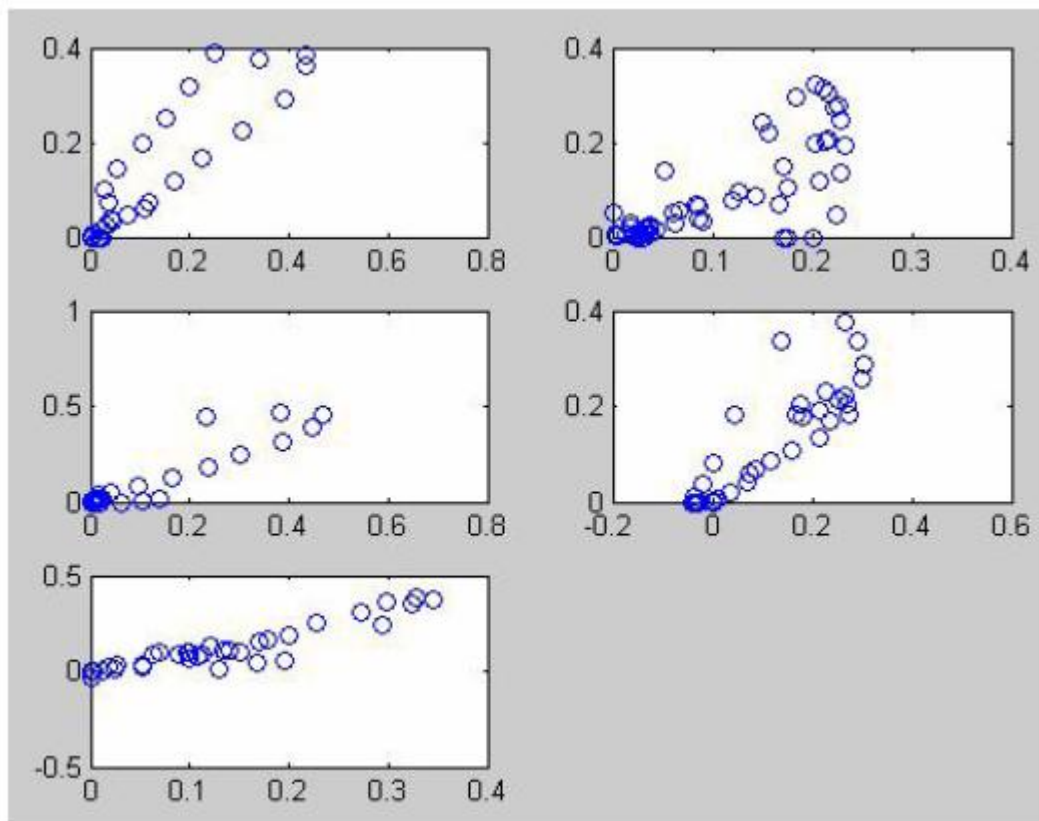


Figure III.42: Correlation of five emission profiles extracted from EEM of extracts taken from nylon fibers dyed with Acid Yellow 17 and 23. Correlation is done by comparing intensity of excitation profile versus wavelength. Five correlation coefficients are as follows top left-0.7564; top right-0.9696; middle left-0.9480; middle right-0.9677, bottom-0.8300.

Figures III.44 and III.45 show the correlation among the intensities of the excitation and fluorescence profiles of the five components predicted from the EEM recorded from the two sets of Acid Red 151 fiber extracts. Close examination of correlation coefficient values in figure III.44 predict strong similarity of excitation profiles among four of the five fluorescence components. Three of the five correlation coefficients in figure III.45 predict strong similarity of fluorescence spectra among three of the five fluorescence components.



*Figure III.44: Correlation of five excitation profiles extracted from EEM of extracts taken from nylon fibers of two different cloths dyed with Acid Red 151. Correlation is done by comparing intensity of excitation profile versus wavelength. Five correlation coefficients are as follows top left-0.93; top right-0.77; middle left-0.94; middle right-0.91, bottom-0.95.*

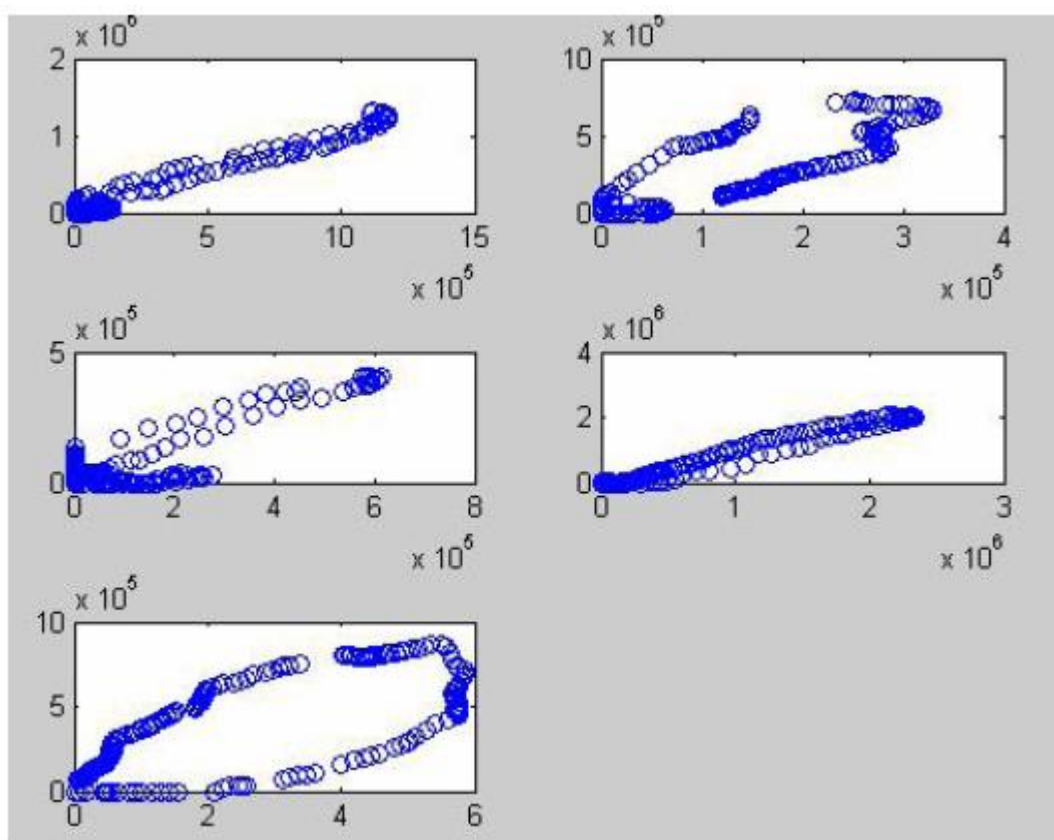


Figure III.45: Correlation of five emission profiles extracted from EEM of extracts taken from nylon fibers of two different cloths dyed with Acid Red 151. Correlation is done by comparing intensity of excitation profile versus wavelength. Five correlation coefficients are as follows top left-0.99; top right-0.85; middle left-0.88; middle right-0.99, bottom-0.77.

Visual inspection of the excitation and fluorescence profiles overlaid in figures III.46 and III.47 confirm these correlations. Considering the number of similar excitation (4) and fluorescence (3) profiles it is safe to assume that three of the five fluorescence components are present in both sets of fibers. Two of the remaining four components are present in only one set of fibers. The differences among the spectra of the two pairs of different components explain the EEM contour differences observed in figures III.34 and III.35. Based on the prediction that two components only exist in one type of fiber extract, MCR-ALS is able to discriminate among Acid Red 151 extracts of fibers collected from two different cloths.

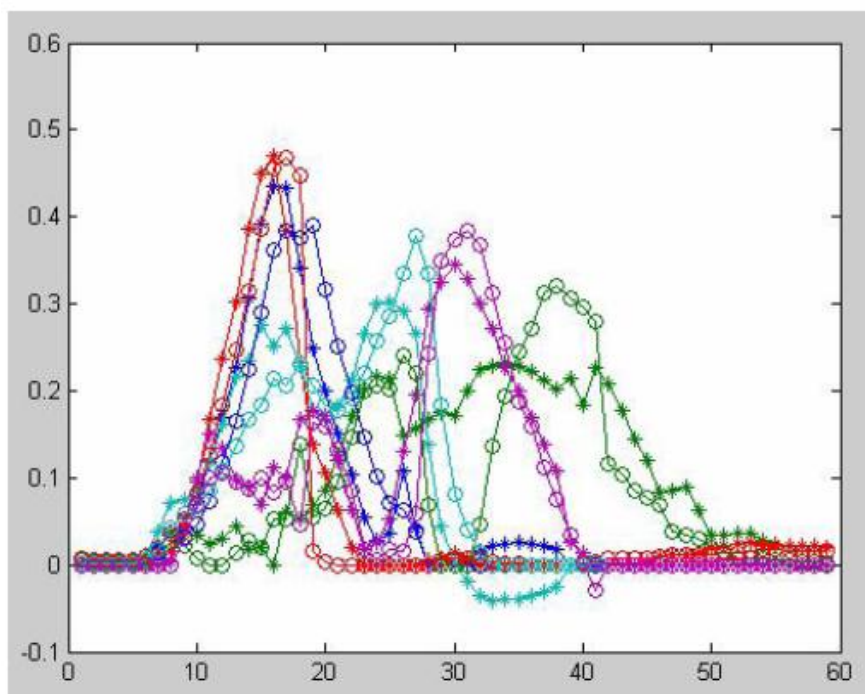


Figure III.46: comparison of the five excitation profiles extracted from EEM of nylon fibers collected from two different clothes dyed with Acid Red 151. Stars represent profiles of Acid Red 151 cloth #1 and Spectra represented by circles are profiles from Acid Red 151 circles. Components one (red spectra), three (blue), four (cyan spectra) and five (purple spectra) show the strongest correlation.

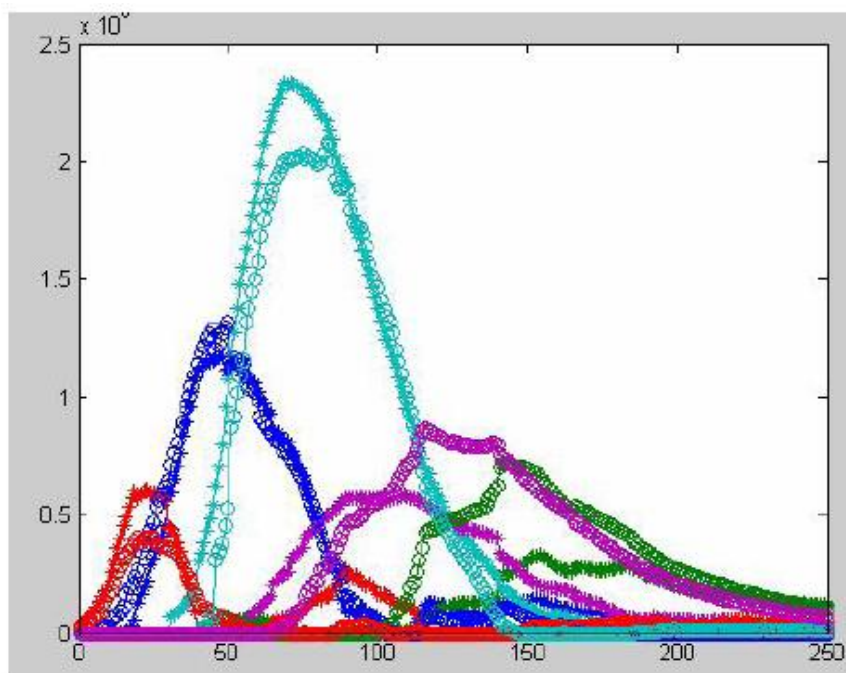


Figure III.47: Comparison of the five extracted emission profiles taken from EEM of nylon fibers from two different clothes dyed with Acid Red 151. Stars represent profiles of Acid Red 151 cloth #1 and Spectra represented by circles are profiles from Acid Red 151 circles. Components one (red spectra), three (blue), and four (cyan spectra) show the strongest correlation.

### III.6. Effects of Environmental Contaminants on the Fluorescence of Textile Fibers

#### III.6.1. Analysis of fibers exposed to cigarette smoke

Solvent extraction of fibers unexposed to cigarette smoke provided n-octane extracts with no fluorescence. This fact agrees well with our previous results from fiber extractions that showed the polar nature of both dyes and fluorescence inherent impurities. Solvent extraction of fibers exposed to cigarette smoke provided n-octane extracts with strong fluorescence. Attributing the observed fluorescence to the adsorption of PAH from cigarette smoke, n-octane fiber extracts were submitted to PAH analysis via HPLC. Chromatographic analysis was carried out via an experimental procedure previously established in our lab [79]. Figure III.48 compares the absorption chromatogram of the EPA-PAH standard mixture to a chromatogram recorded from one fiber extract. Several peaks in the extract chromatogram match the retention times of EPA-PAH. Based on their retention times, the unknown peaks in the fiber extract can be attributed to the presence of naphthalene, phenanthrene, anthracene, pyrene and benzo(a)pyrene.

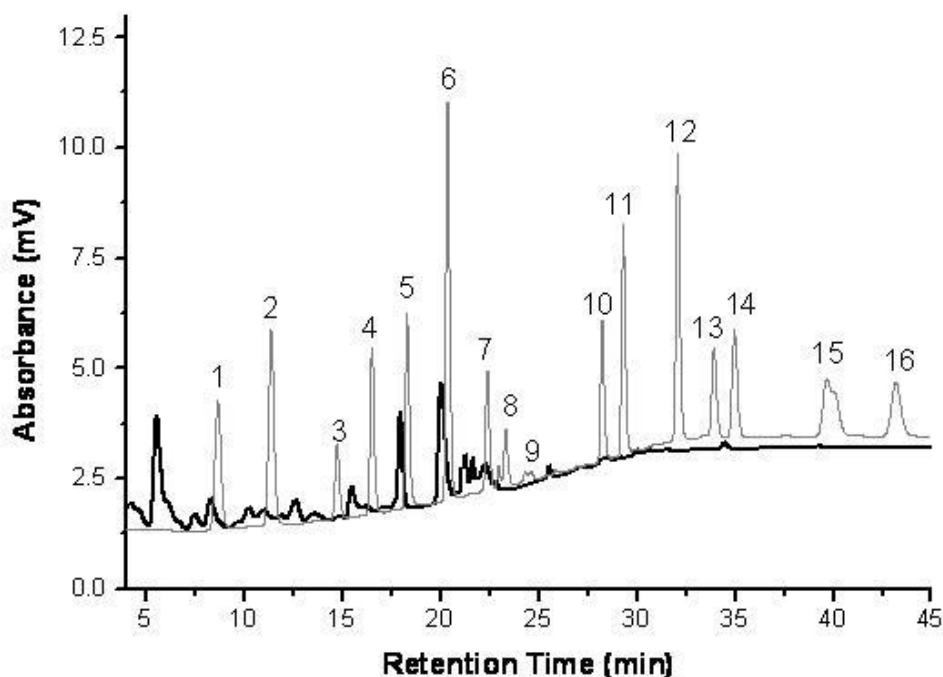


Figure III.48: HPLC chromatograms recorded from a standard 16 EPA-PAH mixture (grey trace) and an n-octane extract taken from 1cm of acetate 154 fiber pre-dyed with Disperse Red 1 previously exposed to cigarette smoke (black trace). Peak assignment as follows: 1-Naphthalene, 2-Acenaphthylene, 3-Acenaphthene, 4-Fluorene, 5-Phenanthrene, 6-Anthracene, 7-Fluoranthene, 8-Pyrene, 9-Benzo(a)anthracene, 10-Chrysene, 11-Benzo(b)fluoranthene, 12-Benzo(k)fluoranthene, 13-Benzo(a)pyrene, 14-Dibenzo(a,h)anthracene, 15-Benzo(g,h,i)perylene, 16-Indeno(1,2,3-cd)pyrene.

#### III.6.2. Spectral Characteristics of Detergents and Fabric Softeners

The absorption and fluorescence characteristics of commercial detergents and fabric softeners were investigated using solutions with typical laundering concentrations. Their concentrations were calculated taking into consideration the average volume (40 L) of a common washing machine and the quantity of detergents and fabric softeners recommended for use by the manufacturer. Of the five detergents and fabric softeners that we investigated four of them

showed strong absorbance in the ultra-violet spectral region. Figure III.49 overlays their spectral profiles and Table III.6 lists their maximum absorption wavelengths.

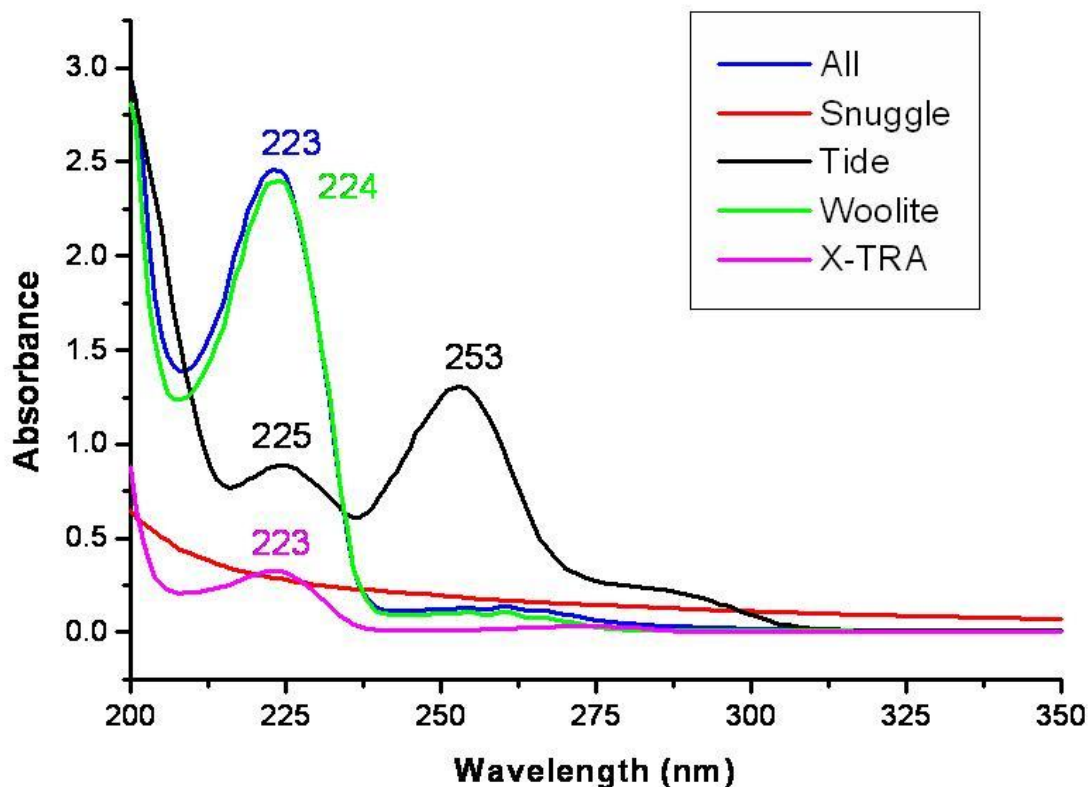


Figure III.49: Absorbance spectra of laundry detergents and fabric softeners overlaid for comparison.

Table III.6: Absorbance Wavelength Maxima of Laundry Detergents

Detergent	Wavelength (nm)
All	223
Snuggle	N/P
Tide	225, <u>253</u>
Woolite	224
XTRA	223

All the investigated detergents and softeners showed strong fluorescence upon excitation in the ultraviolet spectral region. Their excitation and fluorescence spectra are shown in Figure III.50. In all cases, fluorescence extends from the ultraviolet to the visible region. However, sample excitation in the visible region provided negligible fluorescence in all cases.

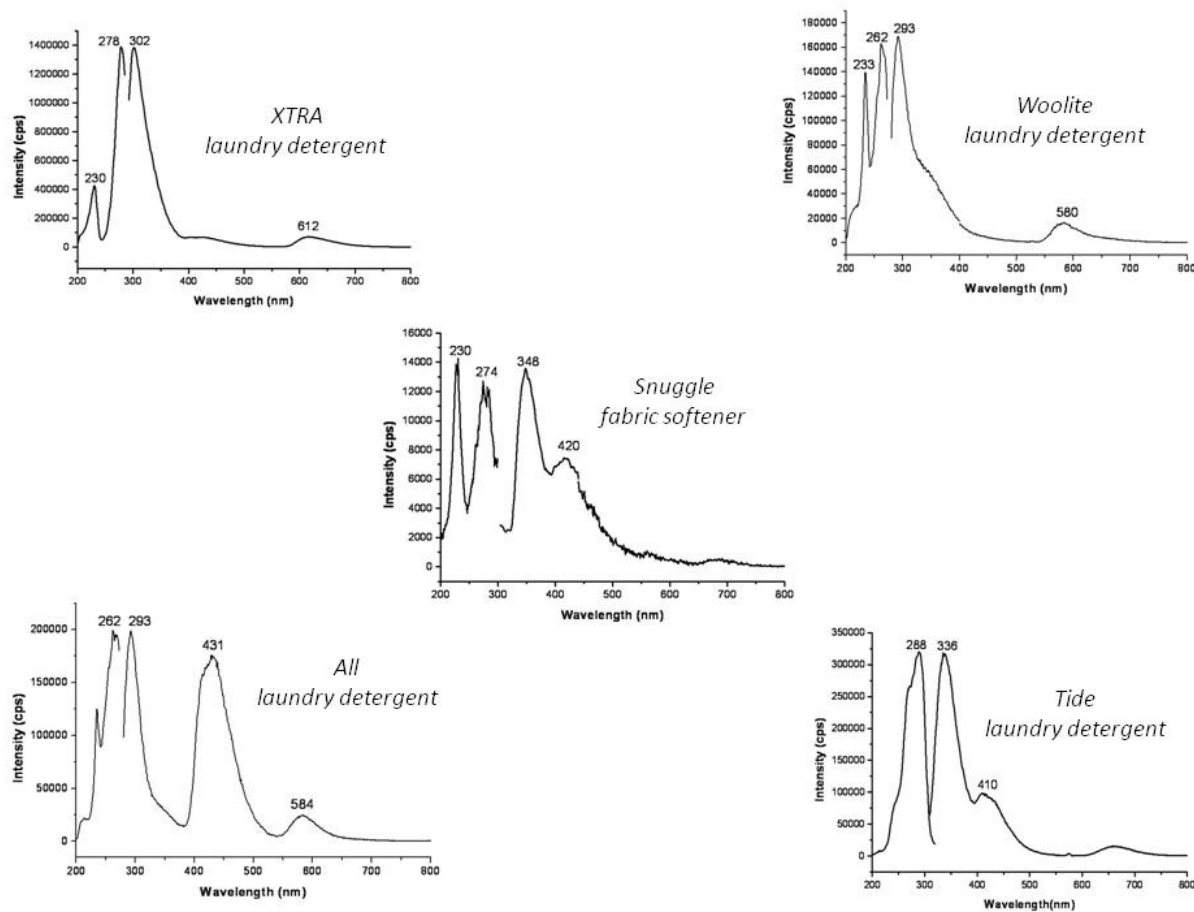


Figure III.50: RTF spectra of detergents and softeners recorded at their respective excitation and fluorescence maximum wavelengths. Excitation and emission slits set at 4 and 2nm band-pass, respectively.

### III.6.3. Fluorescence Characteristics of Disperse Red 4 Fiber Extracts after Laundering

Figure III.51 shows the change in fluorescence spectra of Disperse Red 4 fiber extracts as a function of fiber laundering with ALL detergent. Table III.7 lists the signal intensities measured at the maximum wavelengths of the two fluorescence peaks. All measurements were made upon sample excitation at 291nm, i.e. the maximum excitation wavelength of the fiber extract in the absence of detergent. The comparison of signal intensities in Table III.7 shows no significant change at 344nm. On the other end, a significant intensity enhancement is observed at 414nm. Comparison of the spectral features of ALL III.50 to those in figure III.51 shows that the main fluorescence peak of the extract (maximum wavelength at 344nm) falls within the wavelength valley ( $\sim 320$  nm to  $\sim 400$ nm) at which the detergent emits low fluorescence. The second fluorescence peak of the extract (maximum wavelength at 414nm) strongly overlaps with the fluorescence peak of the detergent at 431nm. The intensity enhancement observed at 414nm could then be attributed to the residual amount detergent on the fiber, which apparently increases with the number of washings.

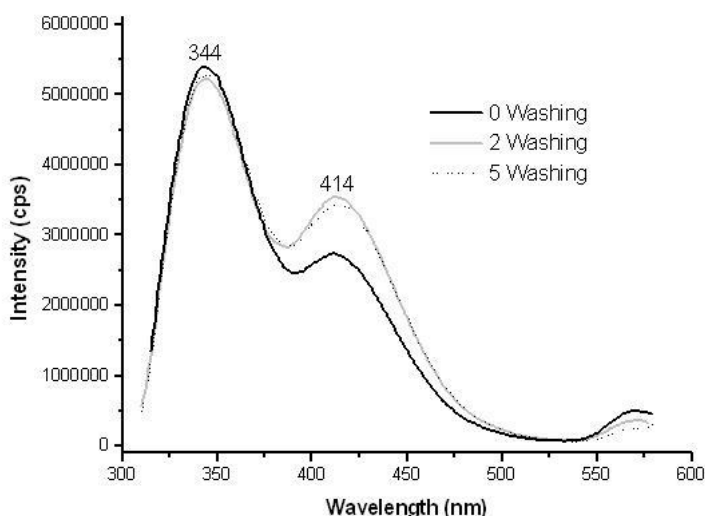


Figure III.51: Fluorescence spectra of extracts taken from fibers pre-dyed with Disperse Red 4 dye after a variable number of launderings in a washing machine. Samples excited at 291 nm with excitation and emission slits set at 4 and 2 nm band pass, respectively.

Table III.7: Fluorescence Intensity from Disperse Red 4 Extracts after Washing

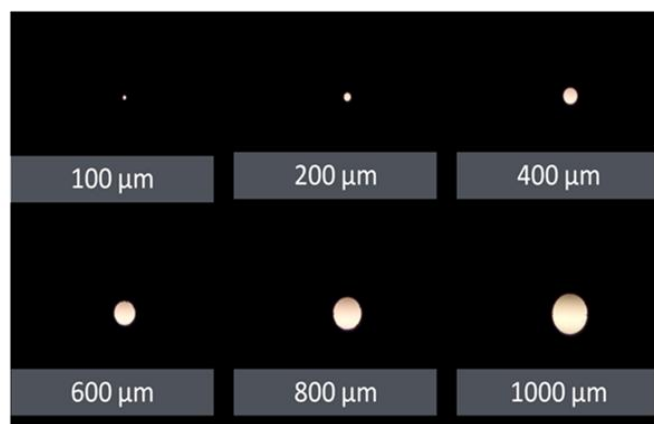
# of Washings	Intensity (cps) <sup>a</sup>	Intensity (cps) <sup>b</sup>
0	$5.40 \times 10^6$	$2.73 \times 10^6$
1	$5.29 \times 10^6$	$2.67 \times 10^6$
2	$5.23 \times 10^6$	$3.52 \times 10^6$
5	$5.27 \times 10^6$	$3.42 \times 10^6$

<sup>a</sup> Intensity measured from peak at 344nm. <sup>b</sup> Intensity measured from peak at 414nm.

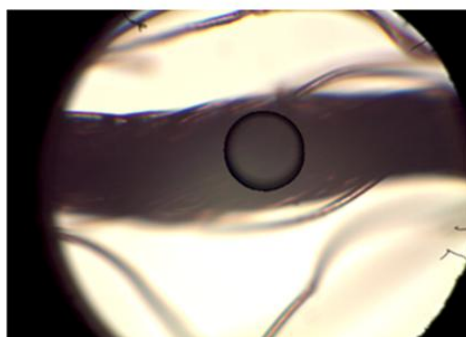
### III.7. Instrumentation for Non-destructive Analysis of Fibers

Two lenses were initially purchased for the analysis of fibers in the ultraviolet (10x-UV) and visible (10xVIS) in the spectral regions. Our selection followed the recommendation made by Olympus representatives, i.e. of the commercial source of our microscope. Figure III.52 shows images recorded from the visible “standard sample” and a textile fiber thread pre-dyed with Basic Red 4. The size of the pinhole correlates well to the size of the illuminated area in the sample. The image of the fiber thread was recorded with no pinhole. For size comparison purposes, the small circle located at the center of the thread corresponds to the area of the 100 micro-metter ( $\mu\text{m}$ ) pinhole diameter.

Figure III.53 overlays several excitation and fluorescence spectra recorded from the visible standard sample. All spectra in “A” were recorded with the same excitation and emission band-pass (5nm). As expected, the intensity of spectra decreases with the size of the pinhole. All spectra in “B” were recorded with the same pinhole diameter but with different excitation and emission band-pass. As expected, the intensity of spectra decreases with the slit-widths of the spectrofluorimeter.

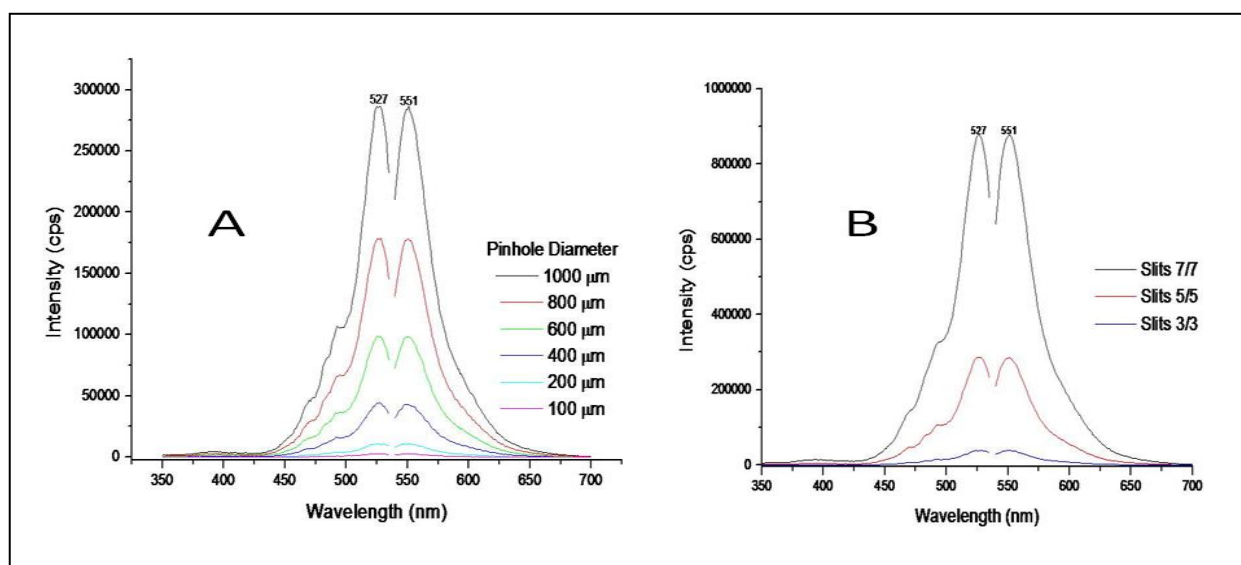


*Images of Capillary Tube Recorded at Various Pinhole Diameters*



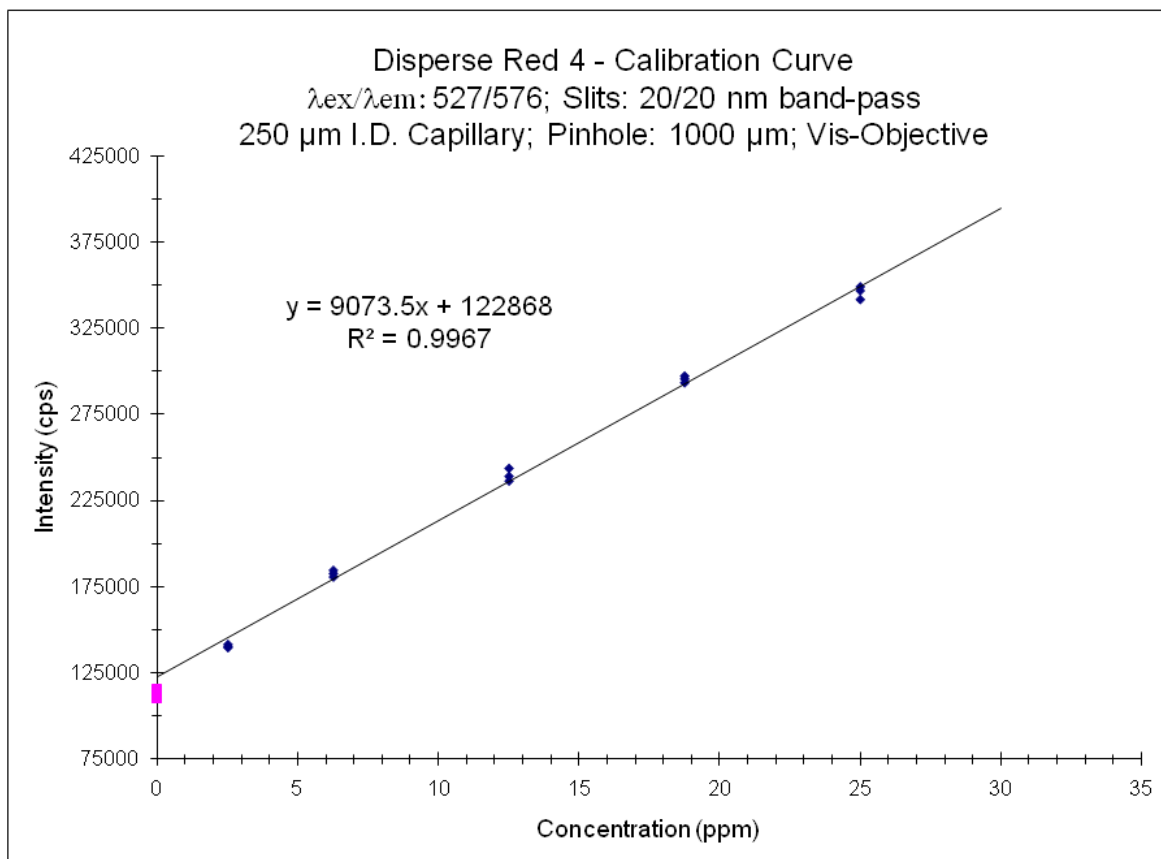
*Image of a Disperse Red 4 Fiber Thread Recorded with No Pinhole*

*Figure III.52: Comparison of pinhole sizes using images of a 250 micro-meters internal diameter capillary tube filled with a metaolic solution of Rhodamine 6G and a Disperse Red 4 fiber thread.*



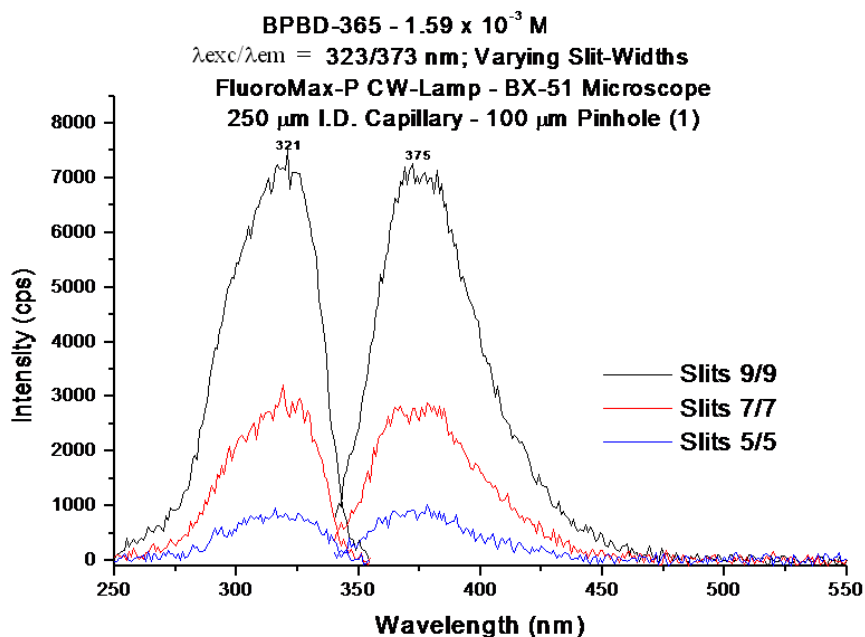
*Figure III.53: Excitation and fluorescence spectra recorded from the visible standard sample. Spectra were recorded at: (A) various pinhole diameters with constant (5nm) excitation and emission band-pass; (B) various excitation/emission bandpass with constant pinhole diameter (1000 micro-meters). Slits refer to band-pass in nm units.*

Figure III.54 shows the calibration curve recorded from several standard samples prepared with various concentrations of Disperse Red 4. Each signal plotted in the calibration graph corresponds to the average fluorescence intensity of three individual measurements made from three capillaries filled with the same concentration of laser dye. Blank measurements were made from pure methanol encapsulated in capillary tubes of 250  $\mu\text{m}$  internal diameter. The excellent linear behavior of the calibration curve demonstrates proper instrumental functioning and outstanding reproducibility of measurements.



*Figure III.54: Calibration curve for Disperse Red 4 obtained with the epi-fluorescence microscope coupled to the spectrofluorimeter.*

The same trend was observed in the ultraviolet spectral region. Figure III.55 shows the spectral features of BPBD-365 recorded with the smaller inner diameter (100 $\mu\text{m}$ ) pinhole at different excitation and emission band-pass.



*Figure III.55: Excitation and fluorescence spectra of the ultraviolet standard sample recorded with the spectrofluorimeter and the microscope at several excitation and emission band-pass. Slits refer to band-pass in nm units.*

Figure III.56 and III.57 show the general trend we observed on the signal-to-background (S/B) ratio of the visible and the ultraviolet standard samples as a function of excitation/emission band-pass and pinhole size. For any given set of excitation and emission band-pass, the value of the S/B ratio of the visible sample increases with the pinhole size. The same is true for the S/B ratio of the ultraviolet sample when recorded with 100 $\mu$ m and 400 $\mu$ m pinhole sizes. When using the 1000 $\mu$ m pinhole, the fluorescence signals recorded with the 7 and 9nm excitation/emission band-pass have the same intensity. This is the result of the detector's saturation at 9nm excitation/emission band-pass with a 1000  $\mu$ m pinhole size. Comparing the trend of the fluorescence signals recorded with 9/9 band-pass (see non-linear trend of blue dots) to those recorded with 3/3nm (see linear trend of green dots), detector saturation with the 9/9 nm band-pass appears to start with the 400 $\mu$ m pinhole. Detector's saturation should be avoided because it would lead to distorted spectra.

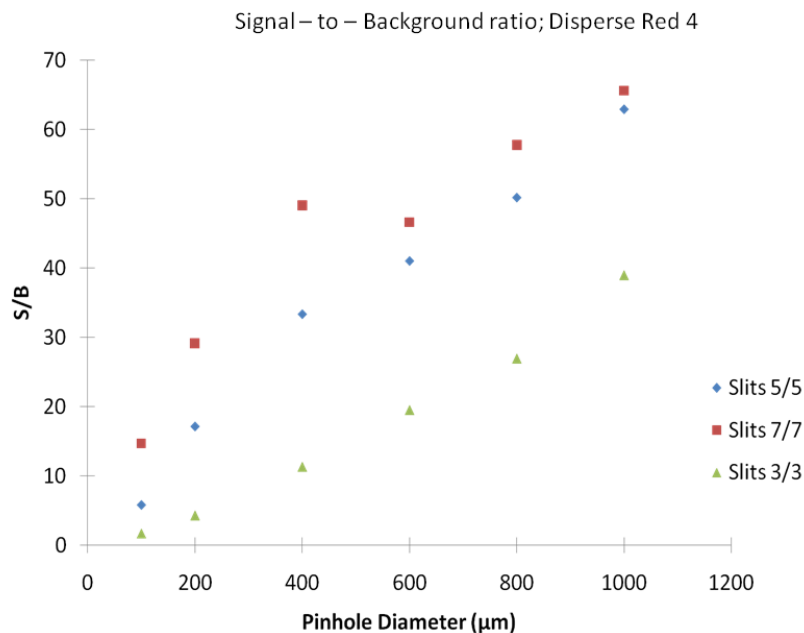


Figure III.56: Signal-to-background ratio of the visible standard sample as a function of pinhole size and slit widths ( $\mu\text{m}$ ). Slits refer to band-pass in nm units.

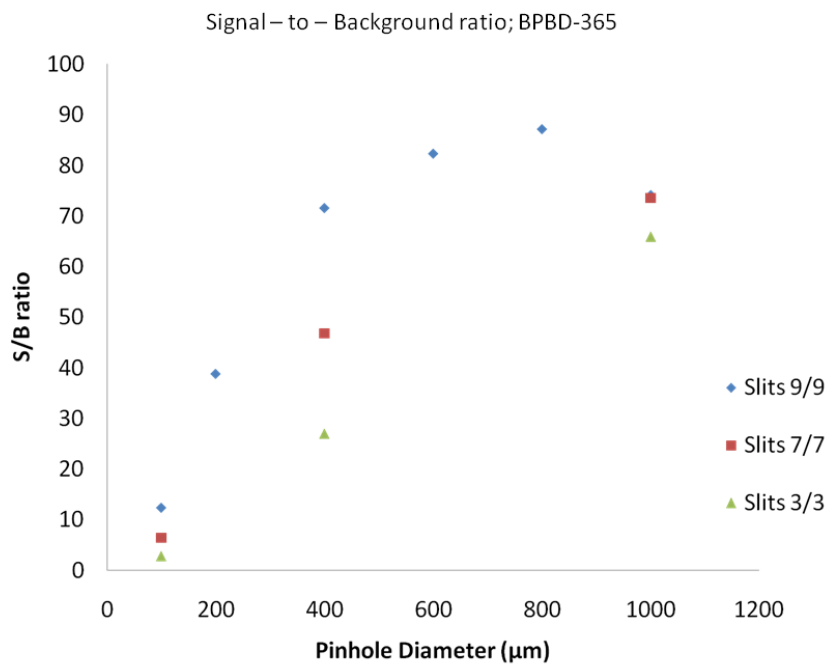


Figure III.57: Signal-to-background ratio of the ultraviolet standard sample as a function of pinhole size and slit widths ( $\mu\text{m}$ ). slits refer to band-pass in nm units.

### III.8. Spectral Reproducibility within the Length of a Single Fiber

Examples of the type of data we have generated are given in figures III.58 and III.59. Figure III.58 compares the spectral profiles (excitation and fluorescence) recorded from different areas of one “A” fiber ( $A_1$ ). The table imbedded in Figure III.58 summaries the average values of nine measurements of fluorescence intensities recorded from areas  $\alpha$ ,  $\beta$  and  $\gamma$  (holes 1-3) of three “A” fibers ( $A_1$ ,  $A_2$  and  $A_3$ ) pre-dyed with Disperse Red 4. Figure III.59 compares the spectral profiles of “B”, “C” and “D” fibers collected from the same piece of cloth in Figure III.58. The table imbedded in Figure III.59 summaries the average values of nine measurements of fluorescence intensities recorded from areas  $\alpha$ ,  $\beta$  and  $\gamma$  (holes 1-3) of three “B”, “C” and “D” fibers collected from the same piece of cloth in Figure III.58. All fluorescence intensities were measured at the maximum excitation (468nm) and emission (603nm) wavelengths. The reproducibility of spectral profiles within the same fiber and among fibers of different sections of the same piece of garment indicates a rather homogeneous composition of fluorophors. The relative standard deviations are within the reproducibility that we usually observe with fluorescence measurements.

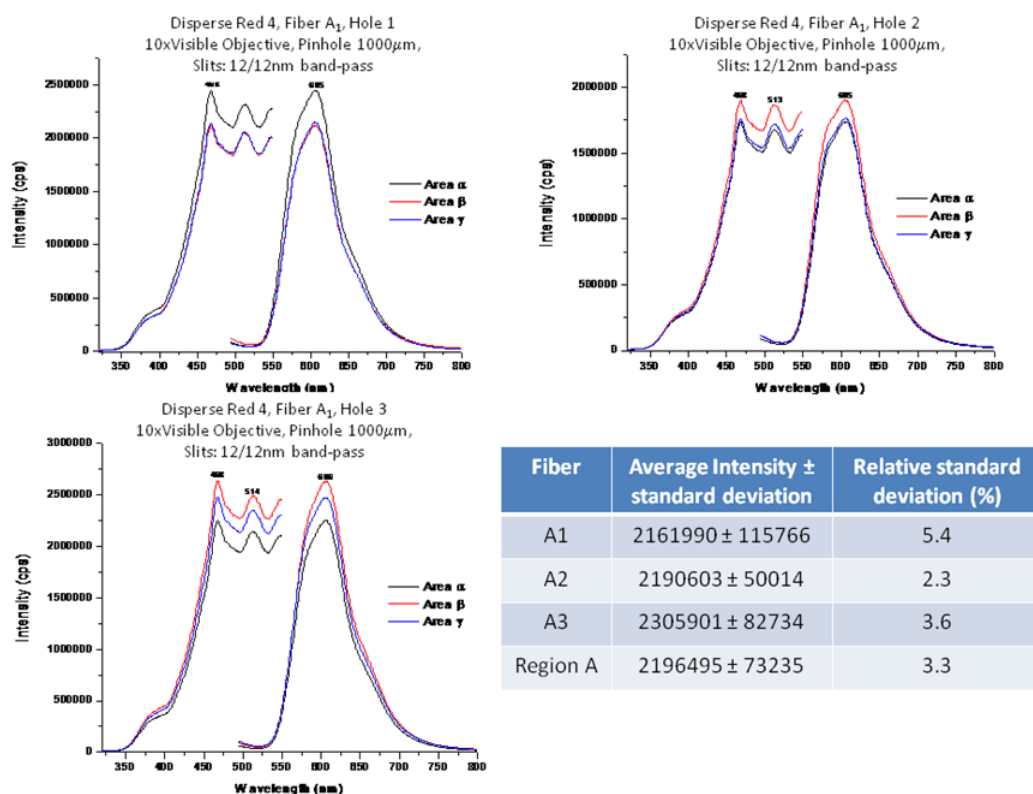


Figure III.58: Reproducibility of measurements made directly from Disperse Red 4 fibers with the spectrofluorimeter and the microscope.  $A_1$ ,  $A_2$ , and  $A_3$  refer to three fibers collected from cloth section A in figure II.7.

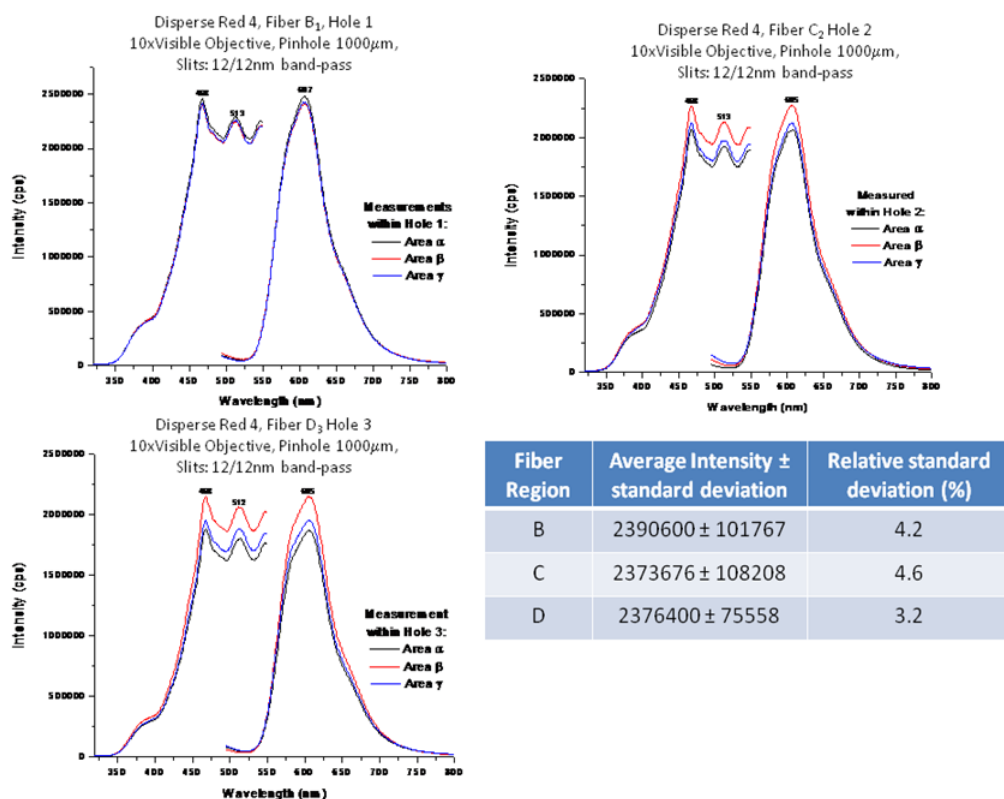
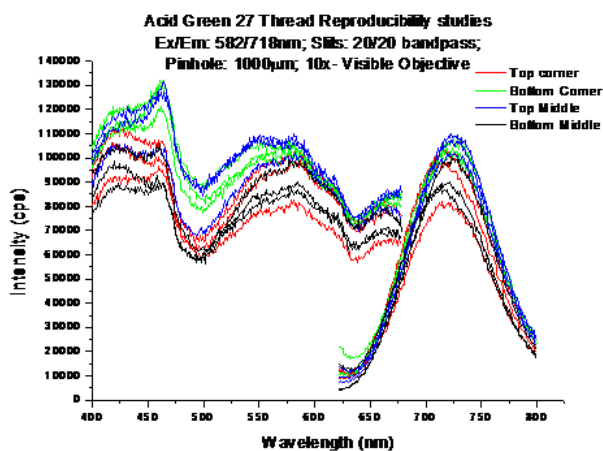


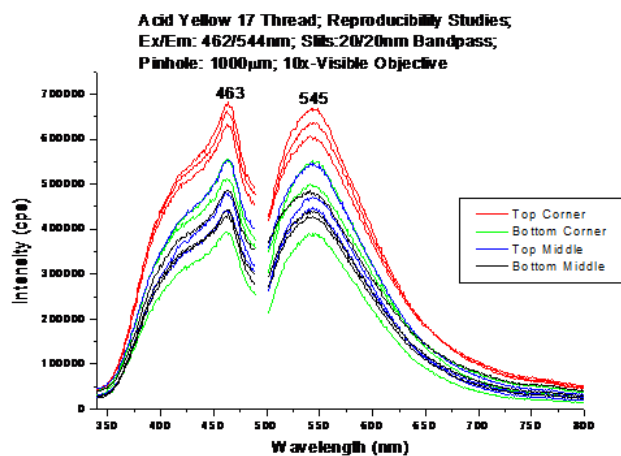
Figure III.59: Reproducibility of measurements made directly from Disperse Red 4 fibers with the spectrofluorimeter and the microscope. B, C, and D refer to three fibers each collected from cloth sections B, C, and D in figure II.7.

Figure III.60 and III.61 show reproducibility studies from fibers pre-dyed with Acid Green 27 and Acid Yellow 17. When compared to other types of fibers in table II.1, fibers pre-dyed with Acid Green 27 and Acid Yellow 17 presented relatively weak fluorescence. Data from Disperse Red 4 in figures III.58 and III.59 was recorded with the same pinhole (1000 $\mu$ m) as the one in figures III.60 and III.61. Although the reproducibility of measurements is worse than the one obtained for Disperse Red 4, the possibility to adjust the excitation and emission band-pass of the spectrofluorimeter to improve signal-to-background ratio still makes possible to record reproducible spectral profiles from textile fibers with weak fluorescence.



Thread Region	Average Intensity $\pm$ Standard Deviation	Relative Standard Deviation (%)
A	93607 $\pm$ 5987	6.4
B	103633 $\pm$ 3740	3.6
C	102947 $\pm$ 3651	3.5
D	90710 $\pm$ 5566	6.1

*Figure III.60: Reproducibility of measurements made directly from Acid Green 27 fibers with the spectrofluorimeter and the microscope. A, B, C, and D refer to three fibers each collected from cloth sections A, B, C, and D in figure II.7.*



Thread Region	Average Intensity $\pm$ Standard Deviation	Relative Standard Deviation (%)
A	635313 $\pm$ 32162	5.1
B	475380 $\pm$ 41726	8.8
C	486423 $\pm$ 25237	5.2
D	449013 $\pm$ 28819	6.4

*Figure III.61: Reproducibility of measurements made directly from Acid Yellow 17 fibers with the spectrofluorimeter and the microscope. A, B, C, and D refer to three fibers each collected from cloth sections A, B, C, and D in figure II.7.*

Figure III.62 shows the possibility to record excitation and fluorescence spectra from un-dyed fibers. These fibers were purchased from Testfabrics, Inc., i.e. the same commercial source of fibers in Table II.1. Although the fabrication process did not involve the use of fluorescence dye materials, their differentiation is still possible on the bases of their excitation and fluorescence profiles.

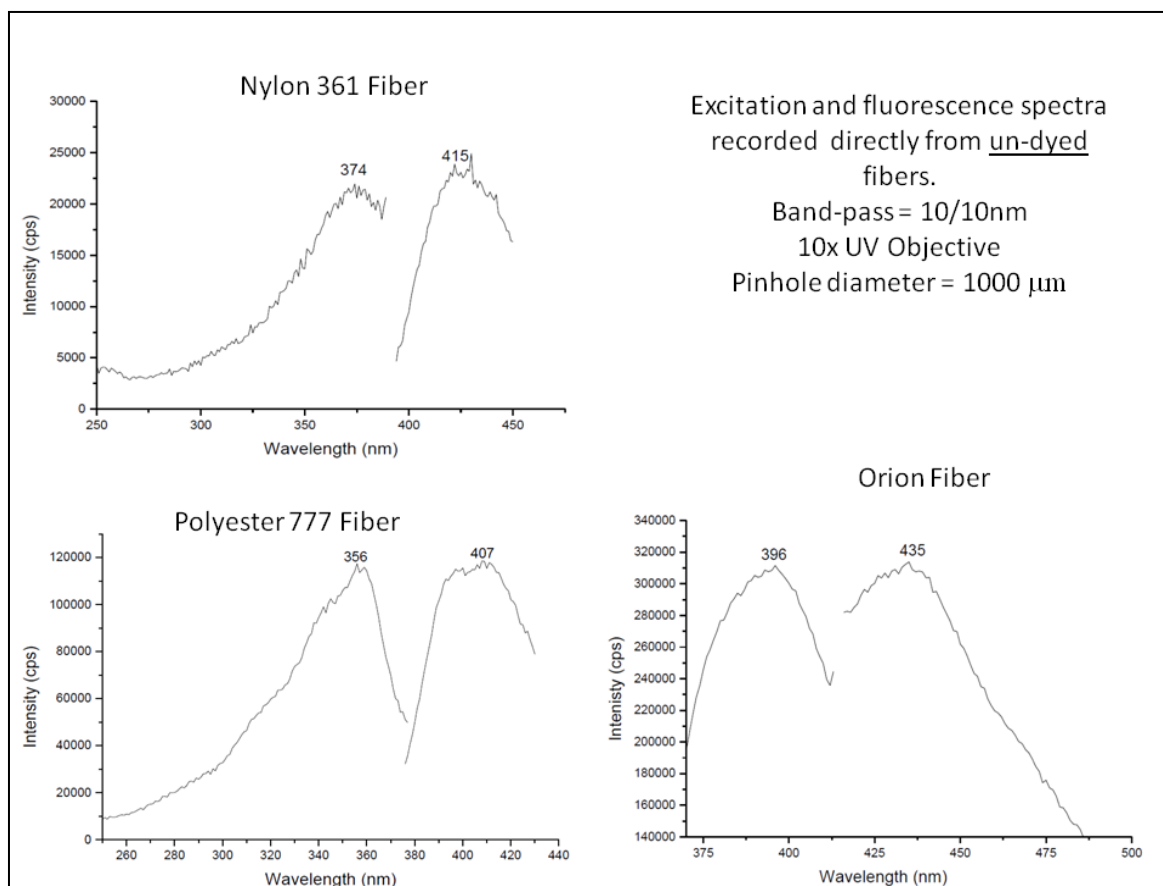


Figure III.62: Excitation and fluorescence spectra recorded from un-dyed fibers (Testfabrics, Inc.) using the spectrofluorimeter and the microscope.

### III.9. Optimization of Microscope Objectives

The type of results we obtained with the UV objectives in table II.4 is summarized in figures III.63-III.65. Fibers pre-dyed with Basic Red 9 are among the weakest fluorescence fibers in Table II.1. Using the 10XUV objective, the diameter of the circular area of fiber probed under the microscope with a 200 $\mu\text{m}$  pinhole approximately matches the width of the fiber (see top right image in figure III.63). With this pinhole size diameter, the spectral features of the fiber are undistinguishable from the spectral features of the background (see top left image in figure III.63). As shown in figure III.64, the use of larger pinholes sizes increases the intensity of both the fluorescence signal (S) from the fiber and the background (B) signal. S increases with the size of the pinhole because of the excitation of larger areas of fiber. Similarly, the background signal increases as a result of the co-irradiation of larger areas of microscope slide. Because the enhancement rate of S as a function of pinhole size diameter is larger than the enhancement rate of B, the spectral features recorded from the fiber improve as the pinhole size diameter increases. Although the best spectral features from the fiber are recorded with an open pinhole,

examination of the bottom left spectra in figure III.63 still shows a strong background contribution to the fluorescence spectrum of the fiber.

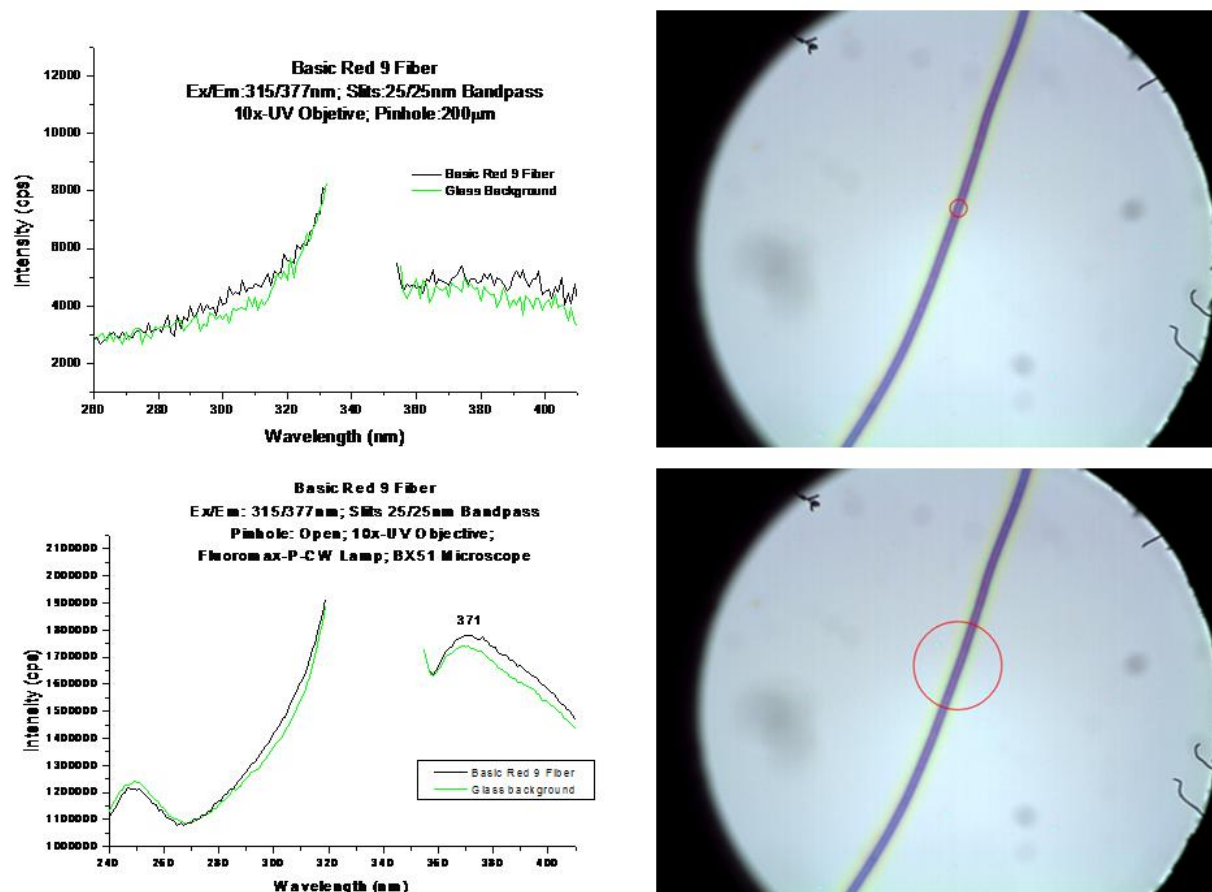
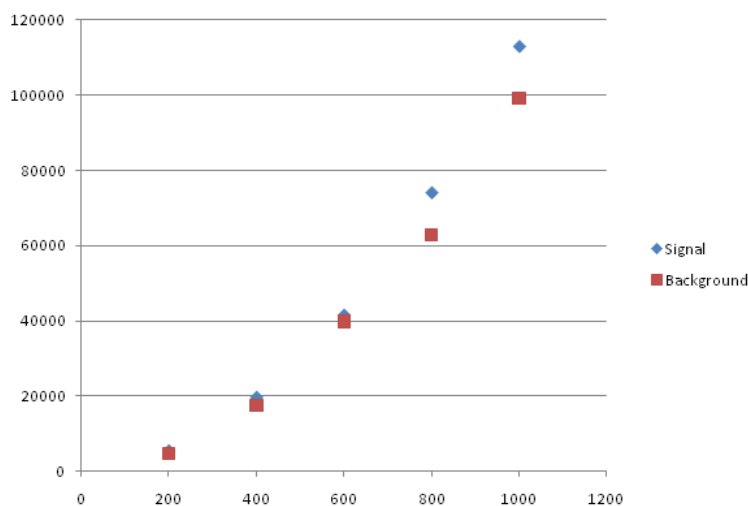


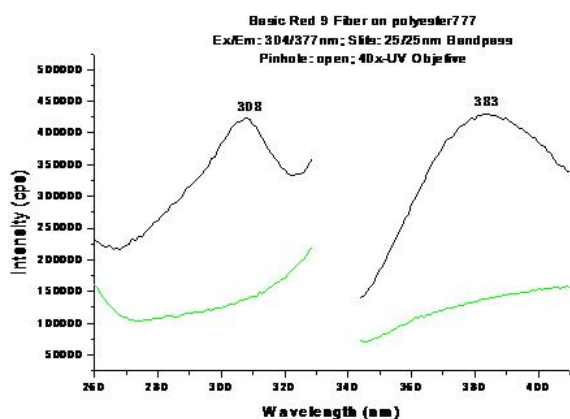
Figure III.63: Data recorded from a single fiber pre-dyed with Basic Red 9 using a 10XUV microscope objective. Left: Excitation and fluorescence spectra recorded with a 200 $\mu\text{m}$  pinhole size diameter (top) and open pinhole (bottom). Right: images of single fiber. The red circle represents the area of fiber probed with a 200 $\mu\text{m}$  (top) and a 1000 $\mu\text{m}$  (bottom) pinhole size diameter.

Pinhole ( $\mu\text{m}$ )	Signal (S, cps)	Background (B, cps)	S-B (cps)
200	5383	4625	758
400	19619	17450	2169
600	41480	39800	1680
800	74050	62810	11240
1000	112970	99280	13690
Open	1800000	1700000	100000



*Figure III.64: Data recorded from a single fiber pre-dyed with Basic Red 9 using a 10XUV microscope objective. Table at the top summarizes the signal (S) and the background (B) intensities recorded at the maximum excitation and fluorescence wavelengths of the fiber. The graph plots the S and B values as a function of pinhole diameter (200-1000 $\mu\text{m}$ ).*

Figure III.65 reports data recorded from the same fiber but with the 40XUV objective. The fiber spectra collected with an open pinhole present distinct features when compared to the background spectra. When compared to the enhancement of B, the enhancement of S as a function of pinhole diameter occurs at a faster rate with the 40XUV objective than with the 10XUV objective (compare graphs in figures III.64 and III.65). This fact results in part from the better C.E. ( $\sim 6.5\text{x}$ ) of the 40XUV objective over the 10XUV objective (C. E.  $\sim 1\%$ ).



Pinhole (μm)	Signal (S, cps)	Background (B, cps)	S - B
400	15040	1430	13610
600	28510	2640	25510
800	42620	4330	38290
1000	56700	6770	49930
Open	430130	138480	291650

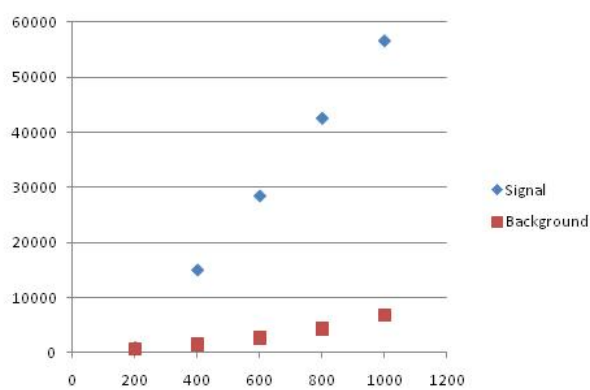
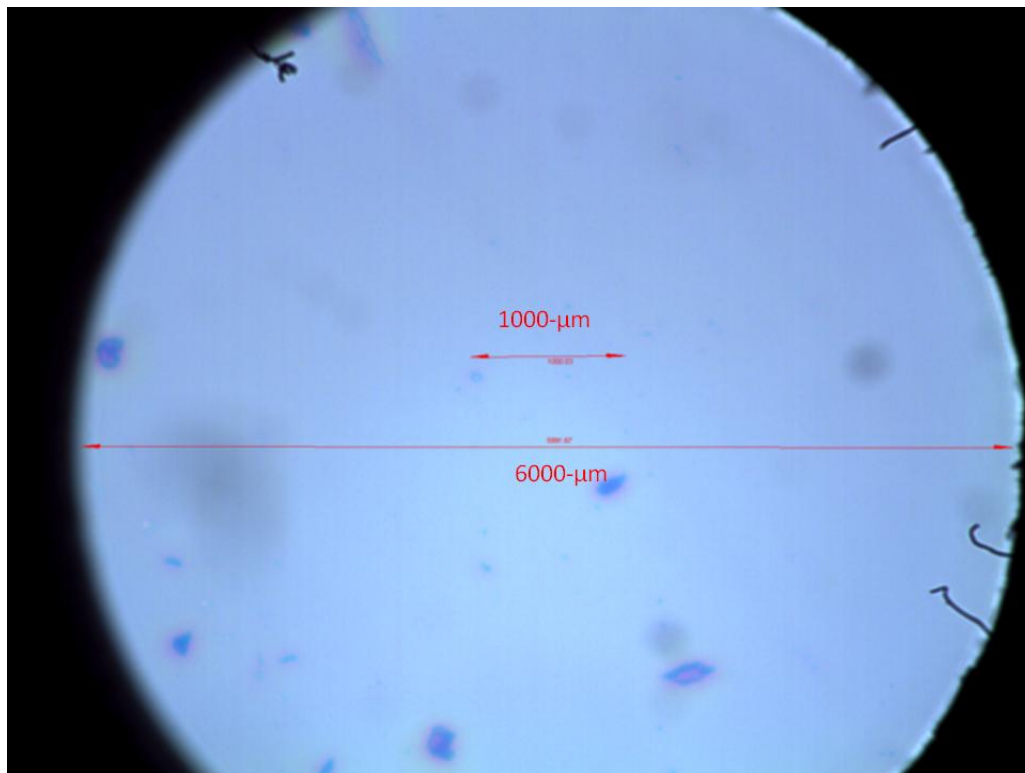


Figure III.65: Data recorded from a single fiber pre-dyed with Basic Red 9 using a 40XUV microscope objective. Top Left: Excitation and fluorescence spectra recorded with the open pinhole. Top Right: image of single fiber. The red circle represents the area of fiber probed with a 600 $\mu$ m pinhole size diameter. Table at the bottom summaries the signal (S) and the background (B) intensities recorded at the maximum excitation and fluorescence wavelengths of the fiber.

Figure III.66 compares the length of the 1000 $\mu$ m pinhole diameter to the length of the open pinhole diameter (6000 $\mu$ m). With the 10XUV objective, the open pinhole diameter corresponds to a 600 $\mu$ m (0.6mm) fiber length. With the 40XUV objective, the open pinhole diameter corresponds to a 150 $\mu$ m (0.15mm) fiber length. Because both fiber lengths are considerably shorter than the ~2mm fiber length typically encountered in crime scenes [74, 75], we decided to carry out all future studies in the ultraviolet region with the 40XUV objective.



*Figure III.66: Image showing the length of the open pinhole diameter (6000 $\mu\text{m}$ ) using the length of the 1000 $\mu\text{m}$  pinhole diameter as a source of comparison.*

The trend we observed with the visible objectives was similar to the trend observed in the ultraviolet region. The better C. E. of 40X lenses provided the best spectral features. The main deciding factor in favor of the 40XVIS-Dry objective over the 40XVIS-oil immersion objective is the fact that the 40XVIS dry objective avoids fiber immersion a potentially extracting medium that could remove fluorescence impurities from the fiber.

### **III.10. Fluorescence Microscopy of Visually Indistinguishable Fibers**

Close microscope examination of single fibers in Table II.5 revealed significant differences among some pairs of fibers. An example of the observed differences is presented in figure III. 67. For the purpose of comparison, figures III.68 – III-70 show images of threads and fibers that we considered truly indistinguishable under the microscope. We concentrated our studies on the pairs of fibers that appeared to be indistinguishable under the microscope, namely Direct Blue 1 and Direct Blue 53, Basic Green 1 and Basic Green 4, and Acid Blue 25 and Acid Blue 41.

## Acid Orange 7 & Acid Orange 10 Nylon

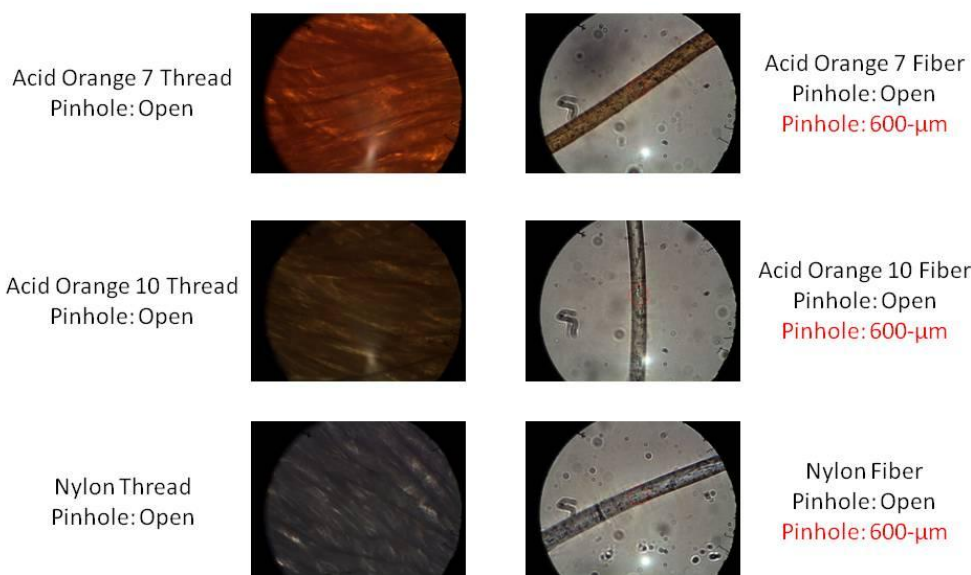


*Figure III.67: Microscope images showing visual differences among threads and single fibers of pairs 7 and 8 in Table II.5.*

## Direct Blue 1 & Direct Blue 53 Cotton 400

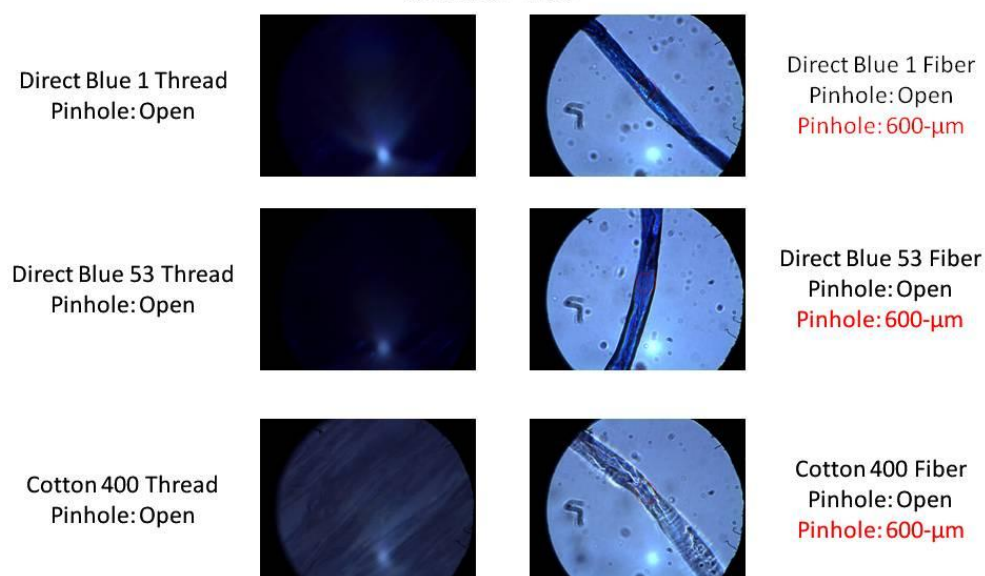


*Figure III.68: Microscope images showing visually indistinguishable threads and single fibers of pairs 5 and 6 in Table II.5.*

## Basic Green 1 & Basic Green 4

Acrylic

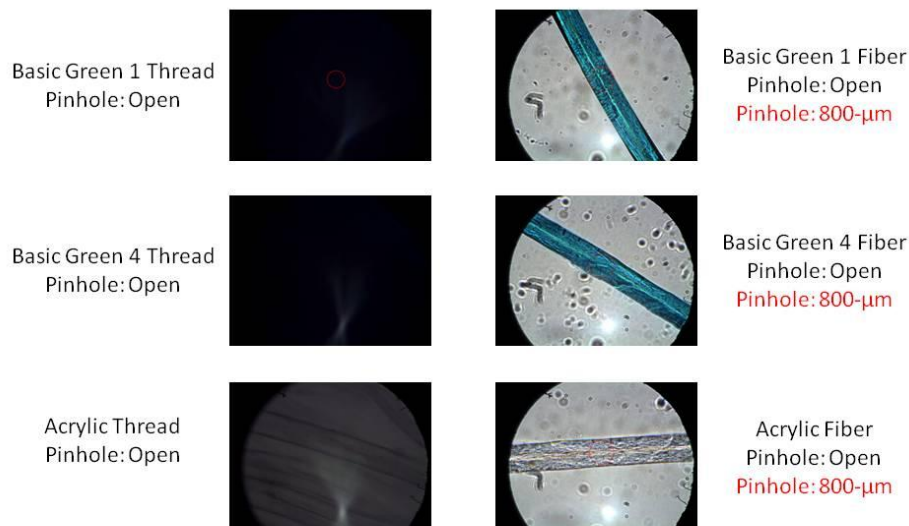


*Figure III.69:  
Microscope images  
showing visually  
indistinguishable  
threads and single  
fibers of pairs 3 and 4  
in Table II.5.*

## Acid Blue 25 & Acid Blue 41

Nylon

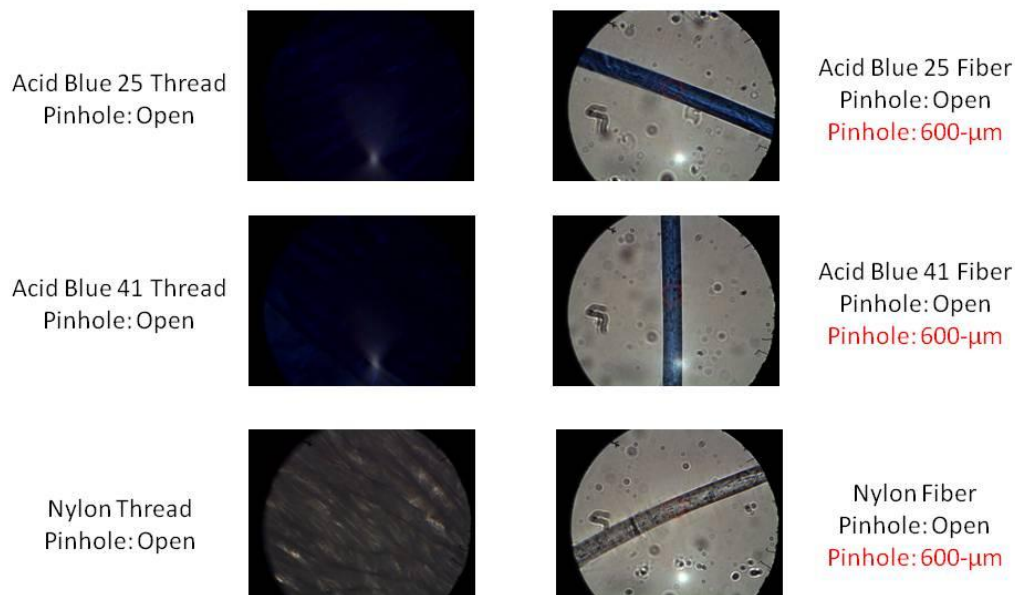


*Figure III.70:  
Microscope  
images showing  
visually  
indistinguishable  
threads and  
single fibers of  
pairs 1 and 2 in  
Table II.5.*

Figure III.71 shows the RTF-EEMs recorded from Direct Blue 1 and direct Blue 53 single fibers within the visible spectral region. The pinhole diameter of the microscope and the excitation and emission band-passes of the spectrofluorimeter were adjusted to provide appropriate signal-to-background ratio.

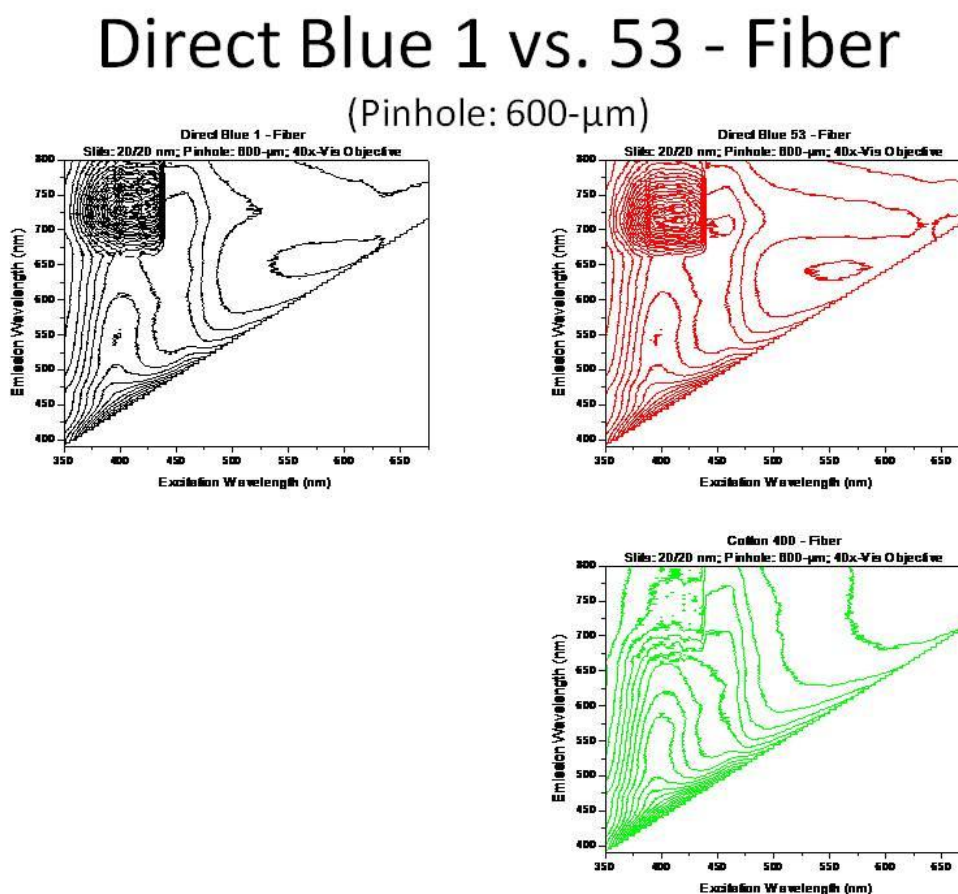


*Figure III.71: RTF-EEMs recorded from visually indistinguishable single fibers. Black contour = Direct Blue 1 fiber; Red contour = Direct Blue 53 fiber; Green contour = Un-dyed cotton fiber.*

The possibility to distinguish the two fibers on the basis of RTF-EEM microscopy is demonstrated in figure III.72, which overlays the contours of the two pre-dyed fibers. Similar results were obtained for the other two pairs of indistinguishable fibers (see figures III.73 and III.74).

## Direct Blue 1 vs. 53 - Fiber

(Pinhole: 600- $\mu\text{m}$ )

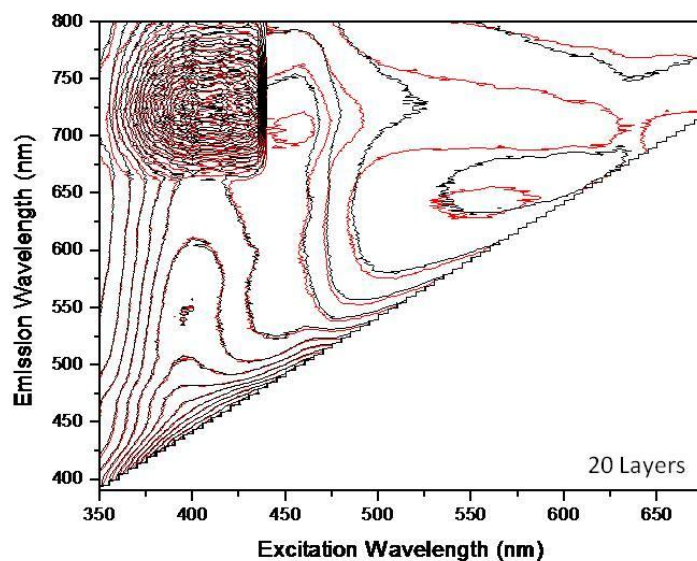


Figure III.72: Superposition of RTF-EEMs recorded single fibers. Black contour = Direct Blue 1 fiber; Red contour = Direct Blue 53 fiber.

## Basic Green 1 vs. 4 - Fiber

(Open Pinhole)

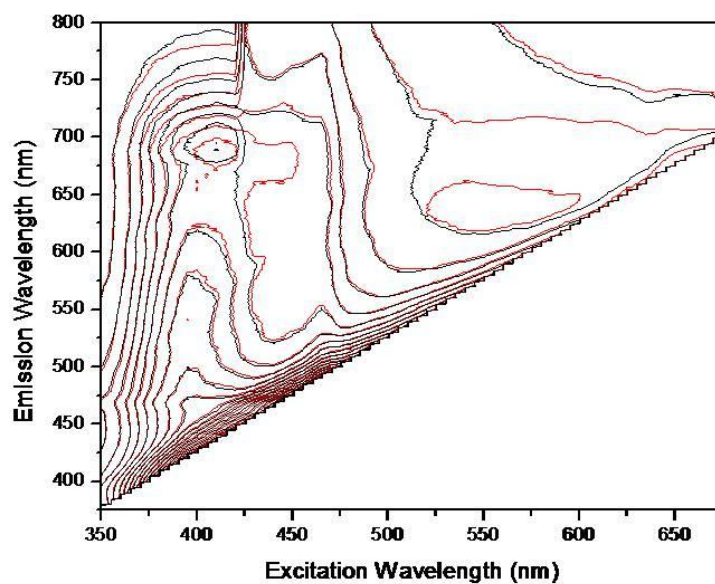


Figure III.73: Superposition of RTF-EEMs recorded single fibers. Black contour = Basic Green 1 fiber; Red contour = Basic Green 4 fiber.

## Acid Blue 25 vs. 41 - Fiber

(Pinhole: 600- $\mu\text{m}$ )

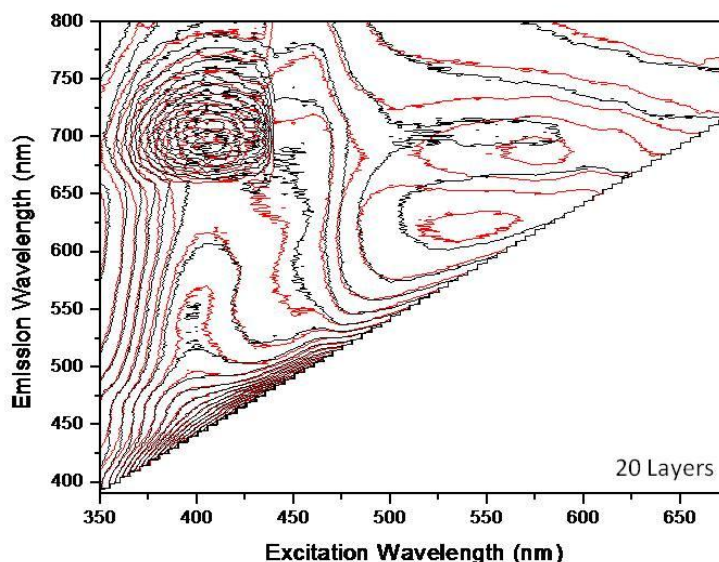


Figure III.74: Superposition of RTF-EEMs recorded single fibers. Black contour = Acid blue 25 fiber; Red contour = Acid Blue 41 fiber.

### IV. Conclusions

#### IV.1. Absorbance and Fluorescence Characteristics of Fiber Extracts

The visual comparison of fluorescence spectra in Appendix B reveals two main types of spectral profiles, i.e. emission spectra with only one and with more than one fluorescent peaks. Spectral comparison within the same type of fiber and the same extracting solvent reveals some cases with strong dependence on the chemical nature of the extracting solvent. The differences observed can be attributed to the chemical affinities of the extracting solvents for fluorescence components in the textile fibers. When fiber extraction was carried out with the best extracting solvent for RTF spectroscopy, all fiber extracts showed excitation and fluorescence profiles different from each other. As shown in Table III.2, the comparison of their maximum excitation and fluorescence wavelengths shows the possibility to discriminate the studied fibers on the basis of their spectral profiles.

Considering the disadvantages associated to selecting the best solvent for fiber extraction prior to RTF spectroscopy in forensic comparisons, we propose a 1:1 acetonitrile:water (v/v) mixture as the common extracting solvent for all the studied fibers. Similar to our observations with the best extracting solvents, the strong fluorescence intensities of fibers in 1:1 acetonitrile:water (v/v) extracts made also possible their analyses with 2mm lengths. The comparison of excitation and fluorescence profiles of the fourteen types of fibers extracted with this solvent showed three distinct groups. Fibers pre-dyed with Disperse Red 1, Direct Blue 1, Disperse Red 13 and Acid Green 27 showed extracts with similar excitation and fluorescence profiles. The same is true for fibers pre-dyed with Basic Red 9, Basic Violet 14, Disperse Blue 56 and Acid Yellow 17. On the other end, fibers pre-dyed with Basic Green 4, Disperse Red 4, Direct Blue 71, Direct Blue 90, Acid Yellow 23 and Acid Red 151 showed distinct excitation and fluorescence spectra. Although

the comparison of fibers within the first two groups would certainly benefit from additional parameters of selectivity, the different excitation and fluorescence maxima still makes possible their visual discrimination on the basis of spectral profiles.

The reproducibility of excitation and fluorescence spectral profiles was demonstrated with two types of experiments. Spectral profiles were recorded from individual extracts belonging to adjacent fibers – i.e. single fibers located immediately next to each other –within the same area of cloth - and from single fibers located in four different areas of the cloth. Both types of experiments provided outstanding reproducibility of spectral profiles with minimum variations in fluorescence intensities. The comparison among the same type of fibers belonging to different pieces of the same type of cloth was only made with three types of fibers, namely Direct Blue 90, Direct Blue 1 and Acid Red 151. All the remaining fibers were acquired as one piece of cloth. Although the differentiation of the same type of fiber from different pieces of cloth appeared to be possible on the basis of two-dimensional excitation and fluorescence spectra, we feel that the forensic examination of textile fibers would certainly benefit from additional selectivity. One possibility that was not explored in our investigations is to enhance possible fluorescence spectral differences via selective excitation of fluorophors specific to one type of fiber.

#### **IV.2. Comparison of Fiber Extracts with Dye Standards**

Absorbance spectra of standards gave spectra closely matching that of dyes from the Sigma Aldrich Handbook of Stains, Dyes and Indicators. As expected, all dye standards had strong peaks in the visible range most likely attributed to the presence of the dyes. The fiber extracts showed similar visible peaks when the dye was extracted, but also showed stronger peaks in the UV region. A distinct possibility is that these peaks confirm the presence of unknown impurities in the fiber.

The majority of dye standards showed relatively weaker fluorescence than their corresponding fiber extracts. Fiber extracts showed the contribution of unknown fluorescence impurities. Several possibilities exist for the origin of these impurities. They could come from impurities present in the impure dyes used to color the fabrics or impurities present in the equipment and reagents used for dyeing the cloths. Since the fluorescence given by the fiber extracts appears to be irrespective of the dyes these fluorescence signals could provide another level of discrimination for forensic fiber analysis beyond examining dyes. The potential exists for differentiating visually indistinguishable fibers, i.e. of the same material, dyed with the same dye but with the presence of different impurities.

#### **IV.3. HPLC of Fiber Extracts**

The separation of fiber extracts via HPLC provides valuable information on the contribution of individual components to the total fluorescence of fibers. The comparison of chromatograms from extracts of fibers collected from different areas of a cloth confirmed the reproducibility of individual fluorescence impurities within the same piece of cloth. The reproducibility of individual impurities agrees well with the fluorescence reproducibility of extracts from fibers of the same cloth. The HPLC analysis of Aldrich-Sigma dyes provided fluorescence chromatograms with different components than those observed from fiber extracts. Further absorption and fluorescence analysis of HPLC fractions confirmed the presence of fluorescence impurities in the fiber extracts that were not present in the Sigma-Aldrich standards.

#### **IV.4. Room Temperature Fluorescence –Excitation Emission Matrix Spectroscopy**

The comparison of 2D excitation and fluorescence spectra to RTF-EEM has demonstrated that the latter is a more powerful data format for fiber discrimination. This advantage results from an

intrinsic characteristic of RTF-EEM data formats, which is their ability to convolute the contribution of all fluorescence components within the ultraviolet and visible spectral regions.

#### **IV.5. Comparison of RTF-EEM Recorded from Fiber Extracts of Visually Indistinguishable Fibers**

MCR-ALS analysis of EEM taken from extracts of nylon fibers pre-dyed with Acid Yellow 17 and 23 predicted five fluorescent components in each type of extract. From differences in the calculated correlation coefficients of two fluorescent components, we were able to discriminate among these two types of visually indistinguishable fibers. MCR-ALS analysis of EEM taken from extracts of nylon fibers pre-dyed with Acid Red 151 also made possible to discriminate among two visually indistinguishable fibers pre-dyed with the same dye in the same textile industry but from different cloths. Although additional studies should be made with a larger number and types of visually indistinguishable fibers, the results presented here provide the foundation to propose the combination of RTF-EEM and MCR-ALS as a promising tool for the forensic analysis of textile fibers.

#### **VI.6. Effects of Environmental Contaminants on the Fluorescence of Textile Fibers**

Many researchers believe that environmental contaminants increase the individualization of the fiber and facilitate forensic fiber discrimination [80-84]. Our original proposition never intended to provide a definite answer to all the questions related to environmental factors. Our original objective was relatively modest as we merely proposed to initiate an investigation on the potential usefulness of environmental concomitants as an additional source of fiber comparison. Based on the results obtained so far, we are inclined to state that the fluorescence of environmental contaminants could prove useful for fiber comparison, mainly in the specific case of visually indistinguishable fibers with similar inherent chemical composition that provide almost identical RTF-EEM data formats. For instance, the spectral features of PAH adsorbed on the fiber could be used to discriminate between fibers on the basis of their exposure history. The same is true with the spectral changes observed upon washing. In the case of non-polar contaminants such as PAH, one possibility is to remove them from the fiber prior to its extraction. Because of the polar nature of intrinsic fluorescence components, fiber rinsing (or even extraction) with a non-polar solvent should be harmless to the inherent fluorescence of the fiber. Because detergents and softeners are soluble in water, the choice of an appropriate solvent for their selective extraction requires further studies. In addition, we feel that fiber discrimination via RTF spectroscopy should benefit from a comprehensive spectral database of commercial detergents and softeners. Comparison of this database to the spectral characteristics of fiber extracts should aid the analyst to track down the exposure of fibers to laundering contaminants.

#### **IV. 7. Instrumentation for Non-destructive Analysis of Fibers**

The installation of the instrumental set up for non-destructive analysis of fibers was successfully accomplished and so it was the alignment of its optical components for best signal-to-background ratio with the 10xUV and 10xVIS objectives.

#### **IV.8. Spectral Reproducibility within the Length of a Single Fiber**

Our studies have shown reproducible spectral profiles along the length of a single fiber. The same is true for spectral profiles of fibers belonging to the same piece of cloth. The possibility to adjust the diameter of the microscope's pinhole and the excitation and emission band-pass of the spectrofluorimeter made possible to record reproducible spectral profiles from fibers with weak fluorescence emission. This possibility includes un-exposed fibers to pre-dying treatments. The differentiation of fibers un-exposed to pre-dying treatments was possible on the bases of their spectral profiles.

#### IV.9. Optimization of Microscope Objectives

The strongest fluorescence signals from all fibers in Table II.1 and best spectral profiles were obtained using open pinholes and 40X objectives in both the ultraviolet and visible spectral regions. With the 40X objectives, the open pinhole diameter corresponds to a 150 $\mu$ m (0.15mm) fiber length. This fiber length is considerably shorter than the ~2mm fiber length typically encountered in crime scenes [74, 75]. From this prospective, the combination of an open pinhole and a 40X objective appears to be well suited for the non-destructive RTF analysis of fibers. Future studies within the period of this project will be carried out with 40X objectives. The main deciding factor in favor of the 40XVIS-Dry objective over the 40XVIS-oil immersion objective is the fact that the 40XVIS dry objective avoids fiber immersion a potentially extracting medium that could remove fluorescence impurities from the fiber.

#### IV. 10. Fluorescence Microscopy of Visually Indistinguishable Fibers

The spectral features of the visually indistinguishable fibers studied in this project provided remarkable different RTF-EEMs. Although a larger pool of visually indistinguishable fibers should be examined in the future, we feel we have successfully achieved the goal of this project. We have presented proof of concept that provides a solid foundation for the development of non-destructive methodology for forensic fiber analysis. Future studies that go beyond the duration of this project should compare the discrimination of visually indistinguishable fibers via RTF-EEM microscopy and micro-spectrophotometry. The new methodology should be tested across multiple types of data frequently encountered in forensic science, in such a way that the practical implications of the results are understandable and the methodology easily explained to juries. If successful, RTF-EEM microscopy should significantly enhance the ‘match’ decision that precedes addressing the question of the weight of the evidence.

#### V. References

- [1] Rendle D. F., *Chem. Soc. Rev.*, **2005**, 34, 1021.
- [2] Goodpaster J. V., Liszewski E. A., *Anal. Bioanal. Chem.*, **2009**, 394, 2009.
- [3] Kirkbride K., Tungol M., Infrared microspectroscopy of fibers. In: Robertson J., Grieve M. (eds) *Forensic Examination of fibers*, 2<sup>nd</sup> edn. CRC, New York, **1999**, pp 179 - 222.
- [4] Macrae R., Dudley R., Smalldon K., *J. Forensic Sci.*, **1979**, 24, 117.
- [5] Adolf F., Dunlop J., Microspectrophotometry/color measurement. In: Robertson J., Grieve M. (eds) *Forensic Examination of fibers*, 2<sup>nd</sup> edn. CRC, New York, **1999**, pp 251- 289.
- [6] Roux C., Scanning electron microscopy and elemental analysis. In: Robertson J., Grieve M. (eds) *Forensic Examination of fibers*, 2<sup>nd</sup> edn. CRC, New York, **1999**.
- [7] Grieve M. C., Dunlop J., Haddock P., *J. Forensic Sci.*, **1990**, 35, 301.
- [8] Grieve M. C., Biermann T. W., Davignon M., *Sci. Justice*, **2001**, 41, 245.
- [9] Grieve M. C., Biermann T. W., Davignon M., *Sci. Justice*, **2003**, 43, 5.
- [10] Biermann T. W., *Sci. Justice*, **2007**, 47, 68.
- [11] Grieve M. C., Dunlop J., Haddock P., *J. Forensic Sci.*, **1988**, 33, 1332.
- [12] Challinor J. M., Fiber identification by pyrolysis techniques. In: Robertson J., Grieve M. (eds) *Forensic Examination of fibers*, 2<sup>nd</sup> edn. CRC, New York, **1999**, pp 223 - 237.
- [13] Wiggins K.G., Thin layer chromatographic analysis for fibre dyes. In: Robertson J, Grieve M (eds) *Forensic examination of fibers*, 2<sup>nd</sup> edn., CRC, New York, **1999**.
- [14] Golding G.M., Kokot S., *J. Forensic Sci.*, **1989**, 34, 1156.
- [15] Rendle D.F., Crabtree S.R., Wiggins K.G., Salter M.T., *J. Soc Dyers Colour*, **1994**, 110, 338.
- [16] Wiggins K.G., Crabtree S.R., March B.B., *J. Forensic sci.*, **1996**, 41, 1042.

- [17] Macrae R., Smalldon K., *J. Forensic Sci.*, **1979**, 24, 109.
- [18] Resua R., *J. Forensic Sci.*, **1980**, 25, 168.
- [19] Wiggins K.G., Cook R., Turner Y.J., *J. Forensic Sci.*, **1988**, 33, 998.
- [20] Beattie I.B., Dudley R.J., Smalldon K.W., *J. Soc Dyers Colour*, **1979**, 95, 295.
- [21] Resua R., DeForest P.R., Harris H., *J. Forensic Sci.*, **1981**, 26, 515.
- [22] Wiggins K.G., Holness J.A., *Sci. Justice*, **2005**, 45, 93.
- [23] Griffin R., Speers J., Other methods of colour analysis: high performance liquid chromatography. In: Robertson J., Grieve M.C. (eds) *Forensic examination of fibers*, 2<sup>nd</sup> edn, CRC, Boca Raton, Florida, **1999**.
- [24] Robertson J., Other methods of colour analysis: capillary electrophoresis. In: Robertson J., Grieve M.C. (eds) *Forensic examination of fibers*, 2<sup>nd</sup> edn., CRC, Boca Raton, Florida, **1999**.
- [25] Trojanowicz M., Wojcik L., Urbaniak-Walczak K., *Chem. Anal.*, **2003**, 48, 607.
- [26] Xu X., Leijenhurst H., Van de Hoven P., de Koeijer J., Logtenberg H., *Sci. Justice*, **2001**, 41, 93.
- [27] Yinon J., Saar J., *J. Chrom.*, **1991**, 586, 73.
- [28] Tuinman A.A., Lewis L.A., Lewis S.A., *Anal. Chem.*, **2003**, 75, 2753.
- [29] Huang M., Yinon J., Sigman M.E., *J. Forensic Sci.*, **2004**, 49, 238.
- [30] Huang M., Russo R., Fookes B.G., Sigman M.E., *J. Forensic Sci.*, **2005**, 50, 526.
- [31] Petrick L.M., Wilson T.A., Fawcett W.R., *J. Forensic Sci.*, **2006**, 51, 771.
- [32] Morgan S.L., Vann B.C., Baguley B.M., Stefan A.R., Advances in discrimination of dyed textile fibers using capillary electrophoresis/mass spectrometry In: 2007 trace evidence symposium, Clearwater beach, Florida, **2007**.
- [33] Soltzberg L.J., Hagar A., Kridaratikorn S., Mattson A., Newman R., *J. Am. Soc. Mass Spectrom.*, **2007**, 18, 2001.
- [34] Suzuki E., Forensic applications of infrared spectroscopy. In: Saferstein R (ed) *Forensic science handbook*. Regents/Prentice Hall, Upper Saddle River, New Jersey, **1993**, pp71-195.
- [35] Gilbert C., Kokot S., *Vibr. Spectro.*, **1995**, 9, 161.
- [36] Kokot S., Crawford K., Rintoul L., Meyer U., *Vibr. Spectro.*, **1997**, 15, 103.
- [37] Kokot S., Tuan N.A., Rintoul L., *Appl. Spectrosc.*, **1997**, 51, 387.
- [38] Keen I.P., White G.W., Fredericks P.M., *J. Forensic Sci.*, **1998**, 43, 82.
- [39] Jochem G., Lehnert R.J., *Sci. Justice.*, **2002**, 42, 215.
- [40] Thomas J., Buzzini P., Massonnet G., Reedy B., Roux C., *Forensic Sci. Int.*, **2005**, 152, 189.
- [41] Massonnet G., Buzzini P., Jochem G., Stauber M., Coyle T., Roux C., Thomas J., Leijenhurst H., Van Zanten Z., Wiggins K.G., Russel C., Chabli S., Rosengarten A., *J. Forensic Sci.*, **2005**, 50, 1028.
- [42] Jurdana L., Ghiggino K. P., Nugent K. W., Leaver I. H., *Textile Research Journal*, **1995**, 65, 593.
- [43] White P. C., Munro C. H., Smith W. E., *Analyst*, **1996**, 121, 835.
- [44] Cho L., Reffner J. A., Gatewood B. M., Wetzell D. L., *J. Forensic Sci.*, **2001**, 46, 1309.
- [45] Kubic T. A., King J. E., Dubey I. S., *Microscope*, **1983**, 31, 213.
- [46] Hartshorne A. W., Laing D. K., *Forensic Sci. Int.*, **1991**, 51, 221.
- [47] Hartshorne A. W., Laing D. K., *Forensic Sci. Int.*, **1991**, 51, 239.
- [48] Palmer R., Chinherende V. A., *J. Forensic Sci.*, **1996**, 41, 802.
- [49] Cantrell S., Roux C., Maynard P., Roberson J., *Forensic Sci. Int.*, **2001**, 123, 43.
- [50] H. A. Deadman, *Proceedings of the American Academy of Forensic Sciences*, **2004**, paper B47, pg. 47.
- [51] Mueller M., Murphy B., Burghammer M., Snigireva I., Riekel C., Gunneweg J., Pantos E., *Applied Physics A: Materials Science & Processing*, **2006**, 83, 183.
- [52] Abu-Rous M., Schuster K.C., Adlassnig W., Lichtscheidl I., *Melliand International*, **2007**, 13, 382.

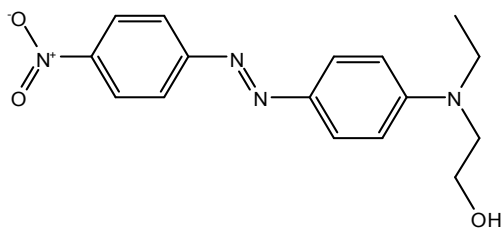
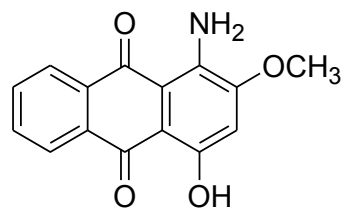
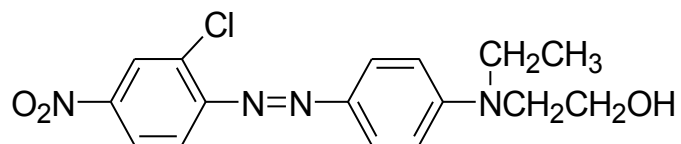
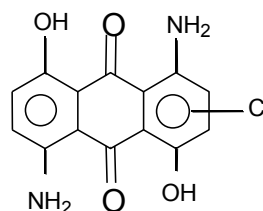
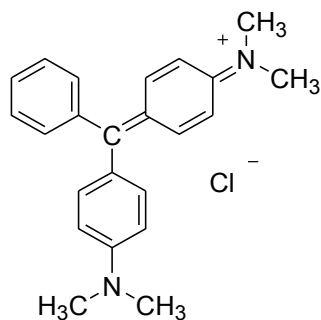
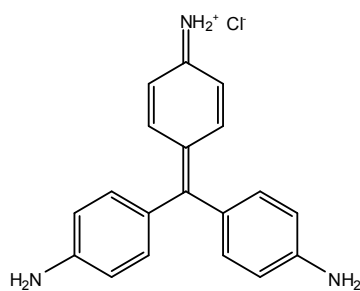
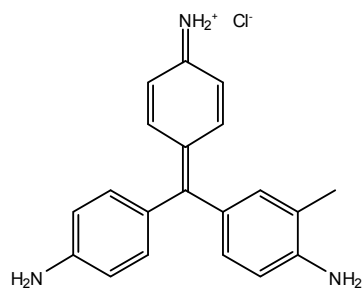
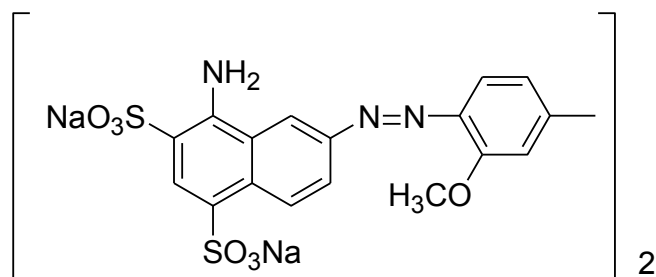
- [53] 24. *Forensic Science Communications* **1999** Vol.1, No. 1  
<http://www.fbi.gov/hq/lab/fsc/backissu/april1999/houckapb.htm>
- [54] Esteves da Silva J. C. G., Tavares M. J. C. G., Tauler R., *Chemosphere*, **2006**, 64, 1939.
- [55] DaCosta R. S., Andersson H., Wilson B. C., *Photochem. Photobiol.*, **2003**, 78, 384.
- [56] Warner I.M., Davidson E.R., Christian G.D., *Anal. Chem.*, **1977**, 49, 2155.
- [57] Warner I.M., Christian G.D., Davidson E.R., *Anal. Chem.*, **1977**, 49, 564.
- [58] Anderson, C.M., Bro, R., *J. Chemom.*, **2003**,17, 200.
- [59] Massart, D.L.; Vandeginste, B.G.M.; Deming, S.N.; Michotte, Y. and Kaufman, L., *Chemometrics: A Textbook* Elsevier, Amsterdam, The Netherlands, **1989**.
- [60] Otto, M., *Chemometrics Statistics and Computer Application in Analytical Chemistry* Wiley-VCH Weinheim, **1999**.
- [61] Harshman, R.A., Lundy, M.E., *Computational Statistics and Data Analysis* **1994**, 18, 39.
- [62] Bystol, A. J.; Campiglia, A. D.; Gillispie, G. D., *Appl. Spectrosc.* **2000**, 54, 910.
- [63] Bystol, A. J.; Campiglia, A. D.; Gillispie, G. D., *Anal. Chem.* **2001**, 73, 5762.
- [64] Campiglia, A. D.; Bystol, A. J.; Yu, S.; *Anal. Chem.* **2006**, 78, 484.
- [65] Huang, M.; Yinon, J.; Sigman, M.E., *J. Forensic Sci.* **2004**, 49, 238.
- [66] Huang, M.; Russo, R.; Fookes, B. G. and Sigman, M. E., *J. Forensic Sci.* **2005**, 50, 526.
- [67] Green, F.J. *Sigma Aldrich Handbook of Stains, Dyes and Indicators*. Aldrich Chem. Co. Library **1990**
- [68] Beattie, I. B., Roberts, H. L. and Dudley R. J.; *Forensic Sci. Int.* **1981**, 17, 57.
- [69] Home J. M. and Dudley R. J.; *Forensic Sci. Int.* **1981**, 17, 71.
- [70] Macrae R., Dudley R. J. and Smalldon K. W.; *J. Forensic Sci.* **1979**, 24, 117.
- [71] Hartshorne A. W. and Laing D. K., *Forensic Science Int.* **1984**, 25, 133.
- [72] Wiersema, S. *CAC Newsletter*, March **1984**, 19.
- [73] Laing, D. K; Dudley, R. J.; Hartshorne, A. W.; Home, J. M.; Rickard, R. A. and Bennett, D.C.; *J. Forensic Sci. Int.* **1991**, 50, 23.
- [74] Pounds, C. W. and Smalldon, K. M.; *J. Forensic Sci. Soc.* **1975**, 15, 17.
- [75] Wiggings, K. G.;Crabtree, S. R.; March, B. B.; *J. Forensic Sci.* **1996**, 41, 1042.
- [76] Isak, S.J., Edward, M. E., Spikes J.D. and Meekins, P.A. *J. Photochem. Photobiol. A: Chemistry* **2000**, 134, 77.
- [77] Toro,C., Thibert, A., De Boni,L., Masunov,A.E., Hernández, F.E. *J. Phys. Chem. B*, **2008**, 112, 929.
- [78] Miler, J. N. and Miller J. C., *Statistics and chemometrics for Analytical Chemistry*, 4<sup>th</sup> Edition, Prentice Hall, New York, 2000.
- [79] Bystol, A. J., Whitcomb, J. L. and Campiglia A. D., *Environ. Sci. & Technol.* **2001**, 35, 2566.
- [80] Goto, S. and Kashiwag, M. I., *Kyoritsu Joshi Daigaku Kaseigakubu Kiyo* **1995**, 41, 39.
- [81] Reifler, F. A., Halbeisen,M., Schmid, H., *Chimia* **1995**, 49, 226
- [82] Schaefer, K. *Mellian Textilberichte* **2001**, 82, E133-E135, 520.
- [83] Kirschenbaum, L. J. and Millington, K. R., *Abstracts of Papers, 222nd ACS National Meeting* Chicago, IL, United States, August 26-30, **2001** ANYL-036.
- [84] Lloyd, J. B. F., Evett, I. W. Dubery, J. M. *J. Forensic Sci.* **1980**, 25, 589.

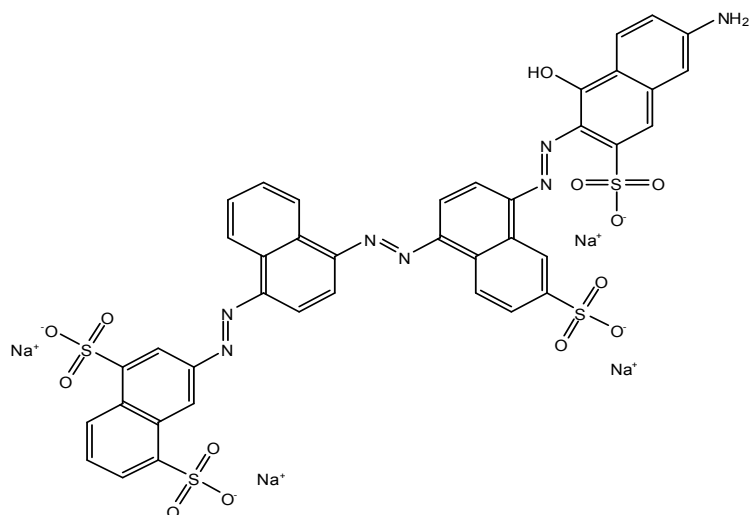
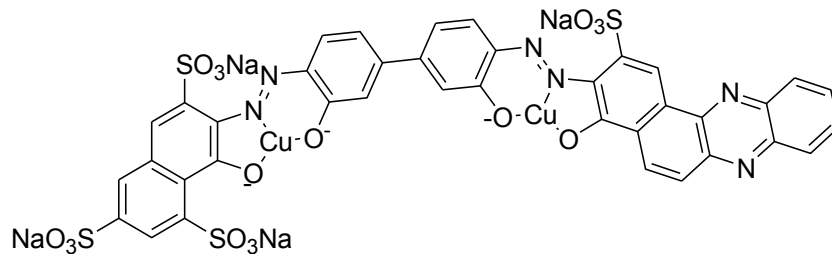
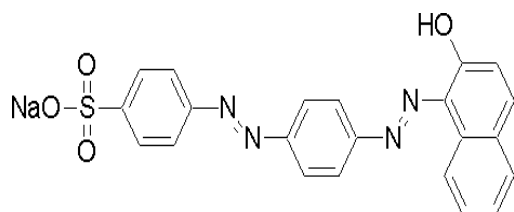
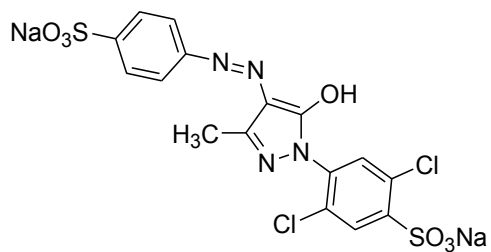
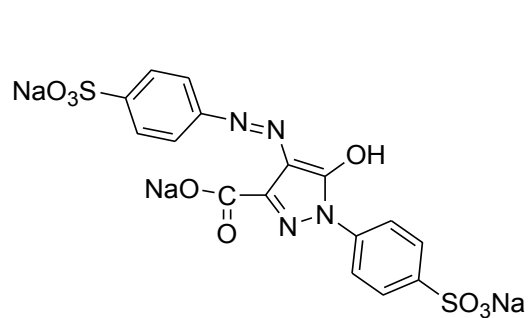
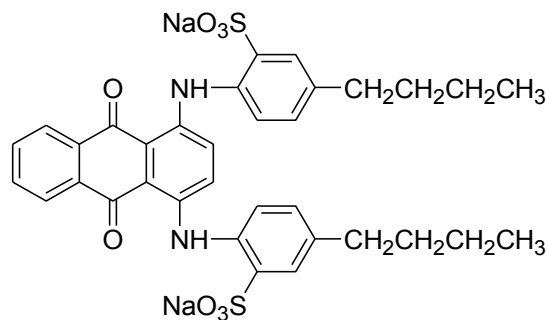
## VI. Dissemination of Research Findings

- *The 31<sup>st</sup> Annual Conference of the Analytical Chemistry & Spectroscopy Societies*, Portland, OR, October 3-7, **2006**. Application of Fluorescence Line Narrowing Spectroscopy to Forensic Fiber Examination. Campiglia A. D. and Sigman M. Abstract Book 291b, page 129. Participation: *Speaker and corresponding author, 20 min presentation.*
- *PITTCON 2006*, Orlando, FL, March 12-17, **2006**. Fluorescence Spectroscopy for Forensic Examination of Textile Fiber Impurities. Rex, M; Moore A.; Campiglia, A. D. Abstract Book 2310-2, page 118. Participation: *Speaker and corresponding author, 20 min presentation.*
- *American Academy of Forensic Sciences 59<sup>th</sup> Anniversary Scientific Meeting*, San Antonio, TX, February 19 – 24, **2007**. Campiglia A. D. Participation: *30 min oral presentation in the General Forensics Research and Development Grantees Meeting, National Institutes of Justice (NIJ).*
- *The 34<sup>th</sup> Annual Conference of the Federation of Analytical Chemistry & Spectroscopy Societies*, Memphis, TN, October 14-18, **2007**. Room-Temperature Fluorescence Analysis of Dye Extracts for Forensic Fiber Examination. Rex M. and Campiglia, A. D. Abstract Book 491, p. 187. Participation: *corresponding author in poster presented by student.*
- *American Academy of Forensic Sciences 60<sup>th</sup> Anniversary Scientific Meeting*, Washington, DC, February 19 – 24, **2008**. Campiglia A. D. Participation: *30 min oral presentation in the General Forensics Research and Development Grantees Meeting, National Institutes of Justice (NIJ).*
- *The 35<sup>th</sup> Annual Conference of the Federation of Analytical Chemistry & Spectroscopy Societies*, Reno, NV, September 28 – October 2, **2008**. Room-Temperature Fluorescence Excitation-Emission Matrices for Comparing Textile Fibers as Physical Evidence. Rex, M.; Goicoechea, H. C. and Campiglia, A. D. Abstract Book 508, p. 185. Participation: *20min oral presentation.*
- *The 35<sup>th</sup> Annual Conference of the Federation of Analytical Chemistry & Spectroscopy Societies*, Reno, NV, September 28 – October 2, **2008**. Evaluation of Chemometric Approaches for the Analysis of Textile Fibers via Room-Temperature Fluorescence Excitation-Emission Matrices. Appalaneni, K. V.; Rex, M; Goicoechea, H. C.; Campiglia, A. D. Abstract Book 212, p. 119. Participation: *Speaker and corresponding author, 20min oral presentation.*
- “Application of Fluorescence Spectroscopy to Forensic Fiber Examination”, Andres D. Campiglia, Mathew Rex, Krishna Veni and Michael Sigman. Poster presented at the *Trace Evidence Symposium*, August 2-7, 2009, Clearwater, FL, USA. Participation: *Poster presenter and corresponding author.*
- “Room Temperature Fluorescence Spectroscopy as a Tool for the Forensic Trace Analysis of Textile Fibers”, Mathew Rex, Ph.D. Dissertation, Major Advisor: Professor Andres D. Campiglia, Department of Chemistry, University of Central Florida, summer Term 2009.

## VII. Appendix Section

## **Appendix A: Molecular Structures of Investigated Dyes**

**Disperse Red 1****Disperse Red 4****Disperse Red 13****Disperse Blue 56****Basic Green 4****Basic Red 9****Basic Violet 14****Direct Blue 1**

**Direct Blue 71****Direct Blue 90****Acid Red 151****Acid Yellow 17****Acid Yellow 23****Acid Green 27**

## **Appendix B: Room-Temperature Excitation and Fluorescence Spectra of Fiber Extracts**

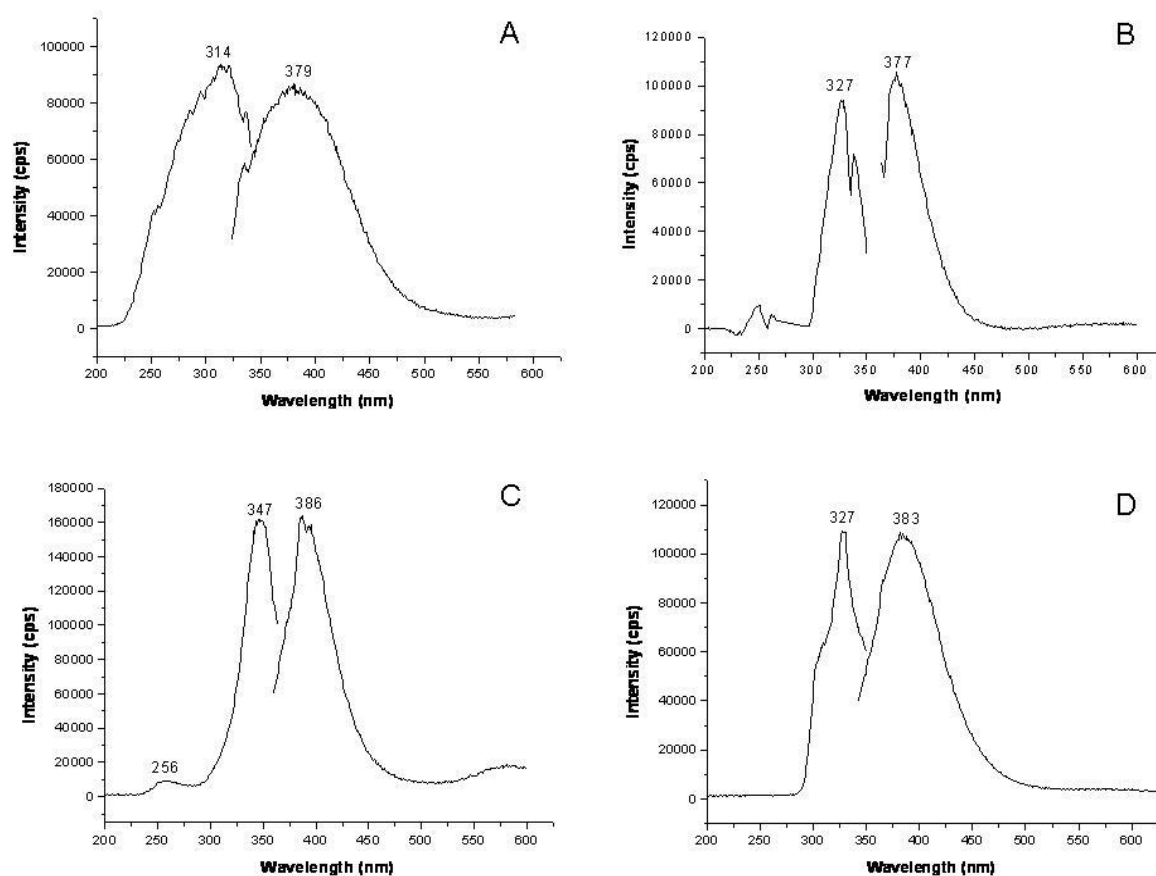


Figure B-1 Fluorescence spectra of extracts taken from acetate fibers dyed with Disperse Red 1 dye. Extracts are in A-1:1 methanol/water (v:v) B-ethanol C-1:1 acetonitrile/water (v:v) D-4:3 pyridine/water (v:v). Excitation and emission set at maximum wavelength.

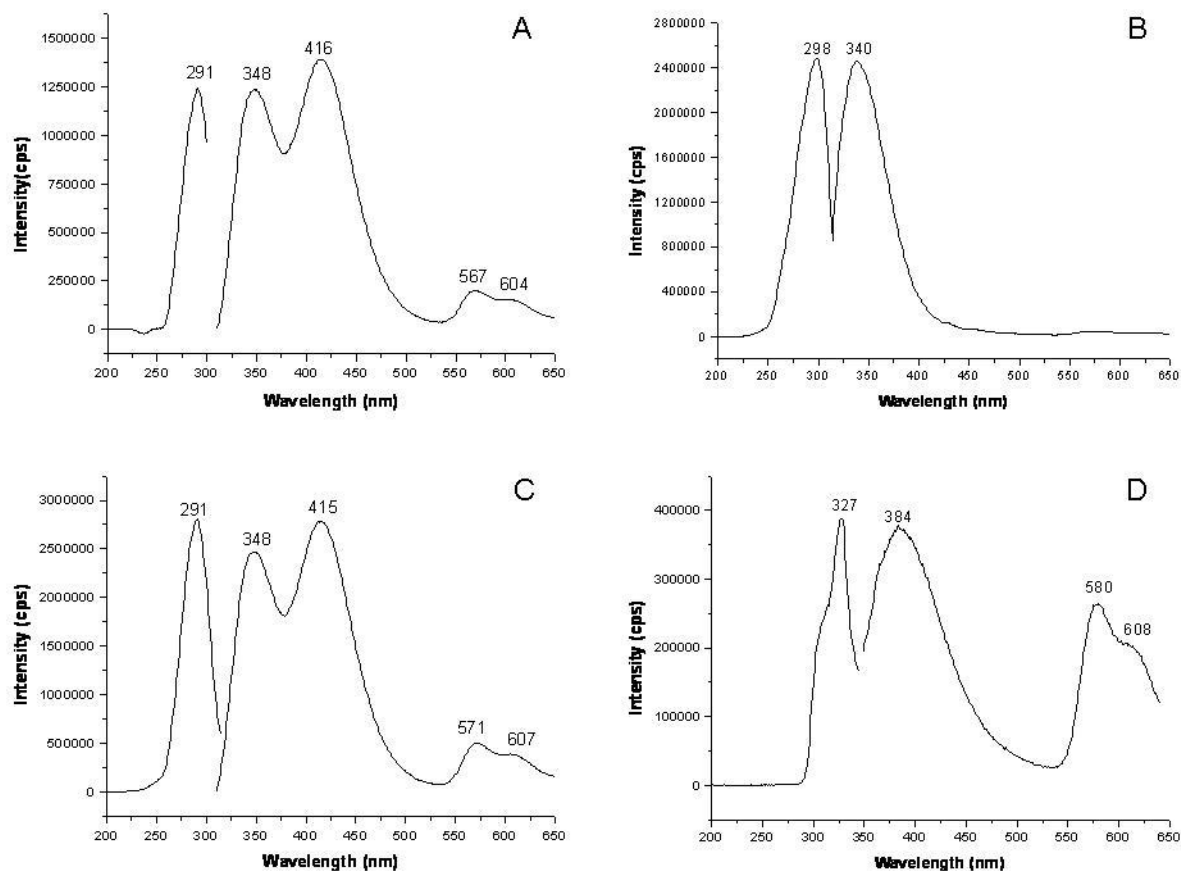


Figure B-2 Fluorescence spectra of extracts taken from polyester fibers dyed with Disperse Red 4 dye. Extracts are in A-1:1 methanol/water (v:v) B-ethanol C-1:1 acetonitrile/water (v:v) D-4:3 pyridine/water (v:v). Excitation and emission set at maximum wavelength.

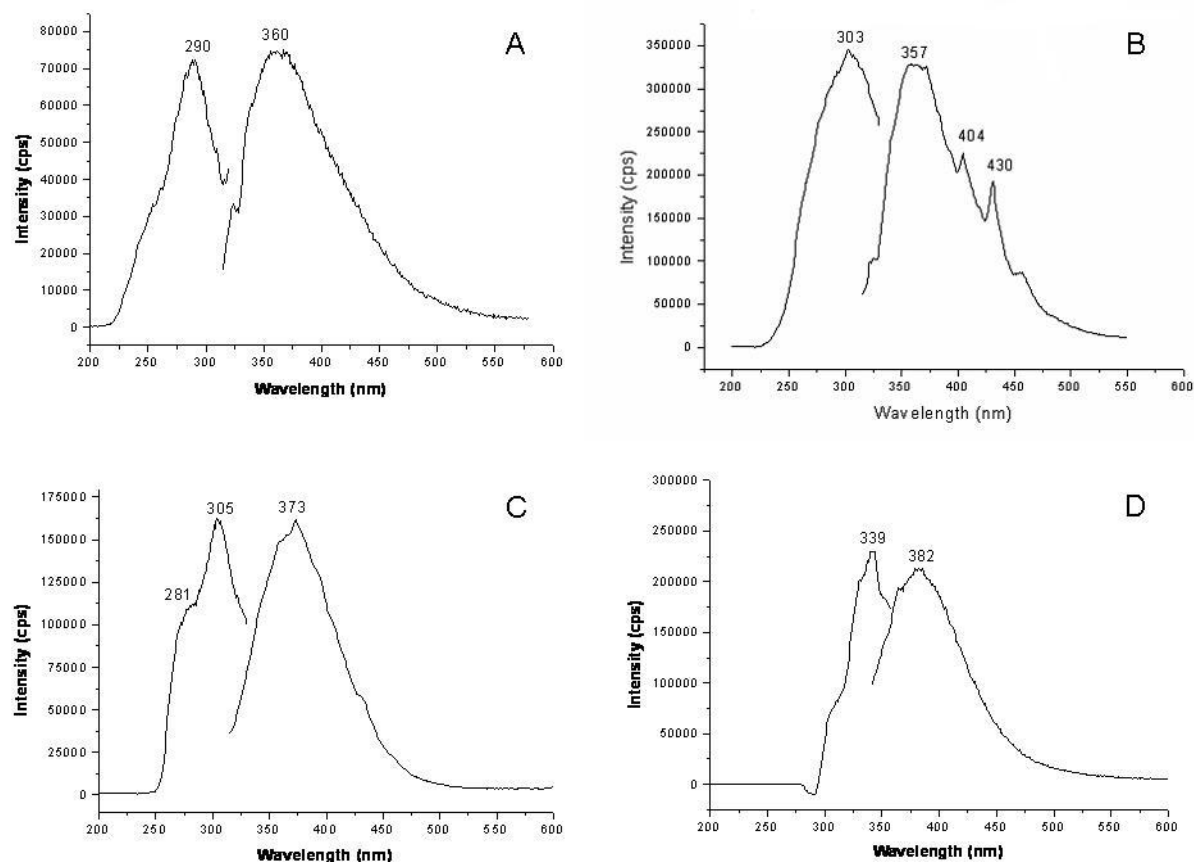


Figure B-3 Fluorescence spectra of extracts taken from polyester fibers dyed with Disperse Red 13 dye. Extracts are in A-1:1 methanol/water (v:v) B-ethanol C-1:1 acetonitrile/water (v:v) D-4:3 pyridine/water (v:v). Excitation and emission set at maximum wavelength.

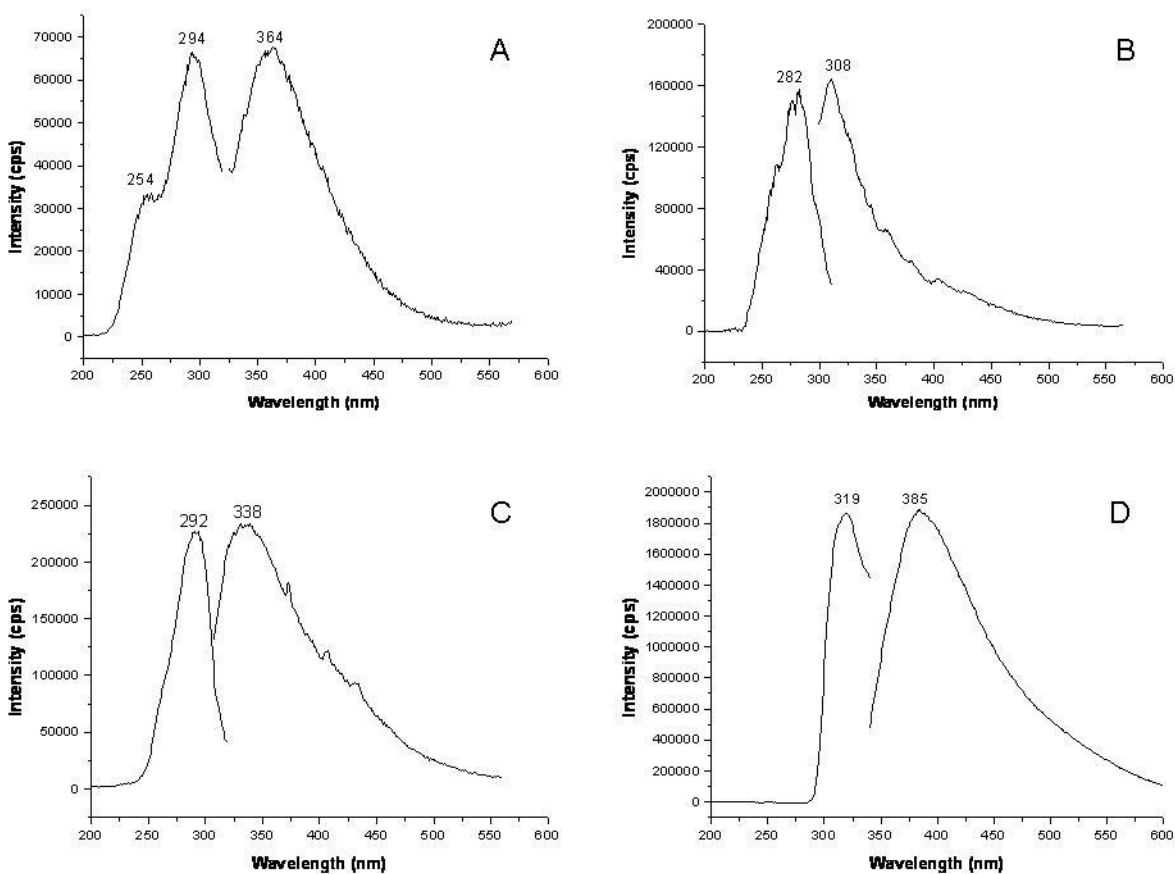


Figure B-4 Fluorescence spectra of extracts taken from polyester fibers dyed with Disperse Blue 56 dye. Extracts are in A-1:1 methanol/water (v:v) B-ethanol C-1:1 acetonitrile/water (v:v) D-4:3 pyridine/water (v:v). Excitation and emission set at maximum wavelength.

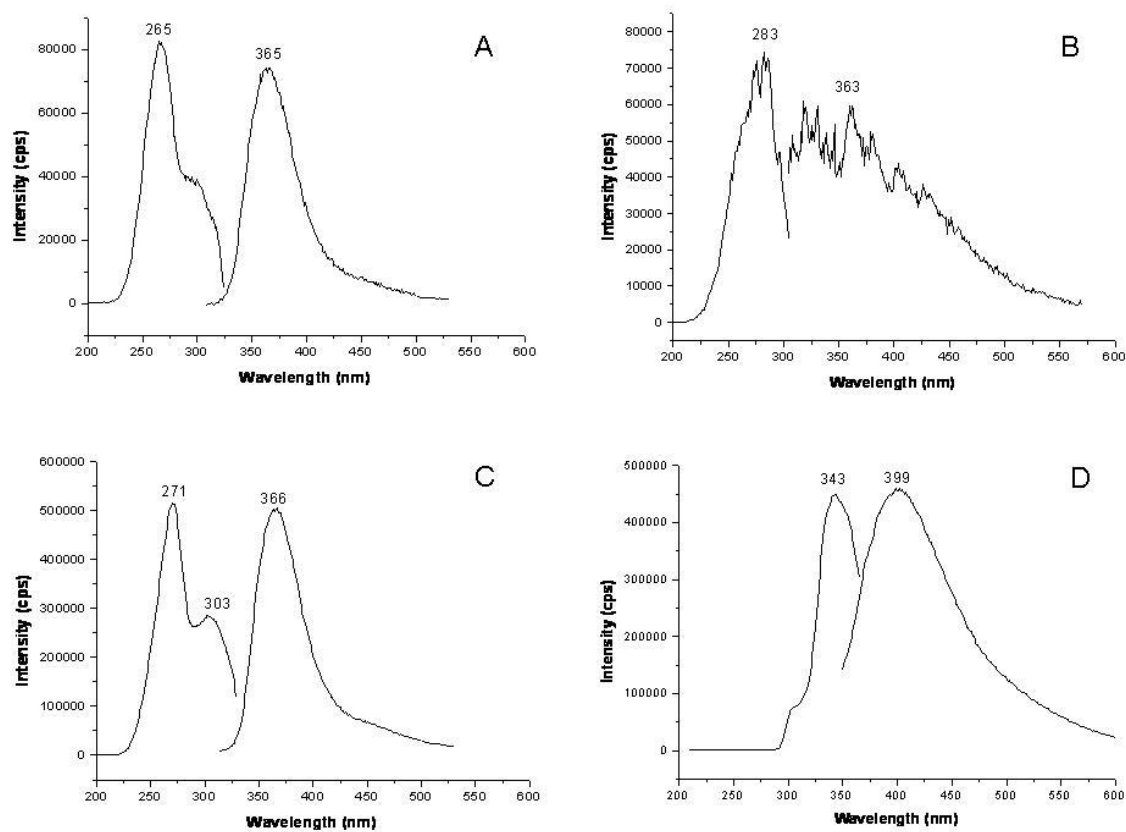


Figure B-5 Fluorescence spectra of extracts taken from poly-acrylic fibers dyed with Basic Green 4 dye. Extracts are in A-1:1 methanol/water (v:v) B-ethanol C-1:1 acetonitrile/water (v:v) D-4:3 pyridine/water (v:v). Excitation and emission set at maximum wavelength.

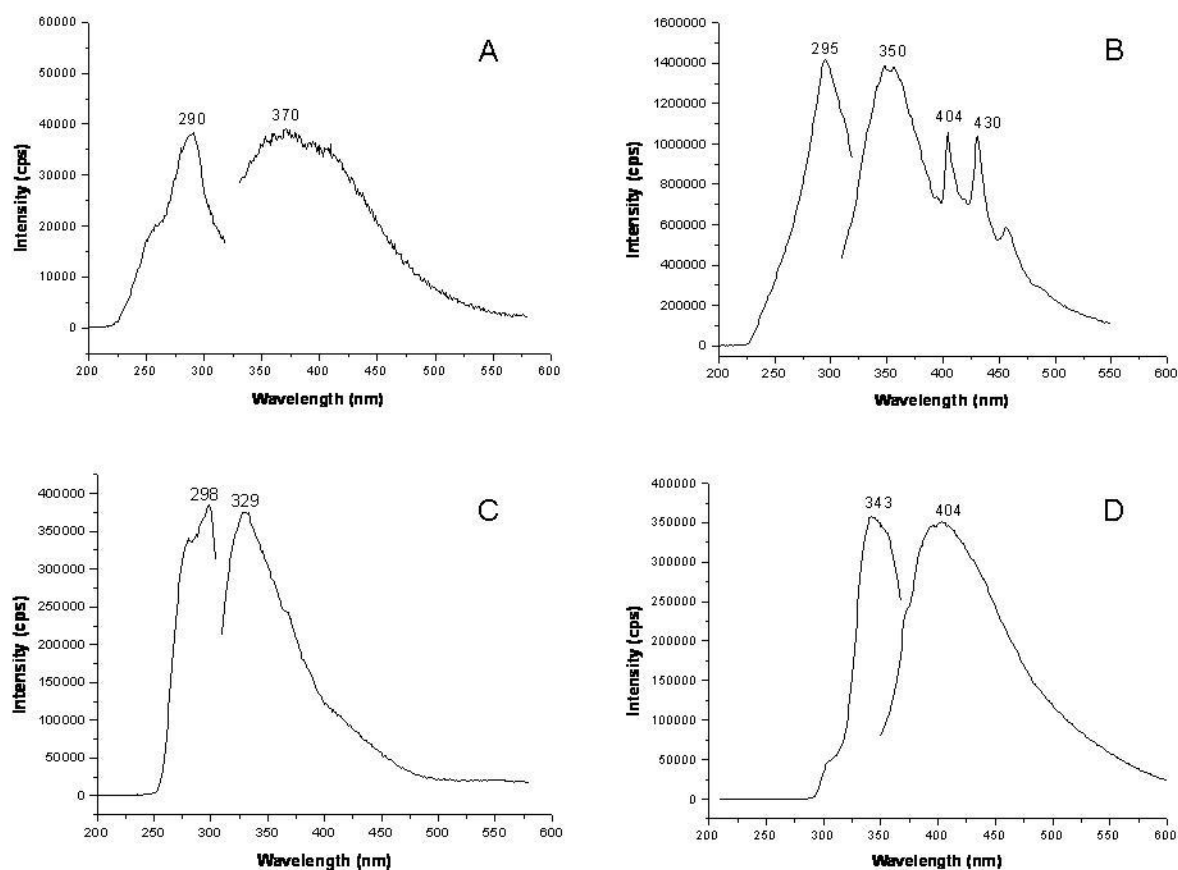


Figure B-6 Fluorescence spectra of extracts taken from polyester fibers dyed with Basic Red 9 dye. Extracts are in A-1:1 methanol/water (v:v) B-ethanol C-1:1 acetonitrile/water (v:v) D-4:3 pyridine/water (v:v). Excitation and emission set at maximum wavelength.

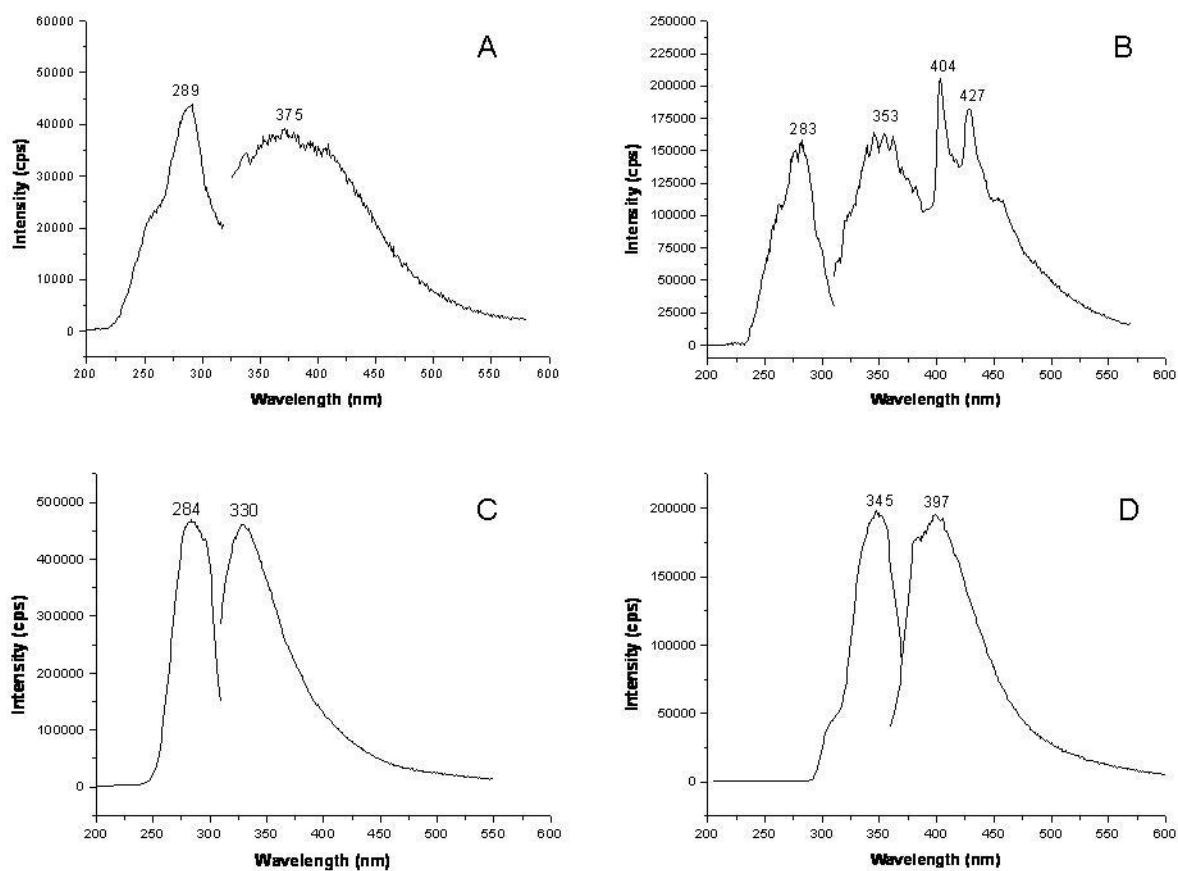


Figure B-7 Fluorescence spectra of extracts taken from polyester fibers dyed with Basic Violet 14 dye. Extracts are in A-1:1 methanol/water (v:v) B-ethanol C-1:1 acetonitrile/water (v:v) D-4:3 pyridine/water (v:v). Excitation and emission set at maximum wavelength.

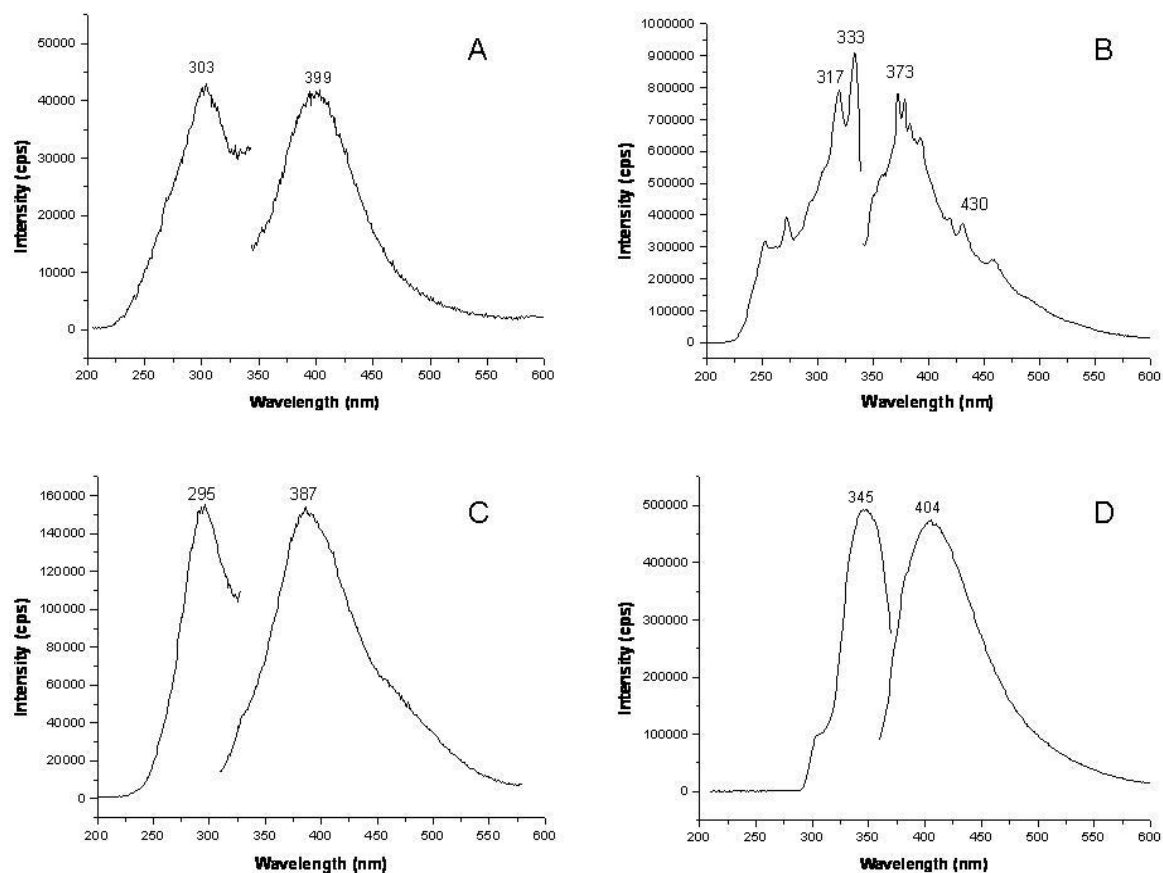


Figure B-8 Fluorescence spectra of extracts taken from cotton fibers dyed with Direct Blue 1 dye. Extracts are in A-1:1 methanol/water (v:v) B-ethanol C-1:1 acetonitrile/water (v:v) D-4:3 pyridine/water (v:v). Excitation and emission set at maximum wavelength.

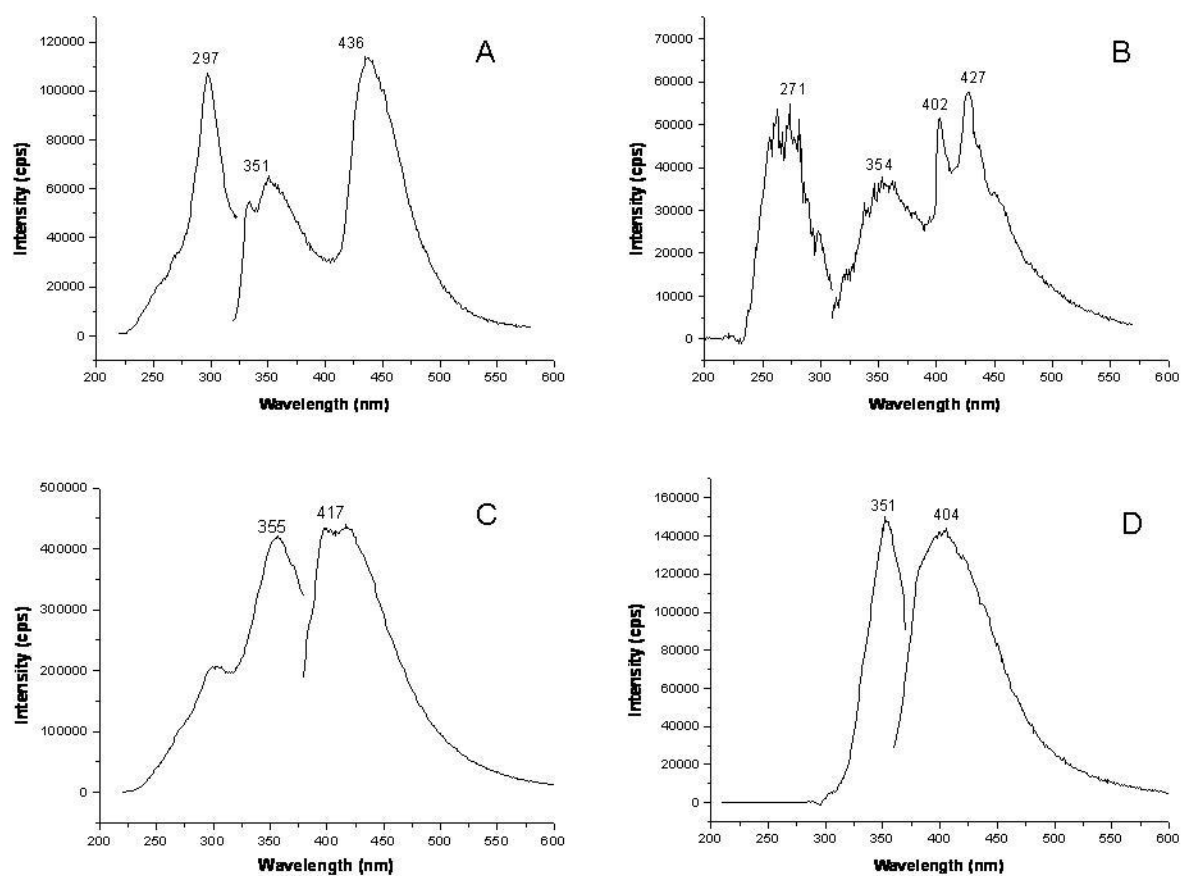


Figure B-9 Fluorescence spectra of extracts taken from cotton fibers dyed with Direct Blue 71 dye. Extracts are in A-1:1 methanol/water (v:v) B-ethanol C-1:1 acetonitrile/water (v:v) D-4:3 pyridine/water (v:v). Excitation and emission set at maximum wavelength.

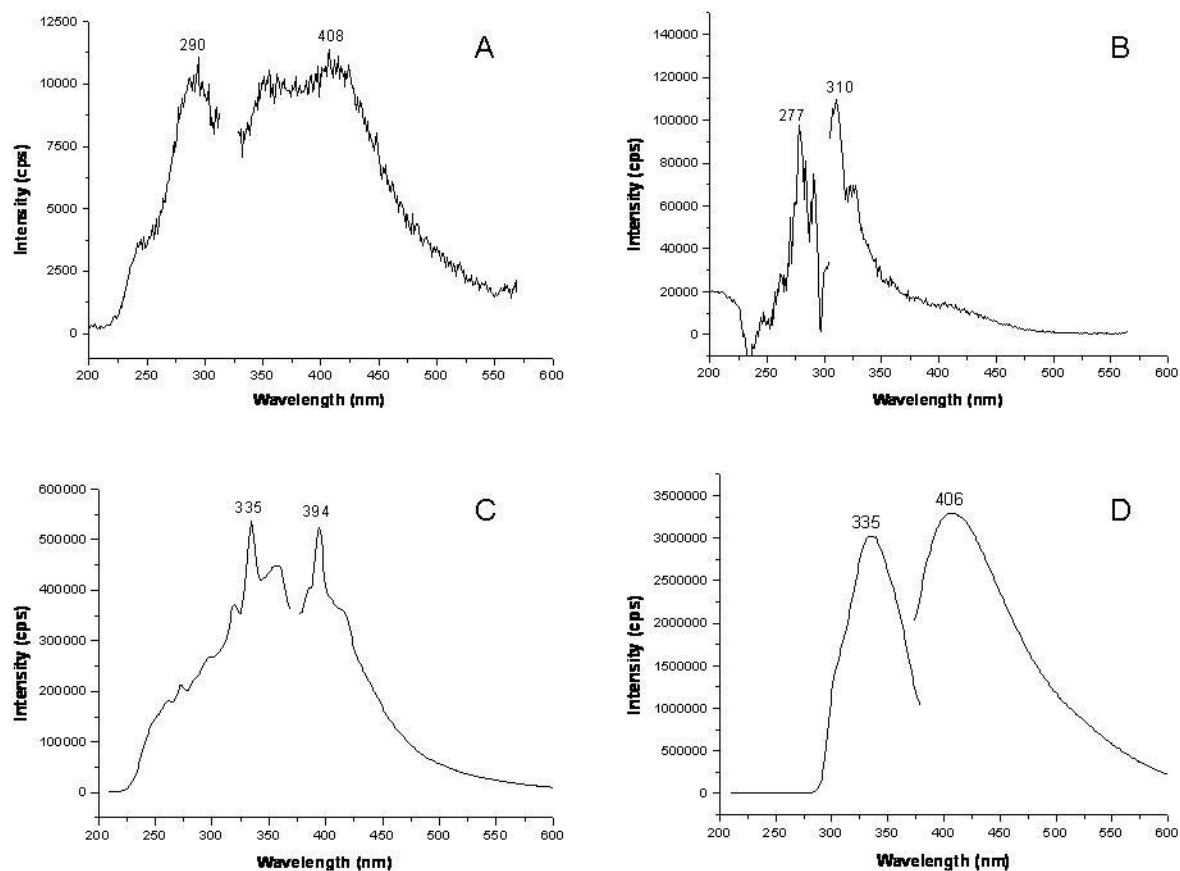


Figure B-10 Fluorescence spectra of extracts taken from cotton fibers dyed with Direct Blue 90 dye. Extracts are in A-1:1 methanol/water (v:v) B-ethanol C-1:1 acetonitrile/water (v:v) D-4:3 pyridine/water (v:v). Excitation and emission set at maximum wavelength.

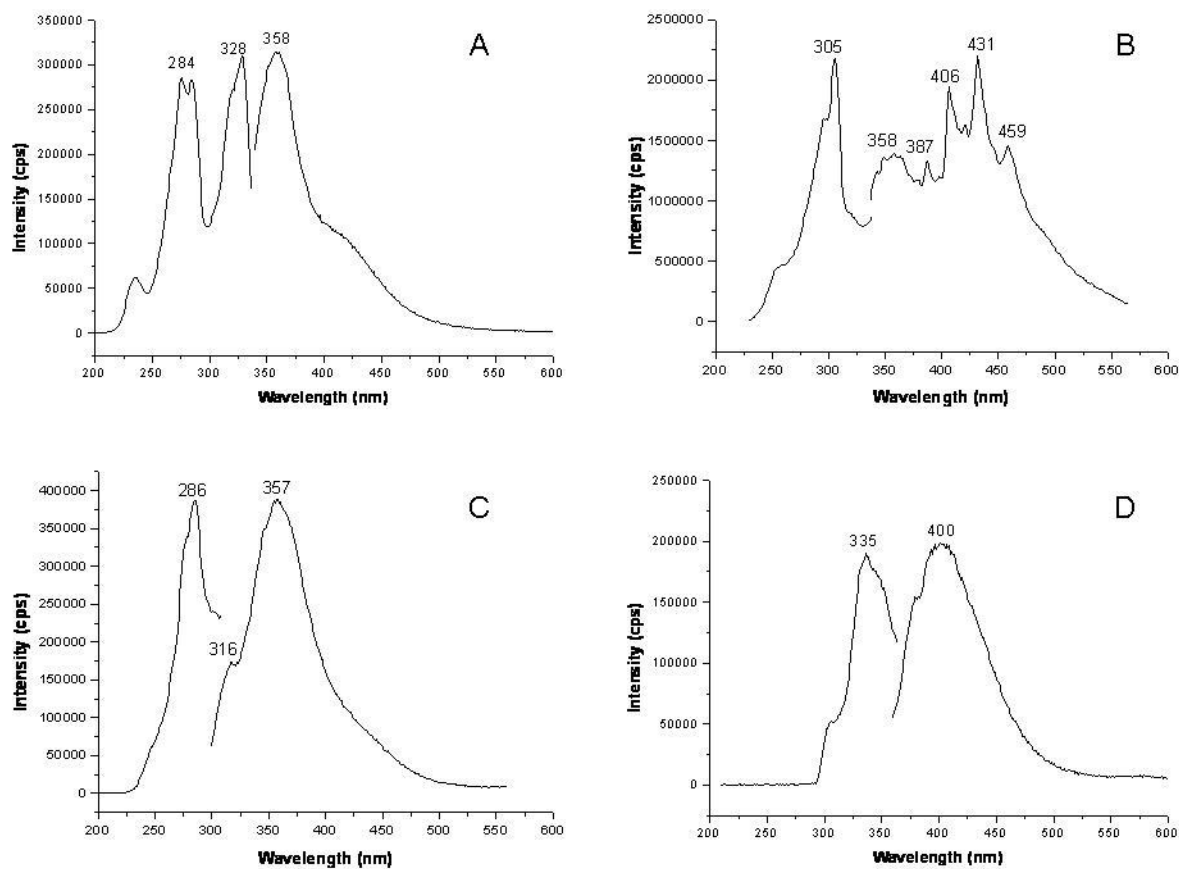


Figure B-11 Fluorescence spectra of extracts taken from nylon fibers dyed with Acid Red 151 dye. Extracts are in A-1:1 methanol/water (v:v) B-ethanol C-1:1 acetonitrile/water (v:v) D-4:3 pyridine/water (v:v). Excitation and emission set at maximum wavelength.

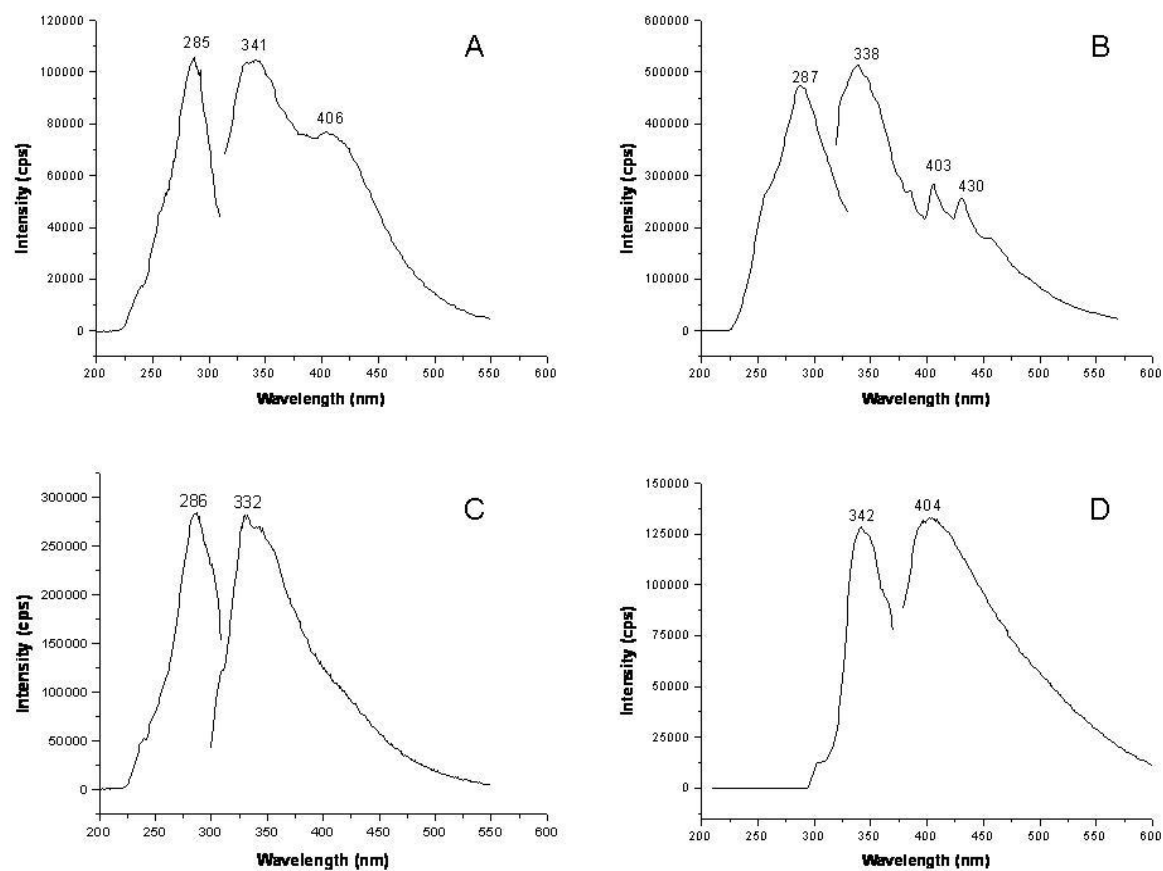


Figure B-12 Fluorescence spectra of extracts taken from nylon fibers dyed with Acid Yellow 17 dye. Extracts are in A-1:1 methanol/water (v:v) B-ethanol C-1:1 acetonitrile/water (v:v) D-4:3 pyridine/water (v:v). Excitation and emission set at maximum wavelength.

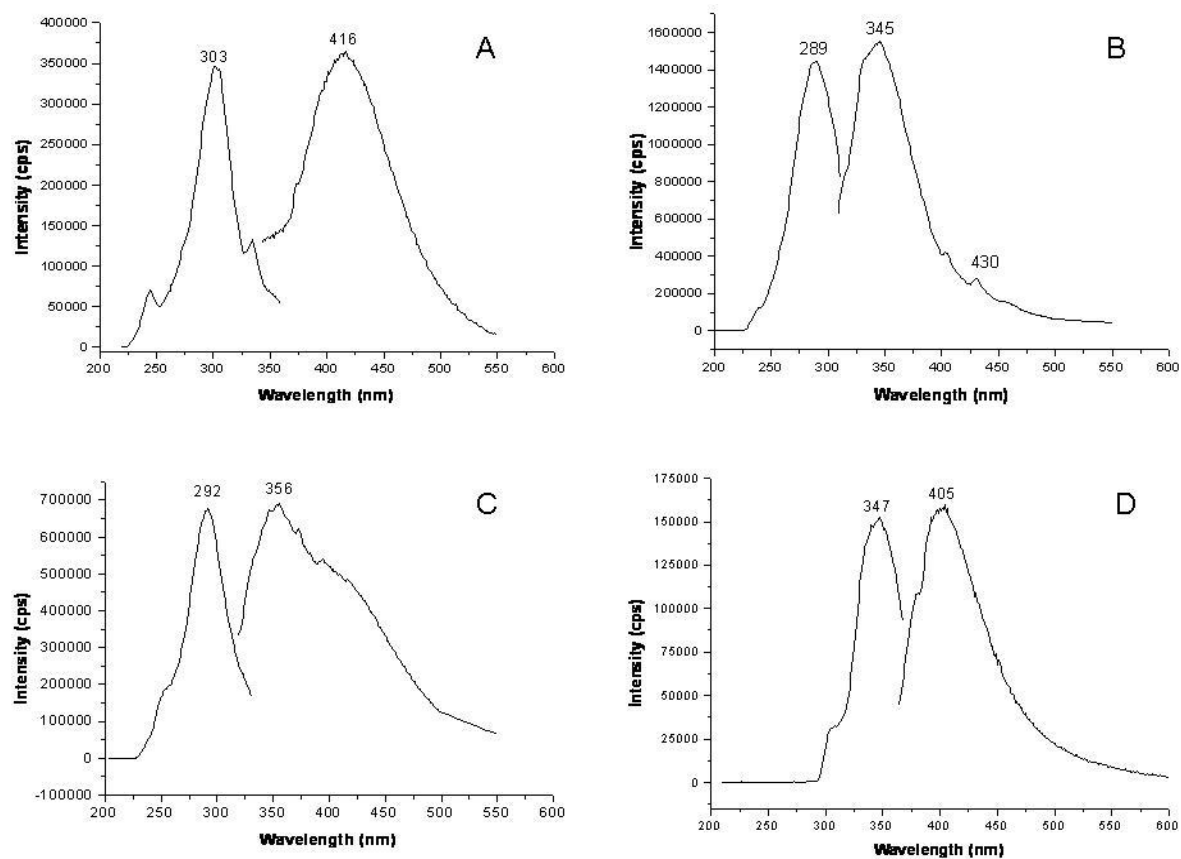


Figure B-13 Fluorescence spectra of extracts taken from nylon fibers dyed with Acid Yellow 23 dye. Extracts are in A-1:1 methanol/water (v:v) B-ethanol C-1:1 acetonitrile/water (v:v) D-4:3 pyridine/water (v:v). Excitation and emission set at maximum wavelength.

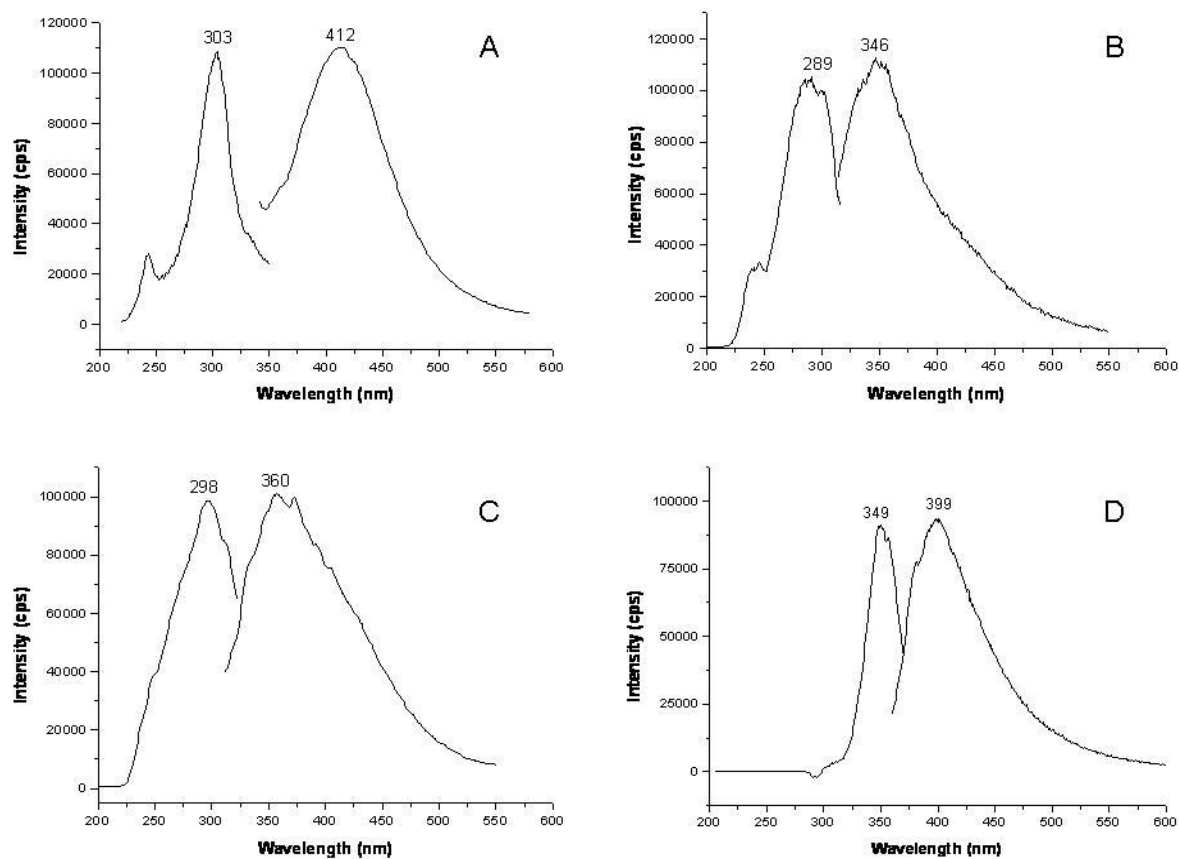


Figure B-14 Fluorescence spectra of extracts taken from nylon fibers dyed with Acid Green 27 dye. Extracts are in A-1:1 methanol/water (v:v) B-ethanol C-1:1 acetonitrile/water (v:v) D-4:3 pyridine/water (v:v). Excitation and emission set at maximum wavelength.

## **Appendix C: Ultraviolet and Visible Absorption Spectra of Sigma-Aldrich Dye Standards and Fiber Extracts at Room Temperature**

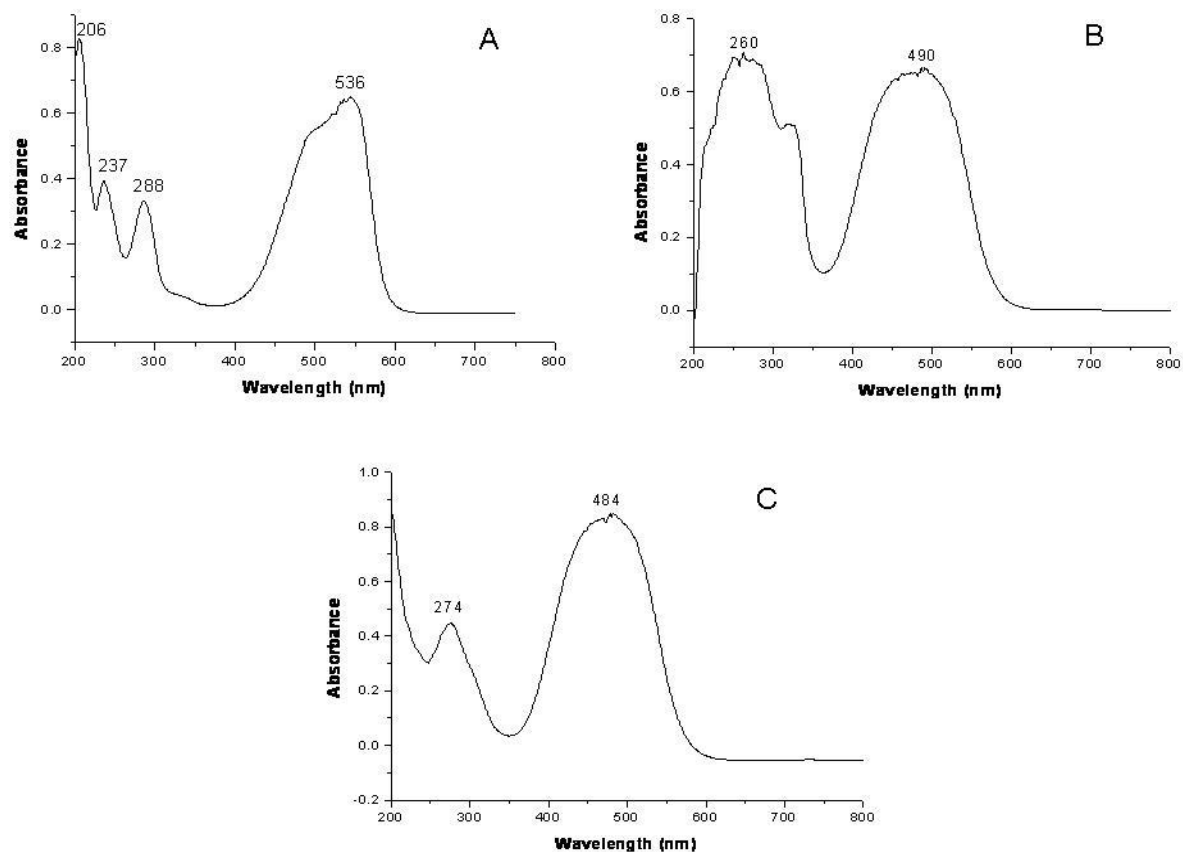


Figure C-1 Absorbance spectra of Disperse Red 1 A-10ppm standard in 1:1 methanol/water (v:v) B-10ppm standard in ethanol C-extract taken from acetate fibers dyed with Disperse Red 1 in ethanol.

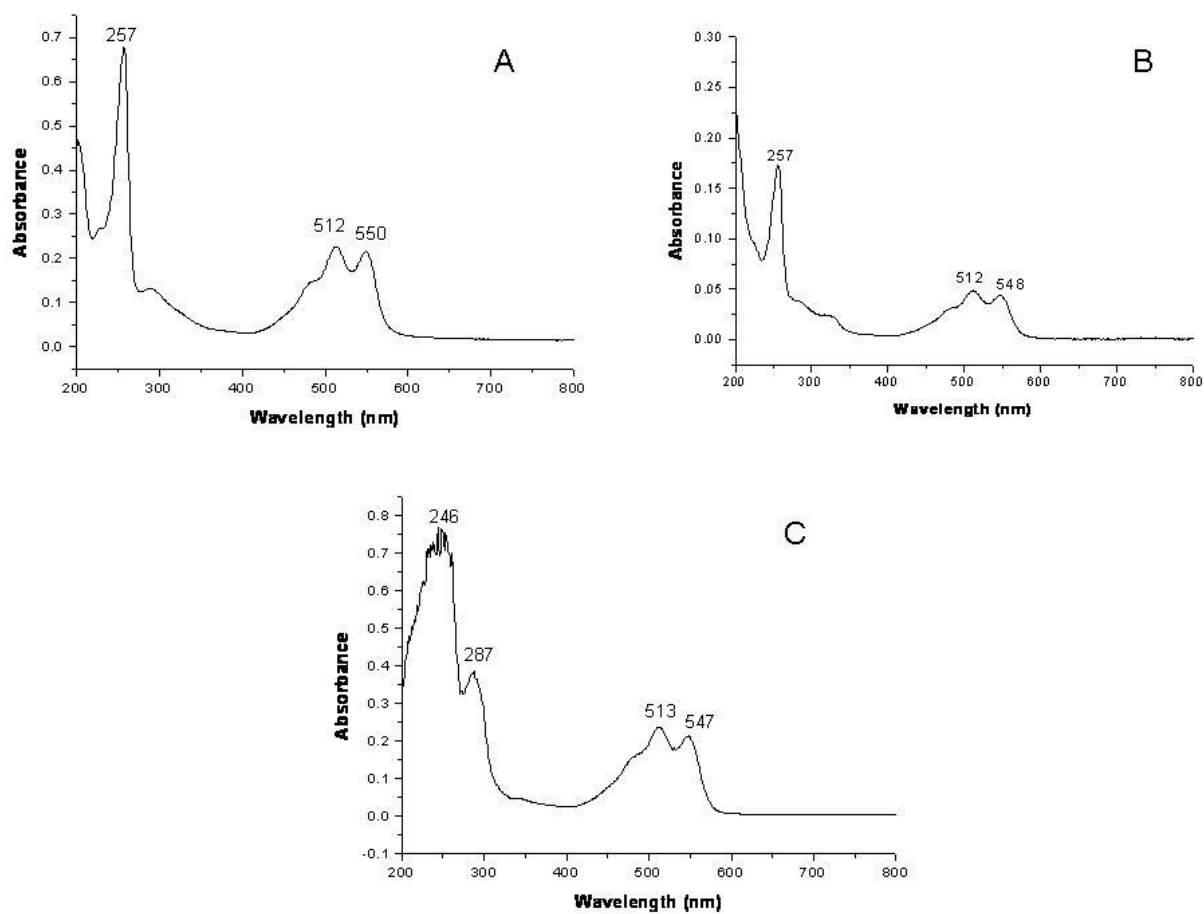


Figure C-2 Absorbance spectra of Disperse Red 4 A-10ppm standard in 1:1 methanol/water (v:v) B-10ppm standard in 1:1 acetonitrile/water (v:v) C-extract taken from polyester fibers dyed with Disperse Red 4 in 1:1 acetonitrile/water (v:v).

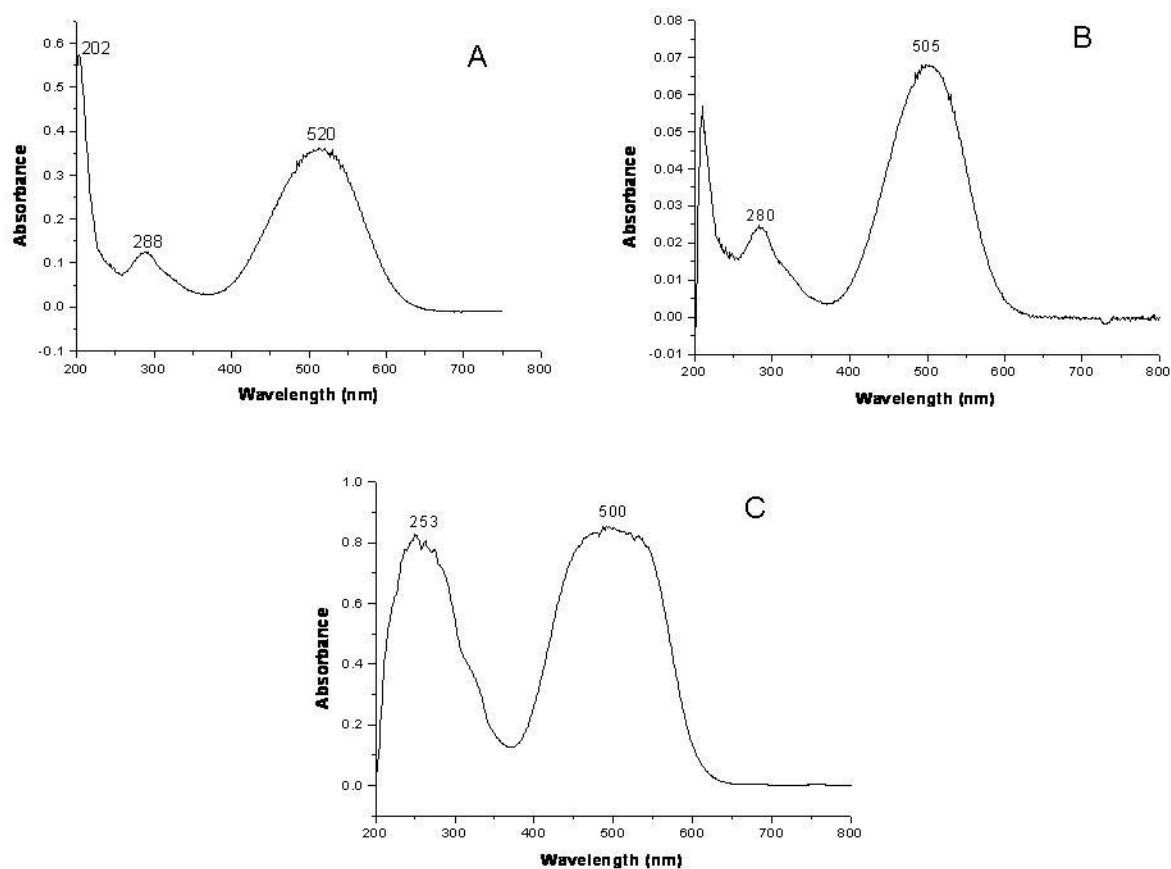


Figure C-3 Absorbance spectra of Disperse Red 13 A-10ppm standard in 1:1 methanol/water (v:v) B-10ppm standard in ethanol C-extract taken from polyester fibers dyed with Disperse Red 13 in ethanol.

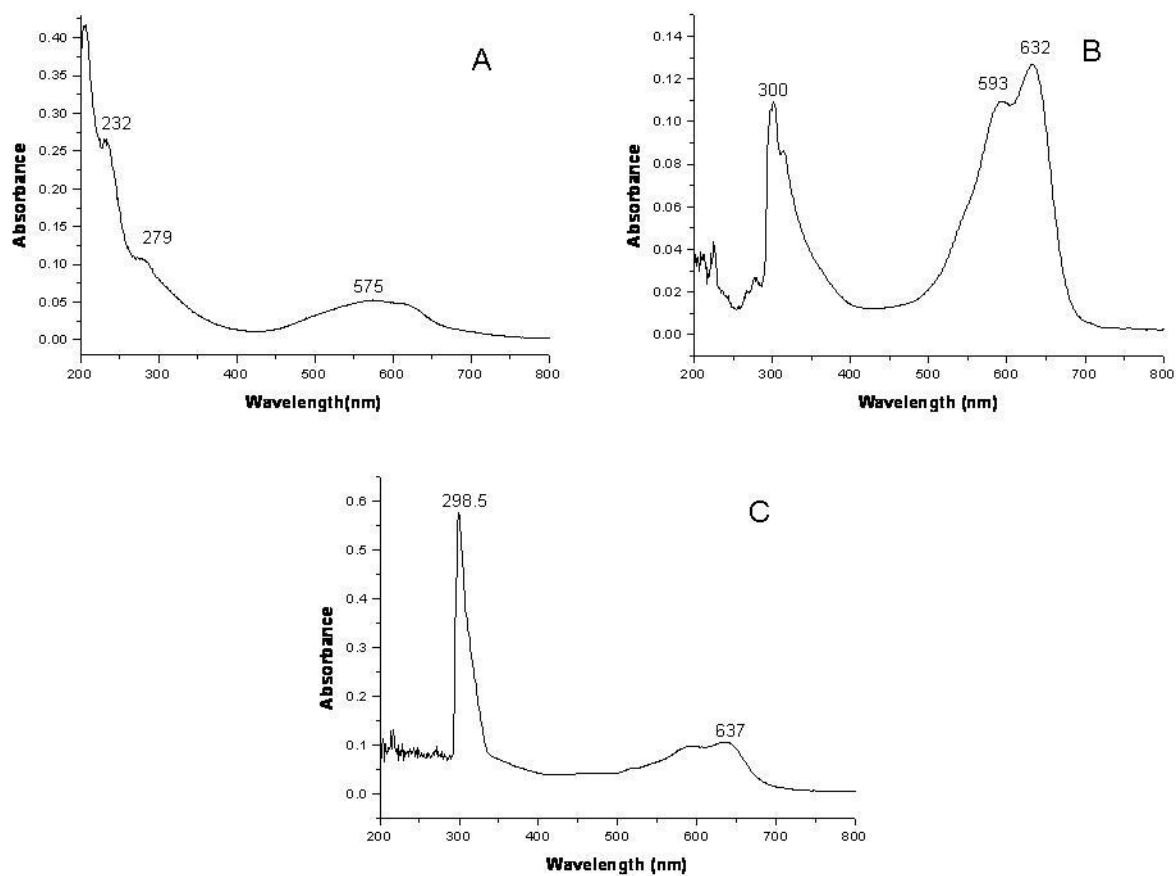
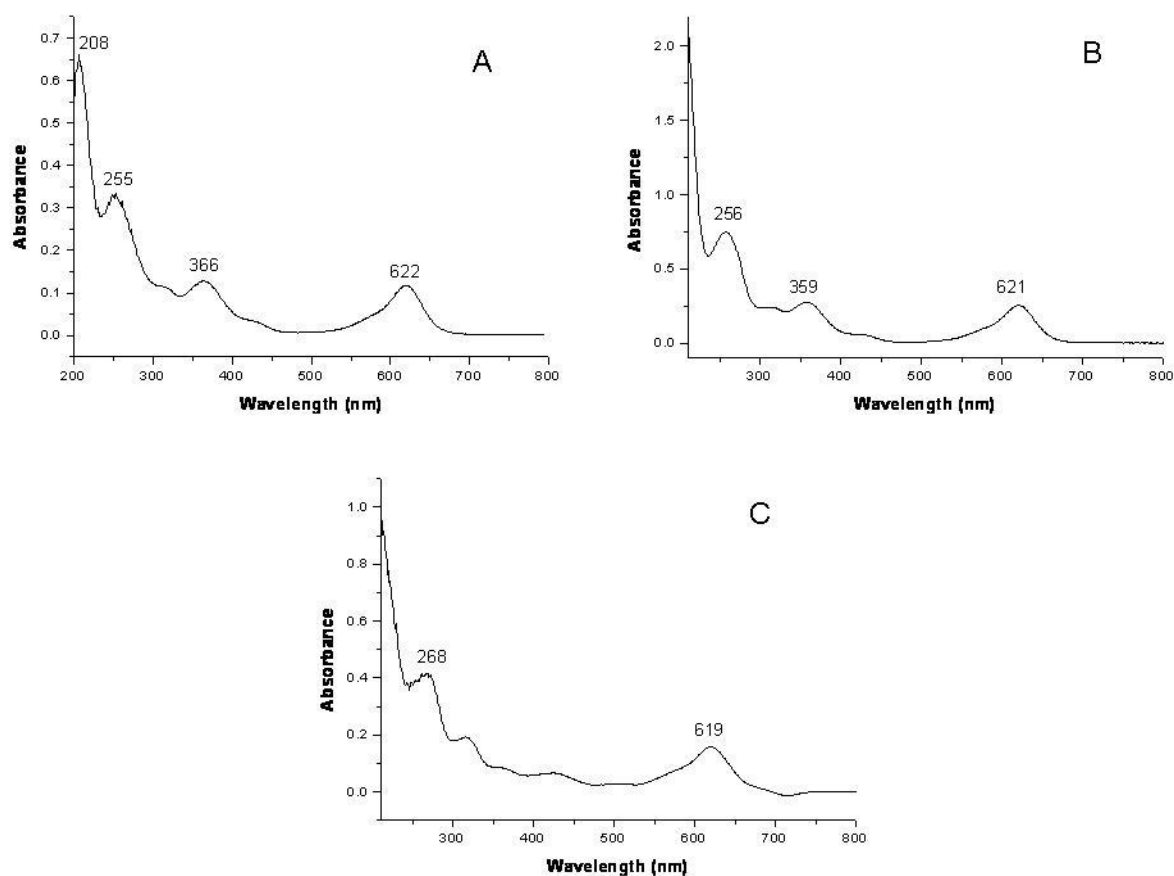


Figure C-4 Absorbance spectra of Disperse Blue 56 A-10ppm standard in 1:1 methanol/water (v:v) B-10ppm standard in 4:3 pyridine/water (v:v) C-extract taken from polyester fibers dyed with Disperse Blue 56 in 4:3 pyridine/water (v:v).



*Figure C-5 Absorbance spectra of Basic Green 4 A-10ppm standard in 1:1 methanol/water (v:v) B-10ppm standard in 1:1 acetonitrile/water (v:v) C-extract taken from poly-acrylic fibers dyed with Basic Green 4 in 1:1 acetonitrile/water (v:v).*

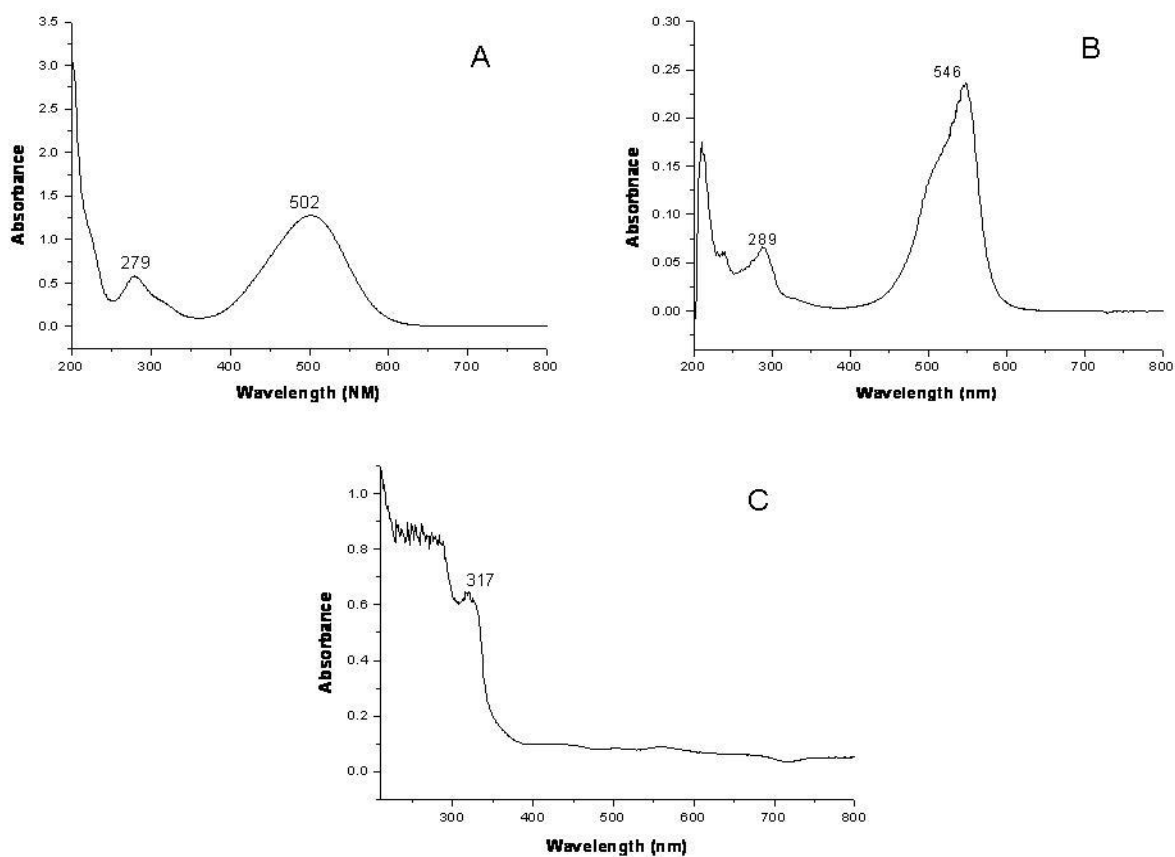
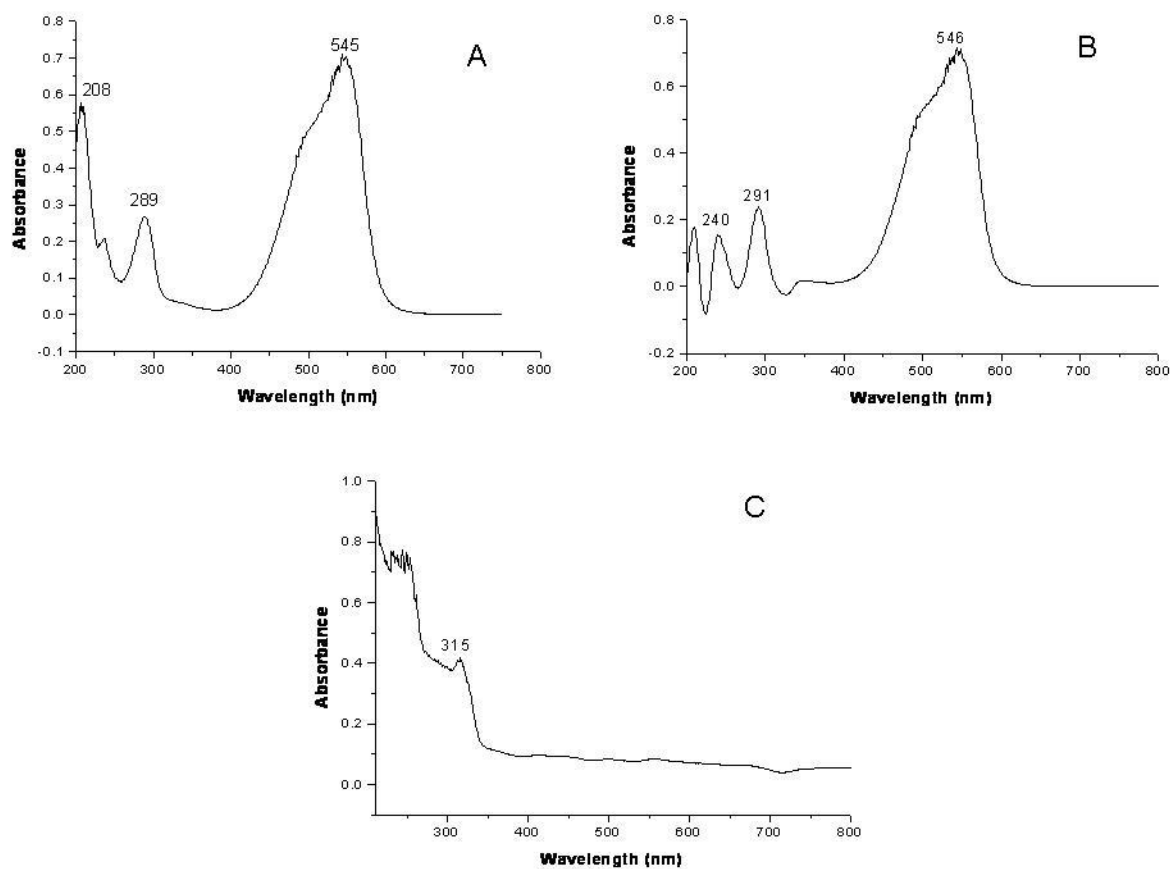
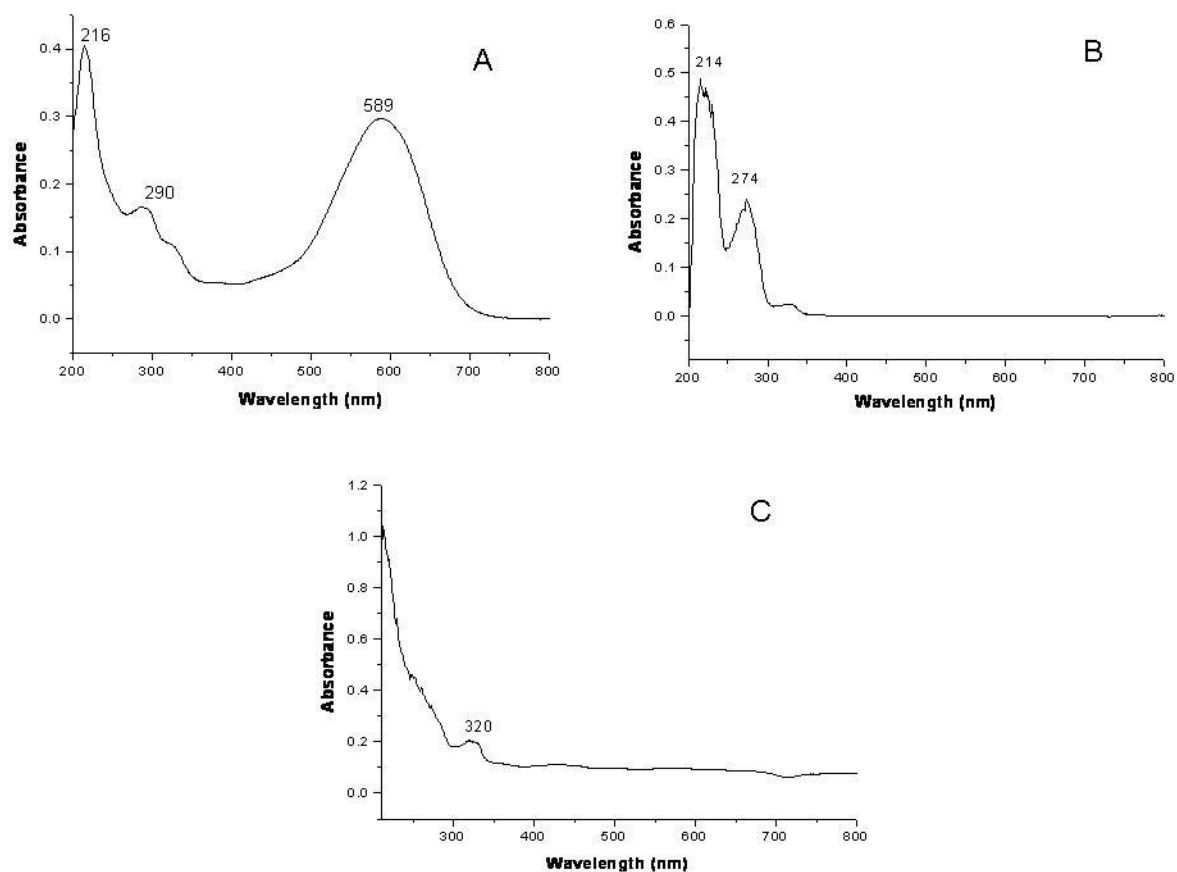


Figure C-6 Absorbance spectra of Basic Red 9 A-10ppm standard in 1:1 methanol/water (v:v) B-10ppm standard in ethanol C-extract taken from polyester fibers dyed with Basic Red 9 in ethanol.



*Figure C-7 Absorbance spectra of Basic Violet 14 A-10ppm standard in 1:1 methanol/water (v:v) B-10ppm standard in 1:1 acetonitrile/water (v:v) C-extract taken from polyester fibers dyed with Basic Violet 14 in 1:1 acetonitrile/water (v:v).*



*Figure C-8 Absorbance spectra of Direct Blue 1 A-10ppm standard in 1:1 methanol/water (v:v) B-10ppm standard in ethanol C-extract taken from cotton fibers dyed with Direct Blue 1 in ethanol.*

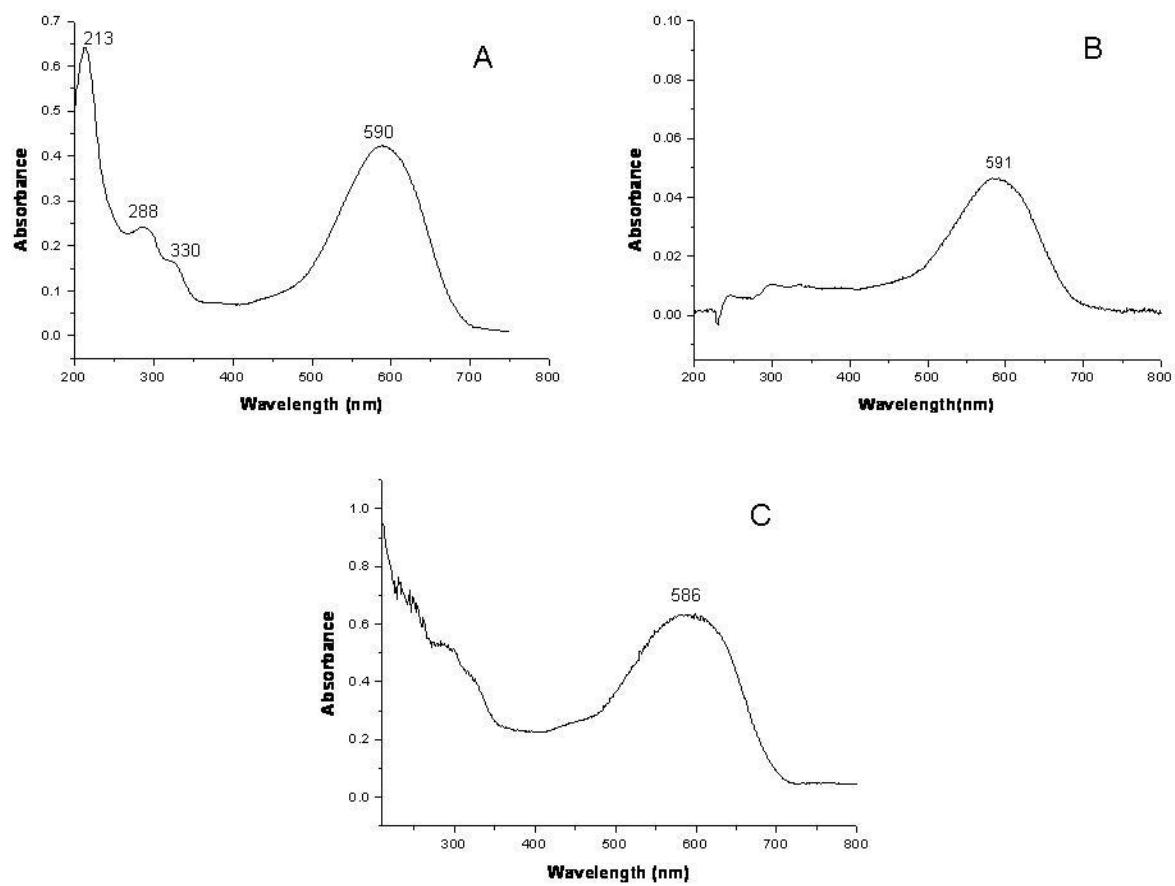


Figure C-9 Absorbance spectra of Direct Blue 71 A-10ppm standard in 1:1 methanol/water (v:v) B-10ppm standard in 1:1 acetonitrile/water (v:v) C-extract taken from cotton fibers dyed with Direct Blue 71 in 1:1 acetonitrile/water (v:v).

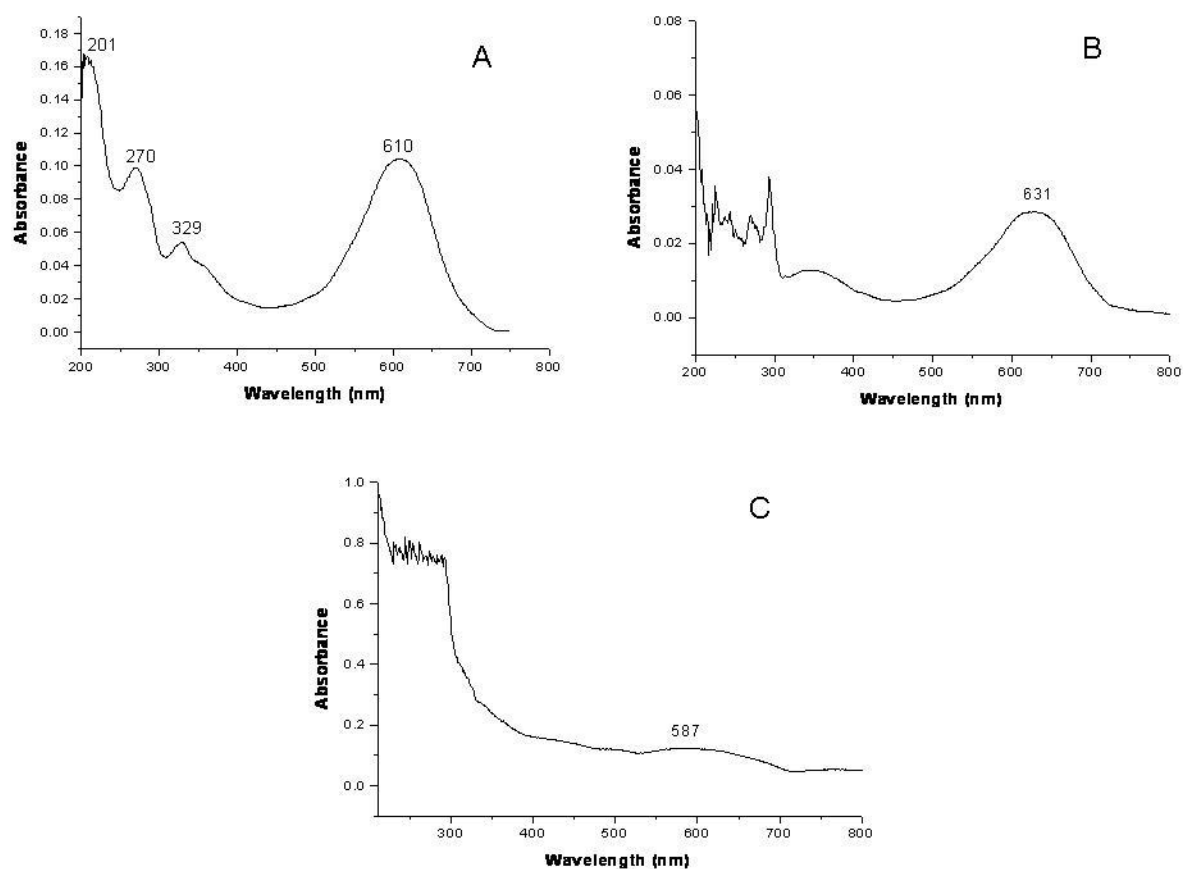


Figure C-10 Absorbance spectra of Direct Blue 90 A-10ppm standard in 1:1 methanol/water (v:v) B-10ppm standard in 4:3 pyridine/water (v:v) C-extract taken from cotton fibers dyed with Direct Blue 90 in 4:3 pyridine/water (v:v).

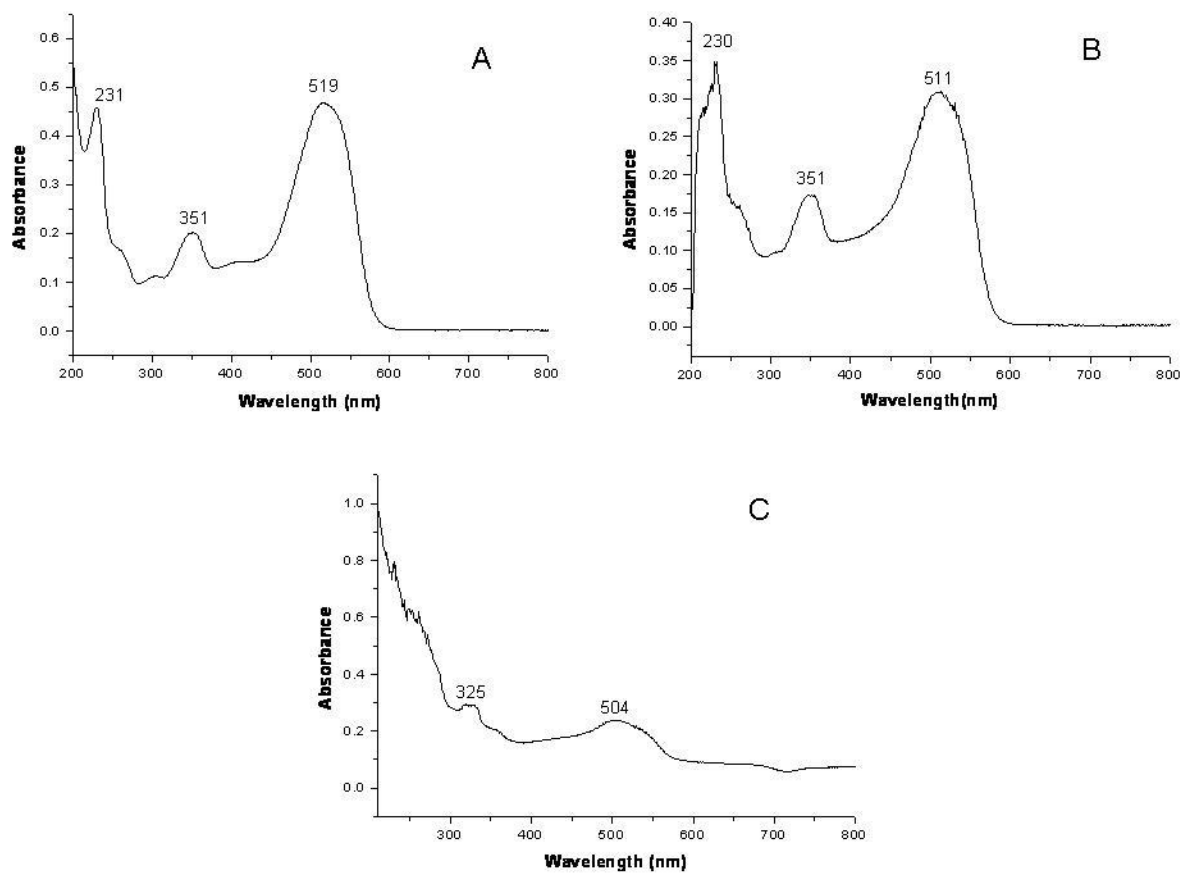


Figure C-11 Absorbance spectra of Acid Red 151 A-10ppm standard in 1:1 methanol/water (v:v) B-10ppm standard in ethanol C-extract taken from nylon fibers dyed with Acid Red 151 in ethanol.

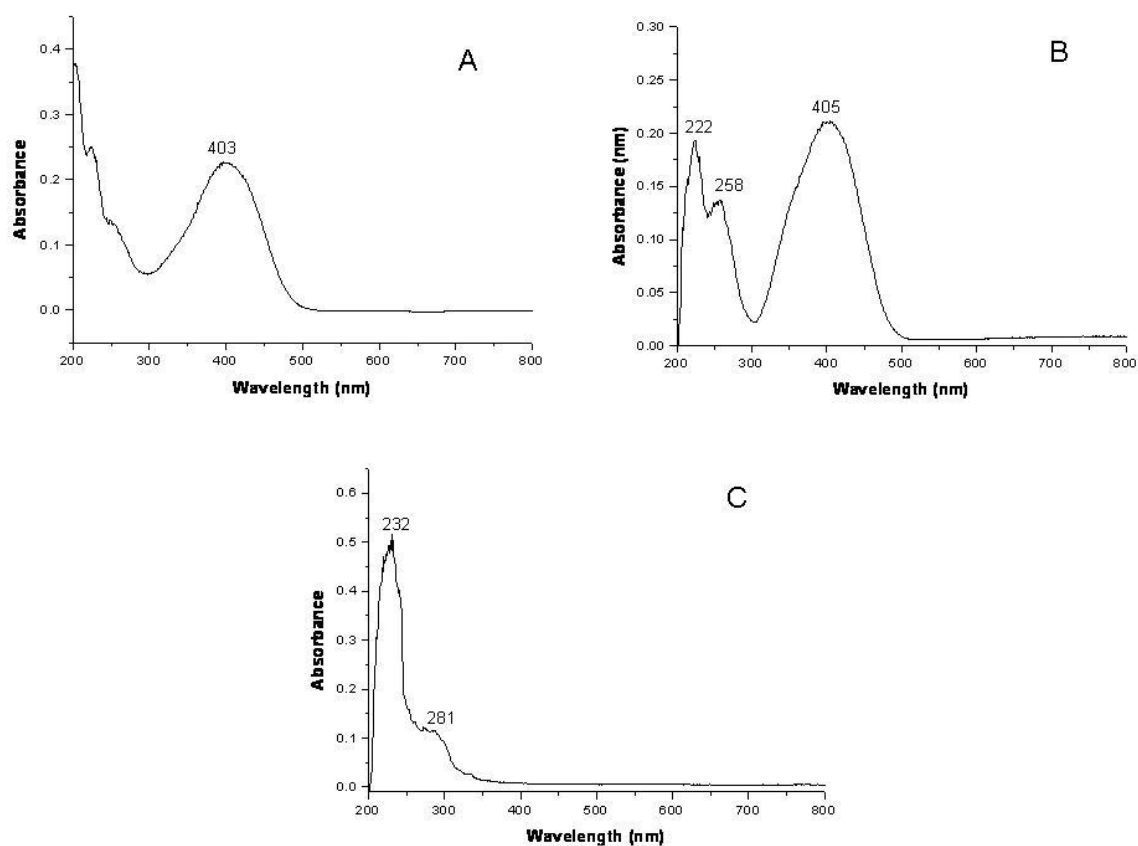


Figure C-12 Absorbance spectra of Acid Yellow 17 A-10ppm standard in 1:1 methanol/water (v:v) B-10ppm standard in ethanol C-extract taken from nylon fibers dyed with Acid Yellow 17 in ethanol.

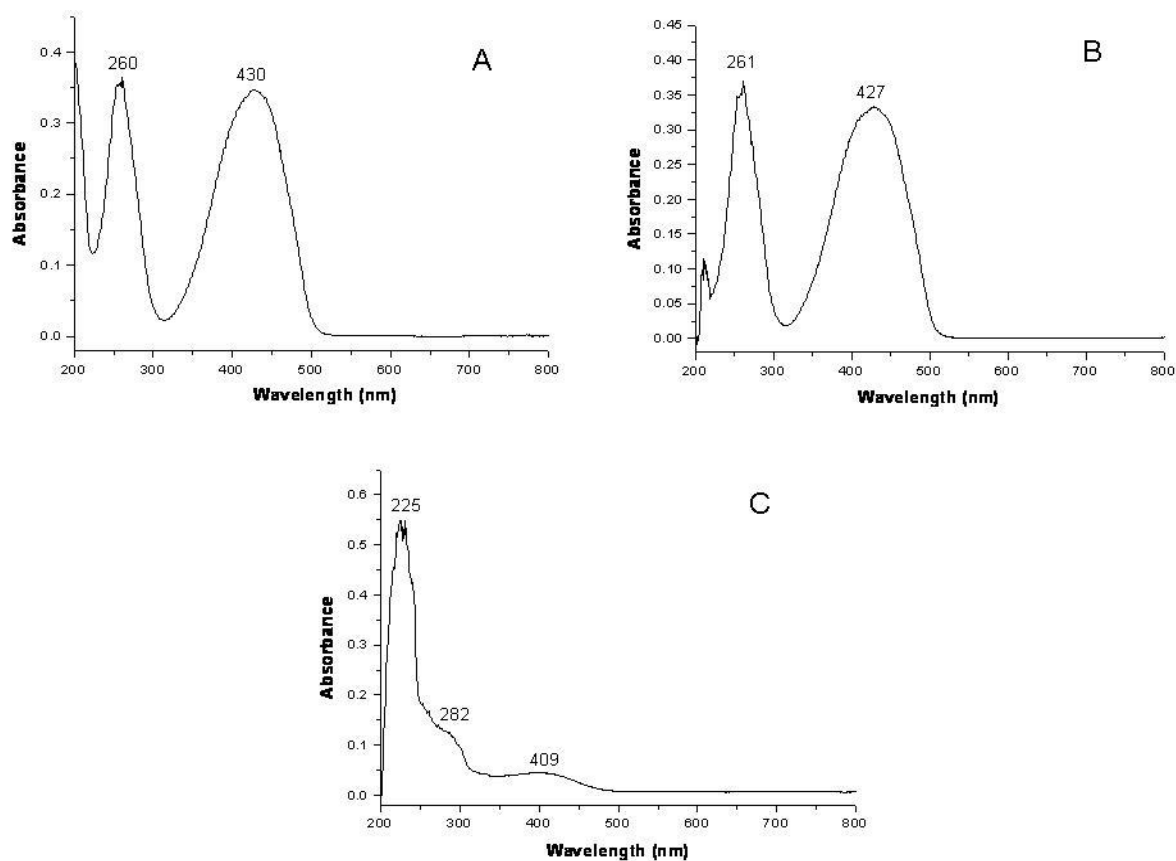
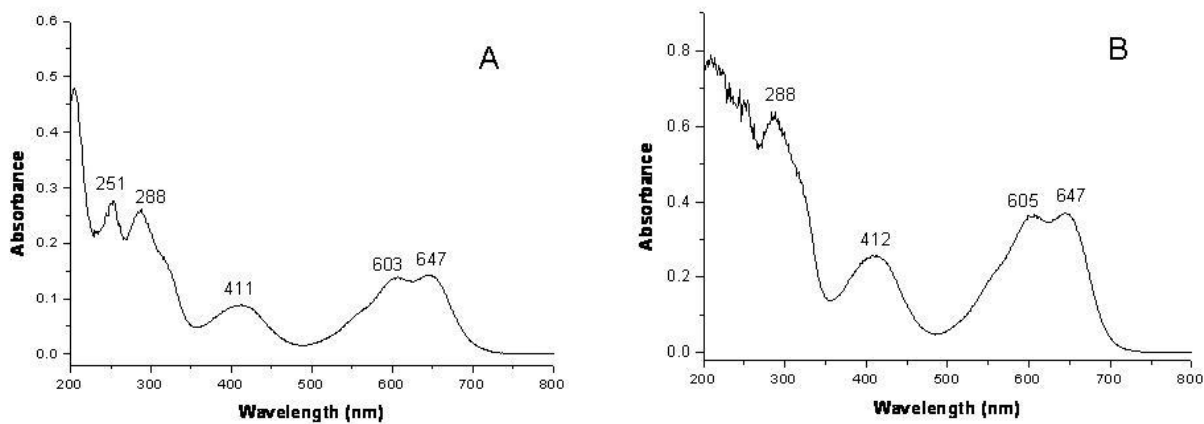


Figure C-13 Absorbance spectra of Acid Yellow 23 A-10ppm standard in 1:1 methanol/water (v:v) B-10ppm standard in ethanol C-extract taken from nylon fibers dyed with Acid Yellow 23 in ethanol.



*Figure C-14 Absorbance spectra of Acid Green 27 A-10ppm standard in 1:1 methanol/water (v:v) B-extract taken from nylon fibers dyed with Acid Green 27 in 1:1 methanol/water (v:v)*

**Appendix D: Room-Temperature Excitation and Fluorescence  
Spectra of Sigma-Aldrich Dye Standards in the Best Fiber  
Extracting Solvent**

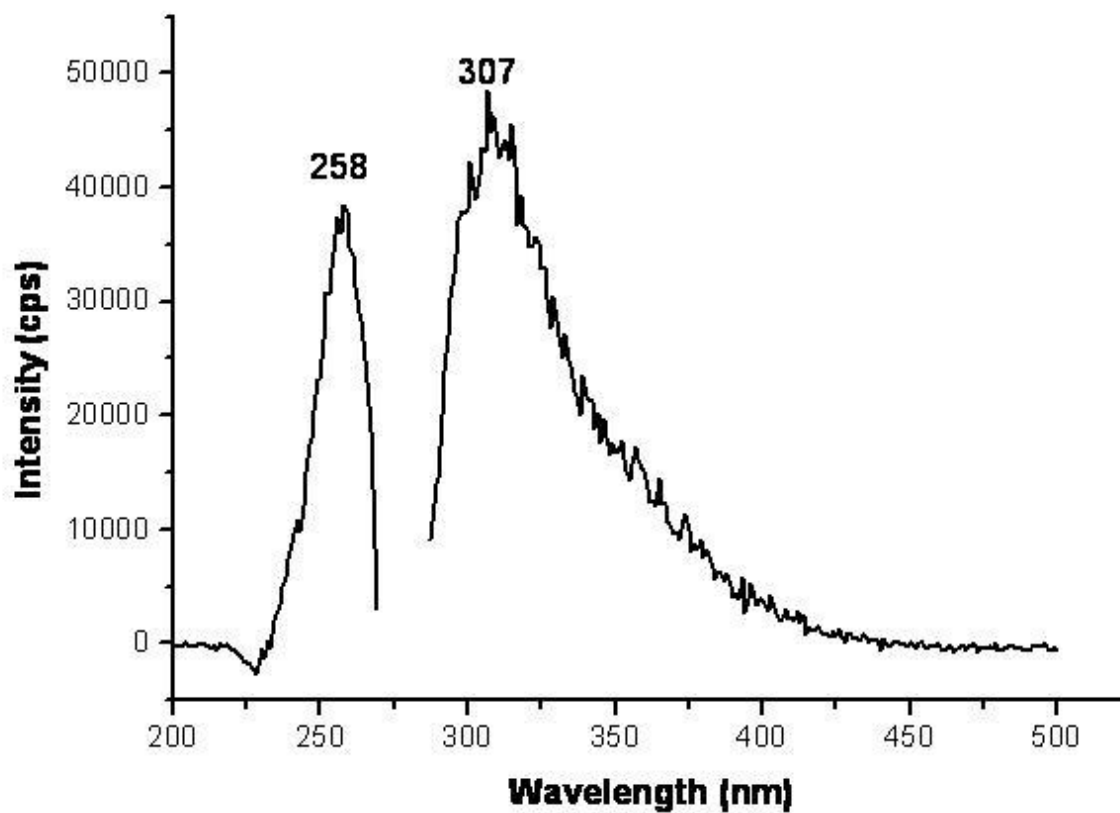


Figure D.1 Excitation Emission Spectrum of Disperse Red 1 Standard in 1:1 Acetonitrile/Water (v:v).  $\lambda_{ex} = 258\text{nm}$  and  $\lambda_{em} = 307\text{nm}$

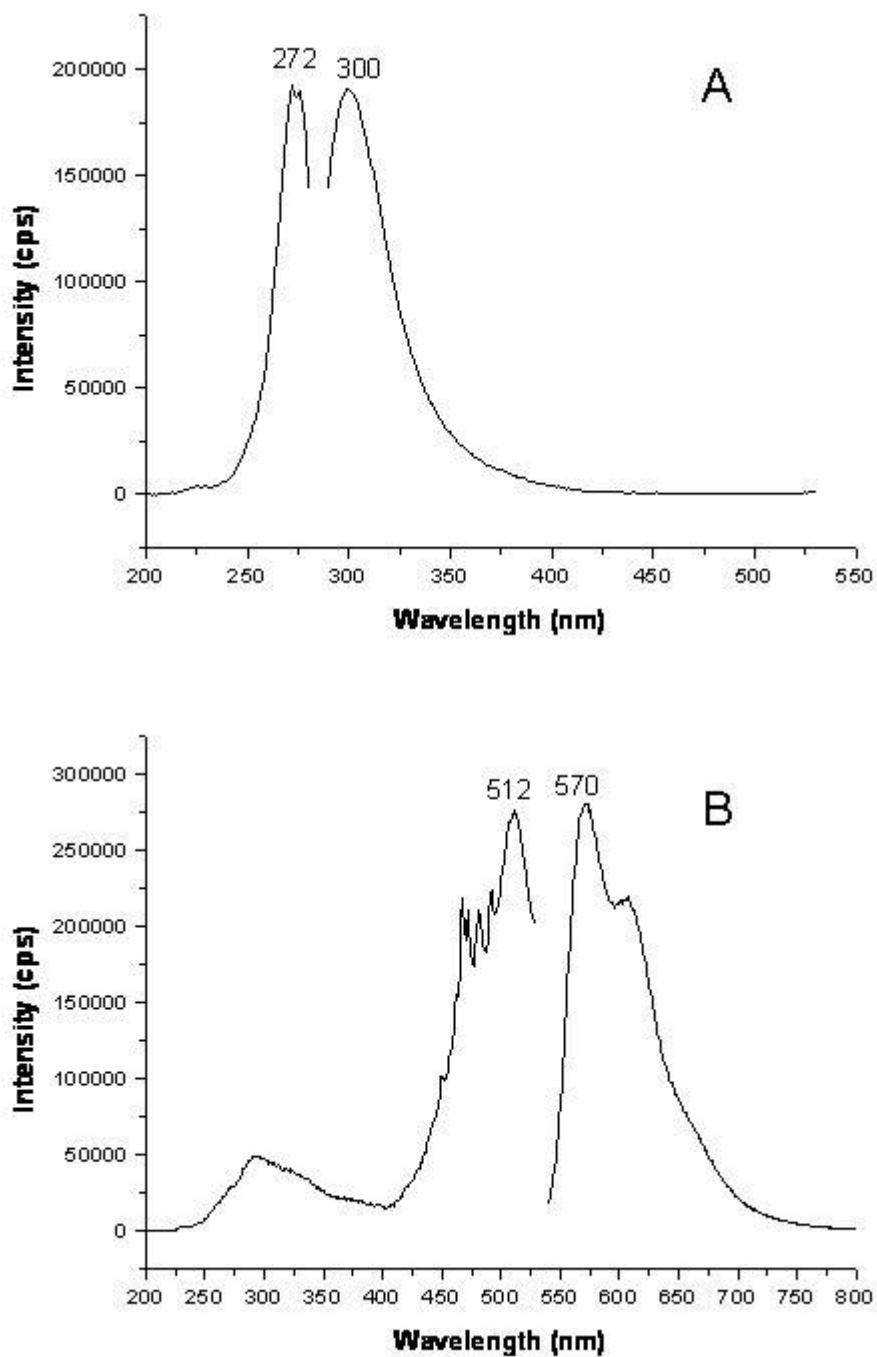


Figure D.2 Excitation Emission Spectrum of Disperse Red 4 Standard in 1:1 Acetonitrile/Water (v:v). A-Ultra-violet region  $\lambda_{ex} = 272\text{nm}$  and  $\lambda_{em} = 300\text{nm}$   
B-Visible region  $\lambda_{ex} = 512\text{nm}$  and  $\lambda_{em} = 570\text{nm}$ .

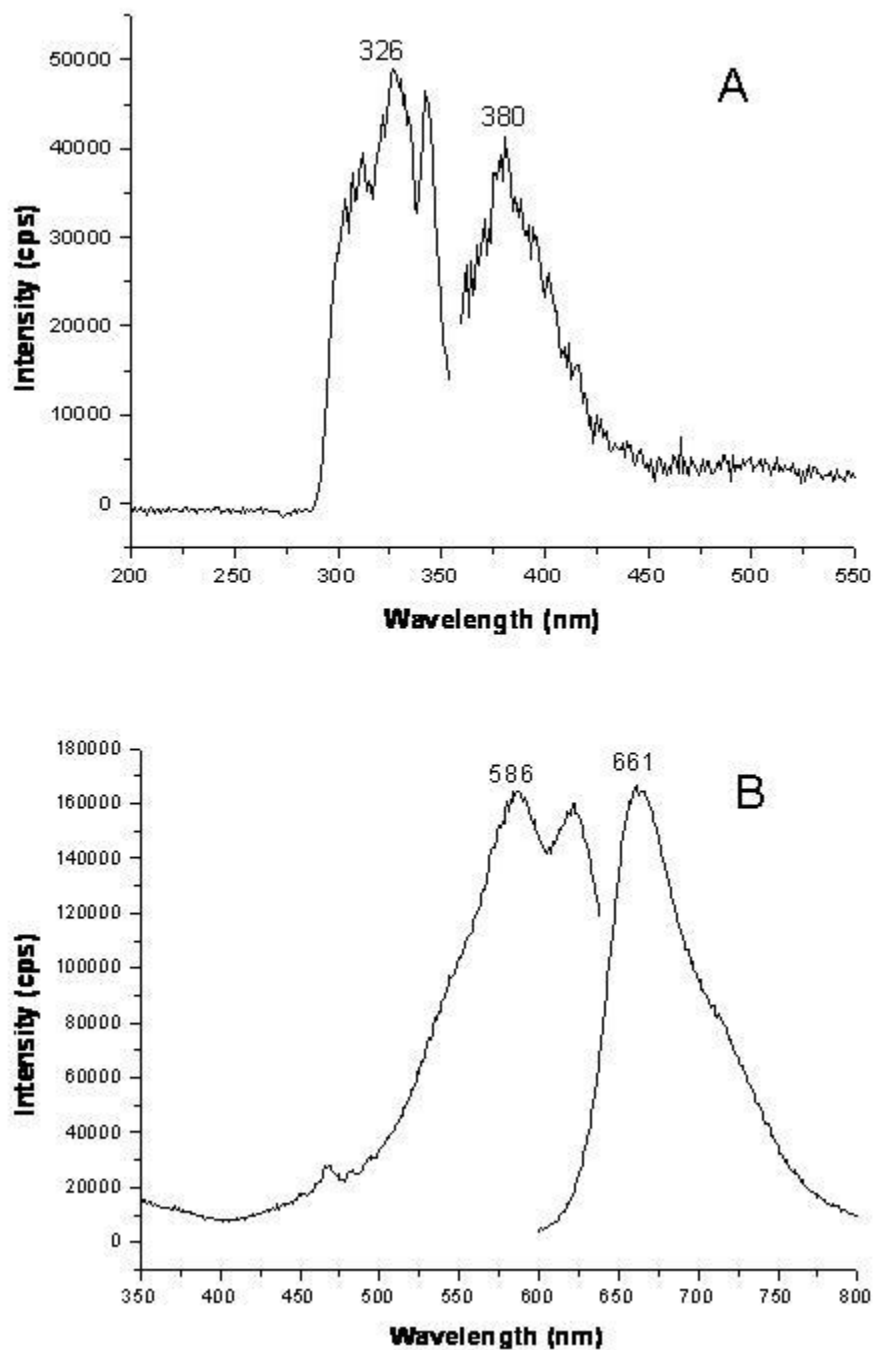


Figure D.3 Excitation Emission Spectrum of Disperse Blue 56 Standard in 4:3 Pyridine/Water (v:v). A-Ultra-violet region  $\lambda_{ex} = 326\text{nm}$  and  $\lambda_{em} = 380\text{nm}$  B-Visible region  $\lambda_{ex} = 586\text{nm}$  and  $\lambda_{em} = 661\text{nm}$ .

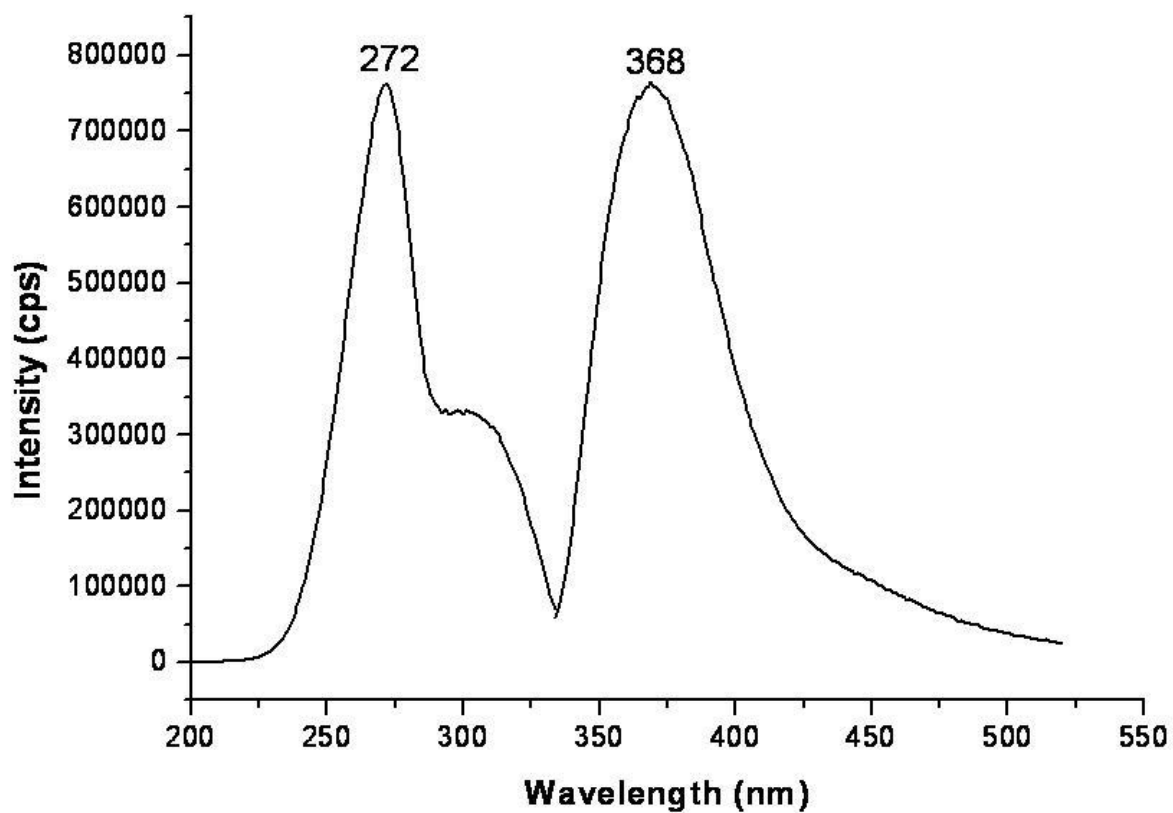


Figure D.4 Excitation Emission Spectrum of Basic Green 4 Standard in 1:1 Acetonitrile/Water (v:v).  $\lambda_{ex} = 272\text{nm}$  and  $\lambda_{em} = 368\text{nm}$

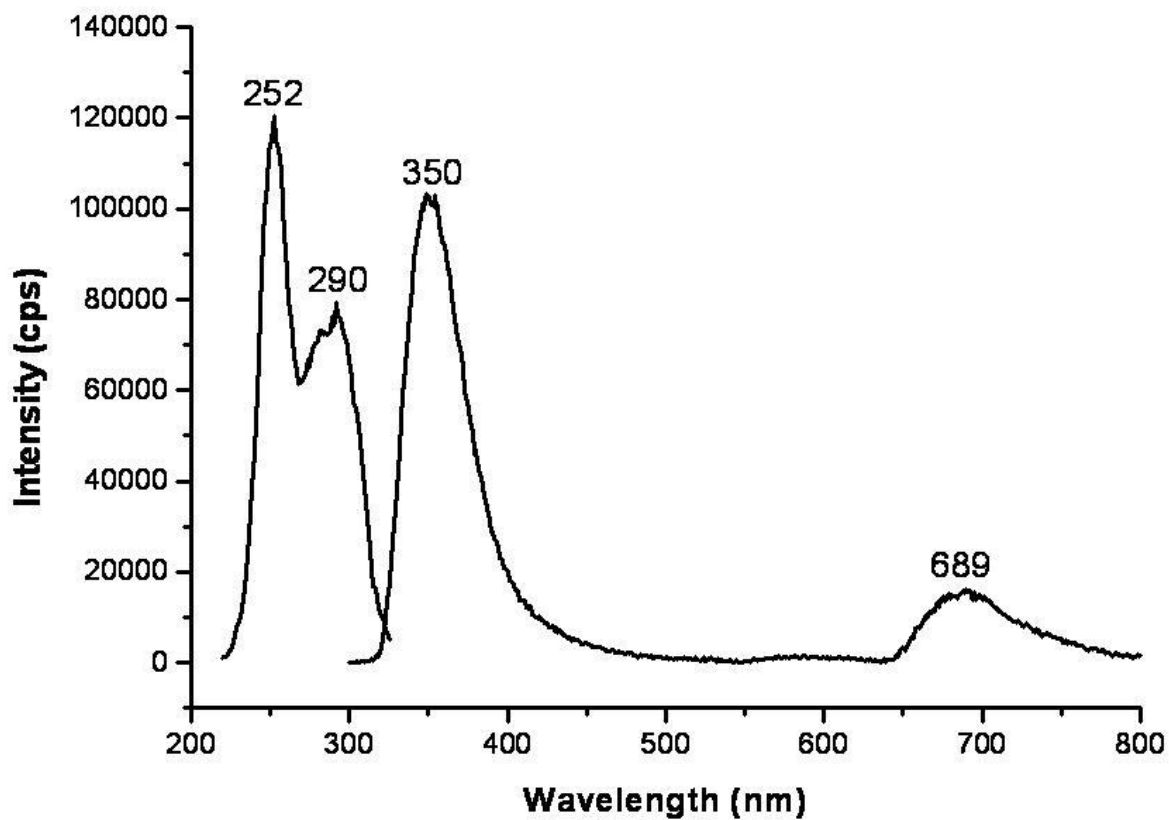


Figure D.5 Excitation Emission Spectrum of Basic Red 9 Standard in Ethanol.  $\lambda_{ex} = 252\text{nm}$  and  $\lambda_{em} = 350\text{nm}$

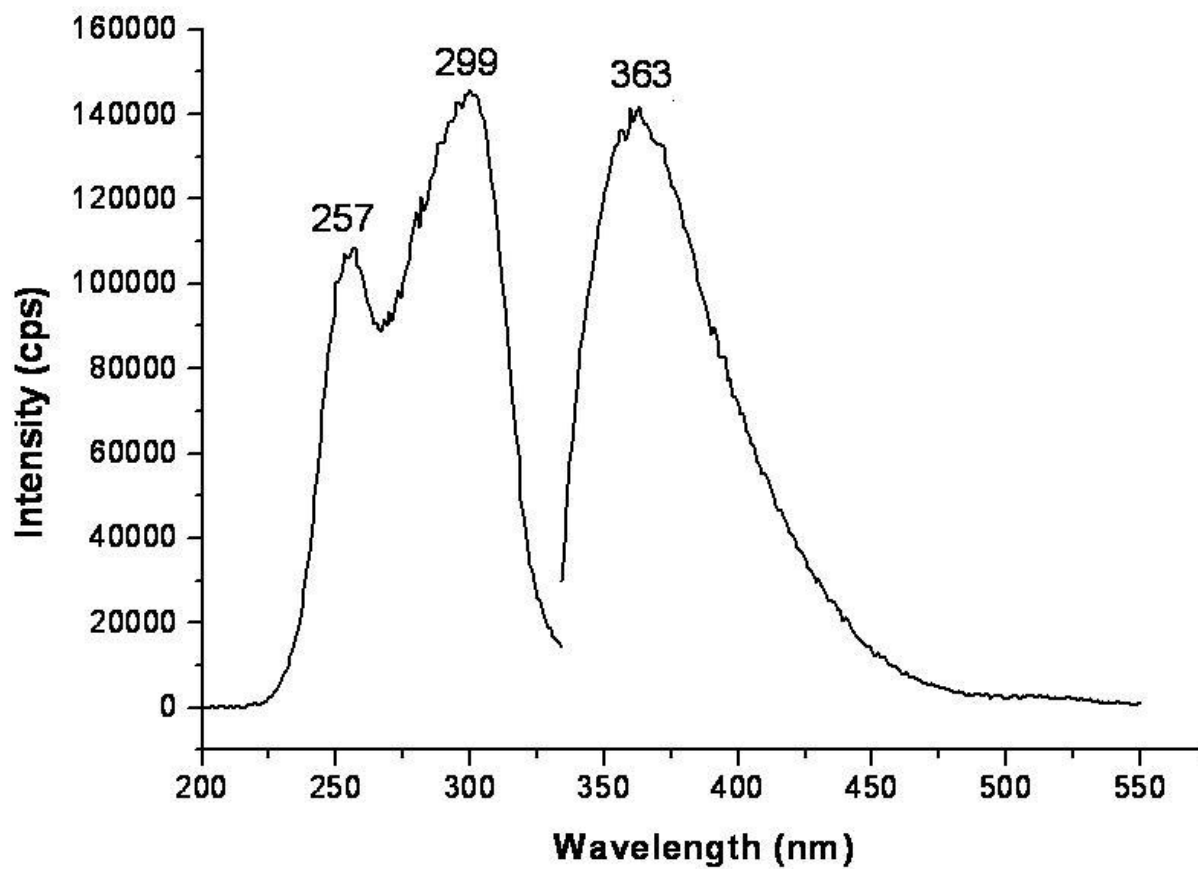


Figure D.6 Excitation Emission Spectrum of Basic Violet 14 Standard in 1:1 Acetonitrile/Water (v:v).  $\lambda_{ex} = 299\text{nm}$  and  $\lambda_{em} = 363\text{nm}$

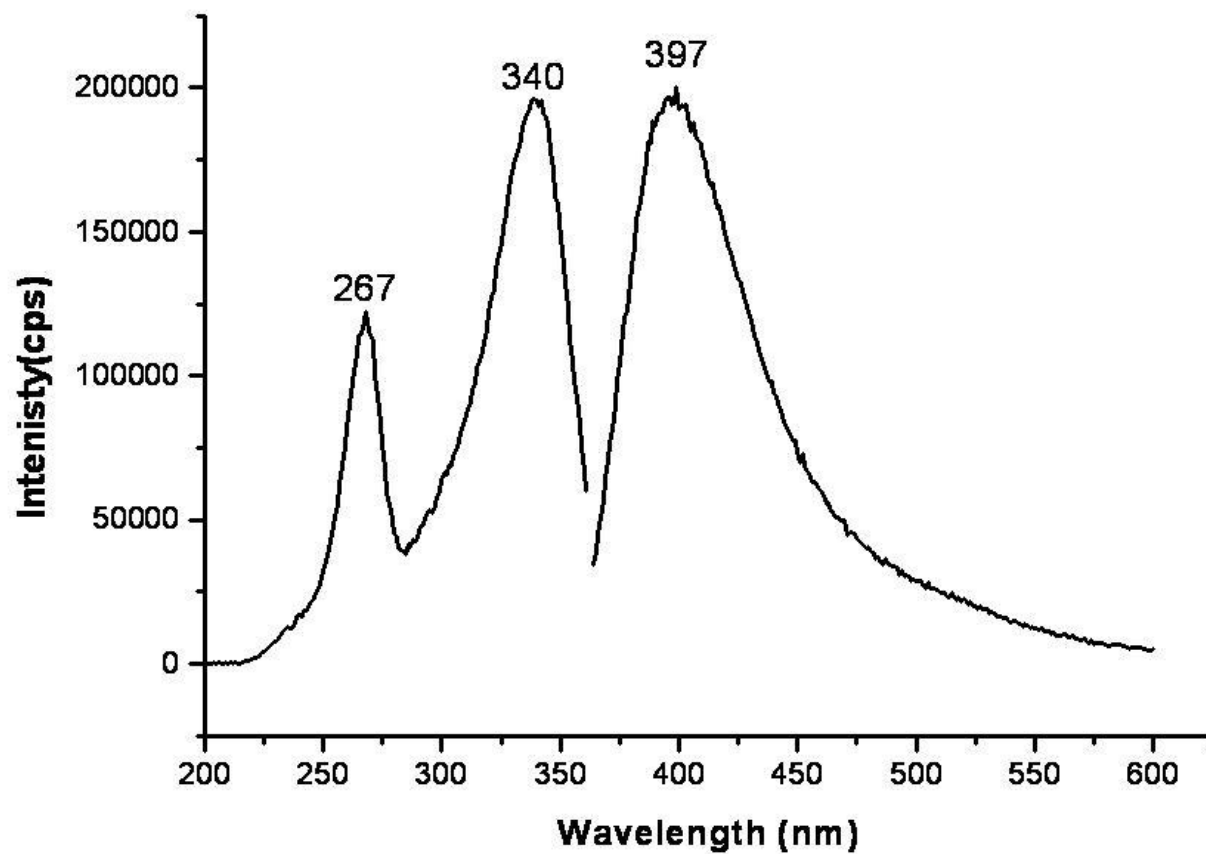


Figure D.7 Excitation Emission Spectrum of Direct Blue 1 Standard in Ethanol.  $\lambda_{ex} = 340\text{nm}$  and  $\lambda_{em} = 397\text{nm}$

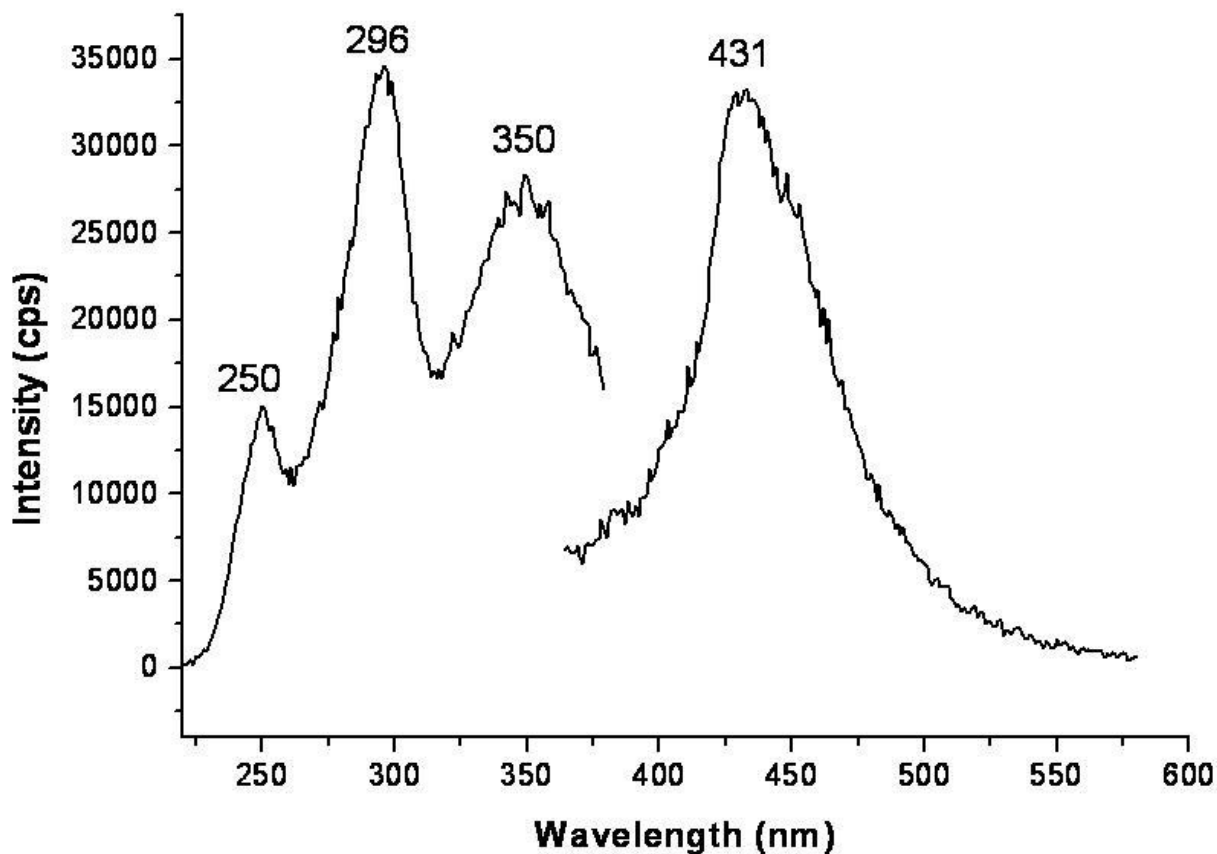


Figure D.8 Excitation and Emission Spectrum of Direct Blue 71 Standard in 1:1 Acetonitrile/Water (v:v).  $\lambda_{ex} = 296\text{nm}$  and  $\lambda_{em} = 431\text{nm}$

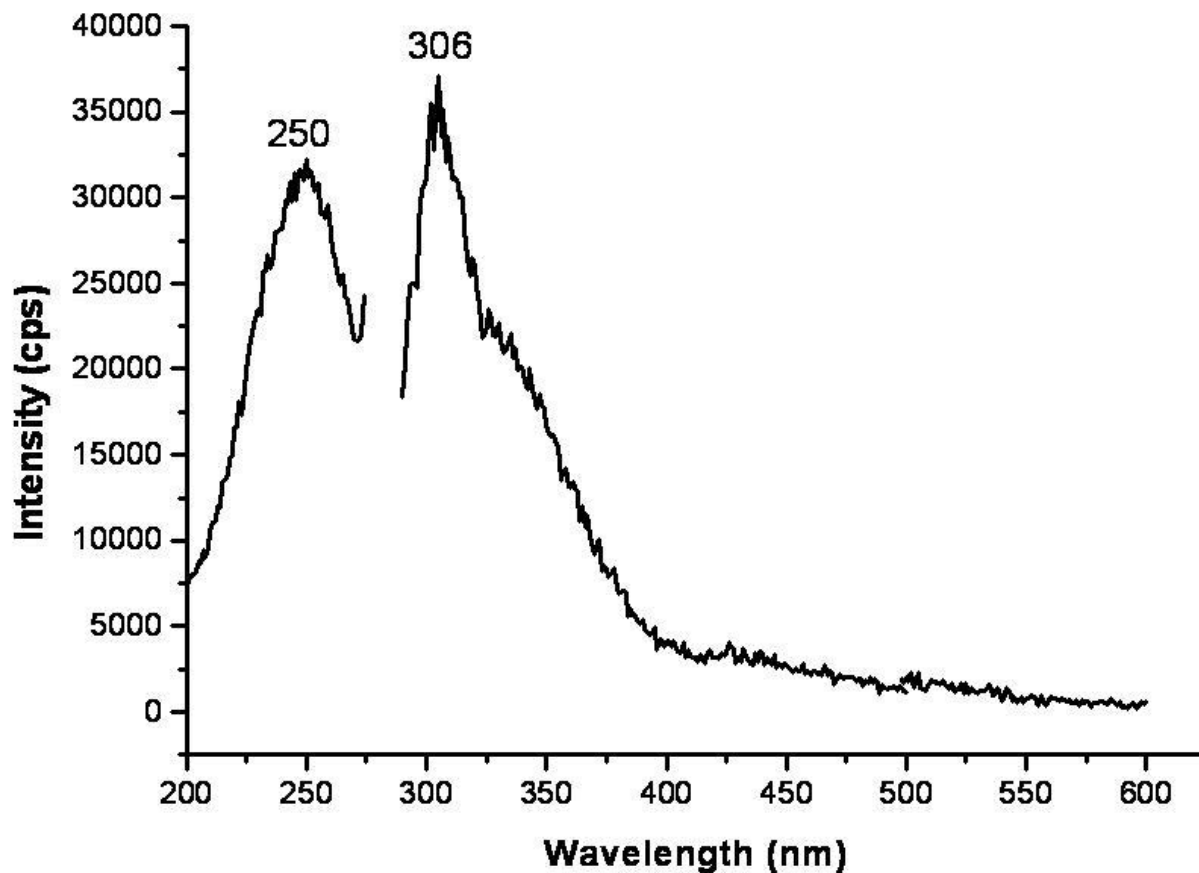


Figure D.9 Excitation Emission Spectrum of Direct Blue 90 Standard in 4:3 Pyridine/Water (v:v).  $\lambda_{ex} = 250\text{nm}$  and  $\lambda_{em} = 306\text{nm}$

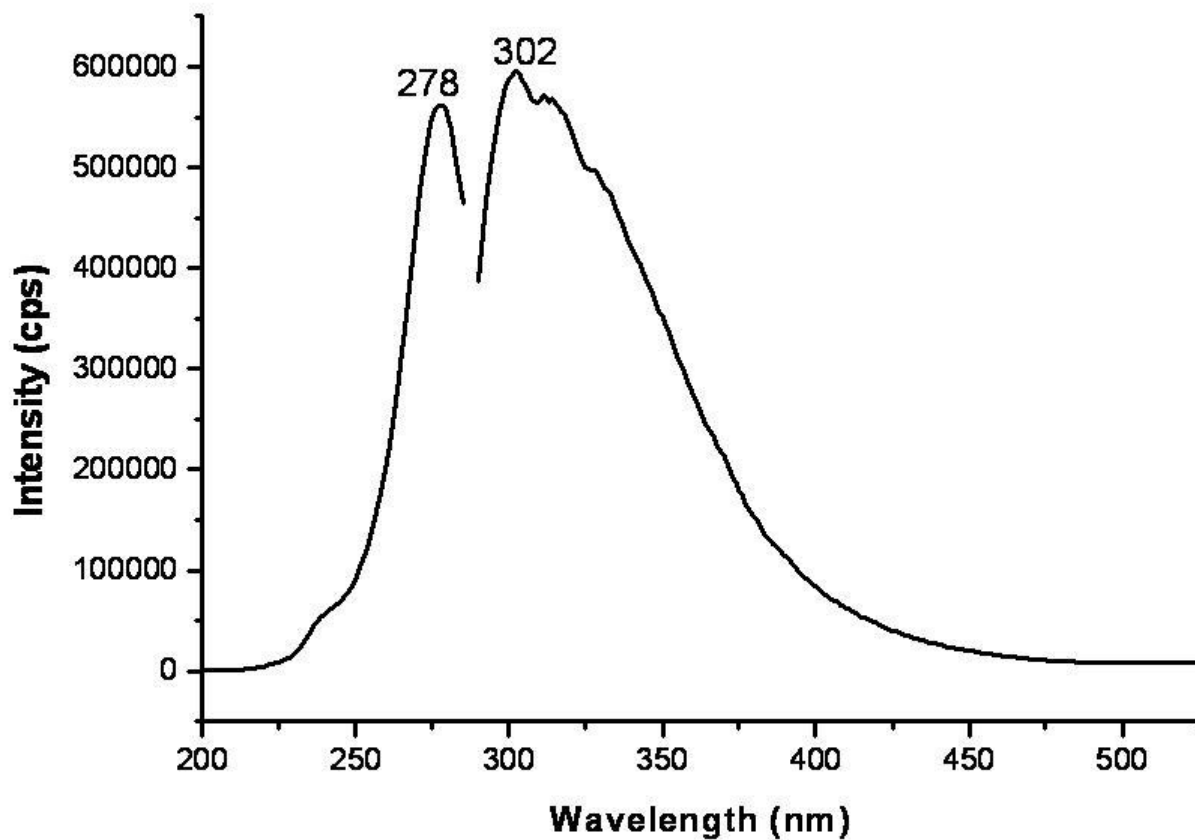


Figure D.10 Excitation and Emission Spectrum of Acid Yellow 17 Standard in Ethanol.  $\lambda_{ex} = 278\text{nm}$  and  $\lambda_{em} = 302\text{nm}$

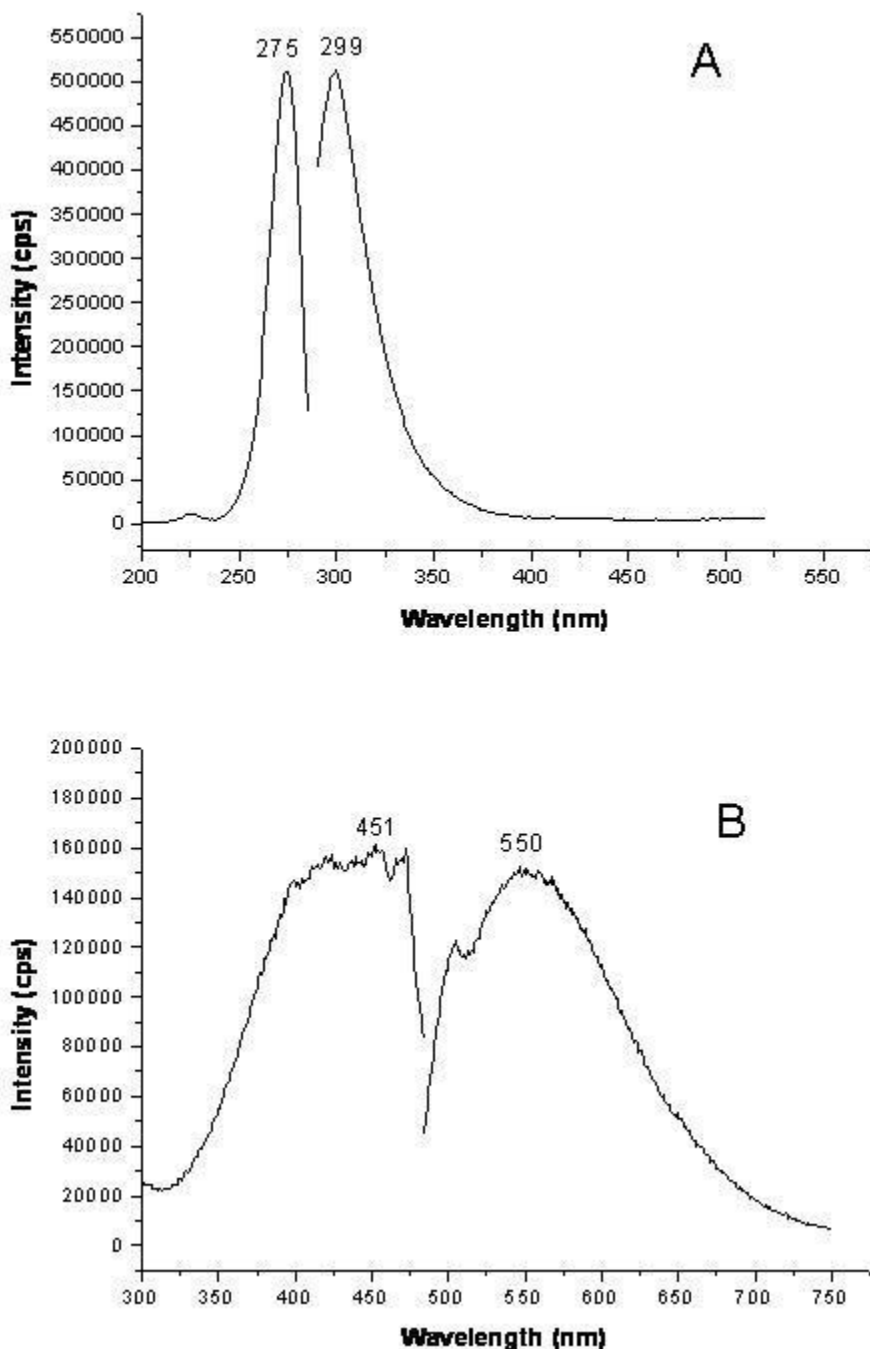


Figure D.11 Excitation Emission Spectrum of Acid Yellow 23 Standard in Ethanol. A-Ultraviolet region  $\lambda_{ex} = 275\text{nm}$  and  $\lambda_{em} = 299\text{nm}$  B-Visible region  $\lambda_{ex} = 451\text{nm}$  and  $\lambda_{em} = 550\text{nm}$ .

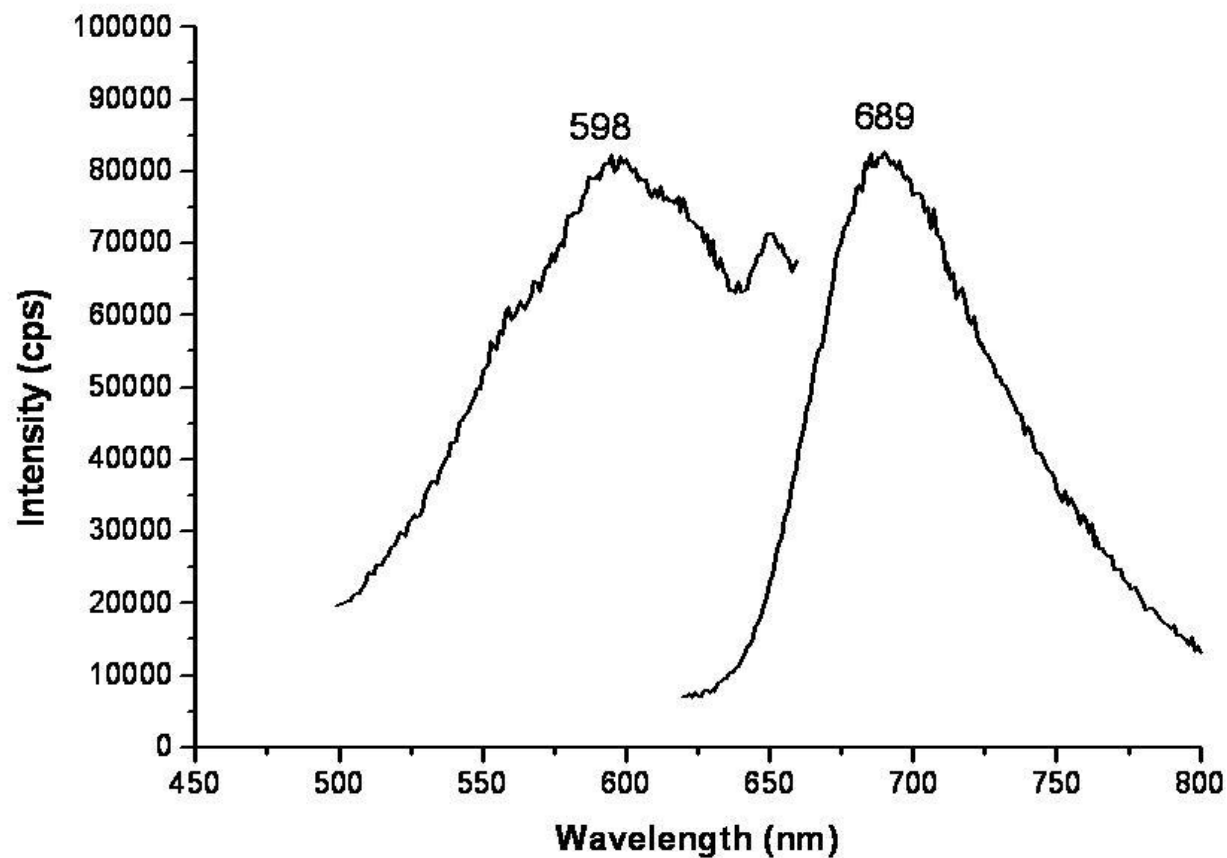


Figure D.12 Excitation and Emission Spectrum of Acid Green 27 Standard in 1:1 Methanol/Water.  $\lambda_{ex} = 598\text{nm}$  and  $\lambda_{em} = 689\text{nm}$

## **APPENDIX E: RTF-EEM of Sigma-Aldrich dye standards and fiber extracts**

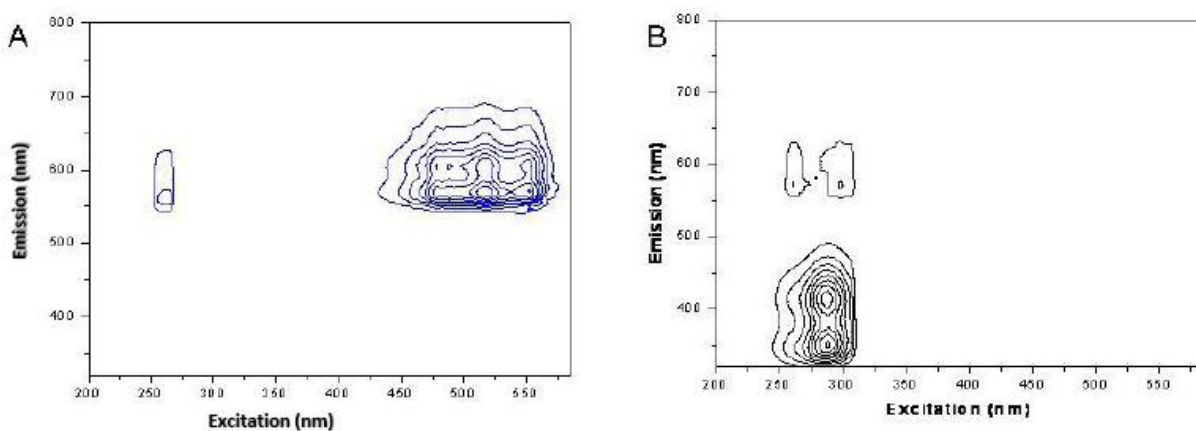


Figure E.1 EEM of Standards and Extracts from Fibers Pre-Dyed with Disperse Red 4 in 1:1 Acetonitrile/Water (v:v)

A-10ppm standard B-Fiber extract

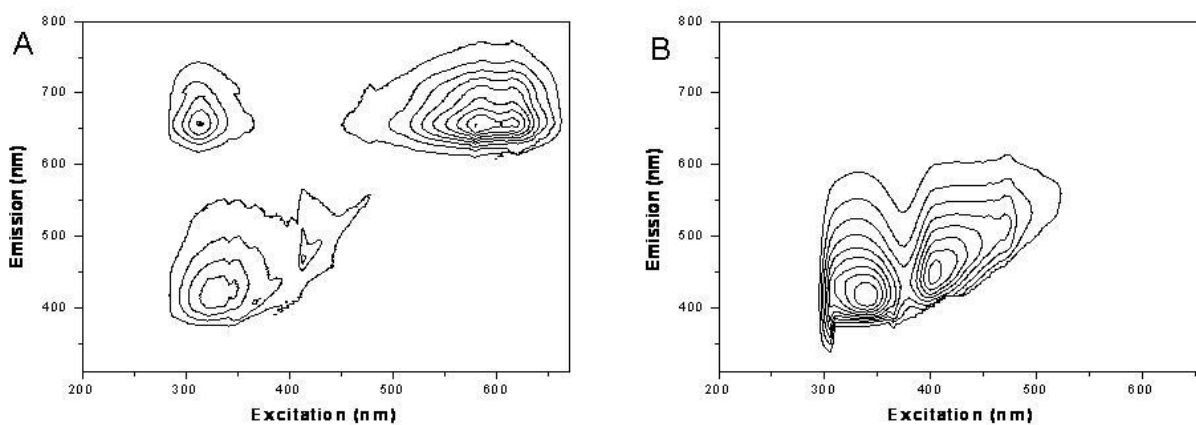


Figure E.2 EEM of Standards and Extracts from Fibers Pre-Dyed with Disperse Blue 56 in 4:3 Pyridine/Water (v:v)

A-10ppm standard B-Fiber extract

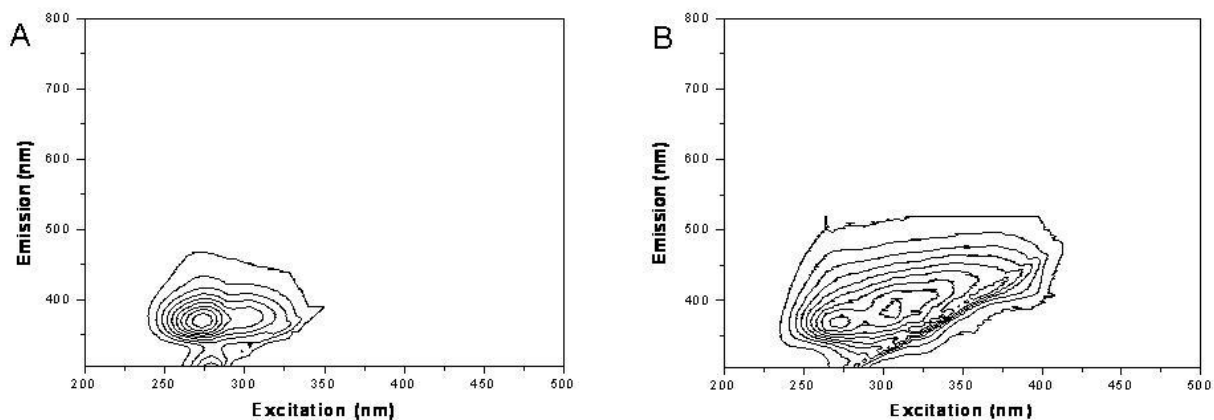


Figure E.3 EEM of Standards and Extracts from Fibers Pre-Dyed with Basic Green 4 in 1:1 Acetonitrile/Water (v:v)  
A-10ppm standard B-Fiber extract

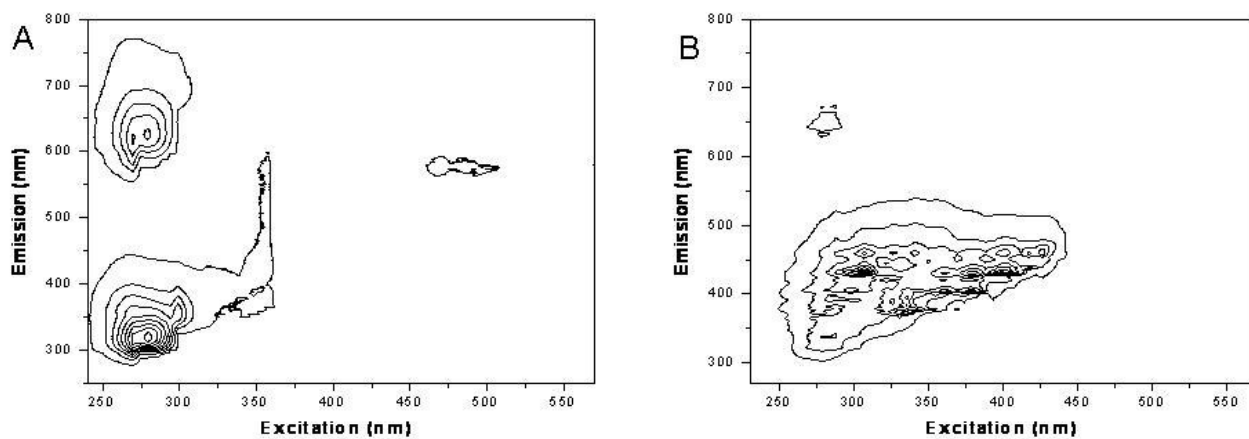
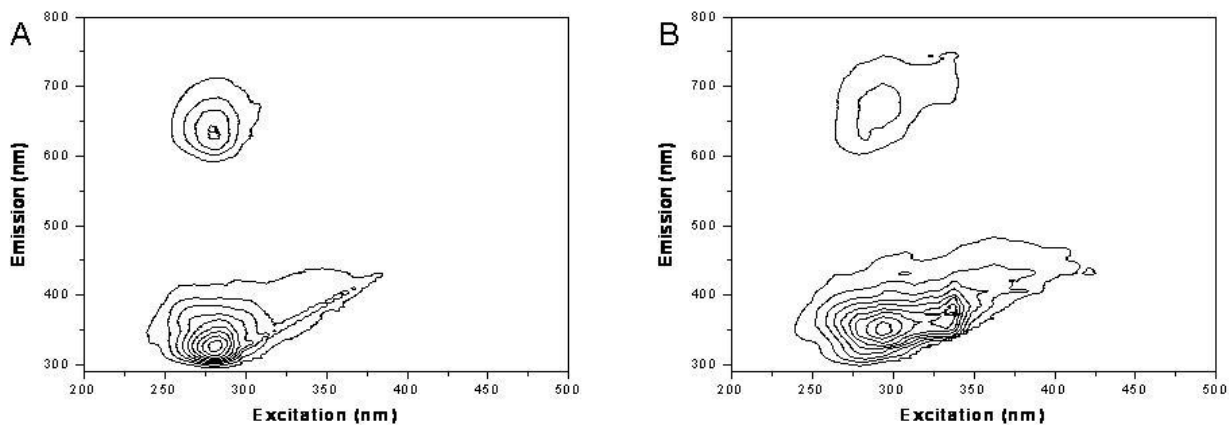
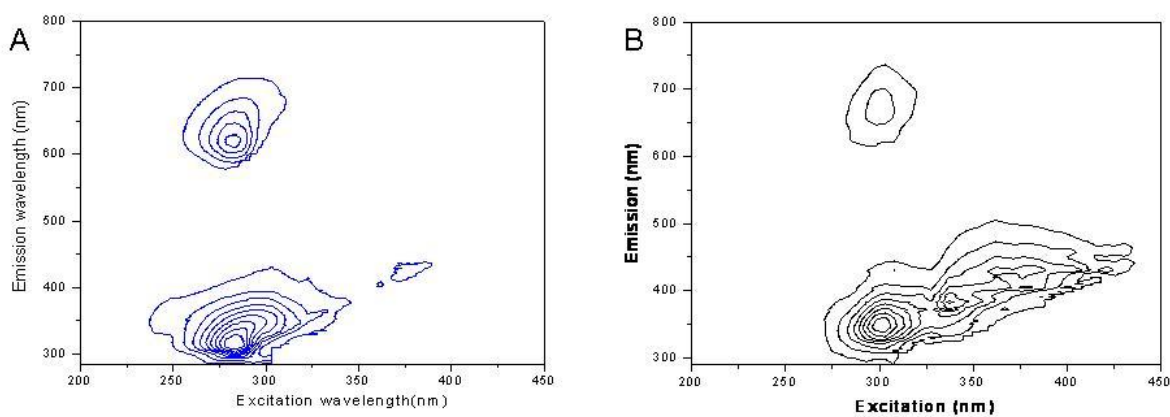


Figure E.4 EEM of Standards and Extracts from Fibers Pre-Dyed with Basic Red 9 in Ethanol  
A-10ppm standard B-Fiber extract



*Figure E.5 EEM of Standards and Extracts from Fibers Pre-Dyed with Acid Red 151 in Ethanol  
A-10ppm standard B-Fiber extract*



*Figure E.6 EEM of Standards and Extracts from Fibers Pre-Dyed with Acid Yellow 17 in Ethanol  
A-10ppm standard B-Fiber extract*

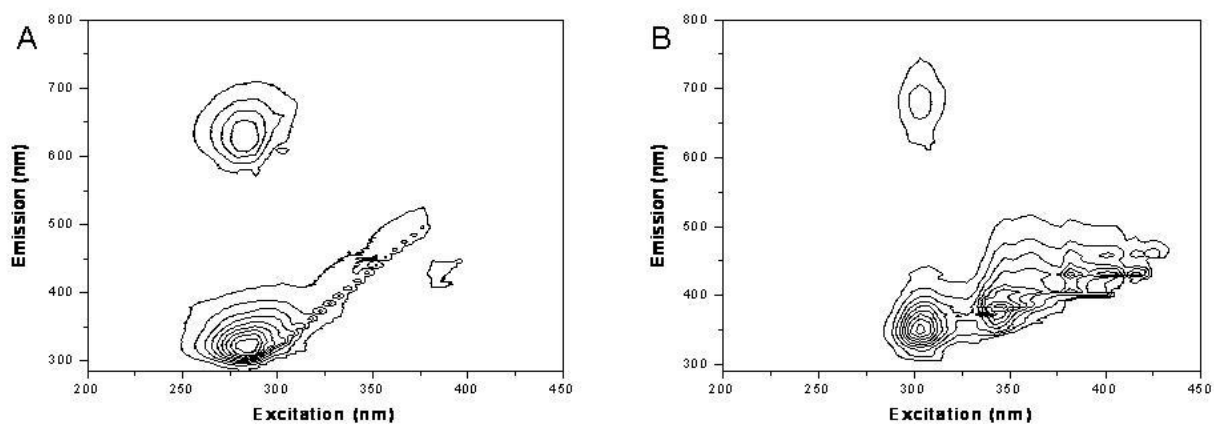


Figure E.7 EEM of Standards and Extracts from Fibers Pre-Dyed with Acid Yellow 23 in Ethanol

A-10ppm standard B-Fiber extract

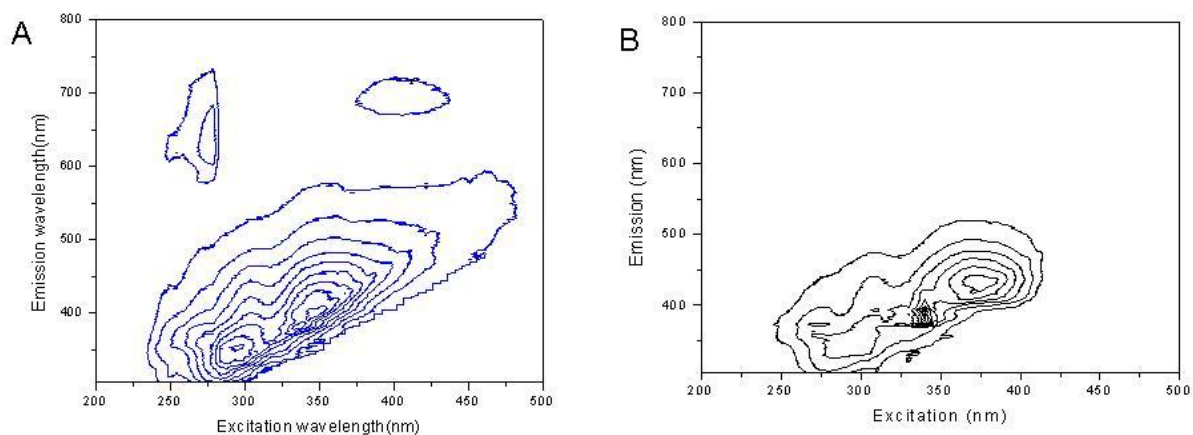


Figure E.8 EEM of Standards and Extracts from Fibers Pre-Dyed with Acid Green 27 in 1:1 Methanol/Water (v:v)

A-10ppm standard B-Fiber extract